UiT
THE ARCTIC UNIVERSITY OF NORWAY

Faculty of Health Sciences
Department of Medical Biology

Novel Inflammatory Mediators in Neuroblastoma Tumorigenesis

—

Conny Tümmler

A dissertation for the degree of Philosophiae Doctor – July 2019

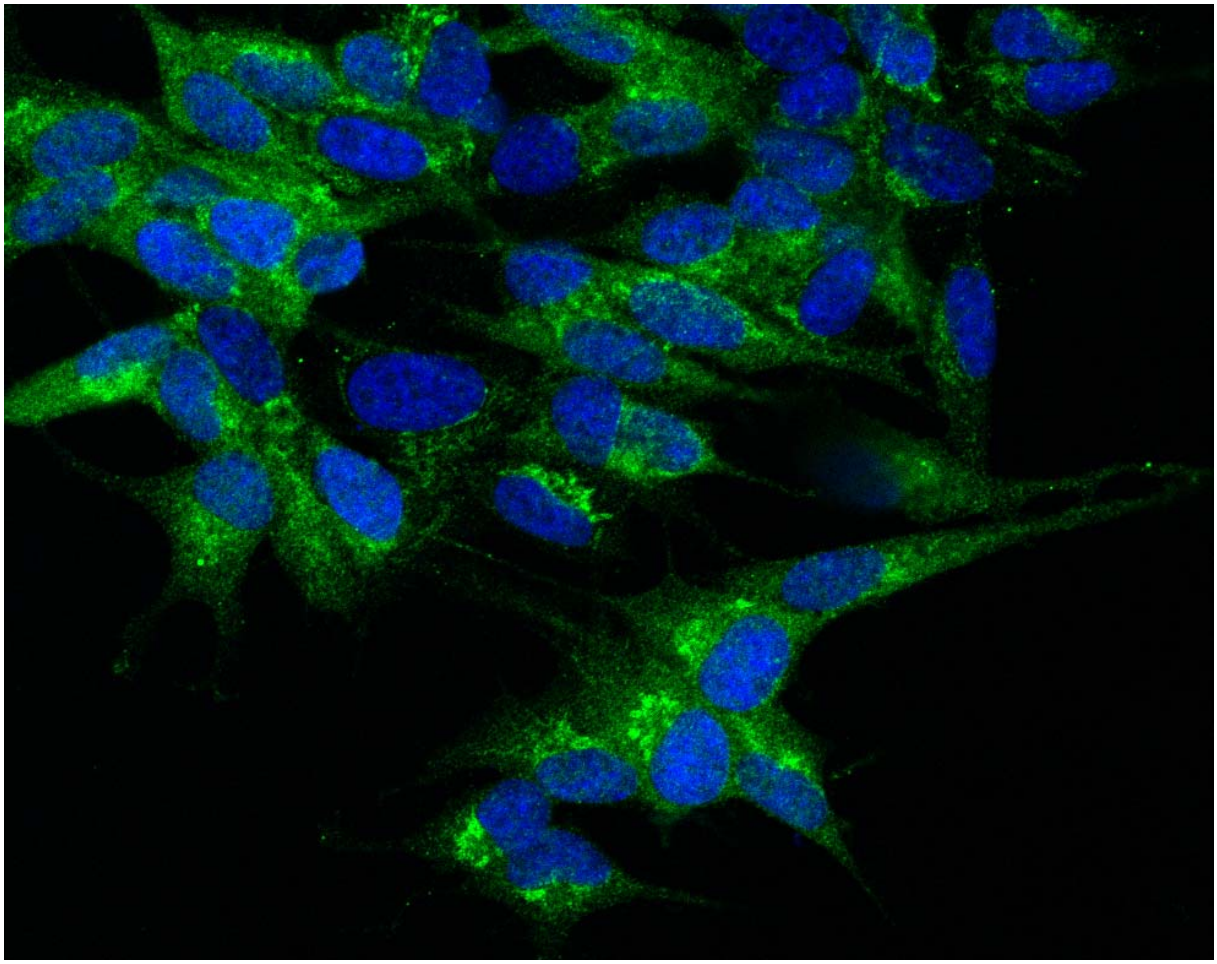

Barnekreft foreningen

THE ARCTIC UNIVERSITY OF NORWAY • UIT •

Novel Inflammatory Mediators in Neuroblastoma Tumorigenesis

Conny Tümmler

A dissertation for the degree of Philosophiae Doctor

Molecular Inflammation Research Group
Department of Medical Biology
Faculty of Health Sciences
UiT–The Arctic University of Norway

July 2019

“I may not have gone where I intended to go, but I think I’ve ended up where I needed to be.”

Douglas Adams

“For a scientist must indeed be freely imaginative and yet skeptical, creative and yet a critic. There is a sense in which he must be free, but another in which his thought must be very precisely regimented; there is poetry in science, but also a lot of bookkeeping.”

Peter B. Medawar
The Strange Case of the Spotted Mice: And Other Classic Essays on Science

CONTENTS

ACKNOWLEDGEMENTS

This work has been carried out at the Molecular Inflammation Research Group, Department of Medical Biology, Faculty of Health Sciences, University of Tromsø, The Arctic University of Norway with funding from the University of Tromsø and financial support from the Norwegian Childhood Cancer Society, the Norwegian Childhood Cancer Society-Region Troms and Finnmark, and the Erna and Olav Aakre Foundation for Cancer Research.

This Ph.D. has been a long, exciting, and sometimes bumpy journey and I would like to express my heartfelt gratitude to the people who supported me – I could not have done it without you.

First, I would like to express my deepest gratitude to my main supervisor Professor Baldur Sveinbjørnsson for introducing me to the fascinating and extremely motivating field of pediatric cancer research. Thank you for always being available usually replying to Emails within five minutes and always patiently answering my never-ending flow of questions. Thank you for your guidance, the extent of your knowledge never ceases to amaze me and I will never comprehend your ability to recall references like a library index. Thank you for always staying positive and encouraging me, even after disposing the umpteenth antibody that is not working. You have a great sense of humor, but your bowling skills could be improved. ☺

My co-supervisor Professor Ugo Moens welcomed me warmly to Tromsø over 12 years ago when I joined his research group for a three months internship. Although you have tried, you simply did not manage to get rid of me over the years and I even returned to your research group to embark on the Ph.D. journey. ☺ You are one of the most helpful, kind persons I know, and I cannot express my gratitude for the support you have given me over the years. Your door is always open and your extensive knowledge is impressive. Thank you for the never-ending supply of fantastic Belgian chocolate and remembering my favorite Belgian beer. ☺

What always impressed me about you, Baldur and Ugo, is that despite your very busy schedule you still regularly work in the lab. You understand how much time experiments can take and are always able to give practical advice. Thank you so much for that.

I would like to thank my co-supervisor Professor Inigo Martinez for always showing interest in my work and my progress and for many educative and extremely interesting cancer biology discussions.

I would like to thank all past (Gianina, Ketil, Liv-Marie, Igor, Ibrahim, Brynjar, Ida Sofie, Julia, Dag, Kristine, and Nannan) and current members (Baldur, Ugo, Maria, Diana, Kashif, Bálint, Aelita, and Marianne) of the Molecular Inflammation Research Group for creating such a nice work environment full of support, helpfulness, amazing cakes, and good humor. Thank you for bowling, mini golf, and escape room adventures and an unforgettable trip to Belgium. Thank you, Maria and Gianina, for keeping the lab going and all your help and support. I would like to thank my past office mates and fellow Ph.D. students Ketil, Liv-Marie, and Igor for great discussions about life, work-outs, fishes and shrimps, superheroes, cooking, and of course work. ☺ Thank you for your support and for making me laugh. Thank you to my other fellow Ph.D. students Kashif, Aelita, and Diana for sharing successes and frustrations. Kashif, you are a great colleague but for a veterinarian you are terrible with fishes. Dianita, thank you for sharing my love for chocolate and always giving me a hug when needed. Thank you, Marianne, for being an amazing Bachelor and Master student. Your initiative, independence, hard work, helpfulness, and kindness have made it a pleasure to work with you.

With the support of an UiT “utenlandsstipend,” I had the great opportunity to spend six months at the Childhood Cancer Research Unit at the Karolinska Institutet in Stockholm. Thank you very much, Per and John Inge. for welcoming me warmly into your research group. I would like to thank all group members (Per, John Inge, Lotta, Malin, Linda, Nina, Cici, Anna, Jelena, Teodora, Diana, and Carl Otto) for making my stay extremely enjoyable, teaching me new methods and a lot about neuroblastoma, and great talks over Fika. Thank you so much Lotta for all your help in practical matters, especially with the animal study. A big thank you to Malin for helping me with the animal studies, great talks about science and life, and always answering my statistics questions. Linda and Nina, you adopted me upon arrival and made sure I did not feel lonely away from home. Thank you for showing me Stockholm and thank you for still being part of my life.

I would also like to express my gratitude to my co-authors: Igor, Malin, Linda, Lotta, Jon-Olof, Per, John Inge, Baldur, Ugo, Gianina, Peter, Andrey, Marianne, and Nina for all your hard work on the papers. It has been a great pleasure to work with you.

Furthermore, I would like to thank the Norsk Biokjemisk Selskap, the Norwegian and Swedish Childhood Cancer Foundations, and the former Norwegian Research School in Medical Imaging for financial support that allowed me to attend extremely valuable courses and conferences.

Thank you Montse and Nina for reading the thesis and the very useful comments and feedback.

A big thank you goes to the 9th floor” lab gang”: Dianita, Adri, Ahmed, Clement, Theresa, Bishnu, Kjersti, Jessin, Katya, Martin, Eric, Mushtaq, Hermoine, and Maria for amazing shared birthday lunches, dinners, hikes, dances, coffee breaks with date pastries, and lots of fun. You are an awesome group of people and I am grateful for being part of this gang.

To the Tromsø ladies (Tracy, Montse, Jai, Ana, Ruomei, the Julias, Irina, Georgina, Ane, Fern, Idun, Elisabeth, Berit, Cris, and Sara) thank you for your support, science-related discussion, and most importantly distractions from work. Montse, thank you for sharing my interest in movies, books, and music. Thank you, Tracy, for many years of friendship, support, and fun adventures. Julia and Theresa, thank you so much for preserving my German language skills☺, for Plätzchen backen, Spätzlehocketsle, and simply for being my friends.

To my “Mädelz” at home, Tini, Anki, Annett, Verena, and Alida, thank you for being part of my life since kindergarten. Thank you for your friendship and never-ending support, even over long distances.

A heartfelt thank you goes to my family, my parents Regina and Peter, my sister Silvana, and my brother-in-law Andi. Thank you for always encouraging and believing in me. Thank you for teaching me the importance of hard work and perseverance. Special thanks go to my amazing niece Lilly for being the best distraction from work, ever. ☺

Last but certainly not least, I want to thank Joe for sharing the past 12 years with me. Thank you for always being there, for supporting and believing in me, for not minding long work hours even on weekends, and for sometimes simply telling me “Come home, you’ve done enough for today”. Thank you for proofreading my manuscripts and the thesis and marveling at the strange and funny expressions we use. Thank you for making me laugh and always having my back.

LIST OF PAPERS

Paper I

Tümmler C, Snapkov I, Wickström M, Moens U, Ljungblad L, Elfman LHM, Winberg JO, Kogner P, Johnsen JI and Sveinbjørnsson B.

Inhibition of chemerin/CMKLR1 axis in neuroblastoma cells reduces clonogenicity and cell viability *in vitro* and impairs tumor growth *in vivo*

Oncotarget, 8(56), 95135-95151. doi:10.18632/oncotarget.19619

Paper II

Tümmler C, Dumitriu G, Wickström M, Coopman P, Valkov A, Kogner P, Johnsen JI, Moens U, and Sveinbjørnsson B.

SYK Inhibition Potentiates the Effect of Chemotherapeutic Drugs on Neuroblastoma Cells *in Vitro*

Cancers (Basel), 11(2), 202. doi:10.3390/cancers11020202

Paper III

Tümmler C, Marken M, Valkov A, Eissler N, Kogner P, Johnsen JI, Moens U, and Sveinbjørnsson B.

The Interleukin 17 Family and Interleukin 23 in the Neuroblastoma Microenvironment

Manuscript

ABBREVIATIONS

^{131}I-miBG	Iodine 123 metaiodobenzylguanidine
Akt	RAC-alpha serine/threonine-protein kinase
ALK	Anaplastic lymphoma kinase
α-NETA	2-(α-naphthoyl) ethyltrimethylammonium iodide
ARID1A	AT-rich interactive domain-containing protein 1A
ARID1B	AT-rich interactive domain-containing protein 1B
ATRX	Alpha thalassemia/mental retardation syndrome X-linked
BET	Bromodomain and extra-terminal motif
BMP	Bone morphogenetic protein
Breg	Regulatory B cells
CAF	Cancer-associated fibroblast
CAR-T	Chimeric antigen receptor T cells
CCL	C-C motif chemokine
CCRL2	C-C chemokine receptor-like 2
CD	Cluster of differentiation
c-Jun	Jun proto-oncogene
CMKLR1	Chemokine-like receptor 1
C-MYC	V-Myc avian myelocytomatosis viral oncogene homolog
COX	Cyclooxygenase
CSF1	Colony-stimulating factor 1
CSF-1R	Colony stimulating factor 1 receptor
CTL	Cytotoxic T lymphocyte
CTLA-4	Cytotoxic T-lymphocyte-associated protein 4
CXCL	C-X-C motif chemokine
CXCR	C-X-C chemokine receptor
DAMP	Damage-associated molecular pattern
DC	Dendritic cell
Dkk-1	Dickkopf-related protein 1
ECM	Extracellular matrix
EGF	Epidermal growth factor
EGFR	Epidermal growth factor receptor
ELISA	Enzyme-linked immunosorbent assay
EMT	Epithelial–mesenchymal transition
ERK	Extracellular signal-regulated kinase
FasL	Fas ligand
FGF	Fibroblast growth factor
FoxD3	Forkhead box D3
GD2	Ganglioside G2
GM-CSF	Granulocyte-macrophage colony-stimulating factor

GPCR	G protein-coupled receptors
GPR1	G protein-coupled receptor 1
HGF	Hepatocyte growth factor
HLA	Human leukocyte antigen
IDO	Indoleamine 2,3-dioxygenase
IFN	Interferon
IGF	Insulin-like growth factors
IL	Interleukin
ILC	Innate lymphoid cell
INRG	International Neuroblastoma Risk Group
INRGSS	International Neuroblastoma Risk Group Staging System
INSS	International Neuroblastoma Staging System
ITAM	Immunoreceptor tyrosine-based activation motif
JAK	Janus kinase
JNK	c-Jun N-terminal kinases
LAG-3	Lymphocyte-activation gene 3
LPS	Lipopolysaccharide
MALAT-1	Metastasis associated lung adenocarcinoma transcript 1
MDSC	Myeloid-derived suppressor cell
MHC	Major histocompatibility complex
MIP	Macrophage inflammatory protein
MMP	Matrix metalloproteinase
mPGES	Microsomal prostaglandin E synthase-1
MSC	Mesenchymal stem cell
MTT	3-(4,5-dimethylthiazol-2-yl)-2,5-diphenyltetrazolium bromide
NF-κB	Nuclear factor kappa-light-chain-enhancer of activated B cells
NGF	Nerve growth factor
NK	Natural killer
NKT	Natural killer T
N-MYC (MYCN)	v-myc avian myelocytomatosis viral oncogene neuroblastoma-derived homolog
NRAS	Neuroblastoma RAS viral oncogene
Nrf2	Nuclear factor erythroid 2-related factor 2
NSAID	Nonsteroidal anti-inflammatory drug
p53	Cellular tumor antigen p53
PAMP	Pathogen-associated molecular pattern
PARP	Poly (ADP-ribose) polymerase
PD-1	Programmed cell death protein 1
PDGF	Platelet-derived growth factor
PD-L1	Programmed death-ligand 1
PGE_2	Prostaglandin E2

Phox2b	Paired-like homeobox 2b
PI3K	Phosphoinositide 3-kinase
PLCγ	Phospholipase C gamma
PTPN11	Tyrosine-protein phosphatase non-receptor type 11
SLP	SH2 domain containing leukocyte protein
STAT3	Signal transducer and activator of transcription 3
SYK	Spleen tyrosine kinase
TAM	Tumor-associated macrophage
TAN	Tumor-associated neutrophils
Tfh cells	T follicular helper cells
TGF-β	Transforming growth factor beta
Th cells	Helper T cells
TIM-3	T-cell immunoglobulin and mucin-domain containing-3
TIME	Tumor immune environment
TIMP	Tissue inhibitors of metalloproteinases
TLR	Toll-like receptors
TME	Tumor microenvironment
TNF-α	Tumor necrosis factor alpha
TRAIL	TNF-related apoptosis-inducing ligand
Treg	Regulatory T cells
Trk	Tropomyosin receptor kinase
VAV	Vav guanine nucleotide exchange factor 1
VEGF	Vascular endothelial growth factor

SUMMARY

Neuroblastoma is a cancer of early childhood and the most frequently diagnosed malignancy in the first year of life. Tumors can arise anywhere in the sympathetic nervous system, predominantly in the adrenal medulla, and metastatic disease is detected in approximately 50% of patients at diagnosis. Neuroblastoma is a biologically and clinically heterogeneous disease ranging from spontaneously regressing to highly aggressive therapy-resistant tumors. Despite intensive multimodal therapy, 50% of high-risk patients are refractory to treatment or relapse within two years. Novel therapeutic approaches are warranted to support existing therapies, improve patient survival, and reduce therapy-related late effects. The tumor microenvironment, a complex and intricate interplay between tumor, immune, and stromal cells as well as the extracellular matrix, constantly evolves to support tumor growth. Inflammatory processes in the tumor microenvironment are an essential part of anti-tumor immunity but can also promote tumor growth. In neuroblastoma, several inflammatory mediators and pathways have already been identified that support tumorigenesis and a deeper understanding of inflammatory processes in the neuroblastoma microenvironment may enable alleviation of tumor-promoting inflammation while preserving anti-tumor immune responses.

This thesis aims to identify novel inflammatory mediators and pathways in neuroblastoma to contribute to a better understanding of neuroblastoma biology, a prerequisite for novel therapeutic approaches. The first study describes a functional chemerin/CMKLR1 axis in neuroblastoma. Chemerin, a multifunctional chemoattractant protein and its receptors CMKLR1 and GPR1 are expressed in neuroblastoma cell lines and tissue. Chemerin promoted pro-tumorigenic signaling pathways in neuroblastoma and blockade of the chemerin/CMKLR1 axis impaired neuroblastoma growth.

The second study demonstrates the presence of spleen tyrosine kinase in neuroblastoma, a non-receptor tyrosine kinase with diverse functions. Inhibition of SYK with commercially available small molecule inhibitors impaired the cell viability of SYK-expressing neuroblastoma cells and potentiated the effect of commonly used chemotherapeutic drugs.

The interleukin 17 family has important functions in host defense but has also been implanted in inflammatory diseases and cancer. The third study describes the expression of interleukin 17 family members and the functionally-related interleukin 23 in neuroblastoma. The interleukin 17 receptors RA, RB, and RC are present in neuroblastoma cell lines and tumor tissue. Their stimulation with recombinant interleukin 17 proteins affected the cell viability of neuroblastoma cells only marginally but modulated HGF and Dkk-1 secretion and *in vitro* migration. Interleukin 23p19 was detected in neuroblastoma cell lines and tissues and the presence of different *IL23A* splice variants in neuroblastoma cell lines was observed.

INTRODUCTION

1 CANCER

"Cancer is a collection of many diseases with common principles, and each disease will have to be understood and more effectively controlled on its own terms."
Harold E. Varmus [1]

In 1989 Harold E. Varmus fittingly described cancer cells as "a distorted version of our normal selves" [2]. During tumorigenesis, the strictly regulated and coordinated processes that govern normal cells and tissues are disturbed. Tumor cells multiply uncontrolled and co-opt non-malignant cells to form a partnership that supports tumor growth and spread to adjacent and distant tissues.

Cancer is a collective term for a heterogeneous group of diseases and despite the fact that cancers are exceptionally diverse and each tumor is unique, advances in cancer research have led to the identification of common biological capabilities that enable and promote tumorigenesis. In 2000 Douglas Hanahan and Robert Weinberg introduced the term "hallmarks of cancer" to conceptualize six characteristics of tumor development: self-sufficiency in growth signals, insensitivity to anti-growth signals, evading apoptosis, limitless replicative potential, sustained angiogenesis, and tissue invasion and metastasis [3]. These hallmarks have since been extended to include deregulation of cellular energetics and avoiding immune destruction and the enabling characteristics of genome instability and tumor-promoting inflammation [4]. In a 2017 review, Yousef Fouad and Carmen Aanei suggested a condensed and revised version of the hallmarks defining seven capabilities that support neoplastic growth: selective growth and proliferative advantage, altered stress response, metabolic rewiring, immune modulation, an abetting microenvironment, vascularization, and invasion and metastasis [5].

Our increased knowledge of cancer biology has led to remarkable advances in cancer therapy. Today, physicians can employ an arsenal of targeted drugs, "magic bullets", a concept already described in the late 19th/early 20th century by Paul Ehrlich, the founder of chemotherapy [6]. However, cancer remains a global health problem as worldwide 1 in 6 deaths are attributed to cancer (estimated 9.6 million deaths in

2018), making it the second most common cause of death [7]. A deeper understanding of the complex processes of tumorigenesis, invasion, metastasis, and drug resistance can improve the utilization of existing treatments and form the basis for the development of novel therapies.

2 THE TUMOR MICROENVIRONMENT

"Cancers are not just masses of malignant cells but complex "rogue" organs."
F.R. Balkwill, M. Capasso & T. Hagemann [8]

With the increasing understanding of tumor biology, cancer is now considered an "ecological disease" [9] characterized by complex and dynamic interactions between malignant cells, supporting immune and stromal cells, and non-cellular factors (Figure 1) [8, 10]. This intricate tumor microenvironment (TME) is not static but evolves to adapt to the needs of the growing tumor, enable invasion into adjoining tissues, and metastatic spread to distant organs.

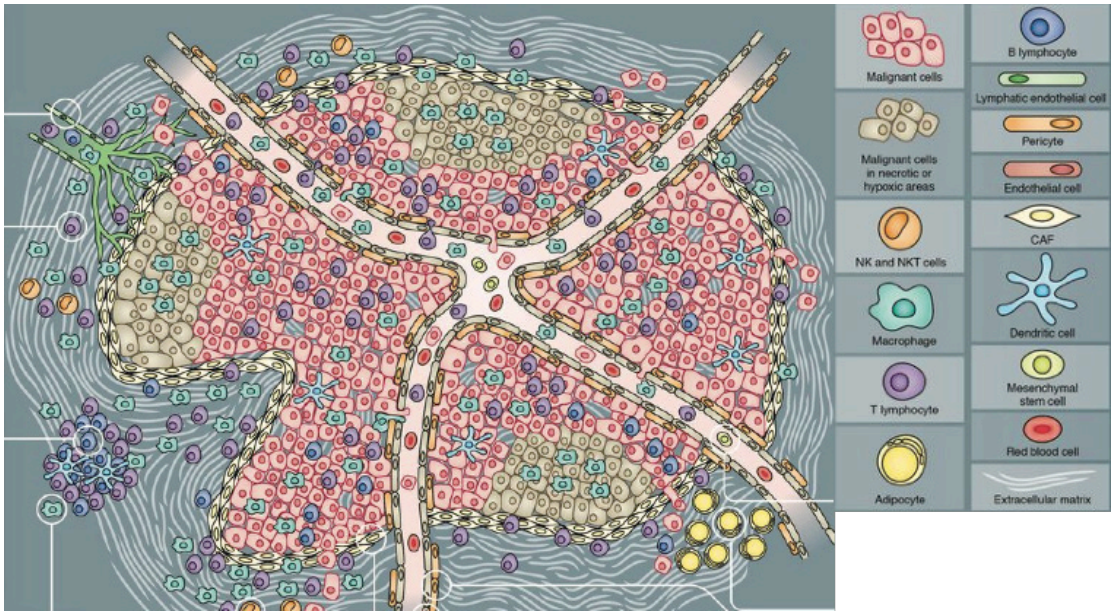

Figure 1: The tumor microenvironment.
The complex interactions of tumor, immune, and stromal cells resemble to some extent the organized structures within tissues and organs. Reproduced/adapted from Journal of Cell Science [8] with permission from The Company of Biologists Ltd.

Solid tumors display commonalities with healthy tissues as they are comprised of the parenchyma, consisting of neoplastic cells, and the stroma that contains

specialized connective tissue cells, blood and lymphatic vessels, immune cells, and the extracellular matrix (ECM) [11].

The cell types described in the following chapters are important contributors to the TME and of prognostic value in different cancer types but do not encompass the entirety of the TME.

2.1 THE TUMOR IMMUNE ENVIRONMENT

The term “tumor immune environment” indicates the complexity of immune cell infiltration in cancer [12]. The composition of the immune infiltrate can vary greatly among tumors and undergo dynamic changes during tumorigenesis. Furthermore, the immunological composition can be an important prognostic factor and affect the response to cancer treatment [13-15]. The increasing knowledge in the field of tumor immunology has led to the classification of “tumor immune environment subclasses” or “immune subtypes” that can inform predictions on disease outcome and response to therapy [12, 16].

Table 1 provides an overview of immune cells that can be present in the TME and have potent tumor supporting and tumor suppressing abilities.

Table 1: Overview of immune cells of the TME. Abbreviations are explained in the list of abbreviations on pages VI-VIII.

Cell type	Signature cytokines	Function	Reviewed in
CD8+ T cells			
Cytotoxic T cells Memory T cells	IFN-γ, TNF-α	• Selectively target tumor cells, induce cell death through perforin and granzyme release and FasL and TRAIL signaling • Functional T cell memory mediates a fast response to a reoccurring antigen • Associated with favorable prognosis in different cancers • CD8+ cells are often dysfunctional in response to suppressive signals in the TME	[17, 18]
CD4+ Helper cells			
Th1	IFN-γ, IL-2, TNF-β	• Promote inflammation • Recruit cytotoxic T cells, NK cells, and macrophages • Regulate the activity of cytotoxic T cells • Mainly associated with favorable prognosis in different cancers • Their contribution to chronic inflammation can also have pro-tumor effects	[19]
Th2	IL-4, IL-5, IL-13	• Regulate activity of different immune cells through cytokine release • Immunosuppressive and immunostimulating effects depending on cytokine secretion pattern • Pro- or anti-tumorigenic effects dependent on cancer type • Th2 cytokines can contribute to immune evasion and escape	[19]
Th9	IL-9	• Anti-tumorigenic functions in some cancers • Promote the recruitment of DCs and cytotoxic T cell function • IL-9 and Th9 also linked to pro-tumorigenic functions particularly in hematological malignancies	[19]
Th17	IL-17, IL-21, IL-22	• Mainly pro-inflammatory and pro-angiogenic • Pro- or anti-tumorigenic effects dependent on cancer type	[19, 20]
Th22	IL-22	• Th22 infiltration linked to poor prognosis in some cancers • Pro-tumorigenic functions mainly linked to increased levels of IL-22 that can promote proliferation, invasion, and angiogenesis • Anti-tumorigenic effects have also been observed	[21]

Tfh	IL-21, IFN-γ, IL-4, IL-9	• Provide help for B cells, different subclasses have been identified • Infiltration of Tfh cells correlates with patient survival in different solid tumors • Positive effects have been attributed to their ability to organize tertiary lymphoid structures and decrease immune suppression although the detailed mechanisms are so far little understood	[20, 22]
Tregs	IL-10, TGF-β, IL-35	• Mainly anti-inflammatory and immunosuppressive • Can effectively impair T cell effector functions • Can contribute to impairment of immunosurveillance • Mainly associated with unfavorable prognosis in different cancers	[23]
γδ T cell	IL-17, IFN-γ, TGF-β, IL-10	• Potent anti-tumor activity (MHC-independent tumor cell killing, phagocytosis) • Positive prognostic marker in different cancers • Pro-tumorigenic functions that have been linked to IL-17 secretion and recruitment of immunosuppressive cells	[24, 25]
Macrophages	IL-1, IL-6, IL-12, IL-23, IL-10, TGF-β	• Versatile cells with potent pro-tumorigenic and anti-tumorigenic abilities • Anti-tumorigenic: antigen presentation and activation of effector immune cells • Pro-tumorigenic: promote tumor cell proliferation and survival, angiogenesis, metastasis, and immunosuppression	[26, 27]
MDSCs	TGF-β, IL-10	• Heterogeneous population of myeloid cells found in peripheral blood and the TME • Potent immunosuppressive cells • Can impair anti-tumor immune responses and immunotherapy	[28, 29]
NK cells	IFN-γ, TNF-α	• Potent anti-tumor abilities (tumor cell killing, release of inflammatory mediators) • Important contributor to immunosurveillance • NK cell presence and activity is a positive prognostic factor in different cancers • Their function is often impaired in cancer	[30, 31]
NKT cells		• Recognize lipids and glycolipids • Various subsets have been identified	[32]
NKT1	IFN-γ	• Contribute to immunosurveillance • Activate DCs, cytotoxic T cells, NK cells but also support Tregs • Can mediate tumor cell lysis	
NKT2	IL-13	• Immunosuppressive • Promotion MDSCs	

DCs	Stimulation and subset dependent	• Important antigen presenting cells • Various subsets • Function often impaired in the TME	[33]
Neutrophils	Subset and context dependent	• Pro- and anti-tumorigenic functions that greatly depend on mediators/signals in the TME • Neutrophil infiltration is mainly a negative prognostic marker but a correlation with good prognosis has also been observed in some cancers • Different subsets may have different functions	[34]
B cells	Subset and context dependent	• Potent anti-tumor functions (production of antibodies, antigen presentation, tumor cell killing) • Also pro-tumor functions (suppression of T cell differentiation and function) • Different subpopulations have been identified with potentially distinct behavior (e.g. Bregs)	[35]
Innate lymphoid cells		• Functions dependent on cytokine environment	[36]
ILC1	IFN-γ	• Anti-tumorigenic functions observed in presence of IL-15 • Pro-tumorigenic functions observed in presence of TGF-β	
ILC2	IL-4, IL-13	• Considered mainly immunosuppressive and pro-tumorigenic but anti-tumorigenic functions have also been described	
ILC3	IL-17, IL-22	• Heterogenic population with pro-tumorigenic (Treg and MDSC recruitment, pro-metastatic) and anti-tumorigenic (NK cell recruitment) functions	
Mast cells	Context dependent	• Heterogeneous and plastic cell population with differences in morphology, surface receptors, and production of specific mediators • tumor promoting, tumor suppressing or inert bystander dependent on tumor type and context • Pro-tumorigenic: promote angiogenesis (VEGFs), ECM remodeling (MMPs), EMT and stem cell features (IL-8), immunosuppression (TGF-β, IL-13, adenosine) • Anti-tumorigenic: cytotoxicity/ growth inhibition (reactive oxygen species, IL-9), DC maturation (histamine)	[37]

2.1.1 T lymphocytes

Different T lymphocyte populations can be present in the tumor bed, the invasive margins, in draining lymph nodes, and lymphoid organs [8]. Both tumor-supportive and tumor-suppressive abilities have been described for different T cell populations that are often highly context-dependent [19]. Furthermore, the assessment of tumor-infiltrating T cell subsets, called the "immunoscore", is a potent prognostic tool in colorectal tumors and other cancers [38-40].

Cytotoxic T cells (CTL)

Cytotoxic ($CD8^+$) effector T cells can induce granzyme-, perforin-, FasL (Fas ligand)-, and TRAIL (TNF-related apoptosis-inducing ligand) -mediated apoptosis in target cells and their presence has been correlated to a good prognosis in various cancers, such as melanoma, colorectal, and breast cancer [13, 18, 41]. However, different mechanisms in the TME can limit/prevent the infiltration of cytotoxic T cells and/or impair their function [17, 42, 43]. Among these mechanisms, the up-regulation of immune checkpoint receptors, such as programmed cell death-1 (PD-1) and cytotoxic T-lymphocyte-associated antigen 4 (CTLA-4), on $CD8^+$ T cells and their ligands PD-L1, PD-L2 and cluster of differentiation 80 (CD80), CD86 on other immune cells, tumor, and stromal cells has been studied intensely in cancer [44]. In health, immune checkpoints are important regulators of immune responses supporting the maintenance of self-tolerance and the prevention of autoimmunity [45]. Among other markers, such as LAG-3 (Lymphocyte-activation gene 3) and TIM-3 (T-cell immunoglobulin and mucin-domain containing-3), PD-1 expression is one of the characteristics of "exhausted", dysfunctional T cells, a condition observed during infections and in cancers [43, 46]. These findings have led to the development of checkpoint inhibitors, antibodies targeting checkpoint receptors or their ligands [44, 47]. Anti-CTLA-4 and anti-PD-1/PD-L1 checkpoint inhibitors have been evaluated in a broad variety of solid tumors as well as hematological malignancies and displayed remarkable therapeutic benefits for some portion of patients with advanced cancers, such as metastatic melanoma, non-small cell lung cancer, and Merkel cell carcinoma [48, 49]. As of September 2018, 2250 clinical trials evaluate the efficacy of PD-1/PD-L1 checkpoint inhibitors in combination with other therapies or as monotherapies in different cancers [50]. Of note, the expression of checkpoint receptors is not limited to cytotoxic T cells.

PD-1 is expressed on different subsets of activated T cells, myeloid cells, and B cells [48]. CTLA-4 expression is restricted to T cells but differs among subsets, as $CD4^+$ T cells show a higher expression than $CD8^+$ T cells [51].

Helper T cells

The world of $CD4^+$ helper T cells (Th cells) is highly complex. So far, seven subsets of Th cells have been identified: Th1, Th2, Th17, Th9, Th22, Tfh, and Treg [20]. Each T helper subset differentiates in response to specific cytokines and transcription factors, produces a characteristic cytokine signature and displays distinct functions [20]. However, specific helper cell subsets can react to environmental changes by acquiring characteristics of a different subset. This plasticity contributes to a fine-tuned balance between the different subsets that regulates their functions in health and disease [20].

Th1 cells differentiate in response to interleukin 12 (IL-12) and target $CD8^+$ cytotoxic T cells, natural killer (NK) cells, and macrophages through the pro-inflammatory cytokines interferon gamma (IFN-γ) and IL-2 [13, 52]. In contrast, Th2 cells differentiate in response to IL-4 and target B cells, eosinophils, basophils, and mast cells through the anti-inflammatory cytokines IL-4, IL-5, and IL-13 [13, 52]. Both, Th1 and Th2 cells have shown prognostic value in different cancers. While Th1 cells generally display anti-tumorigenic functions and correlate with good prognosis, Th2 cells can support tumorigenesis and have mainly been associated with poor prognosis [13, 19].

IL-6, IL-21, and transforming growth factor beta (TGF-β) promote the differentiation of pro-inflammatory Th17 cells that secrete IL-17A, IL-17F, IL-21, and IL-22 and recruit neutrophils and macrophages [53]. Additionally, the presence of IL-23 can maintain differentiated Th17 cells long-term [54]. Th17 cells play a dichotomous role in cancer as they can both promote and suppress tumorigenesis [20]. Furthermore, Th17 cells display great plasticity and in response to changes in their environment they can acquire Th1 properties and gain the ability to secrete IFN-γ while no longer secreting IL-17 [55, 56]. This capability may be one of the reasons for the dichotomy of Th17 cells in cancer.

Regulatory T cells (Tregs) are important for the maintenance of tissue homeostasis. Tregs differentiate in the presence of TGF-β and IL-2 and they suppress lymphocyte effector functions through, among others, TGF-β, IL-10, prostaglandin E2 (PGE_2), idoleamine 2,3-dioxygenase (IDO) and adenosine secretion, sequestration of IL-2, and engagement of

immune checkpoint receptors, such as CLTA-4 and PD-1 [23, 57]. The role of Tregs in the TME is diverse and their presence has been associated to both good and poor prognosis in different cancers [13, 23]. This may be attributed to Treg plasticity as they can display Th17 characteristics when exposed to IL-6 with or without additional IL-23 and IL-1β presence [58].

Furthermore, the presence of cytotoxic CD4+ cells (CD4 CTL) with the ability to kill target cells MHC class II-dependent by secreting perforin and granzyme has also been described in cancers, for example melanoma [59].

γδ T cells

γδ T cells are a potent T cell subset with pleiotropic functions. They can recognize cell surface molecules, such as phosphoantigens, whose expression varies between stressed cells, including malignant cells, and healthy tissue without co-stimulation and MHC-restriction [60]. Tumor cell death can be induced by perforin and granzyme release but also via FasL and TRAIL [24]. There are at least three different human γδ T cell subtypes that differ in their γ- and δ-chain composition, tissue localization and the type of antigens they recognize [60]. The presence of γδ T cells has been observed in different cancer types and their role in tumorigenesis is likely context-dependent [24, 61]. Although γδ T cells have been identified as a good prognostic factor in different cancer types [62] and anti-cancer functions have been observed *in vitro* and *in vivo* [63, 64], pro-tumorigenic functions have also been described [65-67]. Their dichotomous role in cancer may be attributed to the plasticity of γδ T cells. Human γδ T cells are functionally immature and differentiate into IFN-γ-secreting type 1 effector cells with cytotoxic activity in the presence of IL-2 or IL-15 [68]. However, under highly inflammatory conditions γδ T cells can produce IL-17 and display a Th17-like profile [69, 70]. Furthermore, Treg-like profiles, characterized by the production of IL-10 and TGF-β, have also been observed in γδ T cells [71, 72].

2.1.2 Tumor-associated macrophages (TAMs)

TAMs are abundant in different cancer types and function as important regulators of tumorigenesis as they can promote angiogenesis, invasion, and metastasis [26, 73, 74]. In response to environmental factors, macrophages can display different phenotypes along a phenotypic continuum with M1 and M2 being the extremes [27]. M1 or “classically activated”

macrophages secrete pro-inflammatory cytokines, such as IL-6, IL-12, IL-23, and tumor necrosis factor alpha (TNF-α), and have antigen-presenting, phagocytic, and cytotoxic functions [75]. They are activated by IFN-γ, lipopolysaccharide (LPS) or toll-like receptor (TLR) ligands and promote a Th1 type immune response [76]. In contrast, IL-4 and IL-13 activate M2 or "alternatively activated" macrophages, which secrete the anti-inflammatory cytokines IL-10 and TGF-β, vascular endothelial growth factor (VEGF), and matrix metalloproteinases (MMPs), and support a Th2 type immune response [75, 76]. Although the phenotype of TAMs is typically closer to the M2 end of the functional spectrum, TAMs that do not resembles alternatively activated macrophages have also been described [77, 78]. Furthermore, macrophages display great diversity and plasticity, and phenotypic changes of TAMs during tumorigenesis have been observed suggesting that the plasticity of TAMs may be utilized to re-educate TAMs as a therapeutic approach [79, 80].

2.1.3 Myeloid-derived suppressor cells (MDSCs)

MDSCs are immature and immunosuppressive cells that develop in the bone marrow from myeloid progenitor cells and are actively recruited to the tumor and metastatic sites by a variety of chemokines and other factors [28]. Their ability to promote tumor cell survival, angiogenesis, invasion, metastasis, and immune evasion is well established and MDSCs are frequently observed in different cancers [28, 81, 82]. Two large subgroups of MDSCs have been described: granulocytic or polymorphonuclear MDSCs (phenotypically similar to neutrophils), in most cancers the majority of MDSCs, and monocytic MDSCs (phenotypically similar to monocytes) [29]. MDSCs can disrupt immunosurveillance by inducing Tregs [83] and inhibiting dendritic cell (DC)-mediated antigen presentation, NK cell cytotoxicity, M1 polarization, and T cell recruitment, activation, and function through production of reactive oxygen and nitrogen species, IDO, Arginase, IL-10 and TGF-β [10, 84]. Furthermore, hypoxia up-regulates PD-L1 expression on MDSCs [85]. MDSCs are a mixed population of various myeloid cells that display different levels of plasticity and can differentiate into multiple cell types, for example macrophages [82, 86]. Therefore, the re-education of MDSCs is an attractive therapeutic approach [87].

2.1.4 Natural killer (NK) cells

NK cells can recognize stressed, infected, foreign, and also tumor cells, through a variety of receptors in absence of antigen presentation, non-MHC restricted, and mediate cell killing via granzyme B, perforin, FasL, and TRAIL [31]. Furthermore, NK cells can regulate immune responses through secretion of cytokines (e.g. IFN-γ, TNF-α, IL-10 and granulocyte-macrophage colony-stimulating factor (GM-CSF)) and chemokines (e.g. macrophage inflammatory protein-1a (MIP-1α=CCL3), C-X-C motif chemokine 8 (CXCL8=IL-8) and chemokine (C-C) motif ligand 2 (CCL2=MCP-1)) [31]. NK cells are not a homogenous group as distinct NK cell subsets have been described, which differ in localization and function [88]. This is also the case in cancer, as functionally different NK cell phenotypes have been described in different malignancies [30]. Potent anti-tumor and anti-metastatic functions have been demonstrated for NK cells and intratumoral NK cell presence has been associated with good prognosis in various cancers [89-91]. However, tumor, stromal and immune cells can release factors, such as TGF-β, PGE_2, IL-4, and IDO, that impair NK cell infiltration, activation and function, resulting in NK cell anergy [92]. Consequently, restoration of NK cell function by adoptive NK cell therapy or reprogramming of the immunosuppressive TME to harness their full anti-tumor potential are attractive therapeutic approaches that are evaluated in different cancer types [91].

2.1.5 Dendritic cells (DCs)

Dendritic cells are professional antigen presenting cells with important functions in immunosurveillance [33]. They capture antigens from the microenvironment and present them to cells of the adaptive immune system. In addition, they provide important costimulatory signals [93]. Different subsets of DCs have been described that differ in their localization and specific function [33]. DC function is often impaired in the TME as different tumor-derived factors can inhibit their maturation (IL-6, IL-10, VEGF and colony stimulating factor 1 (CSF-1)), activation (PGE_2, IL-10, VEGF), and function (hypoxia, low pH, and high levels of adenosine and lactate) [33, 94]. Additionally, expression of inhibitory molecules, such as PD-L1, TIM-3, and LAG-3, can contribute to the dysfunction of DCs in tumors [95]. PD-1 and PD-L1 blockade has been demonstrated to restore DC function [96].

2.1.6 Tumor-associated neutrophils (TANs)

Different subsets of neutrophils, the most abundant leukocytes in human circulation, have been described in cancer [97]. Neutrophils are multifunctional cells with remarkable plasticity that can both support and suppress tumor growth [34]. They can contribute to an inflammatory TME and immune suppression, support extracellular matrix (ECM) remodeling, and promote angiogenesis and metastasis through, among others, the release of reactive oxygen and nitrogen species, MMPs, arginase-1, cytokines and growth factors, such as TGF-β and VEGF-A, and the expression of PD-L1 [34, 98-100]. Moreover, reactive oxygen species can promote point mutations and genome instability, a hallmark of cancer [101]. In contrast, neutrophils can also effectively kill tumor cells (phagocytosis, degranulation, and release of cytotoxic proteins), promote anti-tumor responses through recruitment and activation of T cells, and inhibit metastasis [102-104].

2.1.7 B lymphocytes

B lymphocytes, important mediators of humoral immune responses, can be present in the tumor margins but are more commonly found in tumor-adjacent tertiary lymphoid structures and draining lymph nodes [8, 12]. Both tumor-promoting and -suppressing capabilities have been attributed to B cells in different cancers [35]. In particular, different subsets of regulatory B cells (Bregs) display tumor promoting functions as they can disrupt cancer immune surveillance through secretion of immune suppressive cytokines, such as IL-10, and expression of the inhibitory molecules PD-L1, CD80 and CD86 [105].

2.2 NON-HEMATOPOIETIC CELLS IN THE TME

In addition to various immune cells, the TME is comprised of blood vessels, lymphatic vessels, and specialized connective tissue cells, such as fibroblasts and mesenchymal stem cells [8]. Furthermore, adipocytes, and other cell types can be present in the microenvironment of specific tumors [42]. Their role in tumorigenesis will be briefly described in the subsequent paragraphs.

2.2.1 Vascular endothelial cells and pericytes

Angiogenesis and neovascularization are important steps in tumorigenesis as a sufficient supply with oxygen and nutrients is needed to enable a tumor to grow beyond a certain size [106]. In response to pro-angiogenic growth factors, such as VEGFs (particularly VEGF-A), platelet-derived growth factors (PDGFs), fibroblast growth factors (FGFs), and angiopoietin 2, vascular endothelial cells form new blood vessels with structural support from pericytes [107, 108]. This tumor vasculature is exceptionally chaotic, leaky, and characterized by an uneven blood flow resulting in varying oxygenation and nutrient supply and potentially impairments of drug distribution and immune cell extravasation [107]. The majority of cells present in the TME have the ability to influence angiogenesis through pro- or antiangiogenic factors. For example, TANs, MDSCs and cancer-associated fibroblasts (CAFs; see 2.2.3) can produce a variety of proangiogenic factors that promote proliferation and migration of endothelial cells and ECM remodeling [108]. However, various cell types, such as B cells, T cells, and macrophages, can display pro- as well as antiangiogenic functions depending on their subtype and microenvironmental factors [108]. In return, vascular endothelial cells are also known to affect cells in the TME. They can express immune checkpoint ligands, such as PD-L1 and PD-L2, as well as TRAIL and FasL, ligands that induce T cell apoptosis [42]. Consequently, angiogenesis, and by extent vascular endothelial cell proliferation, is a promising therapeutic target and multiple drugs have been evaluated in clinical trials with varying results [109]. Of note, there is increasing evidence that not all tumors dependent on angiogenesis and it furthermore has been demonstrated that some tumors can co-opt existing blood vessels [110, 111]. This underlines the complexity of the TME and has to be taken into consideration when targeting angiogenesis.

2.2.2 Lymphatic endothelial cells

Lymphangiogenesis, the formation of new lymphatic vessels by lymphatic endothelial cells, is promoted by VEGF-C and VEGF-D and contributes to the dissemination of tumor cells, a prerequisite for metastasis [112]. Furthermore, lymphatic endothelial cells display immunomodulatory functions, such as tumor antigen cross-presentation, that can promote apoptosis of antigen-specific cytotoxic T cells and thereby supports tolerance [42]. Additionally, the heightened interstitial flow, resulting from an increase in lymphatic vessels,

can cause changes in the tumor stroma, such as a stiffening of the ECM, that can contribute to immune suppression [113].

2.2.3 Cancer-associated fibroblasts (CAFs)

Cancer-associated fibroblasts are myofibroblasts (activated fibroblasts) and a dominant cell type in the microenvironment of many tumors [8]. CAFs are a heterogeneous population of multifunctional cells that can in principle support all stages of cancer development and progression by promoting malignant cell growth, invasion, metastasis, angiogenesis, drug resistance, inflammation, and immune suppression [114]. In contrast to quiescent fibroblasts in healthy tissue, CAFs resemble activated wound healing-associated fibroblasts but display even more pronounced proliferative, secretory, and migratory abilities [114]. While normal fibroblasts can suppress the growth of cancer cells, CAFs have been coerced by the tumor and can display potent tumor promoting functions [115]. CAFs can secrete a variety of factors with tumor-promoting (e.g. epidermal growth factor (EGF), insulin-like growth factor (IGF), hepatocyte growth factor (HGF) and IL-6), immune modulatory (e.g. TGF-β, IL-4, IL-6, PGE_2, CCL2, CXCL12 and GM-CSF), angiogenic (e.g. VEGFA, PDGFα, and TGF-β) and ECM remodeling functions (e.g. MMPs, TIMPs (tissue inhibitors of metalloproteinases), collagens and fibronectin) [116]. Due to their well-established tumor-promoting role, CAFs are considered attractive therapeutic targets and different drugs are under evaluation that target receptors present on or factors secreted by CAFs or aim to normalize or re-educate them to a quiescent or tumor-suppressive state [114]. However, CAFs are functionally heterogeneous and anti-cancer functions have also been observed [116].

2.2.4 Mesenchymal stem cells (MSCs)

Mesenchymal stem cells are multipotent stromal cells, recruited from the bone marrow that can differentiate into, among others, fibroblasts, adipocytes, osteoblasts and chondrocytes [117]. They are rare, migratory cells that support wound healing by regulating the immune response and tissue regeneration [118]. MSCs can be recruited to the TME where they have the potential to promote immune suppression comparable to a wound healing setting [42, 118]. Furthermore, MSCs can promote EMT and bone metastasis by secreting chemokines and attracting tumor cells to the bone marrow [117, 119].

2.3 EXTRACELLULAR MATRIX (ECM)

The ECM, a collection of extracellular molecules, is an important component of healthy organs, but also tumors, as it ensures tissue integrity by providing a structural scaffold for the cells [120]. In the TME, as in any other organ, the ECM undergoes constant remodeling. Proteases, such as MMPs and cathepsins, are secreted by tumor cells, CAFs, and TAMs and degrade ECM components as new components are produced by CAFs [8]. Furthermore, extracellular vesicles released by tumor cells and other cells in the TME have been demonstrated to support tumor growth, angiogenesis, metastasis, immunomodulation, and drug resistance [121, 122]. By no means a bystander in the TME, the ECM can suppress tumorigenesis in early stages but also support cancer progression [10]. The ECM can promote tumor cell proliferation, migration, and invasion, support angiogenesis and simultaneously suppress infiltration, activation, and function of immune cells and contribute to therapy resistance [123].

3 CANCER IMMUNOEDITING

"In the enormously complicated course of fetal and post-fetal development, aberrant cells become unusually common. Fortunately, in the majority of people, they remain completely latent thanks to the organism's positive mechanisms" Paul Ehrlich [124]

Several safety control systems can prevent tumor growth when cells are subjected to malignant transformations. Intrinsic control and repair mechanisms, involving tumor suppressor proteins, aim to restore normal cell behavior or induce apoptosis [4]. Furthermore, the immune system constantly recognizes and eliminates malignant cells. This hypothesis of "immunosurveillance" was developed by Macfarlane Burnet [125] and Lewis Thomas [126] and later extended to the concept of immunoediting [127].

Cancer immunoediting encompasses three phases: elimination, equilibrium, and escape (Figure 2) [127, 128]. During the elimination phase, the innate and adaptive arm of the immune system recognize tumor antigens and danger signals present on, or released by, malignant cells in response to oncogenic stress, leading to the eradication of the emerging tumor [128, 129]. In the equilibrium phase, the tumor is controlled by the immune system and kept functionally dormant [128, 129]. A reduction in tumor immunogenicity, for example through loss of tumor antigens and/or MHC class I expression and the development of an

immunosuppressive TME, can upset the equilibrium leading to immune escape and renewed tumor growth [128, 129]. Importantly, cancer-related inflammation can promote immune escape through various mechanisms [130].

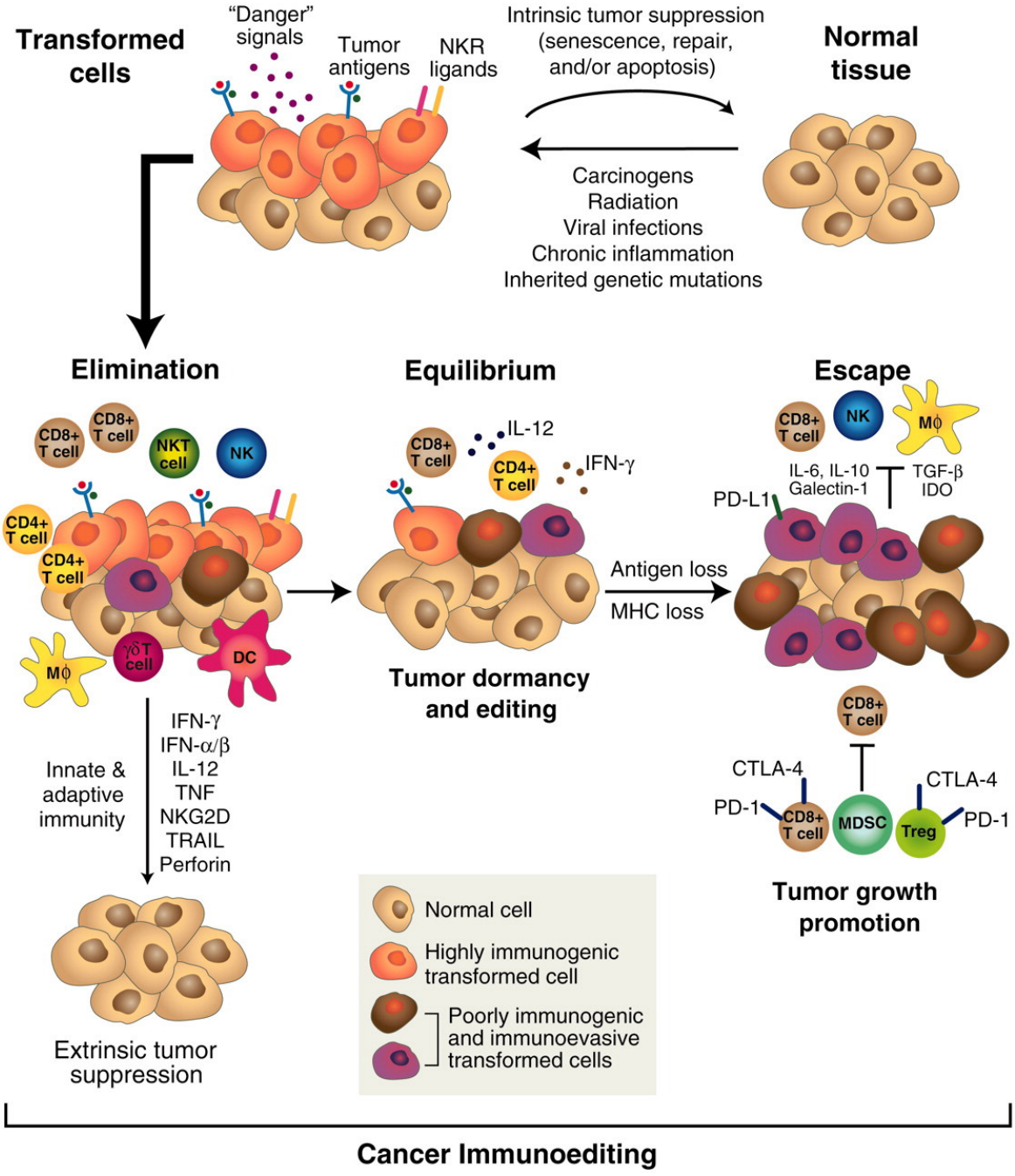

Figure 2: Cancer immunoediting.
Cancer immunoediting engages after the intrinsic cellular mechanisms that prevent malignant growth have failed. The immune system recognizes malignant cells and controls tumor growth (elimination phase) but might fail to eliminate all tumor cells leading to a phase of functional dormancy (equilibrium) in which the immune system prevents progression but cannot eliminate the tumor. In the escape phase, tumor cell populations emerge that evade immune destruction resulting in tumor progression. From [128] reprinted with permission from AAAS, an adapted version from [131] with permission from Annual Reviews, Inc.

4 INFLAMMATION AND CANCER

"Tumors appear to the host in the guise of wounds or, more correctly, of an unending series of wounds that continually initiate healing but never heal completely" Harold F. Dvorak [132]

Inflammation is an essential defense mechanism of the body against harmful stimuli, such as injury, pathogens and other biological or chemical irritants. An acute inflammatory response is characterized by a rapid infiltration of innate immune cells into the damaged tissue and their activation [133]. Depending on type and severity of the damage, adaptive immune cells may also be recruited. Subsequently, coordinated innate and adaptive immune responses lead to the elimination of the harmful stimulus, followed by resolution of inflammation and re-establishment of tissue homeostasis [133]. In contrast, chronic inflammation is the response to a persistent harmful stimulus with continuous recruitment of immune and stromal cells, resulting in lasting immune responses and tissue remodeling [134].

The first observations linking inflammation to tumor growth were made by Rudolf Virchow in 1858 when he observed "lymphoreticular infiltrates" within tumors [135]. Over a century later, in 1986, Harold F. Dvorak compared tumorigenesis to wound healing in his seminal work "Tumors: wounds that do not heal" [132]. Today, the link between inflammation and cancer is firmly established. Approximately 16% of all cancers can be attributed to infections [136] and cancers arise at a higher rate in chronically inflamed tissues [137, 138]. Persistent inflammation can affect every step of tumorigenesis and is recognized as an enabling characteristic for multiple cancer hallmarks [4, 139]. Cytokines and other inflammatory mediators can induce epigenetic changes and genome instability, support cell survival, and proliferation, promote angiogenesis, and contribute to immunosuppression [137, 139, 140]. Inflammatory mediators can contribute to the development of "pre-metastatic niches" in distant organs thereby providing a receptive microenvironment "soil" for the malignant cells "seed" in accordance with Stephen Paget's hypothesis from 1889 [141, 142].

However, inflammation is also an important factor of antitumor immunity and it has been demonstrated that therapy-induced acute inflammation (by specific chemotherapeutic agents, radiation, and targeted therapies) can re-educate the TME and promote antitumor responses [140, 143, 144].

Two cross-talking pathways connect inflammation and cancer: the intrinsic and the extrinsic pathway (Figure 3) [145].

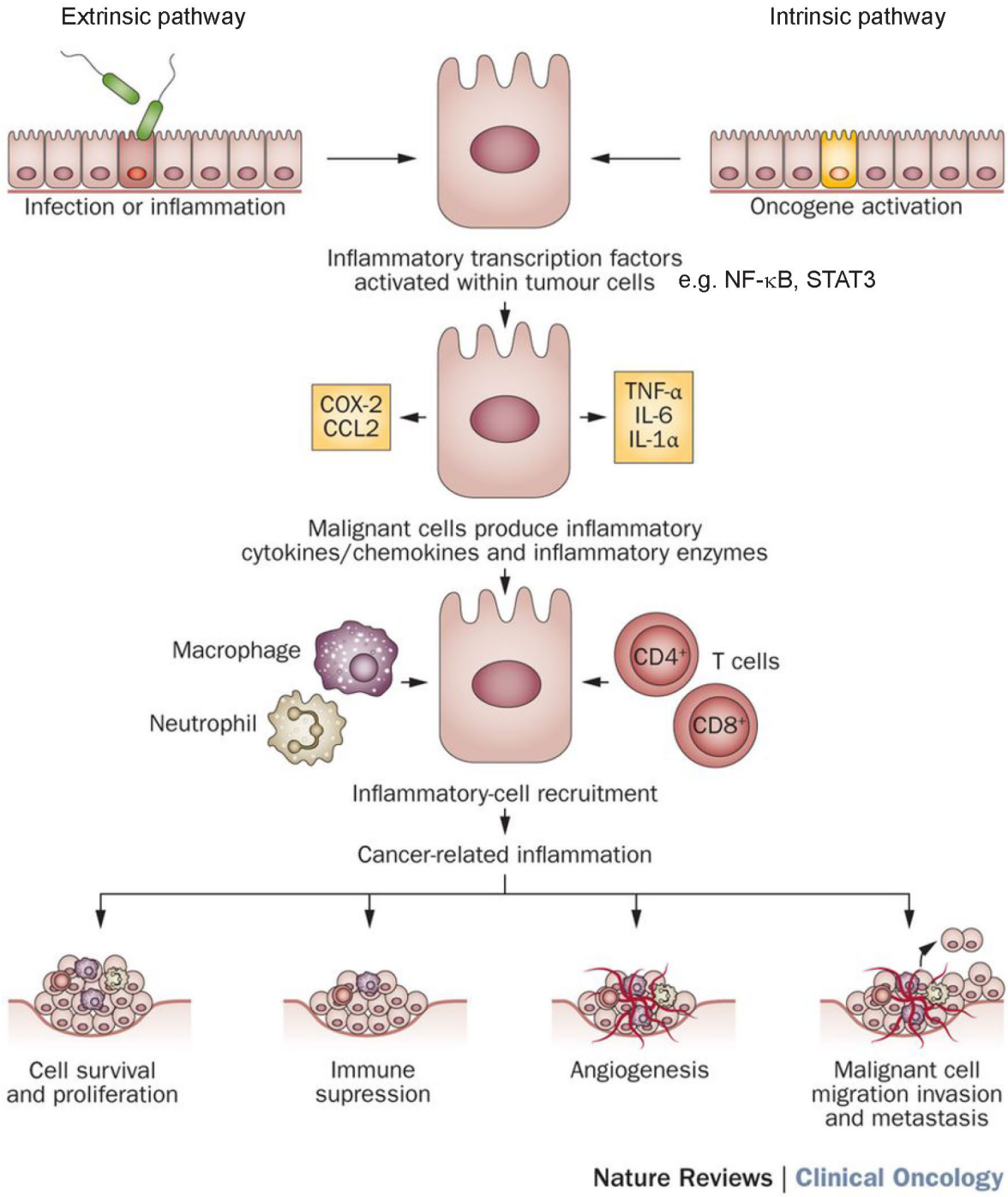

Figure 3: The molecular links between cancer and inflammation
Intrinsic (oncogene activation) or extrinsic (inflammation, infection) factors lead to activation of pro-inflammatory transcription factors, such as NF-κB and STAT3, regulating the expression pro-inflammatory mediators, among others, cytokines and chemokines, promoting the recruitment of inflammatory cells. The resulting inflammatory TME supports various cancer hallmarks, such as angiogenesis and metastasis. Reprinted and adapted by permission from Springer Nature Customer Service Centre GmbH: Springer Nature, Nature Reviews Clinical Oncology [146].

The intrinsic pathway is oncogene-driven and imparts tumor cells with pro-inflammatory characteristics, such as recruitment of inflammatory cells and promotion of angiogenesis [130]. For example, oncogenic Ras induces IL-6, IL-1β, and IL-8 expression in ovarian epithelial cells [147] as well as the expression of GM-CSF in pancreatic epithelial cells [148] and promotes COX-2 expression [149]. In contrast, the extrinsic pathway is driven by inflammatory conditions (e.g. infection or chronic inflammation) and the resulting inflammatory and environmental factors [130]. For example, danger signals (damage-associated molecular patterns or DAMPs) are released in injured/stressed tissues and recognized by the innate immune system initiating the release of pro-inflammatory mediators, such as TNF-α, IL-6, and IL-1 [150].

4.1 INFLAMMATORY MEDIATORS

In the inflammatory TME, chronically activated immune cells, stromal cells, and tumor cells secrete growth factors, cytokines, proteolytic enzymes, chemokines, and other chemoattractant factors, that can promote tumor and stromal cell proliferation and migration, ECM remodeling, metastasis, and immune suppression (Figure 3) [137, 145]. Various therapeutic approaches (examples of which are listed in Table 2) have been developed to either target tumor-supporting inflammatory mediators or promote anti-tumorigenic inflammation and immune responses, with the aim to re-educate the TME and promote anti-cancer functions [47, 130, 138, 146, 151, 152].

Table 2: Examples of therapeutic approaches to alleviate pro-tumorigenic inflammation while promoting anti-tumorigenic immune responses. Based on information from [47, 130, 138, 146, 151-154]

Target		Drugs (examples)
Diverse anti-inflammatory/ immunomodulatory functions		Steroids (Dexamethasone, Prednisolone), Statins, Chemotherapy, Radiotherapy
COX/PGE_2 axis	COX1/2	Aspirin, Ibuprofen
	COX2	Celecoxib
		Omega-3 fatty acids
Inflammatory cytokines and chemokines	TNF-α	Infliximab, Etanercept
	IL-6/IL-6R	Siltuximab, Tocilizumab
	IL-1R	Anakinra
	CXCR4/CXCL12	Plerixafor/ Olaptesed pegol
	CXCR1/CXCR2	Reparixin
	IL-8	HuMax-IL8
	CCL2	Carlumab
Immunosupressive cytokines	TGF-β	Galunisertib

Inflammatory signaling	JAK/ STAT3	Ruxolitinib, AZD9150, NCT02646748, Curcumin, Resveratrol
	NF-κB signaling	Bortezomib (proteasome inhibitor)
Myeloid cells	M-CSF/CSF-1R	BLZ 945, PLX7486, AMG820,
	Diverse functions	Tasquinimod
	Anti-CD47	Hu5F9-G4
	TLR agonists	Motolimod, CMP-001
	Arginase inhibitors	CB-1158
	IDO antagonists	Indoximod, Epacadostat
	PI3Kγ inhibitors	TG100-115
T cell function	Inhibitory target CTLA-4 antagonists PD-1/PD-L1 antagonists LAG-3 antagonists TIM-3 antagonists	 Ipilimumab Pembrolizumab, Avelumab Relatlimab MBG453
	Co-stimulatory target CD40 agonists OX40 agonists	 APX005M PF-04518600
	T cell activation, proliferation	IL-2, Pegilodecakin (Pegylated IL-10) IFN-α

The following inflammatory mediators are merely representatives of an extensive and complex network and will only be described briefly.

4.1.1 Tumor necrosis factor alpha (TNF-α)

TNF-α is a multifunctional inflammatory cytokine with both, pro- and anti-tumorigenic functions [155]. Secreted by tumor and/or stromal cells TNF-α is frequently detected in the tumor tissue and serum of patients with different cancer types and has been identified as a prognostic factor in, among others, breast cancer and prostate cancer [156]. TNF-α can promote tumor cell proliferation and survival, angiogenesis, metastasis, and the recruitment of inflammatory cells [155].

4.1.2 Interleukin 1 (IL-1α and IL-1β)

IL-1α and IL-1β, members of the IL-1 family, are master regulators of inflammation as they promote the expression of other inflammatory mediators (cytokines, chemokines, COX-2, MMPs, etc.) as well as their own expression thereby amplifying the inflammatory response [157, 158]. While the IL-1α precursor is constitutively present and active in cells

under homeostatic conditions, IL-1β expression is stimulated by inflammatory signals and activation of the IL-1β precursor is required for its functionality [158, 159].

IL-1β is an important cytokine in carcinogenesis as it can exert anti-tumorigenic effects but also potent pro-tumorigenic functions by promoting angiogenesis, the development of cancer stem cells, invasion, metastasis, and immune suppression [157, 160]. Furthermore, IL-1β promotes Th17 expansion and in concert with IL-23 the secretion of IL-17 in γδ T cells [161, 162].

4.1.3 Interleukin 6 (IL-6)

Tumor and/or stromal cells can produce IL-6 whose elevated levels are a prognostic marker in different cancers [163]. IL-6 function is often mediated by JAK (Janus kinase)/ STAT3 (signal transducer and activator of transcription 3) signaling supporting proliferation, survival, and invasiveness of malignant cells [164]. Furthermore, IL-6/JAK/STAT3 signaling can modulate immune cell function by exerting negative regulatory effects on, among others, NK cells and effector T cells and positive effects in Tregs and MDSCs [164]. In addition, IL-6 is an adipokine affecting various metabolic processes and has been demonstrated to contribute to cachexia in preclinical models [165].

4.1.4 Interleukin 23 (IL-23)

IL-23 is a pro-inflammatory cytokine consisting of the IL-23p19 and the IL-12p40 subunits that signals through the IL-23R/ IL-12Rβ1 complex activating JAK and STAT signaling pathways [166, 167]. IL-23, and the related cytokine, IL-12, share the p40 subunit and are both secreted in response to microbial pathogens by dendritic cells and macrophages [168]. However, there is a clear functional distinction. While IL-12 promotes Th1 differentiation, IL-23 stabilizes and maintains Th17 populations [54, 169, 170]. In addition to Th17 cells, IL-23 also regulates the function of other IL-17 producing cells, such as γδ T cells, ILCs, and NKT cells [171]. IL-23 has been implicated in different inflammatory diseases, such as psoriasis and Crohn's disease [172, 173]. Furthermore, the efficacy of IL-23-specific antibodies for the treatment of psoriasis has been demonstrated in multiple clinical trials [173].

IL-23 is frequently overexpressed in human cancers [174] and both pro-tumorigenic and anti-tumorigenic functions have been described [175]. IL-23 displays cancer-promoting effects in, among others, colorectal cancer [176-178] and prostate cancer [179]. In contrast,

cancer-suppressing effects of IL-23 have been observed in, for example glioma [180, 181] and melanoma [182]. Tumor- or immune cell- (e.g. MDSCs) derived IL-23 can directly drive tumorigenesis by promoting tumor cell proliferation and survival [179, 183, 184], maintain stemness [185], and promote EMT, migration, and metastasis [178, 186-188]. In addition, IL-23 can support the inflammatory microenvironment and impair immune surveillance (Figure 4) [189].

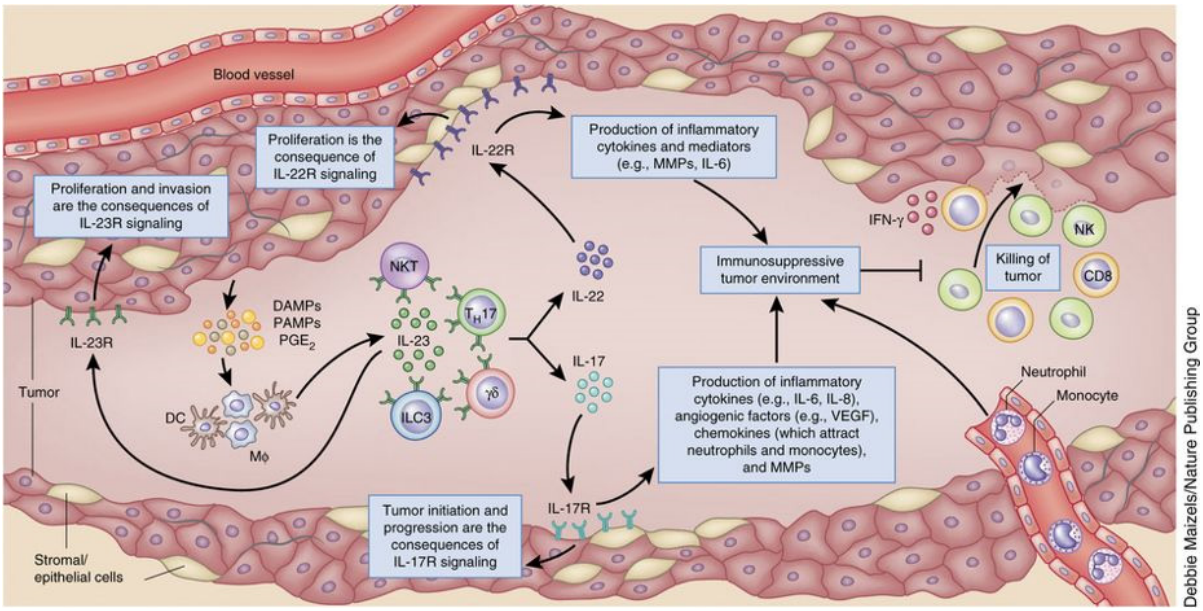

Figure 4: IL-23 functions in tumorigenesis.
Myeloid cells produce IL-23 in response to a variety of signals, such as DAMPs, PAMPs, and PGE_2. IL-23 signals through IL-23R present on a variety of innate and adaptive immune cells resulting in the secretion of IL-17 and IL-22. IL-17 and IL-22 can promote the proliferation of tumor as well as epithelial cells and induce the production of inflammatory mediators thereby contributing to an immunosuppressive TME. Furthermore, IL-23 can directly promote proliferation and invasion of tumor cells expressing IL-23R. Reprinted by permission from Springer Nature Customer Service Centre GmbH: Springer Nature, Nature Medicine [189].

IL-23 can suppress NK cell and $CD8^+$ cell function and contribute to the recruitment of macrophages, neutrophils, and Tregs, thereby affecting cytokine secretion [174, 190-192]. Furthermore, IL-23 produced by pulmonary squamous cancer cells can convert ILC1 to ILC3 cells promoting tumor cell proliferation in an IL-17-dependent manner [193].

Opposing effects have been described for IL-23 and IL-12 in carcinogenesis [194]. In a fibrosarcoma mouse model, for example, outgrowth of dormant tumors was reduced following IL-23p19 depletion, whereas inhibition of IL-12/23p40 promoted tumor growth [195]. This suggests a delicate balance between these two cytokines that might influence the immunoediting process. Furthermore, a complex interaction between cervical cancer cells and stromal cells has been described where cancer-instructed CAFs stimulate IL-23 expression

in DCs and thereby Th17 expansion. Concomitantly, a decreased expression of IL-12p35 in DCs was observed that was linked to tumor cell-derived IL-6 [196]. Based on these findings, therapeutic approaches targeting IL-23 (alone or in combination with other targeted therapies) to restore the IL-23/IL-12 balance have demonstrated great potential for promoting anti-tumor responses in murine models [197-199].

4.1.5 Interleukin 17 family

The IL-17 family consists of six cytokines (IL-17A-F) and five receptors (IL-17RA-IL-17RE) and plays an important role in host defense against pathogens, inflammation, and inflammatory diseases [200]. Functional cytokine/receptor combinations have been established for the majority of the IL-17 family members and the knowledge on their expression in different cell and tissues is constantly expanding (Figure 5).

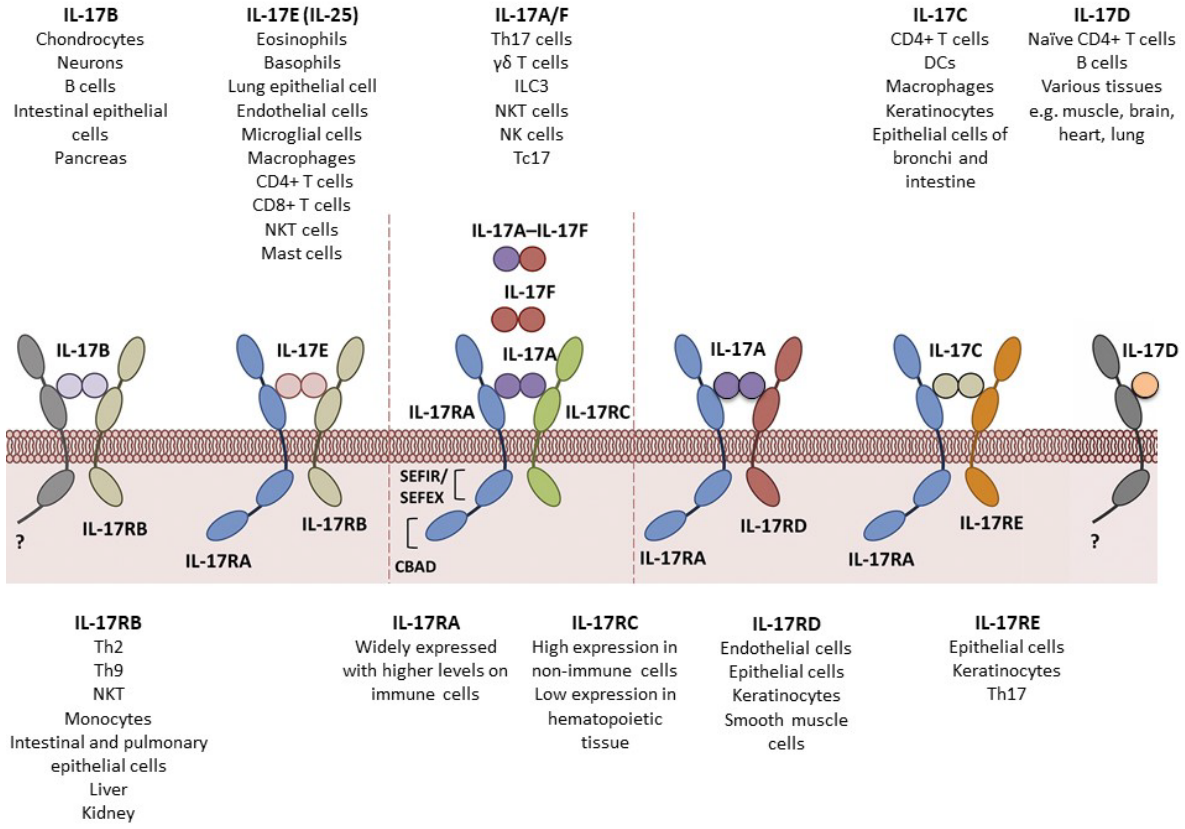

Figure 5: The IL-17 family.
The IL-17 family consists of six cytokines and five receptors. To date, the receptor for IL-17D remains unknown. While some family members are widely expressed in different cell types and tissues, the expression of others is more restricted. Reprinted from [201] with permission from Elsevier and adapted with additional information from [202-207].

IL-17A/F

The best-studied family members IL-17A (often called IL-17) and IL-17F are signature cytokines of the Th17 helper cell subset [208]. Homodimers of IL-17A and heterodimers of IL-17A and IL-17F signal through IL-17RA/RC [206, 209], and overlapping but also specific functions have been described for IL-17A and IL-17F in immune response and host defense [210]. More recently, an additional IL-17F/IL-17RC signaling axis has been established [211]. The major IL-17A/F producing cells (Th17 cells, γδ T cells, ILC3, and NKT cells) express IL-23R and respond to IL-23 stimulation (alone or in concert with other cytokines) with secretion of IL-17A and IL-22, thereby promoting local inflammation [162, 212]. However, IL-23-independent IL-17 expression has also been observed in γδ T cells and NKT cells [213-215].

IL-17A is a potent immune modulator as it can induce/enhance the secretion of pro-inflammatory cytokines (e.g. IL-1β, TNF-α, and IL-6), chemokines (e.g. CXCL9 CXCL10, and CCL2) and other factors, such as MMPs and PGE_2, that promote and facilitate the recruitment of immune cells [212]. IL-17A has been implicated in different autoimmune diseases including psoriasis, inflammatory bowel disease, and multiple sclerosis [200]. Several drugs targeting the IL-23/IL-17 axis have recently been approved for the treatment of psoriasis based on their superior performance in clinical trials [216].

Both tumor-promoting and tumor-suppressing functions have been described for IL-17A, IL-17F, and their producing cells, indicating versatile and context-dependent functions of IL-17A in the TME [20, 60, 217]. Tumor-suppressing functions of IL-17A are often associated with promotion of anti-tumor immune responses through increased recruitment and function of specific immune cells, such a $CD8^+$ T cells and NK cells [218-220]. However, IL-17A-mediated immune cell recruitment can also promote tumorigenesis as has been demonstrated for neutrophil recruitment in breast cancer [221, 222]. Additionally, IL-17A can, among others, inhibit $CD8^+$ T cell infiltration, increase MDSC presence [223], promote tumor cell proliferation [224-226], migration and invasion [227, 228] , angiogenesis [229-231], and metastasis [232, 233] (Figure 6).

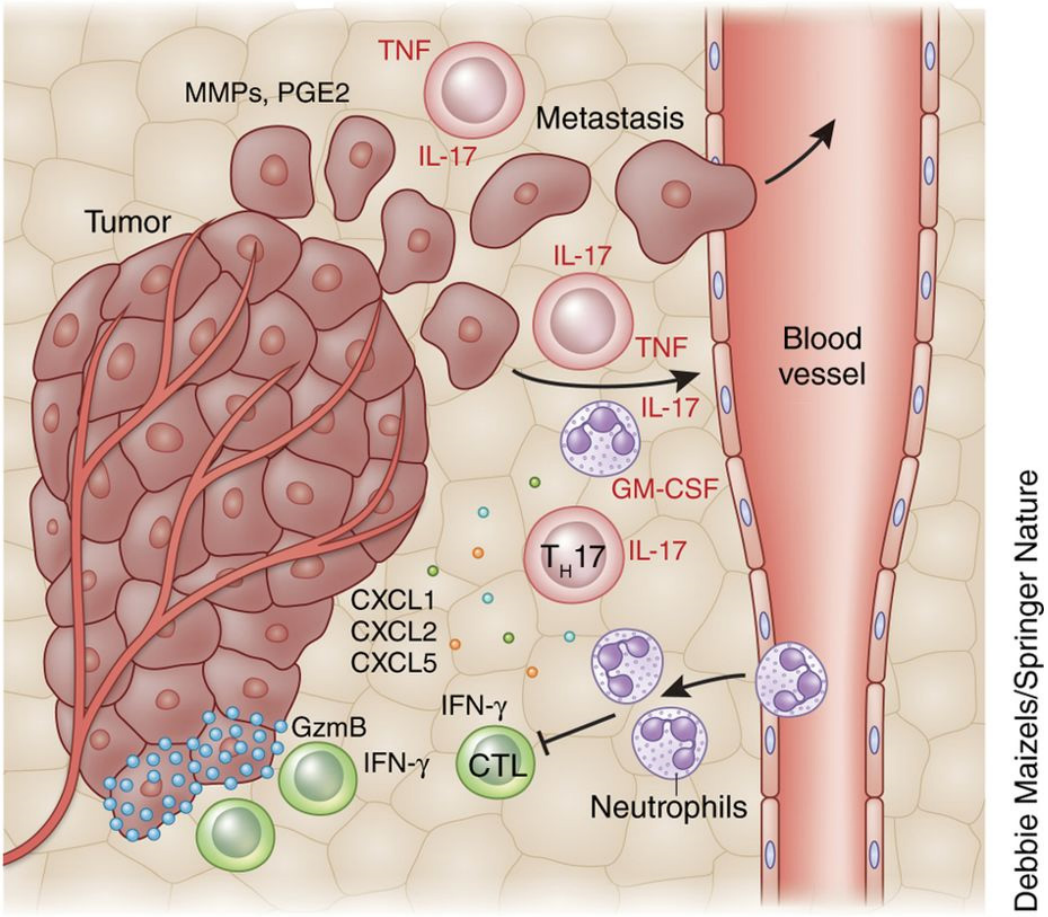

Figure 6: IL-17 functions in tumorigenesis.
IL-17 producing lymphocytes are recruited in response to chemoattractant factors released from the tumor. IL-17 can support anti-tumor immune responses through vasodilation effects and by enhancing immune cell recruitment. However, vasodilation may also support metastasis and IL-17-mediated recruitment of, among others, neutrophils that can support immune suppression. Reprinted by permission from Springer Nature Customer Service Centre GmbH: Springer Nature, Nature Immunology [212].

IL-17B

IL-17B is secreted as a non-disulfide-linked dimer and binds IL-17RB [234, 235]. The IL-17B/IL-17RB axis has been implicated in embryonic development, tissue regeneration, inflammation, inflammatory diseases, and cancer [236]. Furthermore, IL-17B was found to inhibit IL-25-mediated IL-6 production in colon epithelial cells indicating antagonistic functions of both cytokines [237]. IL-17B/RB has been implicated in gastric, pancreatic, breast, and lung cancer where it supports tumorigenesis by promoting tumor cell survival, chemokine expression, migration, and metastasis [238-243].

IL-17C

IL-17C signals through IL-17RA/IL-17RE heterodimers, stimulates epithelial immune responses and contributes to mucosal immunity and barrier maintenance but has also been implicated in various inflammatory diseases, such as psoriasis, rheumatoid arthritis, and inflammatory bowel disease [244-246]. Pro-tumorigenic effects of IL-17C have been observed in colorectal cancer where it promotes cell survival [247] and in lung cancer where it promotes the recruitment of TANs [248].

IL-17D

Although the receptor for IL-17D remains unidentified, several IL-17D functions have been previously been observed. IL-17D can promote the expression of pro-inflammatory cytokines (IL-6, IL-8 and GM-CSF) in endothelial cells [249]. Furthermore, the stress-sensing protein Nrf2 (nuclear factor erythroid 2-related factor 2) induces IL-17D in virus-infected cells and tumors where it contributes to the control of the viral infection or tumorigenesis as IL-17D deficient mice displayed a higher tumor incidence rate and exacerbated viral infections [250]. IL-17D expression is decreased in metastatic prostate cancer compared to primary prostate tumors and advanced grade glioma [251]. Furthermore, IL-17D-mediated NK cell recruitment promotes tumor rejection in preclinical cancer models [251].

IL-17E (IL-25)

IL-17E (also known as IL-25) function is mediated by a heterodimer of IL-17RA and IL-17RB [252, 253]. Important roles in barrier maintenance and the defense against parasites have been demonstrated for IL-25 [254]. It promotes Th2-type inflammations characterized by, among others, high levels of eosinophils and increased expression of IL-4, IL-5, and IL-13, and has been linked to chronic allergies, particularly asthma [255-258]. Furthermore, IL-25 can suppress Th17 responses by up-regulating PD-L1 expression in mesenchymal stromal cells and by inducing IL-13 secretion thereby inhibiting IL-23, IL-1β, and IL-6 expression in DCs, key regulators of Th17 cells [259, 260]. Anti-tumorigenic effects of IL-25 have been demonstrated in breast cancer [261, 262], gastric cancer [263], and colon cancer [264]. However, pro-tumorigenic and pro-metastatic functions of IL-25 have also been observed in breast cancer [265, 266] indicating diverse functions of IL-25 in carcinogenesis.

4.1.6 CXCL12/ CXCR4

Chemokines are chemotactic cytokines with versatile functions in the TME, where they not only regulate immune cell migration but can also affect tumor cell proliferation, angiogenesis, and metastasis [267]. For example, the chemokine CXCL12 and its receptor CXCR4 exert diverse pro-tumorigenic functions in various cancers [268]. In tumor cells, the CXCL12/CXCR4 axis promotes proliferation, stemness [269-272], and metastasis [273-275]. Its effect on endothelial cells drives angiogenesis in synergy with VEGF [276, 277]. Furthermore, the CXCL12/CXCR4 axis is involved in DC recruitment and Treg homing to the TME and bone marrow, respectively [278, 279].

4.1.7 Chemerin/ CMKLR1 axis

Chemerin is a multifunctional chemoattractant factor and adipokine [280, 281] implicated in, among others, obesity and metabolic disorders [282, 283], cardiovascular diseases [284], leukocyte trafficking [285], host defense [286], angiogenesis [287], and inflammation [288].

Furthermore, chemerin has been identified as a biomarker/ prognostic factor in gastric cancer [289], colorectal cancer [290], and non-small cell lung cancer [291]. Although chemerin serum levels are higher in patients with aggressive adrenocortical tumors compared to benign tumors, high chemerin levels correlate with improved overall survival [292].

Secreted as prochemerin with low activity, chemerin's function is regulated by its environment, as it can be further processed by extracellular proteases into different chemerin isoforms with varying activity (Figure 7) [280, 283, 293].

To date, three G protein-coupled receptors (GPCRs) have been identified that bind chemerin: CMKLR1 (Chemokine-like receptor 1), GPR1 (G protein-coupled receptor 1), and CCRL2 (C-C chemokine receptor-like 2) [294-296]. CMKLR1 is expressed by a variety of immune cells, such as macrophages, DCs, and NK cells as well as endothelial cells, adipocytes, and smooth muscle cells [297]. The chemerin/CMKLR1 axis can promote but also suppress inflammation, as functionally different chemerin isoforms may be present at different stages of inflammation and thereby, to some extent, control the severity of the immune response [288, 298]. Serine proteases secreted by, for example neutrophils, during early stages of inflammation generate active chemerin that contributes to recruiting different innate immune

cells, and promoting angiogenesis [288]. Proteases present at a later stage of inflammation, such as mast cell tryptase or cysteine proteases, produced by macrophages can generate chemerin variants with low or no activity promoting phagocytosis and regulating immune cell trafficking [288]. This diverse functionality may form the basis for the complex role of the chemerin/CMKLR1 axis in cancer, as both pro- and anti-tumorigenic effects have been described [299]. While pro-tumorigenic functions have been demonstrated in glioblastoma [300], squamous esophageal cancer [301, 302], gastric cancer [303], oral squamous cell carcinoma [304], and neuroblastoma [305] anti-tumorigenic functions have been observed in hepatocellular carcinoma [306-308], melanoma [309], and adrenocortical tumors [310].

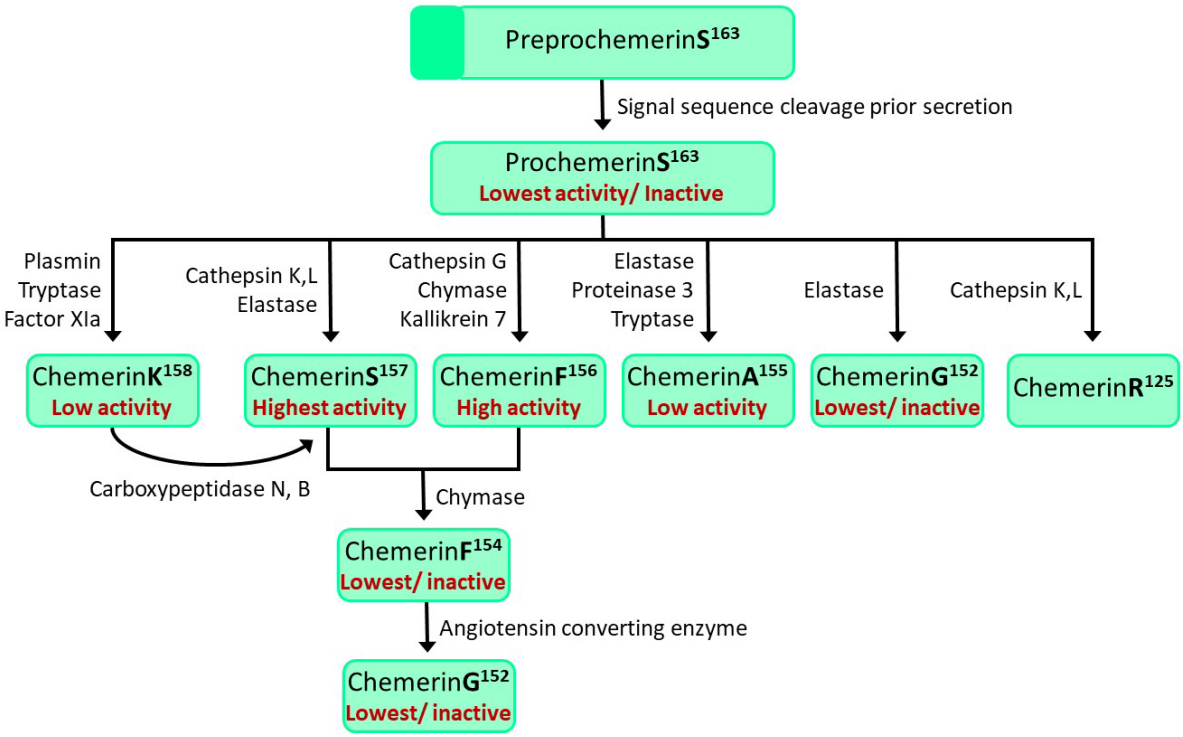

Figure 7: Chemerin processing.
Chemerin can undergo complex post-secretory processing by different proteases resulting in chemerin isoforms with varying activity determined predominantly by chemotaxis and intracellular calcium mobilization assays. While ChemerinR125 does not promote chemotaxis in CMKLR1-postive cells, antimicrobial activity has been demonstrated. Based on [280, 283, 293, 311].

Although most of the known chemerin functions are mediated by CMKLR1, roles for CCRL2 and GPR1 are emerging. In cutaneous squamous cell carcinoma, fibroblast-derived chemerin promotes migration of tumor cells through CCRL2 and GPR1 [312]. Furthermore, CCRL2 has been linked to migration and invasion in glioblastoma [313] and metastasis in colorectal cancer [314]. However, also the function of CCRL2 is complex and context-

dependent, as it has been demonstrated to suppress migration and invasion in breast cancer [315].

Originally cloned in 1994 [316], GPR1 was identified as a chemerin receptor in 2008 [295]. GPR1 mRNA has been detected in different human cell types and tissues, such as the adrenal cortex, smooth muscle cells of blood vessels, kidney tubules, and skin [317]. Although the role of GPR1 in health and disease is so far only partly understood versatile functions are emerging. While GPR1 is a co-receptor in human immunodeficiency virus replication [318], it has also been linked to the regulation of glucose homeostasis [319] and atherosclerosis [320]. Furthermore, pro-tumorigenic effects of chemerin in gastric cancer were recently linked to both CMKLR1 and GPR1 [321].

4.1.8 COX-2/ PGE_2

While normally absent in the majority of cells, cyclooxygenase 2 (COX-2) is upregulated during inflammation and also in various tumors [322]. COX-2 is one of the enzymes that mediates the synthesis of prostanoids, such as PGE_2, a potent pro-inflammatory factor [322]. The COX/PGE_2 axis can promote proliferation, survival, and migration of tumor cells, support angiogenesis, advance immunosuppression through impairment of effector T cells, NK cells, and DCs, and enhance suppressive MDSCs and Treg functions [322-324]. Furthermore, PGE_2, in synergy with IL-23, can promote Th17 expansion *in vitro* [325].

4.2 INFLAMMATORY CELL SIGNALING

Pro-inflammatory cell signaling pathways, such as the JAK/STAT3 pathway or NF-κB (nuclear factor kappa-light-chain-enhancer of activated B cells) signaling, are frequently upregulated in cancer and among the most attractive drug targets for cancer therapy [130, 138, 152].

NF-κB activation occurs in tumors cell and other cells of the TME and can regulate, directly or through cross-talk with other signaling pathways, all known cancer hallmarks [326]. Cytokines and danger signals, such as DAMPs and PAMPs (Pathogen-associated molecular patterns), can among others, activate NF-κB signaling [326]. Similar to NF-κB, the JAK/STAT3 pathway can regulate various cancer hallmarks, such as cell proliferation and survival, invasion and metastasis, inflammation, and immune suppression [327]. Members of the IL-6 family,

TLRs, various GPCRs, and microRNAs can modulate JAK/STAT3 signaling in tumor cells and other cells present in the TME [327].

Spleen tyrosine kinase (SYK) is a non-receptor tyrosine kinase widely expressed in hematopoietic cells mediating signaling by immune receptors, integrins, C-type lectins, and others [328]. Activated SYK can directly interact with VAV and PLCγ family members, phosphoinositide 3-kinase (PI3K) and SLP (Scr homology 2 domain containing leukocyte protein) 76 or 65 activating a broad variety of downstream signaling molecules, such as extracellular signal-regulated kinase (ERK), Akt, c-JUN-NH2 terminal kinase (JNK), the mitogen-activated protein kinase p38, and transcription factors like NF-κB (Figure 8) [328].

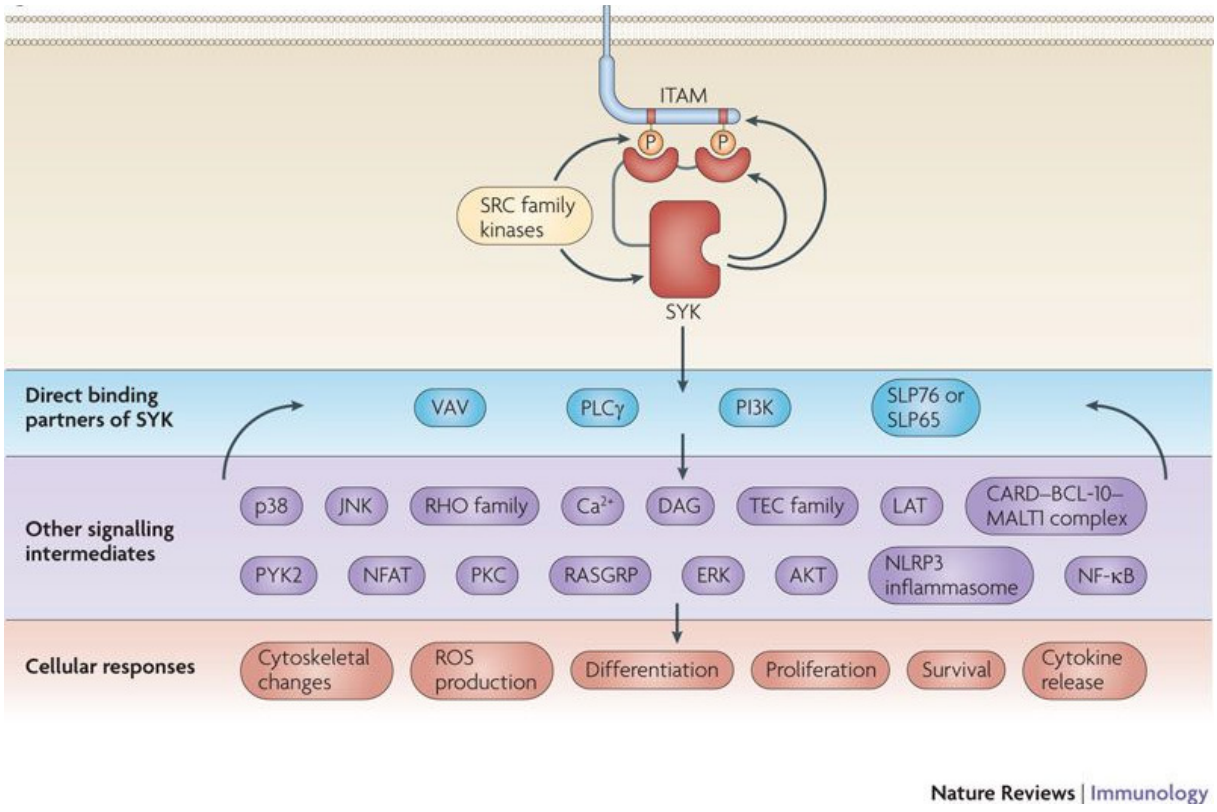

Figure 8: SYK signaling.
In the immunoreceptor-signaling context, SYK is recruited upon ITAM (immunoreceptor tyrosine-based activation motif) phosphorylation leading to SYK activation by phosphorylation (not shown). Active SYK can bind to a variety of signaling molecules that activate various downstream pathways thereby regulating different cellular responses. Feedback mechanisms can further mediate SYK signaling. Reprinted by permission from Springer Nature Customer Service Centre GmbH: Springer Nature, Nature Reviews Immunology [328].

SYK has been implicated in different inflammatory conditions [329] and recently, with fostamatinib, the first SYK inhibitor has been approved for the treatment of immune thrombocytopenia [330]. Both, pro- and anti-tumorigenic SYK functions have been described in hematological cancers and solid tumors indicating SYK's multifunctionality [331]. For

example, SYK inhibits breast cancer tumor growth and lung metastasis formation *in vivo* [332] and functional involvement in cell-cell adhesion has been described *in vitro* [333]. However, SYK has recently been implicated in breast cancer metastasis, where it supports mesenchymal to epithelial transition and metastatic outgrowth [334]. Although SYK expression decreased following TGF-β-mediated EMT its activity increased considerably, indicating that the expression level of the kinase is not necessarily an indicator of its activity [334]. Pro-tumor functions of SYK have been described in Ewing sarcoma where it promotes tumor growth by upregulation of c-Myc and MALAT1 [335]. Furthermore, SYK is expressed in retinoblastoma and inhibition of SYK impairs cell survival *in vitro* and tumor growth *in vivo* [336]. In ovarian cancer, SYK promotes cell migration, invasion, and paclitaxel-resistance [337, 338]. Recently, pro-inflammatory functions of SYK have been described in the glioma TME [339]. Moncayo et al. demonstrated that SYK inhibition not only impaired tumor cell proliferation and invasion but also reduced infiltration of B cells and leukocytes [339]. Furthermore, SYK is present in neuroblastoma tissues and SYK-inhibition potentiates the neuroblastoma cell killing effects of chemotherapeutic drugs *in vitro* [340].

5 PEDIATRIC CANCER

"Children are not just small adults"- saying in pediatrics

Although the common principles of tumorigenesis described above apply to both, pediatric cancers and adult cancers differ in many aspects. The occurrence of malignancies in children and adolescents is rare in comparison to adults. Overall, childhood cancers account for 1.4% of malignancies worldwide [341]. While the risk to develop a childhood cancer is about 1 in 500, adult cancers occur with an approximate risk of 1 in 3 [342]. About 35000 children and adolescents are diagnosed with cancer each year in Europe [343]. The 5-year survival of childhood cancer patients in high-income countries has remarkably improved from 30% in the 1960s to approximately 80% in the 2000s [341]. However, despite improving survival rates, 6000 pediatric cancer patients die every year in Europe, making it the primary cause of disease-related deaths in children above one year of age [343].

While carcinomas are the most frequently occurring cancer type in adults, childhood cancers are more diverse, and carcinomas account for less than 5% of all cases [341]. In children, hematologic malignancies (leukemia and lymphoma) are predominant (40%),

followed by tumors of the central nervous system (25%) and other solid tumors (35%) [342]. However, the distribution varies between different age groups (Figure 9) [341].

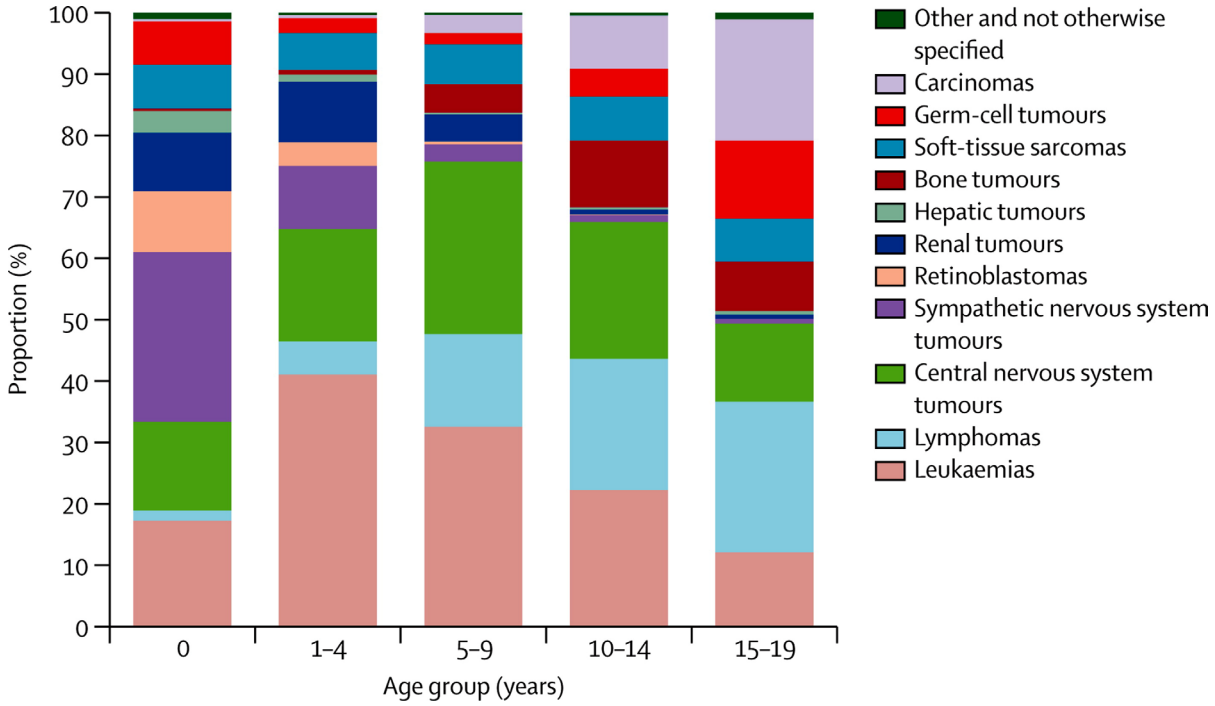

Figure 9: Proportions of pediatric tumor groups in Europe.
The distribution of the 12 main tumor types is displayed according to their occurrence in different age groups. Reprinted from The Lancet Oncology, Vol. 14, [341], an adapted version from The Lancet, Vol. 364 [344] with permission from Elsevier.

Tumor development in adults is a multistep process based on an accumulation of mutations and microenvironmental changes over a long period of time. Many pediatric malignancies, particularly solid tumors, are considered developmental diseases, as they are closely associated with defects in normal organ and tissue development and/or maturation [345, 346]. Cells in developing immature tissues often display a high proliferation rate, prolonged survival, and increased migration ability, typical characteristics of malignant cells. Therefore, it has been suggested that many pediatric solid tumors arise when cells and tissues fail to complete development to mature tissues and organs [345, 346]. Consequently, this poses a challenge for childhood cancer therapy since tumors can be surrounded by normal but equally fast growing developing tissue that will be affected to some extent by chemotherapy and radiation [345].

The repeated observation that the mutation frequency and mutational load is significantly lower in pediatric compared to adult tumors (Figure 10) [347, 348] supports the

notion that fewer defects are necessary to promote pediatric tumorigenesis thereby accelerating cancer development [345, 346].

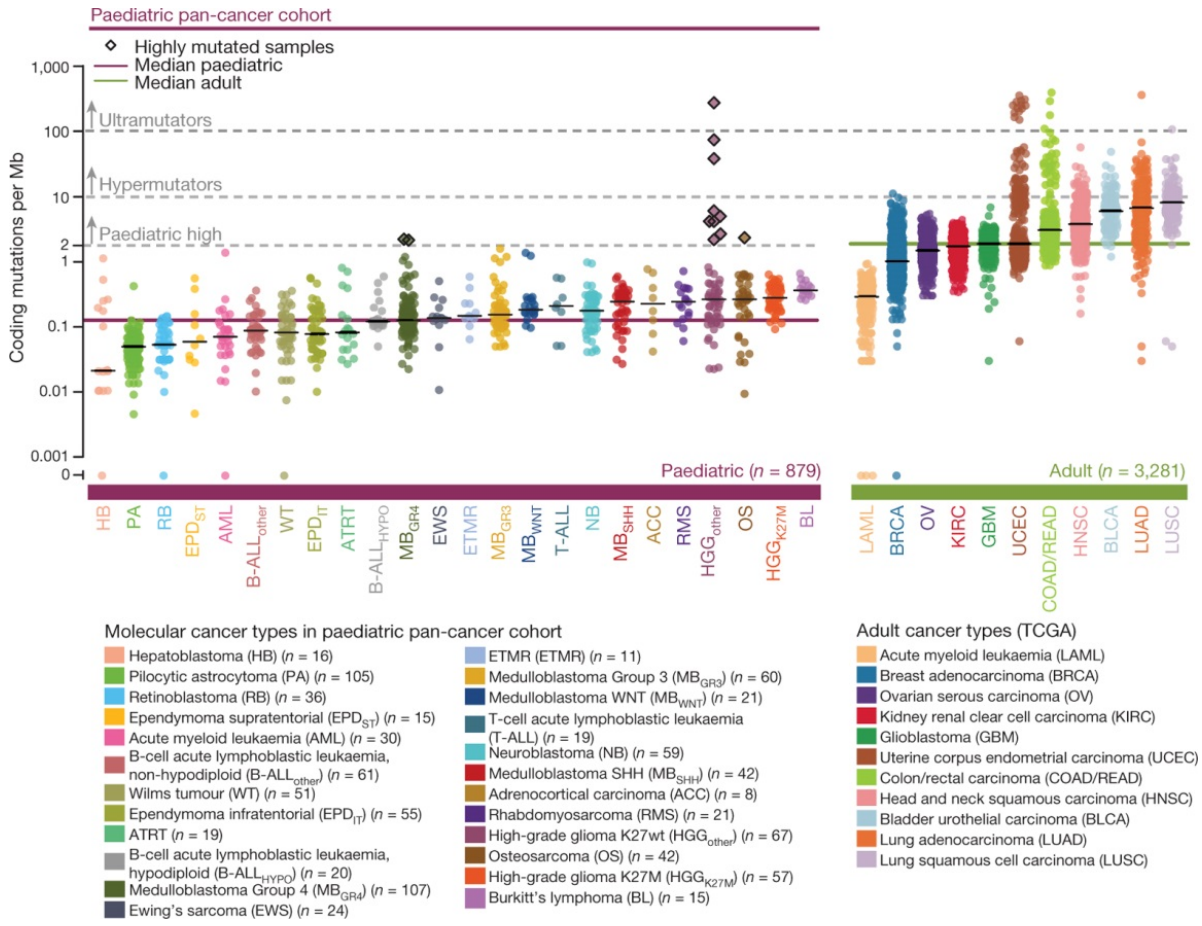

Figure 10: Somatic mutations in pediatric and adult cancers.
Frequency of somatic mutations in 11 pediatric (n=879 primary tumors) and 11 adult (n=3281) cancer types. The solid black lines represent the median mutation load for each cancer type, the solid purple and solid green line the median mutation load across pediatric and adult cancers, respectively. Reprinted from [347] under the Creative Commons Attribution License (CC BY 4.0).

The treatment of pediatric malignancies is particularly challenging considering the young age of the patients and the fact that the majority of the survivors will develop chronic health conditions as a consequence of intensive therapy [349, 350].

6 NEUROBLASTOMA

"Few tumours have engendered as much fascination and frustration for clinical and laboratory investigators as neuroblastoma" Garrett M. Brodeur [351]

Neuroblastoma is a malignancy of early childhood, with 90% of cases being diagnosed within the first 5 years of life and less than 5% in children over 10 years of age [352, 353]. The median age at diagnosis is 18 months [354]. Neuroblastomas account for 6-10% of childhood cancers [355]. It is the most common embryonal cancer, accounting for 44% of embryonal malignancies in Europe [356], and the most frequently diagnosed cancer during the first year of life [357].

Tumors can occur anywhere in the sympathetic nervous system with the majority arising in the adrenal gland (47%) and from paraspinal or other sympathetic ganglia (24% abdominal/retroperitoneal, 15% thoracic, 3% pelvic, 3% in the neck and 8% at other sites) [358]. Approximately 50% of patients present with metastatic disease at diagnosis with the major metastatic sites being the bone marrow and bone (>50%) and to a lesser extent lymph nodes, liver, and intracranial and orbital sites. Metastases are rarely observed in the lung and CNS [357, 359].

6.1 EPIDEMIOLOGY

The annual incidence rate of NB in Europe (1995-2002) is 1.78 per million persons of the general population with a slightly higher occurrence in boys (2.02 per million) than girls (1.56 per million) [356]. The age-standardized incidence rate is 10.9 cases per million children (age 0-14) in Europe (1988–1997) [360]. Although cases of neuroblastomas in adults have been reported, they are exceedingly rare with an incidence rate of fewer than 0.3 cases per million people per year (1973-2002) [361].

In the Nordic countries (Norway, Sweden, Denmark, Finland, and Iceland) neuroblastomas account for 8% of pediatric cancers (Figure 11) [362].

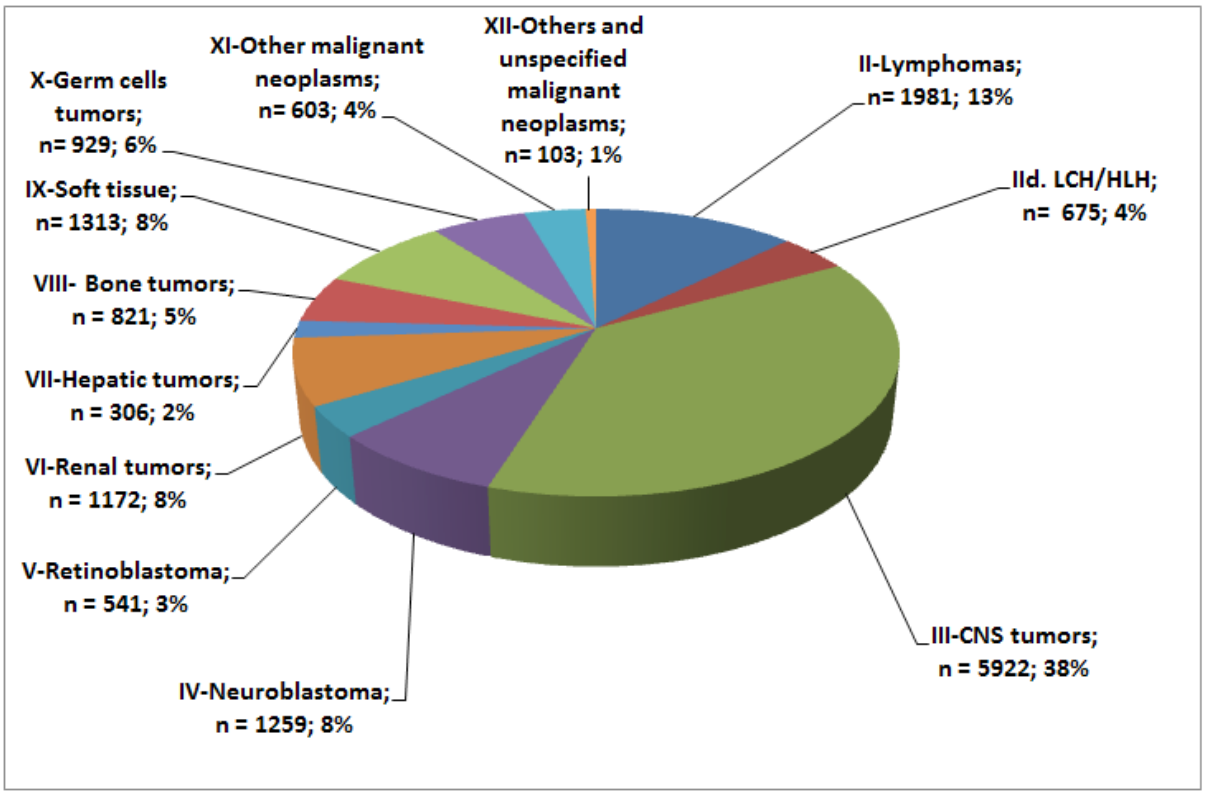

Figure 11: Distribution of pediatric cancer diagnoses in the Nordic countries from 1985-2014.
The proportions of cancer types in children <15 years of age at diagnosis. The Nordic countries include Norway, Sweden, Denmark, Finland, and Iceland. LCH = Langerhans Cell Histiocytosis; HLH = Hemophagocytic Lymphohistiocytosis; Reprinted from [362] with permission from Göran Gustafsson, Solid Tumor Registry Group, NOPHO Annual Report 2016.

Owing to advances in diagnosis and therapy, the 5-year survival has increased from 56% to 74% in the past 30 years (Table 3) representing the most prominent improvement among childhood cancers in the Nordic countries [362].

Table 3: Neuroblastoma 5-year survival estimates over three time periods in the Nordic countries.
OS= overall survival, * p-values between time periods; ** OS at 5 years-whole time period. Adapted and reprinted from [362] with permission from Göran Gustafsson, Solid Tumor Registry Group, NOPHO Annual Report 2016.

	N	Survival at 5 years-Kaplan-Meier (± SD)				OS at 5 years
		1985-1994	*1995-2004*	*2005-2014*	*p-value**	*1985-2014***
Sweden	420	0.61±0.04	0.66±0.04	0.74±0.04	0.045	0.67±0.02
Denmark	268	0.39±0.05	0.68±0.05	0.71±0.06	<0.01	0.59±0.03
Norway	233	0.51±0.05	0.83±0.05	0.88±0.04	<0.01	0.73±0.03
Finland	279	0.68±0.05	0.67±0.05	0.68±0.06	0.93	0.67±0.03
Iceland	11	0.67±0.27	0.75±0.21	0.75±0.21	0.92	0.72±0.14
All countries	1210	0.56±0.02	0.70±0.02	0.74±0.03	<0.01	0.66±0.01

However, despite advances in treatment, neuroblastoma accounts for 12-15% of cancer-related deaths in children [353]. Particularly the treatment of high-risk patients

remains a challenge as approximately 50% of high-risk patients do not respond to therapy or relapse within two years despite intensive treatment regimen [363].

6.2 BIOLOGY AND HISTOLOGY

Neuroblastoma is a neuroendocrine tumor originating from neural crest cells of the sympathoadrenal lineage [364, 365]. The neural crest is a tightly controlled, migratory, and transient cell population during embryogenesis that gives rise to different tissues including the sympathetic nervous system [366]. During this highly complex process,s de-regulated expression of factors that promote proliferation and stemness (e.g. N-Myc, FGF/Stat3, Lin28B, ALK), migration (Wnt, BMP, Rho), and differentiation (e.g. BMP, Phox2b, FoxD3) may lead to the development of malignant neuroblasts that give rise to neuroblastoma [366, 367].

The majority of neuroblastomas are sporadic with familial cases of neuroblastoma accounting for only 1-2% of all neuroblastoma cases [357]. As a major predisposition factor in familial neuroblastoma, mutations in the *ALK* gene, encoding the anaplastic lymphoma receptor tyrosine kinase (ALK) were identified [368].

Several genetic alterations have been identified in neuroblastoma [357]. While whole chromosome gains (triploid and hyperdiploid DNA content) indicate a favorable clinical behavior, segmental chromosome aberrations are connected to clinically unfavorable tumors (Table 4) [369, 370].

Table 4: Prognostic value of genetic alterations in neuroblastoma
Analysis based on 505 patients without *MYCN*-amplification; EFS=event-free survival, OS=overall survival; Reprinted from [370] under the Creative Commons Attribution License (CC BY-NC-SA 3.0).

Parameter	4-year EFS (% ± s.d.)	Log rank (*P*)	4-year OS (% ± s.d.)	Log rank (*P*)
Ploidy				
Hyperdiploid (*n* = 43)	65 ± 6.1	0.05	74 ± 6.6	0.0025
Diploid (*n* = 76)	45 ± 8.9		44 ± 12	
1p status				
Normal (*n* = 290)	63 ± 2.9	0.06	79 ± 2.6	0.11
Deletion (*n* = 205)	55 ± 3.7		72 ± 3.3	
11q status				
Normal (*n* = 207)	75 ± 3	<0.0001	88 ± 2.4	<0.0001
Deletion (*n* = 197)	42 ± 3.8		65 ± 3.9	
17q status				
Normal (*n* = 146)	75 ± 3.6	0.0002	86 ± 2.9	0.0001
Gain (*n* = 118)	49 ± 4.7		72 ± 4.3	
No segmental alterations (*n* = 108)	79 ± 3.9	<0.0001	88 ± 3.2	0.0001
'Segmental' type (*n* = 397)	53 ± 2.7		71 ± 2.5	

The gain of 17q and loss of 1p or 11q are the most common segmental alterations associated with a poor prognosis [371-373]. Recently, distal loss of 6q has been described as a marker of poor prognosis in high-risk neuroblastoma patients [374].

The best-characterized genetic alteration in neuroblastoma is the amplification of the *MYCN* oncogene, a potent genetic marker for aggressive clinical behavior. *MYCN* amplification is observed in approximately 20% of neuroblastomas and more intriguingly in about 40% of high-risk patients, underlining its importance as a prognostic factor [375-379]. N-Myc is a powerful transcription factor that can affect the majority of cancer hallmarks driving tumor progression and metastasis [380, 381].

Neuroblastomas, as the majority of pediatric cancers, are characterized by a low mutational frequency [347, 348, 382]. The most frequently observed changes are activating mutations in *ALK*, *PTPN11, MYCN,* and the *NRAS* oncogene and in addition, inactivating mutations in *ATRX* and *ARID1A/B* [382-385]. However, an increase in mutations and segmental alterations has been observed in relapse neuroblastomas [386, 387] including mutations in the RAS/MAPK pathway, p53, and ALK [388-390]. Recently, a “high” mutational burden (>3) was identified as a prognostic marker independent of age, stage, histology, and *MYCN*-amplification [391].

Neuroblastoma is known for its remarkable ability to spontaneously regress, despite metastatic disease, in infants with only numerical chromosome aberrations and without segmental chromosome aberrations or *MYCN* amplification [392, 393]. Several molecular mechanisms have been suggested to underlie/contribute to spontaneous regression, such as TrkA/NGF-mediated apoptosis or differentiation, immune recognition and tumor elimination, telomere shortening, and epigenetic alterations [393]. However, the exact mechanisms of spontaneous regression still remain uncertain [394].

Histologically, neuroblastoma is a small round blue cell tumor composed of neuroblasts and Schwann cells at different proportions. Neuroblastic tumors display different levels of differentiation and maturation that form the basis for a morphology-based, prognostic classification system [395, 396]. Based on this system neuroblastic tumors can be categorized into four morphologic categories [395-397]:

- *Neuroblastoma* (Schwannian stroma-poor) with undifferentiated, poorly differentiated or differentiating subtype (Figure 12A)
- *Ganglioneuroblastoma, intermixed* (Schwannian stroma-rich)

- *Ganglioneuroma* (Schwannian stoma-dominant) with maturing or mature subtype (Figure 12B)
- *Ganglioneuroblastoma, nodular* (composite Schwannian stroma-rich/stroma-dominant/stroma-poor) with favorable and unfavorable subtype

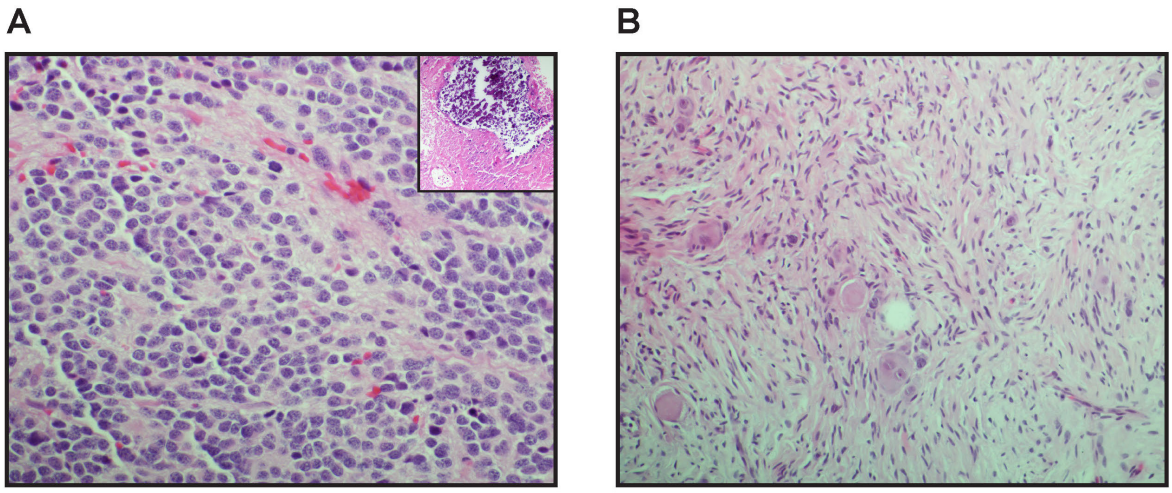

Figure 12: Histology of neuroblastoma and ganglioneuroma.
Typical examples of neuroblastoma (**A**) and ganglioneuroma (**B**), H&E, magnification 900x. A poorly differentiated neuroblastoma (**A**) is characterized by neuroblasts with relatively small nuclei showing salt and pepper chromatin pattern, and a limited quantity of neuropil. Necrosis and calcification are often observed (**insert**). (**B**) Ganglioneuroma with maturing and mature ganglion cells embedded in Schwannian stroma. Images were kindly provided by Andrey Valkov (Department of Clinical Pathology, University Hospital of Northern Norway, Tromsø, Norway).

6.3 NEUROBLASTOMA TME AND IMPLICATIONS OF INFLAMMATORY MEDIATORS

There is increasing evidence that the neuroblastoma TME is characterized by complex interactions between tumor cells, immune cells, other stromal cells, and non-cellular components [398].

Lymphocyte infiltration was established as a positive prognostic marker in neuroblastoma already 50 years ago [399, 400]. In addition, high levels of $CD3^+$ T cell proliferation and organization correlate with positive clinical outcome [401] and a T cell-poor microenvironment and reduced interferon pathway activity have been linked to *MYCN* amplification [402]. Moreover, the presence of a cytotoxic T cell RNA signature corresponds to increased infiltration of T cells and NK cells and a better prognosis in a subgroup of non-*MYCN*-amplified high-risk patients [403]. Furthermore, infiltration with CD8+ T cells with an effector memory phenotype was observed in a panel of neuroblastoma tissues [404].

However, it has been demonstrated that neuroblastoma cells apply different strategies, such as downregulation of MHC class I (HLA-1) expression, upregulation of checkpoint inhibitors (e.g. PD-L1), and secretion of immunosuppressive factors (e.g. TGF-β, IL-10, and arginase-2), to create an immunosuppressive microenvironment and impair T cell function [405-407]. Of note, differentiation of neuroblastoma cells can lead to an upregulation of MHC class I expression increasing sensitivity to CTL- and NK cell-mediated lysis [408].

Great potential for NK cell-mediated neuroblastoma cell killing has been demonstrated *in vitro* and *in vivo* [409]. However, different mechanisms have been described that impair NK cell-mediated immunosurveillance, such as downregulation of MHC class I, downregulation of activating receptors and/or their ligands, and the presence of immunosuppressive NK cell receptor isoforms [409-411].

The importance of myeloid cells in the neuroblastoma TME has been demonstrated in different studies. TAM infiltration correlates with clinical stage, risk classification, and metastasis [412, 413]. Furthermore, a genetic signature representing TAMs was identified as a prognostic marker in children with neuroblastoma at the age of ≥ 18 months without *MYCN* amplification [412]. TAMs can promote neuroblastoma proliferation *in vitro* and *in vivo* in an IL-6-dependent manner [414]. Furthermore, in a murine model lacking *MYCN* amplification TAMs upregulate c-Myc expression and STAT3 activation in neuroblastoma cells in an IL-6-independent manner [415].

MDSCs promote tumor growth in neuroblastoma and contribute to an immunosuppressive TME [416]. The presence of CSF-1R^{+} myeloid cells correlates with poor survival in neuroblastoma patients and blockade of CSF-1R significantly impaired tumor growth and reduced splenic MDSC and TAM numbers in an aggressive murine model of neuroblastoma [417].

As professional antigen presenting cells, DCs play an important role in immunosurveillance [33]. Neuroblastoma cells can impair DC generation, maturation, and function and interestingly, neuroblastoma cell-derived gangliosides have been identified as contributing factors [418, 419].

CAFs play an important role in the neuroblastoma TME by producing mPGES-1, a key enzyme for PGE2 synthesis, thereby supporting tumor growth and angiogenesis [420, 421]. Additionally, a new subtype of CAFs has recently been described in neuroblastoma that

displays phenotypical and functional similarities with mesenchymal stromal cells and stimulates neuroblastoma growth *in vitro* and *in vivo* [422].

Sufficient vascularization ensures the supply of oxygen and nutrients in growing tumors [108]. Several angiogenic factors, such as VEGF, PDGF, and FGF, contribute to angiogenesis in neuroblastoma [398]. Moreover, N-Myc and ALK can promote VEGF production in neuroblastoma [423, 424]. Furthermore, effective VEGF-blockade (VEGF-Trap) in neuroblastoma causes regression of coopted host vasculature [425]. Interestingly, *MYCN* amplification has been observed in microvessel-forming endothelial cells in neuroblastoma, indicating that they may originate from tumor cells [426].

Of note, ECM components, such as reticulin fibers and exosomes, have also been associated with high risk and pro-tumorigenic functions [427, 428].

Various inflammatory mediators have been identified in the neuroblastoma TME. Table 5 presents a selection of inflammatory mediators and their function in neuroblastoma.

Table 5: Inflammatory mediators in the neuroblastoma TME

Inflammatory mediator	Function	Reference
IL-6/IL-6R axis	Promotes cell proliferation, survival, and drug resistance through activation of STAT3	[429] [430]
	IL-6 elevated in blood and bone marrow of patients with high-risk disease compared to low and intermediate risk patients	[431]
COX/mPGES/ PGE_2	IL-1β upregulates COX-2 and the release of PGE_2 in the neuroblastoma cell line SK-N-SH	[432]
	COX-2 is upregulated in neuroblastoma cell lines and tumor tissue; COX inhibition induces cell death *in vitro* and inhibits tumor growth *in vivo*	[433]
	NSAIDs induce apoptosis of neuroblastoma cells *in vitro* and inhibit neuroblastoma growth *in vivo*	[434]
	Combination of low-dose chemotherapy and COX inhibitors potentiates neuroblastoma cell apoptosis and promotes p53 function	[435]
	Selective COX-2 inhibition (Celecoxib) potentiates efficacy of chemotherapeutic drugs *in vitro* and *in vivo*	[436]
	PGE_2 receptors are expressed in neuroblastoma cell lines and tumor tissue; PGE_2 promotes cell viability and Akt signaling, PGE_2 receptor antagonists reduce cell viability	[437]
	Low dose Aspirin (dual COX-1/ COX-2 inhibitor) reduces tumor burden, infiltration with MDSCs, TAMs, DCs, and TGFβ levels	[438]
	β-catenin stabilization is involved in PGE_2-mediated increase in neuroblastoma cell viability	[439]
	11q-deleted neuroblastomas display elevated levels of mPGES and PGE_2, high mPGES expression is associated with poor overall survival in stage 4 neuroblastomas, COX-inhibition reduces tumor growth in an 11q-deletion xenograft model	[421]
	mPGES inhibition reduces CAF-derived PGE2 production, tumor growth, and angiogenesis	[420]
CXCR4/CXCR7/CXCL12	CXCR4 is expressed in neuroblastoma cells and CXCL12 promotes migration of SH-SY5Y cells	[440]
	CXCR4 expression correlates with high clinical stage and metastases in the bone and bone marrow	[441]
	CXCL12 does not stimulate chemotaxis of primary neuroblastoma cells or cell lines	[442]
	CXCR4 promotes growth of primary tumor and liver metastases in an orthotopic tumor model	[443]
	Multiple CRXR4 isoforms are expressed in neuroblastoma cells and CXCR4 downregulation is independent of CXCL12 but correlates with increasing confluency	[444]
	CXCR4 and CXCR7 mediate neuroblastoma cell migration towards mesenchymal stromal cells	[445]
	CXCR7 reduces neuroblastoma growth *in vitro* and *in vivo* and impairs CXCL12/CXCR4 chemotaxis	[446]
	In a tumor cell implantation model CXCR4 or CXCR7 promote neuroblastoma cell dissemination to the liver or adrenal gland and liver, respectively; co-expression of CXCR4 and CXCR7 promotes dissemination to the bone marrow	[447]

M-CSF (CSF-1)/ CSF-1R	Neuroblastoma cells express CSF-1R and CSF-1 at varying levels; targeting CSF-1 using siRNA reduces tumor growth, TAM infiltration, and angiogenesis *in vivo*	[448]
	Neuroblastoma cell-derived M-CSF promotes suppressive functions of myeloid cells; CSF-1R inhibition, alone or in combination with checkpoint blockade limit tumor growth in a transgenic neuroblastoma model	[417]
	CSF-1R inhibition in combination with PD-1 blockade increases T cell infiltration in transgenic neuroblastoma model; correlation between PD-L1 expressing myeloid cells and tumor burden was determined	[449]
	CSF-1R blockade in combination with chemotherapy reduced neuroblastoma tumor growth in a T cell-deficient mouse model	[450]
TNF-α	TNF-α promotes neuroblastoma cell proliferation in the presence of insulin	[451]
	TNF-α activates NF-κB in neuroblastoma cell lines, NF-κB activation does not promote differentiation or proliferation	[452]
	TNF-α induces NF-κB-mediated upregulation of Fas in a subset of neuroblastoma cell lines, TNFα sensitizes those cells to FasL-, cisplatin-, etoposide-induced cell death	[453]
	TNF-α upregulates PD-L1 and HLA-1 in SH-SY5Y and SK-N-FI cells but not *MYCN*-amplified cell lines	[454]
	Cell supernatants from neuroblastoma cell lines can decrease TNF-α and IL-12 production from mature DC's	[455]
	Macrophage-derived TNF-α and IL-1β induce upregulation of arginase-2 in neuroblastoma cells promoting proliferation; high levels of TNF-α and IL-1β in stage 4 tumors are associated with a worse prognosis	[456]

6.4 STAGING AND RISK CLASSIFICATION

Neuroblastoma is a highly heterogeneous disease with its clinical behavior spanning from spontaneously regressing to highly aggressive, metastatic and therapy-resistant tumors [351].

First published in 1988 and revised in 1993, the International Neuroblastoma Staging System (INSS), based on tumor resectability and the extent of metastases, was until recently the most widely used neuroblastoma staging system [457, 458]. However, INSS has the disadvantage that tumor assessment is made after the initial surgery. Therefore, the International Neuroblastoma Risk Group (INRG) developed a pretreatment classification system (INRGSS) to update and replace the INSS in 2009 [459, 460]. The system was developed to enable the comparison of clinical trials conducted at different sites by defining four pretreatment risk groups (very low-, low, intermediate- or high-risk) [459]. The INRGSS is based on image-defined risk factors to determine the extent of the disease at the time of diagnosis (Table 6) and clinically relevant criteria (Table 7) [459, 460].

Table 6: International Neuroblastoma Risk Group Staging System (INRGSS).

Stage	Description
L1	Localized tumor not involving vital structures as defined by the list of image-defined risk factors and confined to one body compartment
L2	Locoregional tumor with presence of one or more image-defined risk factors
M	Distant metastatic disease (except stage MS)
MS	Metastatic disease in children younger than 18 months with metastases confined to skin, liver, and/or bone marrow

NOTE. See text for detailed criteria. Patients with multifocal primary tumors should be staged according to the greatest extent of disease as defined in the table.

Table 7: INRG Consensus Pretreatment Classification schema.
GN, ganglioneuroma; GNB, ganglio-neuroblastoma; Amp, amplified; NA, not amplified. For the definition of L1, L2, M, and MS see Table 6. All blank fields represent any value. Reprinted from [459] with permission. ©2009 American Society of Clinical Oncology. All rights reserved.

INRG Stage	Age (months)	Histologic Category	Grade of Tumor Differentiation	*MYCN*	11q Aberration	Ploidy	Pretreatment Risk Group
L1/L2		GN maturing; GNB intermixed					A Very low
L1		Any, except GN maturing or GNB intermixed		NA			B Very low
				Amp			K High
L2	< 18	Any, except GN maturing or GNB intermixed		NA	No		D Low
					Yes		G Intermediate
	≥ 18	GNB nodular; neuroblastoma	Differentiating	NA	No		E Low
					Yes		H Intermediate
			Poorly differentiated or undifferentiated	NA			
				Amp			N High
M	< 18			NA		Hyperdiploid	F Low
	< 12			NA		Diploid	I Intermediate
	12 to < 18			NA		Diploid	J Intermediate
	< 18			Amp			O High
	≥ 18						P High
MS	< 18			NA	No		C Very low
					Yes		Q High
				Amp			R High

6.5 TREATMENT

The treatment of neuroblastoma is as heterogeneous as the disease itself ranging from observation only to intensive multimodal therapy [357]. The INRGSS pretreatment risk groups serve as important guides for clinicians to decide the best treatment plan (Figure 13).

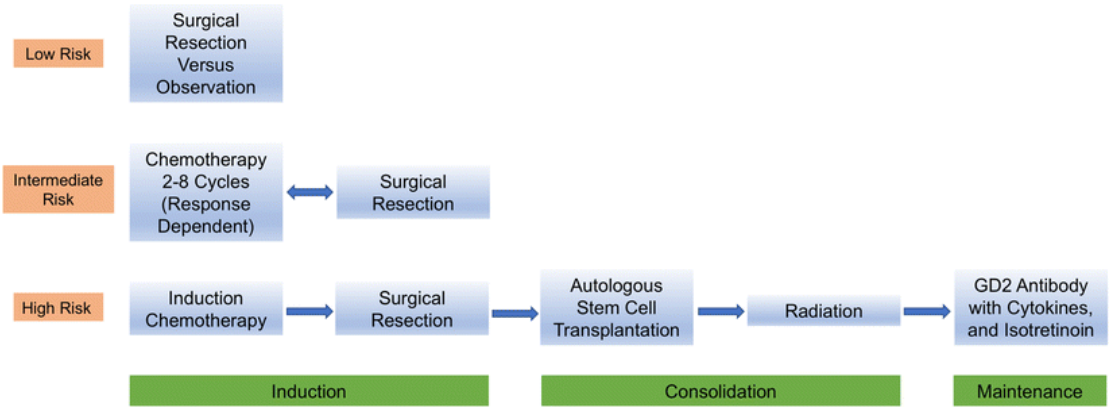

Figure 13: Overview of neuroblastoma treatment based on risk classification.
Surgical resection or observation only is the standard treatment for low risk patients. The treatment of intermediate risk patients includes chemotherapy and surgery while the therapy regimen for the high-risk patients includes chemotherapy, surgery, myeloablation and stem cell transplantation, radiation, immunotherapy, and treatment with a differentiation-inducing agent. Reprinted by permission from Springer Nature Customer Service Centre GmbH: Springer Nature, Cell and Tissue Research [461].

The treatment for patients with very low- and low-risk disease includes observation or surgical resection and intermediate-risk disease is managed with chemotherapy and surgical resection [461]. Increasing evidence supports that observation alone as an appropriate treatment for low-risk patients with favorable histologic and genomic features [462, 463]. Furthermore, several studies demonstrate the possibility to reduce treatment in patients with low- and intermediate-risk disease while maintaining a high overall survival rate (>90%) [464-466].

Although the 5-year overall survival has increased in high-risk neuroblastoma patients from 29% (patients diagnosed between 1990 and 1994) to 50% (patients diagnosed between 2005 and 2010), treatment of high-risk disease remains a challenge [467]. The current therapeutic regimen lasts approximately 18 months and consists of the induction phase (5-8 cycles of intensive chemotherapy and surgical resection), the consolidation phase (myeloablative chemotherapy followed by autologous stem cell transplantation and radiation therapy) and the maintenance phase (treatment with the differentiating agent isotretinoin and anti-GD2 therapy combined with IL-2 and with or without GM-CSF) [468].

The prognosis for patients with refractory or relapsed neuroblastoma remains poor and although partial or complete responses can be achieved these patients are rarely cured [461]. Common salvage therapy includes chemotherapy or ^{131}I-MIBG radiotherapy [461, 469].

The increasing understanding of neuroblastoma biology has led to the identification of various druggable targets, such as ALK, PI3K/mTOR (mammalian target of rapamycin)/Akt, Aurora A kinase, EGFR, Ras/MAPK, histone deacetylase, Wnt/β-catenin, checkpoint kinases 1 and 2 (CHK1/2), Bromodomain and extra-terminal motif (BET) proteins, and VEGF, and the development of targeted therapies [363, 470, 471]. Several targeted drugs have been evaluated or are currently under evaluation in neuroblastoma clinical trials [363, 470, 471].

The inclusion of monoclonal antibodies targeting the disialoganglioside GD2 (known as dinutuximab or ch14.18) in combination with IL-2 and GM-CSF into maintenance therapy has significantly improved event-free survival in high-risk neuroblastoma patients [472]. In addition, the efficacy of anti-GD2 therapy as part of consolidation therapy has also been demonstrated [473]. This has led to the

development of humanized anti-GD2 monoclonal antibodies and different approaches targeting GD2, such as bispecific antibodies or CAR-T cells [474]. Furthermore, combination therapy of anti-GD2 with chemotherapy, NK cells or PD-1 blockage has displayed great promise in clinical trials or pre-clinical studies [475-477]. Intense neuropathic pain is one of the major adverse effects related to anti-GD2 therapy and modifications in the treatment regimen, such as long-term antibody infusion, aim at reducing toxicity [478].

Other immunotherapy approaches, among others, immune checkpoint blockage (anti-CTLA-4 and anti-PD-1), NK cell therapy, and ALK CAR (chimeric antigen receptor) T cell therapy, have been investigated in neuroblastoma with mixed results or are currently under investigation [479-483]. Recently, Parihar et al. demonstrated that genetically modified NK cells target MDSCs and improve the activity of GD2 CAR-T cells in a neuroblastoma xenograft model [484]. Furthermore, antibodies targeting $CD105^{+}$ cells (MSCs, monocytes, and endothelial cells) improved immunotherapy with dinutuximab and activated NK cells in a neuroblastoma murine model [485]. These findings underline that a thorough understanding of the neuroblastoma TME can lead to novel therapeutic approaches.

AIMS OF THE THESIS

The overall aim of this thesis was to investigate novel inflammatory mediators and inflammatory pathways in neuroblastoma and evaluate their therapeutic potential.

The specific aims were:

Paper I: To assess the functional significance of the Chemerin/CMKLR1 axis in neuroblastoma tumorigenesis.

Paper II: To evaluate spleen tyrosine kinase (SYK) as a potential therapeutic target in neuroblastoma.

Paper III: To investigate the role of the IL-17 family and the associated cytokine IL-23 in the neuroblastoma microenvironment.

METHODOLOGICAL CONSIDERATIONS

This section aims to give a general overview of the methods used in this thesis, the rationale for choosing them, and their limitations. The specific materials and conditions used in this work are described in detail in **papers I-III**.

1 BIOLOGICAL MATERIAL

Cancer cell lines are an extremely useful tool to study diverse biological processes and the efficacy of therapeutic agents. A broad variety of neuroblastoma cell lines with specific morphological and genetic characteristics is available that can represent different aspects of neuroblastoma biology, such as presence or absence of *MYCN*-amplification, ALK mutations, and segmental chromosome aberrations [486]. Neuroblastoma cell lines are a convenient tool as their handling is uncomplicated and their relatively short doubling times allow extensive experimental set ups. However, one has to keep in mind that cancer cell lines have undergone many passages that unavoidably have caused changes in the cells. They should, therefore, be considered a useful model that can however not replace patient material and *in vivo* studies.

Primary cell cultures can be a valuable alternative to established cell lines as they display a more native phenotype. However, primary cell cultures are difficult to obtain for rare diseases, such as neuroblastoma with 233 registered cases in Norway between 1985 and 2014 [362]. Furthermore, specific ethical guidelines apply for the work with primary cells.

1.1 CELL LINES (PAPER I-III)

To confirm the identity of the cell lines used in this work STR (short tandem repeat) profiling was performed at the Centre of Forensic Genetics, University of Tromsø. The cell lines were routinely grown without antibiotics as it has been demonstrated that antibiotics can affect the proliferation and gene regulation of cultured cells [487, 488]. Furthermore, the use of antibiotics can hide low level contaminations and mycoplasma infections [489]. Mycoplasma tests were performed regularly.

1.2 HUMAN TISSUE SAMPLES (PAPER I-III)

Neuroblastoma tumor tissues were obtained in accordance with the ethical approval from the Stockholm Regional Ethical Review Board and the Karolinska University Hospital Research Ethics Committee (approval ID 2009/1369-31/1 and 03-736) at the Astrid Lindgren Children's Hospital, Karolinska University Hospital. Informed consent (written or verbal) for the use of tumor samples in research was provided by the parents or guardians.

1.3 *IN VIVO* STUDIES (PAPER I AND III)

All animal studies were conducted at the Department of Comparative Medicine, Karolinska University Hospital in accordance with the local guidelines and the European Directive 2010/63/EU. The studies were approved by the regional ethics committee (ethical permits N231/14 and N42/12). The 3R's (replacement, refinement, and reduction) were considered while planning and conducting all experiments involving animals.

2 GENE EXPRESSION STUDIES

2.1 SCREENING OF PUBLICALLY AVAILABLE GENE EXPRESSION DATABASES (PAPER I-III)

The R2: Genomics Analysis and Visualization Platform (http://r2.amc.nl) was used to screen different neuroblastoma datasets for the expression of relevant genes and their prognostic implications (comparison of high and low expression in relation to overall or event-free survival), and to examine correlations between genes. Both microarray-based data sets (**paper I-III**) and RNA-sequencing-based data sets (**paper III**) were used. Furthermore, the MegaSampler feature was utilized to compare gene expression between neuroblastoma cohorts, the neural crest, and neurofibroma (benign tumors of the peripheral nervous system) to determine differences in expression levels. Since neuroblastoma is a rare disease, an advantage of employing the R2: Genomics Analysis and Visualization Platform is access to data from a greater

number of patients. In addition, the availability of a variety of neuroblastoma datasets enables comparisons between the data sets.

2.2 ENDPOINT RT-PCR (PAPER I-III)

Endpoint reverse transcription (RT-) PCR was used to detect the presence or absence of gene transcripts. Endpoint PCR is not a quantitative method and does, at most, allow for semi-quantitative estimations if normalization to a housekeeping gene is performed. If the quantification of gene expression would have been the aim, a different method, such as quantitative real-time PCR or Droplet Digital PCR, should have been chosen. One advantage of endpoint PCRs is the ability to estimate PCR product sizes following agarose gel electrophoresis. For the majority of genes examined in this study, intron-spanning primers were used to ensure that amplification of residual genomic DNA is clearly distinguishable from the amplification of transcript-based cDNA based on the PCR-product size.

3 PROTEIN DETECTION

Most methods for protein detection depend on the availability of reliable and thoroughly validated antibodies. For extensively studied proteins, such as housekeeping proteins like GAPDH (Glyceraldehyde-3-phosphate dehydrogenase) or cell signaling proteins like Akt and ERK1/2, this poses no problem since a variety of verified antibodies are available. However, it can be difficult to find reliable antibodies for less extensively studied proteins. The availability of thoroughly validated antibodies in particular for members of the IL-17 family and CMKLR1/chemerin was a major challenge in this work. Commercially available antibodies frequently do not perform as promised even on suggested positive controls. For **paper III** we tested seven different antibodies for IL-17RB alone for the use in western blot and/or IHC to find one that works satisfactory for each method. Our difficulties are mirrored in two recent publications demonstrating the challenge to find reliable IL-17A and IL-17B antibodies [490, 491].

Fortunately, the problem of antibody reliability has gained increasing attention in the past years [492] and there are several initiatives, such as the Human Protein Atlas (www.proteinatlas.org) [493] aiming to improve validation and reliability of

antibodies. Furthermore, guidelines on antibody validation are emerging [494, 495]. However, antibody validation remains largely the responsibility of the researcher and antibody suppliers could provide better support to enable a more effective validation by the researcher. Greater transparency of antibody origins would help to select antibodies and prevent the purchase of the same antibody from different suppliers. In addition, suppliers could provide more detailed information concerning their validation practices, to enable the researcher to evaluate the antibodies for their specific needs more time- and cost-effectively.

3.1 WESTERN BLOT (PAPER I-III)

Western blot is a common method used to detect specific proteins in cell or tissue lysates. Briefly, protein lysates are separated according to their size by SDS-PAGE (sodium dodecyl sulfate–polyacrylamide gel electrophoresis) and transferred to a membrane. Unspecific binding sites are subsequently blocked and the membranes are incubated in the primary antibody solution, with the primary antibody being directed against the protein of interest. Following washing steps to remove unbound antibodies, the membranes are incubated in a secondary antibody solution containing antibodies directed against the species of the primary antibody. The secondary antibody is conjugated with an enzyme, for example horseradish peroxidase (HRP), or a fluorescent dye. If an enzyme-conjugated secondary antibody is used, the addition of, for example a chemoluminescent substrate, leads to substrate conversion and a chemoluminescent signal that can be detected. A marker containing proteins of a known size allows for size estimation of the obtained signal/protein band. This is a major advantage of western blotting because information can be gained concerning antibody specificity based on the number of visible bands and size estimations. Western blotting is a semi-quantitative method allowing comparisons of band strength, corresponding to protein amounts, between samples on the same gel/membrane. The amount of the protein of interest should be normalized to the amount of a housekeeping protein (ideally in the same size range) to ensure equal sample input and even protein transfer and blocking.

Western blot analyses were used in this work to determine the presence of different proteins in neuroblastoma cell lysates and to evaluate the specificity of antibodies.

3.2 IMMUNOCYTOCHEMISTRY AND IMMUNOHISTOCHEMISTRY (PAPER I-III)

Immunocytochemistry (ICC) and immunohistochemistry (IHC) are methods that determine the localization of proteins in cells (ICC) or tissues (IHC). The use of different fluorescent dyes or chromogens allows for multiplexing and colocalization studies. Either primary (direct detection) or secondary antibodies (indirect detection) can be conjugated to a fluorescent dye or chromogen. Indirect detection has the advantage of greater sensitivity since multiple secondary antibodies can bind to a primary antibody leading to an amplification of the signal. The use of isotype control antibodies (same species as the primary antibody) instead of primary antibodies is important to control for unspecific binding. A crucial step in IHC is the use of the optimal antigen retrieval approach (heat induced or enzymatic) to unmask epitopes, as cross-linking of proteins during fixation can mask antigens.

ICC and IHC are commonly used to determine the subcellular location of a specific protein (ICC/IHC) and to study protein expression pattern in different cell types and areas of tissues (IHC). A prerequisite for successful ICC and IHC is the availability of high quality antibodies to avoid false positive staining (lack of specificity) or false negative staining (lack of sensitivity). In this work, ICC and IHC were used to determine the presence/absence and localization of specific proteins in neuroblastoma cell lines and tissues.

3.3 ELISA (PAPER I AND III)

Enzyme-linked immunosorbent assay (ELISA) is a method to quantify proteins in cell supernatants, plasma, serum, and tissue lysates. In this work, commercially available, validated sandwich ELISAs were used to determine the concentration of chemerin, Dkk-1, and HGF in cell supernatants of stimulated neuroblastoma cell lines. In typical sandwich ELISAs, plates are coated with an antibody directed against the

protein of interest. Unspecific binding sites are blocked followed by addition of the samples. An additional antibody specific to the protein of interest is added that is either directly enzyme-conjugated (e.g. HRP) or tagged (e.g. biotin). If a tagged antibody is used, an enzyme-conjugated antibody targeting the tag is added. Thorough washing between each step is essential to remove unbound sample and antibodies. Finally, the appropriate substrate, such as TMB (3,3',5,5'-tetramethylbenzidine), for HPR is added and after sufficient color development, the reaction is stopped. Absorbance measurements at the appropriate wavelength (e.g. 450nm for TMB) are performed to quantify the amounts of the reaction product. A dilution series of known protein concentrations is included in each run to draw a standard curve, allowing for the extrapolation of the concentration of the protein of interest in the samples.

3.4 IMMUNOPRECIPITATION (PAPER II)

Immunoprecipitation was used in **paper II** to concentrate neuroblastoma cell-derived SYK to enable the detection of specific phospho-sites. Phospho-specific antibodies are raised against a specific phospho-residue, a very small antigen. This can result in very weak signals particularly if no prior stimulation of phosphorylation took place as not all copies of the protein may be phosphorylated at the same time. In this work, we wanted to determine the phosphorylation state of SYK under normal growth conditions. Through immunoprecipitation, we were able to concentrate and purify total SYK protein enabling us to detect the phosphorylation of specific sites and in addition, reduce unspecific background staining observed for some of the phospho-specific antibodies.

3.5 FLOW CYTOMETRY (PAPER III)

Flow cytometry was used in **paper III** to evaluate the presence of IL-23p19 in tumors, sera, spleen, liver, and lung of TH-MYCN mice. Multi-color flow cytometry is a common technique to determine the presence of specific cell populations in more or less heterogeneous samples (e.g. tissue lysates, cell cultures, sera) and to determine the presence/absence of a specific target in different cell populations. High

quality antibodies and the inclusion of extensive controls are, among others, important factors that determine the quality of flow cytometry analyses.

4 REGULATION OF CELL SIGNALING PATHWAYS

4.1 PHOSPHO-SPECIFIC WESTERN BLOTS (PAPER I-II)

Phospho-specific western blots were used in **paper I and II** to determine the activation or inhibition of specific cell signaling pathways in response to specific stimuli or inhibitors. Normalization to the corresponding total protein and/or a house keeping protein are important to ensure equal loading and consequently that the differences observed are in fact due to stimulation or inhibition and not a result of unequal protein input. During our work on **paper II**, we experienced difficulties to completely remove phospho-antibodies prior to re-probing with the total-protein antibodies. This can lead to signals from the remaining phospho-antibodies or can impair the binding of the total protein antibodies. Incomplete antibody removal is a well-recognized problem for relative phospho-protein quantification [496]. We, therefore, chose an approach to circumvent this problem, which was running separate gels for phospho- and total protein and to normalize each to its loading control before calculating phospho/total protein ratios.

4.2 CALCIUM MOBILIZATION (PAPER I)

Calcium is an important second messenger connected to GPCR signaling. In **paper I**, calcium mobilization from intracellular compartments was detected by live cell imaging. The cells were loaded with a calcium sensitive fluorescent dye and probenecid to ensure the retention of the fluorescent dye within the cells. Calcium mobilization in response to GPCR activation resulted in an increase of fluorescence that was detected with a confocal laser scanning microscope.

We also attempted to establish a protocol for plate-reader based calcium mobilization measurements but observed that the automated injection of media (without stimuli) to the cells caused an increase in calcium mobilization by itself. This may be attributed to the high pressure of the injection causing mechanical stress in the cells, as the same effect was not observed when media was carefully added

manually to the control cells in the microscopy based set up. Intracellular calcium mobilization has previously been linked to mechanical stimulation in a variety of cell types [497].

5 MTT CELL VIABILITY ASSAY (PAPER I-III)

The MTT assay was used to determine cell viability in response to stimuli, inhibitors or drugs. The cell viability was determined in comparison to control cells that were set as 100% viable cells. There are a variety of colorimetric or fluorescence based cell viability assays. We chose the MTT assay because it is inexpensive, widely used, and a well-established method in our lab. MTT is tetrazolium dye that is reduced to a purple insoluble formazan by nicotinamide adenine dinucleotide phosphate (NADPH)-dependent cellular oxidoreductase enzymes (mainly mitochondrial dehydrogenases present in living cells) [498]. Therefore, the production of formazan is a measure of metabolic activity/cell viability. The MTT assay can also be used as a proliferation assay as an increase in cell numbers correlates with an overall increase in cellular activity. However, it is important to note that more specific assays are available to determine proliferation directly, such as the BrdU assay or the 3H-thymidine incorporation assay, whose measures of DNA synthesis are more specific to determining proliferation.

6 CLONOGENIC ASSAY (PAPER I)

The clonogenic assay also known as colony formation assay is a cell survival assay that assesses the ability of a cell to divide without restrictions. In **paper I** we used this assay to determine whether CMKLR1 inhibition affected the ability of neuroblastoma cells to form cell colonies (>50 cells) from a single cell.

7 PARP-1 CLEAVAGE (PAPER II)

PARP-1 is a nuclear protein with important functions in DNA damage repair but also in, among others, cell death and inflammation. In the context of cell death, PARP is an *in vivo* target for caspase-3- and caspase-7-cleavage resulting in fragments of 89 kDa and 24 kDa [499]. It has been observed that other cell-death related proteases can also cleave PARP-1 resulting in different fragment sizes. Therefore, the size of

PARP-1 fragments can give an indication towards which form of cell death the cells are undergoing [499]. In **paper II**, PARP-1 cleavage, represented by the presence of the 89 kDa fragment, was detected using western blot to supplement MTT cell viability data. A reduction in cell viability in combination with an increase in cleaved PARP-1 indicated that SYK-inhibition in combination with chemotherapy induced cell death rather than reducing cell proliferation. However, further studies would be required to determine the extent and type of cell death or the extent of proliferation inhibition.

8 SCRATCH ASSAY (*IN VITRO* MIGRATION ASSAY) (PAPER III)

The scratch assay also called wound healing assay is a well-established method to assess two dimensional cell migration *in vitro* [500]. In **paper III** we utilized the scratch assay to determine whether recombinant IL-17 proteins affect the migration of neuroblastoma cell lines *in vitro*. However, additional studies using specific chemotaxis assays are required to investigate if the migration of the cells is directed towards the recombinant proteins. Chemotaxis assays are based on creating a gradient of the respective stimulus to examine if the cells migrate towards the highest concentration of the stimulus.

9 KNOCKDOWN/ KNOCKOUT STUDIES

9.1 SIRNA MEDIATED DOWNREGULATION OF GENE EXPRESSION (PAPER II)

Transient downregulation of SYK expression was achieved using small interfering RNA (siRNA). siRNAs are specifically designed to complementary bind to transcripts from genes of interest promoting their degradation and preventing translation. In **paper II**, cells were transfected with SYK mRNA-targeting siRNAs using liposome-based transfection. High transfection efficiency is the prerequisite for substantial downregulation of gene expression. In both SYK-positive cell lines, we observed a pronounced reduction in SYK protein following siRNA transfection. However, we did not achieve a complete knockdown of SYK expression, which can be attributed to the sub-optimal transfection efficiency we previously observed in these cell lines with liposome-based transfection methods.

Alternative transfection methods, such as electroporation, could improve transfection efficiency and consequently result in complete knockdowns. Alternatively, gene knockout using CRISPR/Cas9 or stable gene knockdown through genome-integrated shRNA mediated by, for example lentiviral transduction, can be used to permanently downregulate target gene expression.

9.2 CRISPR/CAS9 GENE KNOCKOUT (PAPER I)

In **paper I** we attempted CRISPR/Cas9 (clustered regularly interspaced short palindromic repeats/CRISPR-associated protein 9)-mediated CMKLR1 knockout in the neuroblastoma cell line SK-N-AS. CRISPR/Cas9 has revolutionized the field of genome editing and many additional applications beyond genome editing have been described [501]. In our work, we used commercially available sgRNA/Cas9 plasmids. Modifications to the supplied protocol were necessary as one of the difficulties we encountered was achieving sufficient transfection efficiency while maintaining cell viability. We, therefore, changed the transfection reagent from the supplied EndoFectin™Max (GeneCopoeia) to jetPRIME® (Polyplus-transfection®) since it resulted in higher transfection efficiency. Furthermore, SK-N-AS cells were very sensitive to mechanical stress and flow cytometry-based single cell sorting could not be utilized. Therefore, manual serial dilutions were made to establish clones derived from a single cell.

10 MMP ACTIVITY ASSAY (PAPER I)

Real-time zymography was used to study the degradation of gelatin by MMP-2 and MMP-9. The use of fluorescent (2-methoxy-2, 4-diphenyl-3(2H)-furanone (MDPF)-labeled) gelatin in the acrylamide gel allowed us to follow the degradation of gelatin by MMP-2 and MMP-9 in real time without additional staining of the gel. Areas of gelatinase activity (degradation of gelatin) were apparent as dark bands against the bright fluorescent background of undegraded gelatin.

11 *IN VIVO* STUDIES

11.1 XENOGRAFT MODEL (PAPER I)

Immunodeficient nude mice were used to investigate the effect of the CMKLR1 inhibitor α-NETA on the growth of SK-N-AS xenografts. This was an appropriate model to evaluate the effect of CMKLR1 inhibition on tumor cell growth *in vivo*. Nude mice are deficient of T cells due to a mutation in the transcription factor *FOXN1* required for thymus development [502-504]. T cells are important contributors to the TME, therefore, an immunocompetent mouse model would be more appropriate to study the effect of chemerin/CMKLR1 axis on the neuroblastoma microenvironment.

11.2 TH-MYCN TRANSGENIC MODEL (PAPER III)

The transgenic TH-MYCN model overexpresses human *MYCN* under the control of the rat tyrosine hydroxylase promoter (TH) in neuroectodermal cells causing tumors that resemble human neuroblastomas [505]. The tumors express neuronal markers (e.g. synaptophysin) and display neuronal differentiation at varying degrees. As an immunocompetent model, TH-MYCN mice are frequently used in immunological studies of neuroblastoma [417, 438]. Macroscopic metastases are occasionally observed in liver, lung, and ovaries of the TH-MYCN mice [505]. However, bone marrow involvement or bone metastases, which are frequently observed in neuroblastoma patients are rarely seen in TH-MYCN mice [359, 505]. A murine neuroblastoma model with pronounced secondary tumors in the bone marrow was recently developed [506]. Additional murine neuroblastoma models have been developed in the past years to extend the knowledge on neuroblastoma biology, among others, models expressing mutated ALK and a model resembling *MYCN* non-amplified tumors [415, 507-509].

SUMMARY OF MAIN RESULTS

PAPER I: Inhibition of chemerin/CMKLR1 axis in neuroblastoma cells reduces clonogenicity and cell viability *in vitro* and impairs tumor growth *in vivo*

A correlation between high *CMKLR1* and *GPR1* expression and a reduced overall survival probability was observed in two neuroblastoma gene expression cohorts. Chemerin, CMKLR1, and GPR1 protein were detected in a panel of neuroblastoma cell lines and tumor tissues. IL-1β, TNF-α, and serum increased the secretion of chemerin in SK-N-AS cells. Chemerin induced calcium mobilization, promoted phosphorylation of Akt and ERK1/2, and stimulated MMP-2 synthesis. The CMKLR1 antagonist α-NETA reduced the cell viability and clonogenicity of neuroblastoma cell lines. Furthermore, early and prolonged treatment of nude mice, carrying SK-N-AS xenografts with α-NETA impaired tumor growth *in vivo.*

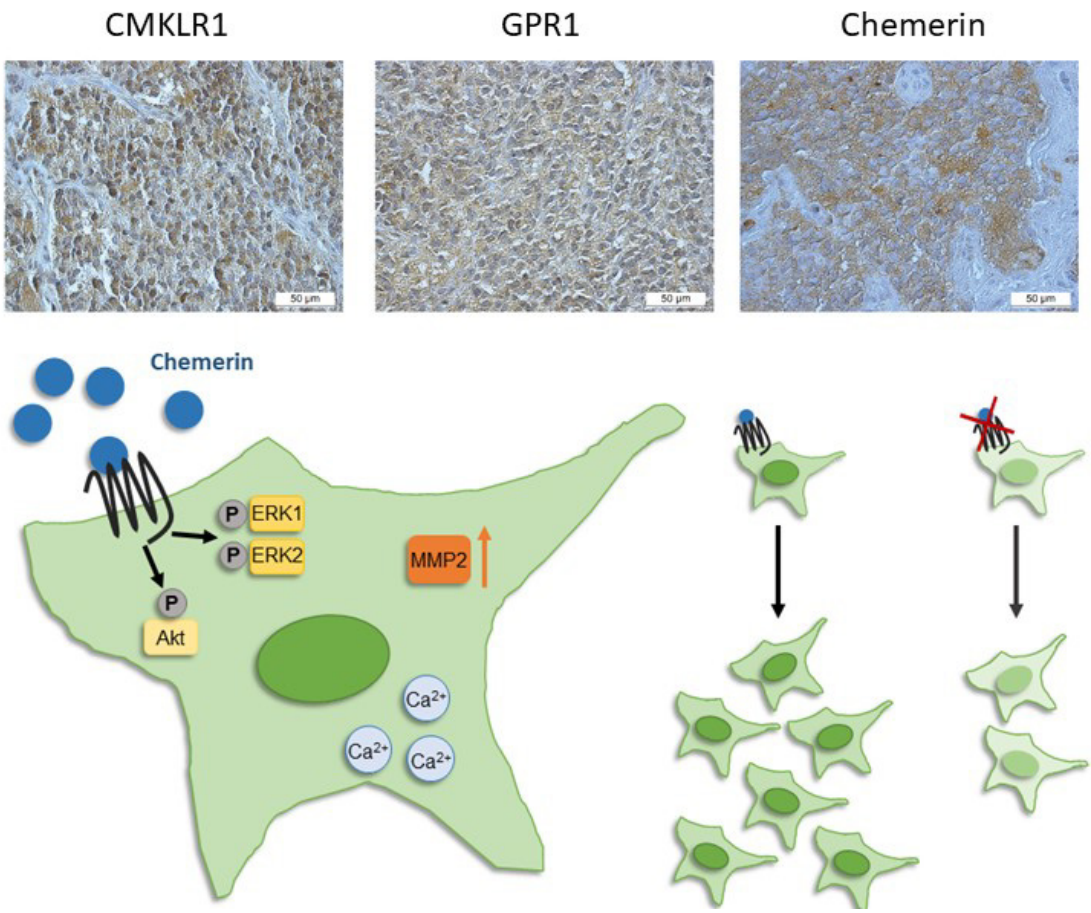

PAPER II: SYK inhibition potentiates the effect of chemotherapeutic drugs on neuroblastoma cells *in vitro*

SYK expression was elevated in neuroblastoma compared to neural crest and benign neurofibroma. SYK and phosphorylated SYK were observed in the majority of examined neuroblastoma tissues. *SYK* mRNA and less frequently SYK protein were detected in neuroblastoma cell lines. Phosphorylation at tyrosine 525/526, tyrosine 352, and tyrosine 323 was observed in SYK-expressing SH-SY5Y cells. The cell viability of SYK-positive neuroblastoma cells was reduced by siRNA-mediated SYK downregulation or SYK inhibition. In addition, Akt and ERK1/2 phosphorylation was reduced by SYK inhibition. The selective SYK inhibitor BAY 61-3606 enhanced the effect of chemotherapeutic drugs on SYK-expressing neuroblastoma cells illustrated by decreased cell viability and increased PARP cleavage. Furthermore, the cell viability of neuroblastoma cells was increased following transient expression of a constitutive active SYK variant independent of endogenous SYK levels.

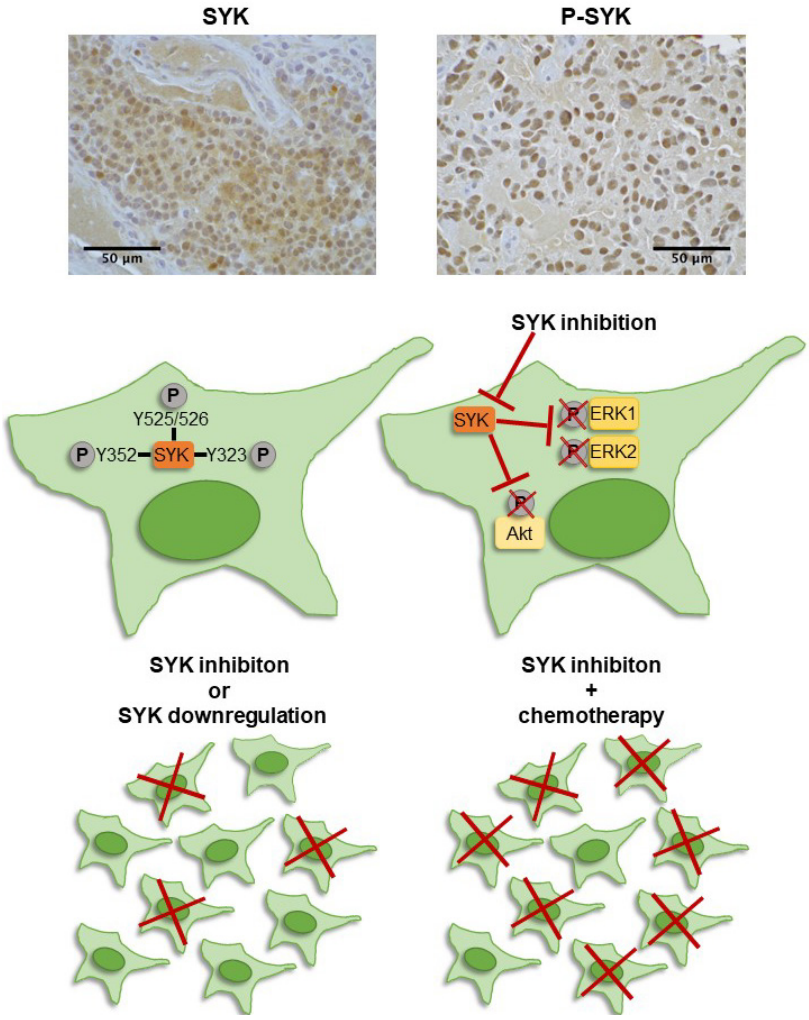

PAPER III: Interleukin 17 family and interleukin 23 in the neuroblastoma microenvironment

High expression of *IL17A*, *IL17B, IL17C*, *IL25 (IL17E)*, and *IL17F* and the receptors *IL17RA*, *IL17RB,* and *IL17RD* correlated with a reduced overall survival probability in a neuroblastoma expression cohort. IL-17RA, IL-17RB, and IL-17RC proteins were detected in neuroblastoma tissues and neuroblastoma cell lines. Recombinant IL-17A, IL-17A/F, IL-17B, and IL-25 stimulated the cell viability of neuroblastoma cell lines at varying degrees. Of note, high concentrations of IL-25 impaired the cell viability of neuroblastoma cell lines. In addition, IL-17A and IL-17B promoted *in vitro* migration of SK-N-BE(2) cells. IL-17A, IL-17B, and IL-25 modulated HGF secretion in SK-N-AS cells. Moreover, IL-25 increased Dkk-1 secretion in SK-N-AS cells while decreasing Dkk-1 secretion in SK-N-BE(2) cells. Furthermore, IL-23p19 was detected in neuroblastoma cell lines and tumor tissue. Additionally, different splice variants of *IL23A* were observed in neuroblastoma cell lines.

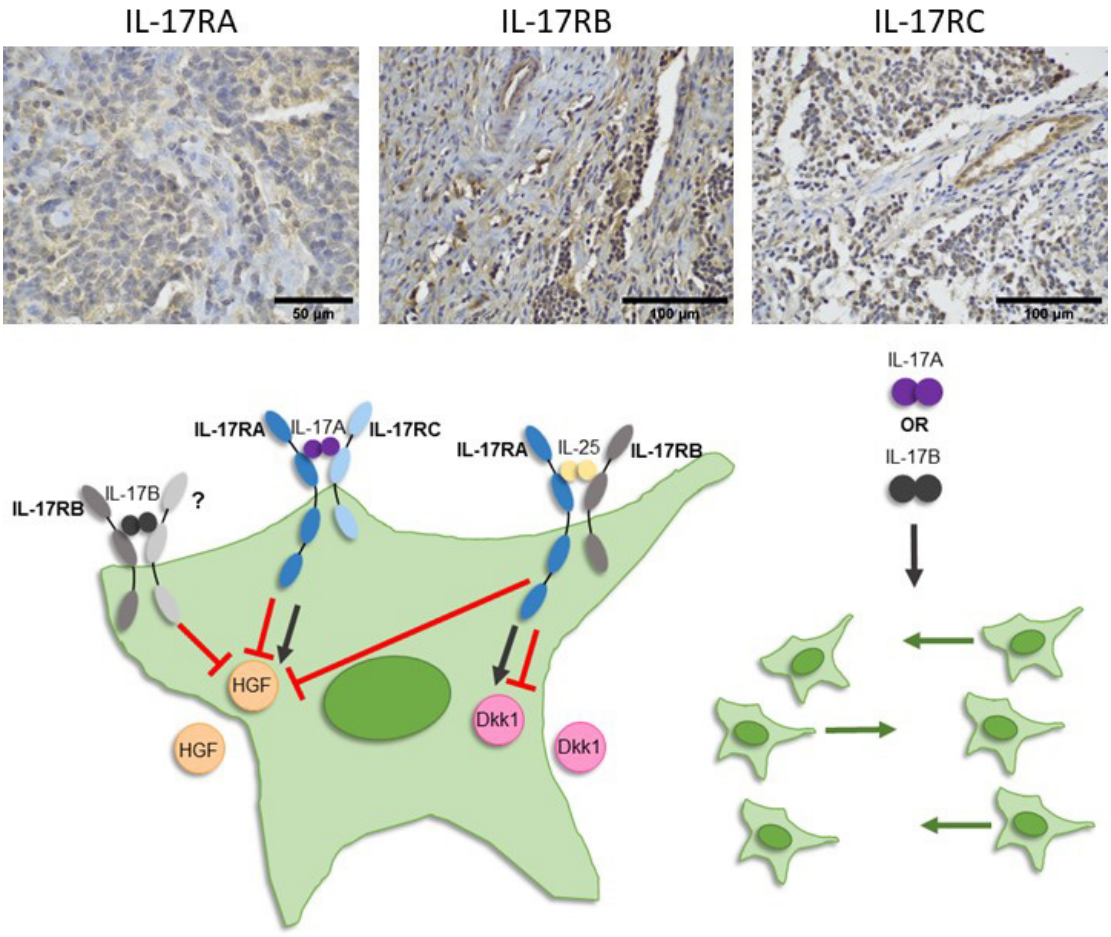

GENERAL DISCUSSION

In the past decades, great advances in the treatment of pediatric malignancies led to current 10-year survival rates of above 80% [350]. According to estimates, approximately 1 in 1000 individuals of the general adult population in high-income countries is a childhood cancer survivor [341, 342]. By 2020 the number of childhood cancer survivors in Europe may be as high as 500000 [343]. However, most childhood cancer survivors suffer from severe chronic health conditions and by the age of 45, the cumulative burden of chronic health conditions is twice as high as in the general population [350].

Neuroblastomas are tumors arising from the developing sympathetic nervous system and the most common malignancies during the first year of life [461]. As a biologically and clinically highly heterogeneous disease, the treatment of neuroblastoma is equally heterogeneous ranging from observation and surgery for low-risk tumors to intensive multimodal therapy for high-risk disease [461]. In consequence, a broad variety of late effect (therapy-related morbidities) is observed in neuroblastoma survivors, with severe chronic health conditions, such as heart, pulmonary and gonadal dysfunction, hearing loss, and secondary malignancies, occurring in patients that underwent intensive treatment protocols [510]. This underlines the necessity for improved and novel therapy approaches to reduce late effects and enable childhood cancer survivors to live a high-quality life.

Among the most promising new therapeutic approaches for neuroblastoma treatment are targeted therapies, among other, inhibitors of ALK, Aurora A and B, PI3K/Akt, and BET [471]. However, intrinsic or acquired resistance to targeted therapies is a well-established challenge and various combination strategies are emerging to utilize the full potential of targeted therapies [511]. A recent phase II clinical trial of the Aurora A kinase inhibitor alisertib in combination with irinotecan and temozolomide demonstrated antitumor activity especially in patients with *MYCN* non-amplified tumors [512]. Spleen tyrosine kinase (SYK) is a non-receptor tyrosine kinase and a promising therapeutic target in pediatric retinoblastoma and Ewing sarcoma [335, 336]. Recently, the first SYK inhibitor Fostamatinib was approved by the US Food and Drug Administration for use in chronic immune thrombocytopenia [330].

In **paper II** we evaluated the efficacy of SYK inhibition in combination with chemotherapeutic drugs in neuroblastoma cell lines. We observed a more pronounced inhibitory effect on cell viability when SYK inhibition was combined with chemotherapy. Combinations of targeted therapies, conventional therapy, and immunotherapy may allow the use of lower doses and lead to a reduction in late effects. Furthermore, targeted therapies hold great promise for patients that cannot be treated with conventional therapies. This was recently observed in a neuroblastoma patient with DNA repair defects that resulted in severe toxicities in response to chemotherapy. The identification of a gain-of-function ALK mutation allowed the successful treatment of the patient with the ALK inhibitor ceritinib [513].

In **paper II**, we established the presence of SYK in neuroblastoma cell lines and tumor tissue and demonstrated that SYK inhibition reduces neuroblastoma cell viability and Akt- and ERK-phosphorylation. Furthermore, we observed that chemotherapeutic drugs affect SYK levels in neuroblastoma cells. SYK is a multifunctional kinase that can support but also suppress tumor growth in different cancers [331]. Novel functions of SYK in tumor cells and also other cells present in the TME are constantly emerging. Recently, SYK has been implicated in mesenchymal to epithelial transition and metastatic growth in breast cancer [334]. SYK participation has also been described in the regulation of energy metabolism as SYK inhibition promoted a shift from glycolysis to oxidative phosphorylation (anti-Warburg effect) in glioma stem cells [514]. Yu et al. previously linked SYK function to migration and invasion of ovarian cancer cells as it phosphorylates the actin binding proteins cortactin and cofilin, which are involved in actin assembly and the formation of invadopodia [338]. Interestingly, a chemerin/CMKLR1/SYK signaling axis has previously been described in macrophages in connection to actin polymerization and phagocytosis [515]. In **paper I** we investigated the chemerin/CMKLR1 axis in neuroblastoma, but a potential link between chemerin/CMKLR1 and SYK remains to be investigated. Furthermore, there is increasing evidence that inhibition of SYK in tumor-supporting immune cells, can contribute to the overall tumor-suppressing effects of SYK inhibition [339, 516]. Metastatic disease is detected in approximately 50% of patients at diagnosis, with bone and bone marrow being the major metastatic sites [359]. Studies in a preclinical prostate cancer model demonstrated that SYK

supported bone metastasis formation whereas SYK depletion by knockdown and overexpression of a kinase dead SYK variant reduced the metastatic burden [517]. Consequently, further studies (both *in vitro* and *in vivo*) are needed to determine the specific functions of SYK in the neuroblastoma microenvironment and the efficacy of SYK inhibition both alone and in combination with conventional therapies.

The tumor microenvironment is composed of tumor cells, immune cells, stromal cells, and the ECM whose complex interactions evolve constantly to support the growing tumor [8, 10]. Inflammation is an indispensable defense mechanism against harmful stimuli and an essential factor of antitumor immunity [140]. However, chronic inflammatory processes in the TME can essentially support all stages of tumor growth and can be considered a hallmark of cancer [137, 139]. A thorough understanding of the inflammatory processes in the TME is therefore required to target excessive tumor-promoting inflammation while supporting inflammatory processes essential to anti-tumor immunity, basically walking a tightrope. In **paper I and III** we investigated the chemerin/CMKLR1 axis and the IL-17 family with the aim to expand the knowledge on inflammatory mediators and pathways in the neuroblastoma microenvironment.

Chemerin is a versatile chemoattractant protein with context-dependent functions, and both tumor-promoting and tumor-suppressing functions of chemerin have been described [299]. Chemerin undergoes extensive post-secretory processing resulting in isoforms with varying activity [293]. In **paper I** we demonstrated that chemerin is secreted by neuroblastoma cells, however, we did not determine the presence of specific chemerin isoforms. To our knowledge, there are to date no isoform-specific chemerin antibodies commercially available. However, mass spectrometric analyses could be performed to determine chemerin isoforms and/or the presence of specific proteases that may mediate chemerin cleavage. Chemerin binds to three G protein-coupled receptors (CMKLR1, GPR1, and CCRL2) [294-296]. While CMKLR1 is the most studied chemerin receptor, functions for GPR1 and CCRL2 in the TME are emerging. Recently GPR1 was implicated in migration and invasion of gastric cancer cells [321]. Furthermore, CCRL2 (and CMKLR1) have been demonstrated to mediate a chemerin-induced downregulation of IL-6 and GM-CSF and to reduce MDSC infiltration in hepatocellular carcinoma [307]. In **paper I** we describe the

presence of CMKLR1 and GPR1 protein in neuroblastoma cell lines and tumor tissues as well as *CCRL2* mRNA in neuroblastoma cell lines. However, further studies are necessary to determine whether the observed chemerin functions are mediated by CMKLR1 and/or GPR1 and if CCRL2 protein is present and functional in neuroblastoma. As a chemoattractant, chemerin's function in the TME is often not only associated with its direct effects on tumor cells but also effects on immune cells and stromal cells [299]. For example, anti-tumorigenic effects of chemerin have been linked to the recruitment of NK cells in melanoma and also NK cells and CD8+ T cell in breast cancer [309, 518]. Furthermore, chemerin promotes proliferation and migration of endothelial cells and vessel formation [287, 519]. In **paper I** we investigated the effect of CMKLR1 inhibition on tumor growth in a neuroblastoma xenograft model. However, further studies, particularly in immunocompetent mice are warranted to determine potential functions of chemerin and its receptors on the neuroblastoma microenvironment with focus on immune cell infiltration and angiogenesis. In our studies, we observed that IL-1β promotes chemerin secretion. A pilot study in **paper III** indicates increased levels of IL-1β in tumors and serum of tumor-bearing TH-MYCN transgenic mice. A possible *in vivo* link between IL-1β and chemerin could, therefore, be investigated using the TH-MYCN murine model. Of note, recent work by Fultang et al. demonstrates increased IL-1β expression in stage 4 compared to stage 1 neuroblastomas and a correlation between high *IL1B* expression and a poor overall survival [520]. In their work, macrophages were identified as the source of IL-1β and TNFα [520].

The IL-17 family consist of six cytokines with important functions in immunity and host defense but also autoimmunity and cancer [200]. In **paper III** we examined the expression and prognostic implications of the IL-17 cytokines A-F and their receptors RA-RE. Furthermore, we aimed to gain insight into potential functions in neuroblastoma tumorigenesis. However, considering the multifunctional nature of the IL-17 family, we hardly scratched the surface. The most intensely studied family member IL-17A, which occurs as IL-17A homodimers and IL-17A/F heterodimers, was discovered over 25 years ago and is a versatile cytokine with highly context dependent functions [209, 521, 522]. In **paper III** we demonstrate the expression of the IL-17A receptors RA and RC in neuroblastoma cell lines and tumor tissue. We observed

modest effects of IL-17A or the IL-17A/F heterodimer on the cell viability of certain neuroblastoma cell lines. Furthermore, we found that IL-17A could modulate HGF secretion and *in vitro* cell migration. Interestingly, the effect of IL-17A and IL-17A/F differed between cell lines and more extensive studies are needed to investigate the cell-line specific effects in depth. It has previously been noted in different cell systems that while the *in vitro* effects of IL-17A can be relatively modest more pronounced *in vivo* effects occur [200]. IL-17A has strong immunomodulatory effects and both pro-tumorigenic and anti-tumorigenic functions of IL-17A have been linked to immune cell recruitment (e.g. T cells, NK cells, DCs neutrophils, and MDSCs) and their functional activation or impairment [217]. Furthermore, IL-17 can promote tumor cell proliferation, migration, angiogenesis, and metastasis [217]. *In vivo* studies are therefore necessary to obtain a more complete picture of IL-17A functions in the neuroblastoma TME.

Recently, IL-17RD was identified as an additional functional receptor for IL-17A indicating there might be receptor-ligand combinations that have so far not been discovered [207]. Of note, we observed *IL17RD* mRNA in the majority of neuroblastoma cell lines and the presence of IL-17RD protein and its functions could be an interesting subject for a new study especially with respect to the positive correlation between *IL17RD* and *MYCN* expression we observed in **paper III**.

Differentiation therapy using 13-cis-retinoic acid (isotretinoin) is part of the maintenance regimen for high-risk neuroblastomas [461]. In recent work in pancreatic ductal adenocarcinoma, it was demonstrated that retinoic acid produced by DCs as well as other cells in the TME, modulates the balance between Tregs and IL-17A-producing helper cells and that ATRA (all-trans retinoic acid) attenuates IL-17A and IFN-γ secretion [523]. Various immune modulatory functions have been described for retinoic acid [524]. In the context of neuroblastoma, it has previously been established that retinoids sensitize tumor cells to lysis by CTLs [525]. Further studies could be of interest to investigate the effect of retinoids on the neuroblastoma TME especially with respect to IL-17A.

The COX-2/mPGES/PGE_2 axis is a well-established contributor to neuroblastoma tumorigenesis [420, 421, 433, 434, 436, 437]. Interestingly, PGE_2 can modulate Th17 differentiation and IL-17A secretion [526-529]. Furthermore, IL-17A

has been shown to upregulate COX-2 in cancer cell lines [530]. In addition, PGE_2 can stimulate IL-23 production in, among other, breast cancer cells and dendritic cells [531-534]. A potential link between PGE_2, IL-23, and IL-17 in the neuroblastoma TME may, therefore, be examined. In **paper II** we investigated SYK as a potential therapeutic target in neuroblastoma. Interestingly, SYK has been described as a mediator of IL-17A signaling in keratinocytes and multiple myeloma cells [535, 536].

IL-17A and IL-17F are cytokines at the crossroads of innate and adaptive immunity as they are produced by adaptive immune cells (Th17), innate immune cells (ILC3, NK cells) and cells associated with both innate and adaptive immunity (NKT, γδ T cells) [212]. γδ T cells can target cells without co-stimulation and MHC-restriction suggesting they have an application in cancers with low mutational loads, such as many pediatric malignancies including neuroblastoma [60, 347]. The efficacy of γδ T cell-mediated neuroblastoma cell killing in combination with anti-GD2 or Zolendronate has been demonstrated *in vitro* and in immunodeficient mouse models [537-540]. Although no effect was observed on the production of a panel of cytokines, including IL-17A, in a co-culture study of neuroblastoma cell lines and different γδ T cell subsets, potential effects on cytokine production in the TME were not evaluated [537, 538]. Furthermore, in a recent study GD2 CAR γδ T cells (vδ1 and vδ2) displayed specific neuroblastoma cell lysis [541]. However, further studies are required to determine the efficacy of GD2 CAR γδ T cells and potential microenvironmental effects *in vivo*. A phase 1 study by Pressey et al. evaluated the safety of γδ T cell expansion using Zolendronate and IL-2 in four refractory neuroblastoma patients [542]. Of note, when compared to healthy controls γδ T cell levels were significantly decreased in neuroblastoma patients. Although the treatment was well tolerated only a slight increase in γδ T cells was observed. In addition, an increase in Tregs was also seen. However, the small number of heavily treated patients made it difficult to observe clear trends and the article does not indicate whether cytokine analyses were performed. Furthermore, a recent study by Zoine et al. demonstrated the efficacy of neuroblastoma patient-derived and *ex vivo* expanded γδ T cells against neuroblastoma cells, which was further increased by the addition of dinutuximab [540]. In a neuroblastoma xenograft model, a combination of γδ T cells, dinutuximab and temozolomide reduced tumor growth significantly compared to untreated tumors

or either monotherapy [540]. However, the article did not indicate whether IL-17 expression was examined in the study.

Although the remaining IL-17 family members have to date been less extensively studied, cancer-related functions have been described for all of them. The IL-17B/RB axis has been demonstrated to promote tumor cell survival, migration, metastasis, and chemokine expression [238-243]. In **paper III** we observed that high expression of *IL17B* and *IL17RB* correlated with a reduced overall survival probability in neuroblastoma. We detected the presence of IL-17RB protein in neuroblastoma cell lines and tissue and of *IL17B* RNA in neuroblastoma cell lines. IL-17B promoted the cell viability of neuroblastoma cell lines, the *in vitro* migration of SK-N-BE(2) cells, and reduced HGF secretion from SK-N-AS cells. Our data indicates the presences of a functional IL-17B/RB axis in neuroblastoma cells whose role in tumorigenesis should be further explored.

IL-17C can promote tumor cell survival, angiogenesis, and the recruitment of TANs [247, 248]. Interestingly, neurotrophic effects have been described for IL-17C in the peripheral nervous system where it promotes neurite growth and branching and has a protective effect during virus reactivation [543]. In **paper III** we noticed that high *IL17C* expression correlates with a lower overall survival probability in neuroblastoma and that *IL17RC* mRNA was present in some of the examined neuroblastoma cell lines. Furthermore, expression of the IL-17C receptors IL-17RA (mRNA and protein) and *IL17RE* (mRNA) was observed in the majority of neuroblastoma cell lines. Of note, high expression of *IL17RE* correlated with a higher overall survival probability. Further studies are warranted to determine potential functions of the IL-17C/IL-17RA/RE axis in neuroblastoma especially with respect to the previously described neurotrophic effect of IL-17C.

Although the receptor for IL-17D is not yet identified, IL-17D has been demonstrated to promote NK cell recruitment and tumor rejection in preclinical glioma and prostate cancer models [251]. In our study, we observed that high *IL17D* expression correlates to a higher neuroblastoma overall survival and that *IL17D* mRNA was present in the majority of the examined neuroblastoma cells. IL-17D knockdown or overexpression studies could give indications toward IL-17D functions in neuroblastoma even though the receptor is to date unknown.

IL-17E was given a different name, IL-25, to emphasize its distinct functions in promoting type II immunity [200]. Opposing functions of IL-25 and other IL-17 family members have previously been described [237, 259]. For example, while IL-25 promoted colon inflammation and allergic asthma, IL-17B displayed anti-inflammatory effects [237]. Moreover, IL-17B reduced IL-25-induced IL-6 expression likely by blocking their shared receptor IL-17RB [237]. In our work, we observed that high concentrations of IL-25 impaired the cell viability of neuroblastoma cells lines, in particular of SK-N-DZ cells after 72h. Furthermore, we noted that while low concentrations of IL-17A, IL-17B, and IL-25 reduced HGF secretion, high concentrations of IL-17A stimulated the secretion of HGF in contrast to IL-17B and IL-25. Furthermore, we found that IL-25 had opposite effects on Dkk-1 secretion in SK-N-AS and SK-N-BE(2) cells.

IL-17F is mainly co-produced with IL-17A and functional redundancy is often observed [212, 544]. However, differences in activity and distinct functions have also been described [212]. Recently, co-culture studies demonstrated that malignant T cell-derived IL-17F promoted sprouting and tube formation in HUVEC cells [545]. In **paper III** we observed that high *IL17F* expression correlated with a reduced overall survival probability in neuroblastoma and that recombinant IL-17A/F moderately promoted the cell viability of certain neuroblastoma cell lines.

Our data indicate overlapping but also distinct effects of IL-17 family members in neuroblastoma that are likely cell-type and context dependent. Additional work is necessary to explore cytokine- and cell type- specific effects further, and evaluate the presence of reoccurring patterns.

Studies of autoimmune disorders indicate that the functions of the IL-23/IL-17A axis are complex, fine-tuned, and highly context dependent [173]. While the blockade of IL-17A or IL-17RA alleviates the symptoms of psoriasis patients, blockade of IL-17A can exacerbate Crohn's disease [173, 212]. Furthermore, work in a colitis murine model demonstrated that the blockade of IL-23 improved symptoms while the IL-17A blockade worsened the disease [546]. IL-17A contributes to the maintenance of barrier integrity in the gut and following acute injury, the production of IL-17A by γδ T cells is IL-23-independent [214]. In this context, Teng et al. suggested that IL-23 blockade may eliminate excessive disease-related IL-17A while not affecting

protective IL-17A in the gut [189]. These findings underline that the presence and function of IL-23 should be taken into consideration when studying IL-17A (and IL-17F) in any specific context.

IL-23 stabilizes Th17 populations and promotes the secretion of IL-17A from Th17, γδ T cells, ILC3, NKT and NK cells [212]. Recently, lung cancer cell-derived IL-23 was shown to convert ILC1 to ILC3 cells promoting IL-17A production and subsequent IL-17-dependent tumor cell proliferation [193]. Furthermore, cervical fibroblasts stimulate IL-23 production in cervical cancer-educated DCs consequently promoting Th17 expansion [196]. These examples demonstrate the complexity of the IL-23/IL-17 axis in the TME. In **paper III** we demonstrate the presence of IL-23p19 in neuroblastoma cell lines and tumor tissue. However, *in vivo* studies are indispensable to investigate the role of IL-23/IL-17 in the neuroblastoma microenvironment. In a pilot study, we observed the presence of IL-23 in myeloid cells and tumor-stroma cells in the TH-MYCN mouse model, indicating this model may be suitable to study IL-23 function in neuroblastoma using IL-23-specifc antibodies to block its function.

With a median age of 18 months at diagnosis, neuroblastoma is a malignancy of early childhood [354]. Children are not small adults and potential differences in immunological and inflammatory processes during tumorigenesis should be considered when studying embryonal and pediatric malignancies. System immunology studies have expanded our knowledge on immune system changes in early life. After birth, the immune system undergoes dramatic changes. For example, high MDSC and Breg numbers that are abundantly observed in cord blood after birth decrease quickly and in addition, a slow reduction of neutrophils is observed whereas CD4+ and CD8+ T cells gradually increase [547]. Moreover, the first three months of life are important for B cells, NK cells, and DCs as adult-like phenotypes are developing [547]. Tregs are observed early in the thymus during fetal development and can be detected in the blood of newborns [548]. Interestingly, cord blood-derived γδ T cells express more diverse combinations of Vγ and Vδ TCR chains and while Vδ1+ T cells are the predominant subset in early life Vγ9Vδ2+ T cell are the main subset in adult blood and Vδ1+ T cells occur in skin and mucosa [60, 549]. In addition, it has been suggested that γδ T cell function compensates for the relative immaturity of the αβ compartment at birth as they display stronger functional responsiveness including IFN-γ production

[550]. Furthermore, the T helper cell response is skewed towards Th2 in newborns [548, 551]. This may in part be attributed to decreased IL-12 levels, resulting from reduced transcription of the p35 subunit in DCs [552, 553]. In consequence, cord neonatal innate immune cells secrete less IL-12, IFN-α, and IFN-γ (Th1 polarizing cytokines) and more IL-6, IL-1β, and IL-23 (Th17 polarization) as well as IL-10 in response to TLR engagement [554]. Vanden Eijnden et al. demonstrated that neonatal DCs secrete functional IL-23 in response to TLR-ligands and that LPS-stimulated DCs induced IL-17 production in neonatal $CD8^+$ T cells [555]. In conclusion, the authors suggested that "a functional IL-23/IL-17 axis might compensate a suboptimal IL-12/IFN-γ pathway in early life". Moreover, Olin et al. observed elevated levels of IL-17A and IL-12B (IL-12p40) in stage 4 and 5; distinct developmental stages where stage 5 corresponds to 3 months of age [547]. Collectively, these studies suggest that the IL-23/IL-17 axis may have important functions in early life immunity. Interestingly, IL-12 has previously been demonstrated to promote anti-tumor immunity in neuroblastoma mouse models [556-558]. Considering that IL-12 and IL-23 can exert opposing effects in tumorigenesis [194] more research on the IL-23/IL-17 axis and IL-12 in neuroblastoma a warranted.

CONCLUSION

Despite continuing therapeutic advances, the survival of high-risk neuroblastoma patients remains poor. Neuroblastoma is a malignancy of early childhood and survivors often experience severe chronic health conditions later in life. The aim of neuroblastoma therapy is, therefore, to improve the survival of neuroblastoma patients while reducing treatment-related morbidities to ensure a high and lasting quality of life.

A thorough understanding of the neuroblastoma microenvironment and associated inflammatory pathways contributes to the understanding of the disease and can thereby lead to the discovery of novel therapeutic approaches and the improvement of existing therapies. The tumor microenvironment is a complicated jigsaw puzzle and only when we turn around enough pieces and fit them together a clear picture will emerge. With this work, I hope to contribute some small pieces to the puzzle of neuroblastoma biology.

REFERENCES

1. Varmus H. NIH cancer chief wants more with less: by Meredith Wadman. Nature. 2011;475(7354):18.
2. Varmus HE. Nobel Prize Banquet speech NobelPrize.org. Nobel Media AB 2018. Wed. 22 Aug 2018.1989 [Available from: https://www.nobelprize.org/prizes/medicine/1989/varmus/speech/.
3. Hanahan D, Weinberg RA. The hallmarks of cancer. Cell. 2000;100(1):57-70.
4. Hanahan D, Weinberg RA. Hallmarks of cancer: the next generation. Cell. 2011;144(5):646-74.
5. Fouad YA, Aanei C. Revisiting the hallmarks of cancer. Am J Cancer Res. 2017;7(5):1016-36.
6. Strebhardt K, Ullrich A. Paul Ehrlich's magic bullet concept: 100 years of progress. Nature reviews Cancer. 2008;8(6):473-80.
7. World Health Organization. http://www.who.int/news-room/fact-sheets/detail/cancer 2018 [
8. Balkwill FR, Capasso M, Hagemann T. The tumor microenvironment at a glance. Journal of cell science. 2012;125(Pt 23):5591-6.
9. Barcellos-Hoff MH, Lyden D, Wang TC. The evolution of the cancer niche during multistage carcinogenesis. Nature reviews Cancer. 2013;13(7):511-8.
10. Quail DF, Joyce JA. Microenvironmental regulation of tumor progression and metastasis. Nature medicine. 2013;19(11):1423-37.
11. Connolly JL, Schnitt SJ, Wang HH, Longtine JA, Dvorak A, Dvorak HF. Tumor Structure and Tumor Stroma Generation. In: Kufe D, Pollock R, Weichselbaum Rea, editors. Holland-Frei Cancer Medicine. 6th ed. Hamilton, Ont. ; Lewiston, NY: BC Decker; 2003.
12. Binnewies M, Roberts EW, Kersten K, Chan V, Fearon DF, Merad M, et al. Understanding the tumor immune microenvironment (TIME) for effective therapy. Nature medicine. 2018;24(5):541-50.
13. Fridman WH, Pages F, Sautes-Fridman C, Galon J. The immune contexture in human tumours: impact on clinical outcome. Nature reviews Cancer. 2012;12(4):298-306.
14. Bindea G, Mlecnik B, Tosolini M, Kirilovsky A, Waldner M, Obenauf AC, et al. Spatiotemporal dynamics of intratumoral immune cells reveal the immune landscape in human cancer. Immunity. 2013;39(4):782-95.
15. Gentles AJ, Newman AM, Liu CL, Bratman SV, Feng WG, Kim D, et al. The prognostic landscape of genes and infiltrating immune cells across human cancers. Nature medicine. 2015;21(8):938-45.
16. Thorsson V, Gibbs DL, Brown SD, Wolf D, Bortone DS, Ou Yang TH, et al. The Immune Landscape of Cancer. Immunity. 2018.
17. Reiser J, Banerjee A. Effector, Memory, and Dysfunctional CD8(+) T Cell Fates in the Antitumor Immune Response. J Immunol Res. 2016;2016:8941260.
18. Martinez-Lostao L, Anel A, Pardo J. How Do Cytotoxic Lymphocytes Kill Cancer Cells? Clin Cancer Res. 2015;21(22):5047-56.
19. Chraa D, Naim A, Olive D, Badou A. T lymphocyte subsets in cancer immunity: Friends or foes. J Leukoc Biol. 2019;105(2):243-55.
20. Knochelmann HM, Dwyer CJ, Bailey SR, Amaya SM, Elston DM, Mazza-McCrann JM, et al. When worlds collide: Th17 and Treg cells in cancer and autoimmunity. Cell Mol Immunol. 2018;15(5):458-69.
21. Perusina Lanfranca M, Lin Y, Fang J, Zou W, Frankel T. Biological and pathological activities of interleukin-22. J Mol Med (Berl). 2016;94(5):523-34.
22. Qin L, Waseem TC, Sahoo A, Bieerkehazhi S, Zhou H, Galkina EV, et al. Insights Into the Molecular Mechanisms of T Follicular Helper-Mediated Immunity and Pathology. Front Immunol. 2018;9:1884.
23. Togashi Y, Shitara K, Nishikawa H. Regulatory T cells in cancer immunosuppression - implications for anticancer therapy. Nature reviews Clinical oncology. 2019.
24. Chitadze G, Oberg HH, Wesch D, Kabelitz D. The Ambiguous Role of gammadelta T Lymphocytes in Antitumor Immunity. Trends Immunol. 2017;38(9):668-78.
25. Wu D, Wu P, Qiu F, Wei Q, Huang J. Human gammadeltaT-cell subsets and their involvement in tumor immunity. Cell Mol Immunol. 2017;14(3):245-53.

26. Prenen H, Mazzone M. Tumor-associated macrophages: a short compendium. Cell Mol Life Sci. 2019.
27. Mosser DM, Edwards JP. Exploring the full spectrum of macrophage activation. Nature Reviews Immunology. 2008;8(12):958-69.
28. Groth C, Hu X, Weber R, Fleming V, Altevogt P, Utikal J, et al. Immunosuppression mediated by myeloid-derived suppressor cells (MDSCs) during tumour progression. British journal of cancer. 2019;120(1):16-25.
29. Gabrilovich DI. Myeloid-Derived Suppressor Cells. Cancer Immunol Res. 2017;5(1):3-8.
30. Chiossone L, Dumas PY, Vienne M, Vivier E. Natural killer cells and other innate lymphoid cells in cancer. Nature reviews Immunology. 2018;18(11):671-88.
31. Paul S, Lal G. The Molecular Mechanism of Natural Killer Cells Function and Its Importance in Cancer Immunotherapy. Frontiers in Immunology. 2017;8.
32. Terabe M, Berzofsky JA. Tissue-Specific Roles of NKT Cells in Tumor Immunity. Front Immunol. 2018;9:1838.
33. Veglia F, Gabrilovich DI. Dendritic cells in cancer: the role revisited. Curr Opin Immunol. 2017;45:43-51.
34. Galdiero MR, Varricchi G, Loffredo S, Mantovani A, Marone G. Roles of neutrophils in cancer growth and progression. J Leukoc Biol. 2018;103(3):457-64.
35. Liu M, Sun Q, Wang J, Wei F, Yang L, Ren X. A new perspective: Exploring future therapeutic strategies for cancer by understanding the dual role of B lymphocytes in tumor immunity. International journal of cancer Journal international du cancer. 2018.
36. Bruchard M, Ghiringhelli F. Deciphering the Roles of Innate Lymphoid Cells in Cancer. Front Immunol. 2019;10:656.
37. Varricchi G, Galdiero MR, Loffredo S, Marone G, Iannone R, Marone G, et al. Are Mast Cells MASTers in Cancer? Front Immunol. 2017;8:424.
38. Galon J, Costes A, Sanchez-Cabo F, Kirilovsky A, Mlecnik B, Lagorce-Pages C, et al. Type, density, and location of immune cells within human colorectal tumors predict clinical outcome. Science. 2006;313(5795):1960-4.
39. Pages F, Mlecnik B, Marliot F, Bindea G, Ou FS, Bifulco C, et al. International validation of the consensus Immunoscore for the classification of colon cancer: a prognostic and accuracy study. Lancet. 2018;391(10135):2128-39.
40. Angell H, Galon J. From the immune contexture to the Immunoscore: the role of prognostic and predictive immune markers in cancer. Curr Opin Immunol. 2013;25(2):261-7.
41. Gajewski TF, Schreiber H, Fu YX. Innate and adaptive immune cells in the tumor microenvironment. Nature immunology. 2013;14(10):1014-22.
42. Turley SJ, Cremasco V, Astarita JL. Immunological hallmarks of stromal cells in the tumour microenvironment. Nature reviews Immunology. 2015;15(11):669-82.
43. Thommen DS, Schumacher TN. T Cell Dysfunction in Cancer. Cancer cell. 2018;33(4):547-62.
44. Topalian SL, Drake CG, Pardoll DM. Immune checkpoint blockade: a common denominator approach to cancer therapy. Cancer cell. 2015;27(4):450-61.
45. Carreno BM, Collins M. The B7 family of ligands and its receptors: new pathways for costimulation and inhibition of immune responses. Annu Rev Immunol. 2002;20:29-53.
46. Wherry EJ. T cell exhaustion. Nature immunology. 2011;12(6):492-9.
47. Mazzarella L, Duso BA, Trapani D, Belli C, D'Amico P, Ferraro E, et al. The evolving landscape of 'next-generation' immune checkpoint inhibitors: A review. European journal of cancer. 2019;117:14-31.
48. Buchbinder EI, Desai A. CTLA-4 and PD-1 Pathways: Similarities, Differences, and Implications of Their Inhibition. Am J Clin Oncol. 2016;39(1):98-106.
49. Nghiem PT, Bhatia S, Lipson EJ, Kudchadkar RR, Miller NJ, Annamalai L, et al. PD-1 Blockade with Pembrolizumab in Advanced Merkel-Cell Carcinoma. The New England journal of medicine. 2016;374(26):2542-52.
50. Tang J, Yu JX, Hubbard-Lucey VM, Neftelinov ST, Hodge JP, Lin Y. Trial watch: The clinical trial landscape for PD1/PDL1 immune checkpoint inhibitors. Nature reviews Drug discovery. 2018;17(12):854-5.
51. Chan DV, Gibson HM, Aufiero BM, Wilson AJ, Hafner MS, Mi QS, et al. Differential CTLA-4 expression in human CD4+ versus CD8+ T cells is associated with increased NFAT1 and inhibition of CD4+ proliferation. Genes Immun. 2014;15(1):25-32.

52. Zhu JF, Yamane H, Paul WE. Differentiation of Effector CD4 T Cell Populations. Annu Rev Immunol. 2010;28:445-89.
53. Dong C. TH17 cells in development: an updated view of their molecular identity and genetic programming. Nature reviews Immunology. 2008;8(5):337-48.
54. Stritesky GL, Yeh N, Kaplan MH. IL-23 promotes maintenance but not commitment to the Th17 lineage. Journal of immunology. 2008;181(9):5948-55.
55. Lee YK, Turner H, Maynard CL, Oliver JR, Chen D, Elson CO, et al. Late developmental plasticity in the T helper 17 lineage. Immunity. 2009;30(1):92-107.
56. Muranski P, Restifo NP. Essentials of Th17 cell commitment and plasticity. Blood. 2013;121(13):2402-14.
57. Halvorsen EC, Mahmoud SM, Bennewith KL. Emerging roles of regulatory T cells in tumour progression and metastasis. Cancer Metast Rev. 2014;33(4):1025-41.
58. Yang XO, Nurieva R, Martinez GJ, Kang HS, Chung Y, Pappu BP, et al. Molecular antagonism and plasticity of regulatory and inflammatory T cell programs. Immunity. 2008;29(1):44-56.
59. Quezada SA, Simpson TR, Peggs KS, Merghoub T, Vider J, Fan X, et al. Tumor-reactive CD4(+) T cells develop cytotoxic activity and eradicate large established melanoma after transfer into lymphopenic hosts. The Journal of experimental medicine. 2010;207(3):637-50.
60. Lo Presti E, Pizzolato G, Corsale AM, Caccamo N, Sireci G, Dieli F, et al. gammadelta T Cells and Tumor Microenvironment: From Immunosurveillance to Tumor Evasion. Front Immunol. 2018;9:1395.
61. Tosolini M, Pont F, Poupot M, Vergez F, Nicolau-Travers ML, Vermijlen D, et al. Assessment of tumor-infiltrating TCRVgamma9Vdelta2 gammadelta lymphocyte abundance by deconvolution of human cancers microarrays. Oncoimmunology. 2017;6(3):e1284723.
62. Gentles AJ, Newman AM, Liu CL, Bratman SV, Feng W, Kim D, et al. The prognostic landscape of genes and infiltrating immune cells across human cancers. Nature medicine. 2015;21(8):938-45.
63. Lo Presti E, Dieli F, Meraviglia S. Tumor-infiltrating gamma delta T lymphocytes: pathogenic role, clinical significance, and differential programing in tumor microenvironment. Frontiers in Immunology. 2014;5.
64. Fournie JJ, Sicard H, Poupot M, Bezombes C, Blanc A, Romagne F, et al. What lessons can be learned from gamma delta T cell-based cancer immunotherapy trials? Cellular & Molecular Immunology. 2013;10(1):35-41.
65. Rei M, Goncalves-Sousa N, Lanca T, Thompson RG, Mensurado S, Balkwill FR, et al. Murine CD27((-)) V gamma 6((+)) gamma delta T cells producing IL-17A promote ovarian cancer growth via mobilization of protumor small peritoneal macrophages. P Natl Acad Sci USA. 2014;111(34):E3562-E70.
66. Ma SB, Cheng Q, Cai YF, Gong HL, Wu Y, Yu X, et al. IL-17A Produced by gamma delta T Cells Promotes Tumor Growth in Hepatocellular Carcinoma. Cancer research. 2014;74(7):1969-82.
67. Wu P, Wu D, Ni C, Ye J, Chen W, Hu G, et al. gamma delta T17 Cells Promote the Accumulation and Expansion of Myeloid-Derived Suppressor Cells in Human Colorectal Cancer. Immunity. 2014;40(5):785-800.
68. Ribot JC, Ribeiro ST, Correia DV, Sousa AE, Silva-Santos B. Human gamma delta Thymocytes Are Functionally Immature and Differentiate into Cytotoxic Type 1 Effector T Cells upon IL-2/IL-15 Signaling. Journal of immunology. 2014;192(5):2237-43.
69. Caccamo N, La Mendola C, Orlando V, Meraviglia S, Todaro M, Stassi G, et al. Differentiation, phenotype, and function of interleukin-17-producing human Vgamma9Vdelta2 T cells. Blood. 2011;118(1):129-38.
70. Ness-Schwickerath KJ, Jin C, Morita CT. Cytokine requirements for the differentiation and expansion of IL-17A- and IL-22-producing human Vgamma2Vdelta2 T cells. Journal of immunology. 2010;184(12):7268-80.
71. Hu GM, Wu P, Cheng P, Zhang ZG, Wang Z, Yu XY, et al. Tumor-infiltrating CD39(+) gamma delta Tregs are novel immunosuppressive T cells in human colorectal cancer. Oncoimmunology. 2017;6(2).
72. Peters C, Kabelitz D, Wesch D. Regulatory functions of gamma delta T cells. Cellular and Molecular Life Sciences. 2018;75(12):2125-35.
73. Qian BZ, Pollard JW. Macrophage diversity enhances tumor progression and metastasis. Cell. 2010;141(1):39-51.

74. Albini A, Bruno A, Noonan DM, Mortara L. Contribution to Tumor Angiogenesis From Innate Immune Cells Within the Tumor Microenvironment: Implications for Immunotherapy. Frontiers in Immunology. 2018;9.
75. Aras S, Zaidi MR. TAMeless traitors: macrophages in cancer progression and metastasis. British journal of cancer. 2017;117(11):1583-91.
76. Mills CD, Kincaid K, Alt JM, Heilman MJ, Hill AM. M-1/M-2 macrophages and the Th1/Th2 paradigm. Journal of immunology. 2000;164(12):6166-73.
77. Gabrilovich DI, Ostrand-Rosenberg S, Bronte V. Coordinated regulation of myeloid cells by tumours. Nature Reviews Immunology. 2012;12(4):253-68.
78. Franklin RA, Liao W, Sarkar A, Kim MV, Bivona MR, Liu K, et al. The cellular and molecular origin of tumor-associated macrophages. Science. 2014;344(6186):921-5.
79. Biswas SK, Allavena P, Mantovani A. Tumor-associated macrophages: functional diversity, clinical significance, and open questions. Semin Immunopathol. 2013;35(5):585-600.
80. Pyonteck SM, Akkari L, Schuhmacher AJ, Bowman RL, Sevenich L, Quail DF, et al. CSF-1R inhibition alters macrophage polarization and blocks glioma progression. Nature medicine. 2013;19(10):1264-72.
81. Kumar V, Patel S, Tcyganov E, Gabrilovich DI. The Nature of Myeloid-Derived Suppressor Cells in the Tumor Microenvironment. Trends in Immunology. 2016;37(3):208-20.
82. Stromnes IM, Greenberg PD, Hingorani SR. Molecular Pathways: Myeloid Complicity in Cancer. Clinical Cancer Research. 2014;20(20):5157-70.
83. Huang B, Pan PY, Li Q, Sato AI, Levy DE, Bromberg J, et al. Gr-1+CD115+ immature myeloid suppressor cells mediate the development of tumor-induced T regulatory cells and T-cell anergy in tumor-bearing host. Cancer research. 2006;66(2):1123-31.
84. Ostrand-Rosenberg S, Sinha P. Myeloid-derived suppressor cells: linking inflammation and cancer. Journal of immunology. 2009;182(8):4499-506.
85. Noman MZ, Desantis G, Janji B, Hasmim M, Karray S, Dessen P, et al. PD-L1 is a novel direct target of HIF-1alpha, and its blockade under hypoxia enhanced MDSC-mediated T cell activation. The Journal of experimental medicine. 2014;211(5):781-90.
86. Corzo CA, Condamine T, Lu L, Cotter MJ, Youn JI, Cheng P, et al. HIF-1alpha regulates function and differentiation of myeloid-derived suppressor cells in the tumor microenvironment. The Journal of experimental medicine. 2010;207(11):2439-53.
87. Shirota Y, Shirota H, Klinman DM. Intratumoral injection of CpG oligonucleotides induces the differentiation and reduces the immunosuppressive activity of myeloid-derived suppressor cells. Journal of immunology. 2012;188(4):1592-9.
88. Vivier E, Tomasello E, Baratin M, Walzer T, Ugolini S. Functions of natural killer cells. Nature immunology. 2008;9(5):503-10.
89. Larsen SK, Gao Y, Basse PH. NK cells in the tumor microenvironment. Crit Rev Oncog. 2014;19(1-2):91-105.
90. Glasner A, Levi A, Enk J, Isaacson B, Viukov S, Orlanski S, et al. NKp46 Receptor-Mediated Interferon-gamma Production by Natural Killer Cells Increases Fibronectin 1 to Alter Tumor Architecture and Control Metastasis (vol 48, pg 107, 2018). Immunity. 2018;48(2):396-8.
91. Souza-Fonseca-Guimaraes F, Cursons J, Huntington ND. The Emergence of Natural Killer Cells as a Major Target in Cancer Immunotherapy. Trends Immunol. 2019;40(2):142-58.
92. Pietra G, Vitale C, Pende D, Bertaina A, Moretta F, Falco M, et al. Human natural killer cells: news in the therapy of solid tumors and high-risk leukemias. Cancer Immunol Immun. 2016;65(4):465-76.
93. Shortman K, Naik SH. Steady-state and inflammatory dendritic-cell development. Nature reviews Immunology. 2007;7(1):19-30.
94. Gardner A, Ruffell B. Dendritic Cells and Cancer Immunity. Trends Immunol. 2016;37(12):855-65.
95. Fu C, Jiang A. Dendritic Cells and CD8 T Cell Immunity in Tumor Microenvironment. Front Immunol. 2018;9:3059.
96. Karyampudi L, Lamichhane P, Krempski J, Kalli KR, Behrens MD, Vargas DM, et al. PD-1 Blunts the Function of Ovarian Tumor-Infiltrating Dendritic Cells by Inactivating NF-kappaB. Cancer research. 2016;76(2):239-50.
97. Shaul ME, Fridlender ZG. Cancer related circulating and tumor-associated neutrophils - subtypes, sources and function. FEBS J. 2018.

98. Coffelt SB, Wellenstein MD, de Visser KE. Neutrophils in cancer: neutral no more. Nature reviews Cancer. 2016;16(7):431-46.
99. Casbon AJ, Reynaud D, Park C, Khuc E, Gan DD, Schepers K, et al. Invasive breast cancer reprograms early myeloid differentiation in the bone marrow to generate immunosuppressive neutrophils. Proc Natl Acad Sci U S A. 2015;112(6):E566-75.
100. Wang TT, Zhao YL, Peng LS, Chen N, Chen W, Lv YP, et al. Tumour-activated neutrophils in gastric cancer foster immune suppression and disease progression through GM-CSF-PD-L1 pathway. Gut. 2017;66(11):1900-11.
101. Gungor N, Knaapen AM, Munnia A, Peluso M, Haenen GR, Chiu RK, et al. Genotoxic effects of neutrophils and hypochlorous acid. Mutagenesis. 2010;25(2):149-54.
102. Granot Z, Henke E, Comen EA, King TA, Norton L, Benezra R. Tumor Entrained Neutrophils Inhibit Seeding in the Premetastatic Lung. Cancer cell. 2011;20(3):300-14.
103. Finisguerra V, Di Conza G, Di Matteo M, Serneels J, Costa S, Thompson AAR, et al. MET is required for the recruitment of anti-tumoural neutrophils. Nature. 2015;522(7556):349-+.
104. Sionov RV, Fridlender ZG, Granot Z. The Multifaceted Roles Neutrophils Play in the Tumor Microenvironment. Cancer Microenviron. 2015;8(3):125-58.
105. Sarvaria A, Madrigal JA, Saudemont A. B cell regulation in cancer and anti-tumor immunity. Cell Mol Immunol. 2017;14(8):662-74.
106. Folkman J. Tumor angiogenesis: therapeutic implications. The New England journal of medicine. 1971;285(21):1182-6.
107. Carmeliet P, Jain RK. Molecular mechanisms and clinical applications of angiogenesis. Nature. 2011;473(7347):298-307.
108. De Palma M, Biziato D, Petrova TV. Microenvironmental regulation of tumour angiogenesis. Nature reviews Cancer. 2017;17(8):457-74.
109. Jayson GC, Kerbel R, Ellis LM, Harris AL. Antiangiogenic therapy in oncology: current status and future directions. Lancet. 2016;388(10043):518-29.
110. Donnem T, Reynolds AR, Kuczynski EA, Gatter K, Vermeulen PB, Kerbel RS, et al. Non-angiogenic tumours and their influence on cancer biology. Nature reviews Cancer. 2018;18(5):323-36.
111. Kuczynski EA, Vermeulen PB, Pezzella F, Kerbel RS, Reynolds AR. Vessel co-option in cancer. Nature reviews Clinical oncology. 2019.
112. Stacker SA, Williams SP, Karnezis T, Shayan R, Fox SB, Achen MG. Lymphangiogenesis and lymphatic vessel remodelling in cancer. Nature reviews Cancer. 2014;14(3):159-72.
113. Swartz MA, Lund AW. Lymphatic and interstitial flow in the tumour microenvironment: linking mechanobiology with immunity. Nature reviews Cancer. 2012;12(3):210-9.
114. Chen X, Song E. Turning foes to friends: targeting cancer-associated fibroblasts. Nature reviews Drug discovery. 2019;18(2):99-115.
115. Alkasalias T, Moyano-Galceran L, Arsenian-Henriksson M, Lehti K. Fibroblasts in the Tumor Microenvironment: Shield or Spear? International journal of molecular sciences. 2018;19(5).
116. Kalluri R. The biology and function of fibroblasts in cancer. Nature reviews Cancer. 2016;16(9):582-98.
117. Ridge SM, Sullivan FJ, Glynn SA. Mesenchymal stem cells: key players in cancer progression. Mol Cancer. 2017;16(1):31.
118. Yagi H, Soto-Gutierrez A, Parekkadan B, Kitagawa Y, Tompkins RG, Kobayashi N, et al. Mesenchymal stem cells: Mechanisms of immunomodulation and homing. Cell Transplant. 2010;19(6):667-79.
119. Valkenburg KC, de Groot AE, Pienta KJ. Targeting the tumour stroma to improve cancer therapy. Nature reviews Clinical oncology. 2018;15(6):366-81.
120. Bonnans C, Chou J, Werb Z. Remodelling the extracellular matrix in development and disease. Nature reviews Molecular cell biology. 2014;15(12):786-801.
121. Kosaka N, Yoshioka Y, Fujita Y, Ochiya T. Versatile roles of extracellular vesicles in cancer. The Journal of clinical investigation. 2016;126(4):1163-72.
122. Steinbichler TB, Dudas J, Skvortsov S, Ganswindt U, Riechelmann H, Skvortsova, II. Therapy resistance mediated by exosomes. Mol Cancer. 2019;18(1):58.
123. Leight JL, Drain AP, Weaver VM. Extracellular Matrix Remodeling and Stiffening Modulate Tumor Phenotype and Treatment Response. Annual Review of Cancer Biology. 2017;1(1):313-34.

124. Ehrlich P. Ueber den jetzigen stand der Karzinomforschung Nederlandsch Tijdschrift voor Geneeskunde. Ned Tijdschr voor Geneeskd. 1909;5.
125. Burnet M. Cancer; a biological approach. I. The processes of control. Br Med J. 1957;1(5022):779-86.
126. Thomas L. On immunosurveillance in human cancer. Yale J Biol Med. 1982;55(3-4):329-33.
127. Dunn GP, Bruce AT, Ikeda H, Old LJ, Schreiber RD. Cancer immunoediting: from immunosurveillance to tumor escape. Nature immunology. 2002;3(11):991-8.
128. Schreiber RD, Old LJ, Smyth MJ. Cancer immunoediting: integrating immunity's roles in cancer suppression and promotion. Science. 2011;331(6024):1565-70.
129. Mittal D, Gubin MM, Schreiber RD, Smyth MJ. New insights into cancer immunoediting and its three component phases elimination, equilibrium and escape. Current Opinion in Immunology. 2014;27:16-25.
130. Nakamura K, Smyth MJ. Targeting cancer-related inflammation in the era of immunotherapy. Immunology and Cell Biology. 2017;95(4):325-32.
131. Vesely MD, Kershaw MH, Schreiber RD, Smyth MJ. Natural Innate and Adaptive Immunity to Cancer. Annual Review of Immunology, Vol 29. 2011;29:235-71.
132. Dvorak HF. Tumors: wounds that do not heal. Similarities between tumor stroma generation and wound healing. The New England journal of medicine. 1986;315(26):1650-9.
133. Albini A, Sporn MB. The tumour microenvironment as a target for chemoprevention. Nature reviews Cancer. 2007;7(2):139-47.
134. Manresa MC, Godson C, Taylor CT. Hypoxia-sensitive pathways in inflammation-driven fibrosis. Am J Physiol Regul Integr Comp Physiol. 2014;307(12):R1369-80.
135. Virchow R. Cellular Pathology as Based Upon Physiological and Pathological Histology: J. B. Lippincott; 1863.
136. de Martel C, Ferlay J, Franceschi S, Vignat J, Bray F, Forman D, et al. Global burden of cancers attributable to infections in 2008: a review and synthetic analysis. Lancet Oncology. 2012;13(6).
137. Grivennikov SI, Greten FR, Karin M. Immunity, inflammation, and cancer. Cell. 2010;140(6):883-99.
138. Todoric J, Antonucci L, Karin M. Targeting Inflammation in Cancer Prevention and Therapy. Cancer Prev Res (Phila). 2016;9(12):895-905.
139. Colotta F, Allavena P, Sica A, Garlanda C, Mantovani A. Cancer-related inflammation, the seventh hallmark of cancer: links to genetic instability. Carcinogenesis. 2009;30(7):1073-81.
140. Shalapour S, Karin M. Immunity, inflammation, and cancer: an eternal fight between good and evil. Journal of Clinical Investigation. 2015;125(9):3347-55.
141. Psaila B, Lyden D. The metastatic niche: adapting the foreign soil. Nature Reviews Cancer. 2009;9(4):285-93.
142. Paget S. THE DISTRIBUTION OF SECONDARY GROWTHS IN CANCER OF THE BREAST. The Lancet. 1889;133(3421):571-3.
143. Hagemann T, Balkwill F, Lawrence T. Inflammation and cancer: A double-edged sword. Cancer cell. 2007;12(4):300-1.
144. Galluzzi L, Senovilla L, Zitvogel L, Kroemer G. The secret ally: immunostimulation by anticancer drugs. Nature Reviews Drug Discovery. 2012;11(3):215-33.
145. Mantovani A, Allavena P, Sica A, Balkwill F. Cancer-related inflammation. Nature. 2008;454(7203):436-44.
146. Crusz SM, Balkwill FR. Inflammation and cancer: advances and new agents. Nature Reviews Clinical Oncology. 2015;12(10):584-96.
147. Liu J, Yang G, Thompson-Lanza JA, Glassman A, Hayes K, Patterson A, et al. A Genetically Defined Model for Human Ovarian Cancer. 2004;64(5):1655-63.
148. Pylayeva-Gupta Y, Lee KE, Hajdu CH, Miller G, Bar-Sagi D. Oncogenic Kras-Induced GM-CSF Production Promotes the Development of Pancreatic Neoplasia. Cancer cell. 2012;21(6):836-47.
149. Araki Y, Okamura S, Hussain SP, Nagashima M, He PJ, Shiseki M, et al. Regulation of cyclooxygenase-2 expression by the Wnt and ras pathways. Cancer research. 2003;63(3):728-34.
150. Chen GY, Nunez G. Sterile inflammation: sensing and reacting to damage. Nature Reviews Immunology. 2010;10(12):826-37.

151. Ritter B, Greten FR. Modulating inflammation for cancer therapy. The Journal of experimental medicine. 2019.
152. Coussens LM, Zitvogel L, Palucka AK. Neutralizing tumor-promoting chronic inflammation: a magic bullet? Science. 2013;339(6117):286-91.
153. Steggerda SM, Bennett MK, Chen J, Emberley E, Huang T, Janes JR, et al. Inhibition of arginase by CB-1158 blocks myeloid cell-mediated immune suppression in the tumor microenvironment. J Immunother Cancer. 2017;5(1):101.
154. Dempke WCM, Fenchel K, Uciechowski P, Dale SP. Second- and third-generation drugs for immuno-oncology treatment-The more the better? European journal of cancer. 2017;74:55-72.
155. Balkwill F. Tumour necrosis factor and cancer. Nature Reviews Cancer. 2009;9(5):361-71.
156. Balkwill F. TNF-alpha in promotion and progression of cancer. Cancer Metast Rev. 2006;25(3):409-16.
157. Voronov E, Dotan S, Krelin Y, Song X, Elkabets M, Carmi Y, et al. Unique Versus Redundant Functions of IL-1alpha and IL-1beta in the Tumor Microenvironment. Front Immunol. 2013;4:177.
158. Mantovani A, Dinarello CA, Molgora M, Garlanda C. Interleukin-1 and Related Cytokines in the Regulation of Inflammation and Immunity. Immunity. 2019;50(4):778-95.
159. Dinarello CA, Simon A, van der Meer JW. Treating inflammation by blocking interleukin-1 in a broad spectrum of diseases. Nature reviews Drug discovery. 2012;11(8):633-52.
160. Bent R, Moll L, Grabbe S, Bros M. Interleukin-1 Beta-A Friend or Foe in Malignancies? International journal of molecular sciences. 2018;19(8).
161. Sutton CE, Lalor SJ, Sweeney CM, Brereton CF, Lavelle EC, Mills KH. Interleukin-1 and IL-23 induce innate IL-17 production from gammadelta T cells, amplifying Th17 responses and autoimmunity. Immunity. 2009;31(2):331-41.
162. Gaffen SL, Jain R, Garg AV, Cua DJ. The IL-23-IL-17 immune axis: from mechanisms to therapeutic testing. Nature reviews Immunology. 2014;14(9):585-600.
163. Taniguchi K, Karin M. IL-6 and related cytokines as the critical lynchpins between inflammation and cancer. Semin Immunol. 2014;26(1):54-74.
164. Johnson DE, O'Keefe RA, Grandis JR. Targeting the IL-6/JAK/STAT3 signalling axis in cancer. Nature Reviews Clinical Oncology. 2018;15(4):234-48.
165. Jones SA, Jenkins BJ. Recent insights into targeting the IL-6 cytokine family in inflammatory diseases and cancer. Nature reviews Immunology. 2018;18(12):773-89.
166. Oppmann B, Lesley R, Blom B, Timans JC, Xu Y, Hunte B, et al. Novel p19 protein engages IL-12p40 to form a cytokine, IL-23, with biological activities similar as well as distinct from IL-12. Immunity. 2000;13(5):715-25.
167. Parham C, Chirica M, Timans J, Vaisberg E, Travis M, Cheung J, et al. A receptor for the heterodimeric cytokine IL-23 is composed of IL-12Rbeta1 and a novel cytokine receptor subunit, IL-23R. Journal of immunology. 2002;168(11):5699-708.
168. Tait Wojno ED, Hunter CA, Stumhofer JS. The Immunobiology of the Interleukin-12 Family: Room for Discovery. Immunity. 2019;50(4):851-70.
169. Langrish CL, Chen Y, Blumenschein WM, Mattson J, Basham B, Sedgwick JD, et al. IL-23 drives a pathogenic T cell population that induces autoimmune inflammation. The Journal of experimental medicine. 2005;201(2):233-40.
170. O'Garra A, Arai N. The molecular basis of T helper 1 and T helper 2 cell differentiation. Trends Cell Biol. 2000;10(12):542-50.
171. Guo L, Junttila IS, Paul WE. Cytokine-induced cytokine production by conventional and innate lymphoid cells. Trends Immunol. 2012;33(12):598-606.
172. Gooderham MJ, Papp KA, Lynde CW. Shifting the focus - the primary role of IL-23 in psoriasis and other inflammatory disorders. J Eur Acad Dermatol Venereol. 2018;32(7):1111-9.
173. Bianchi E, Rogge L. The IL-23/IL-17 pathway in human chronic inflammatory diseases-new insight from genetics and targeted therapies. Genes Immun. 2019.
174. Langowski JL, Zhang X, Wu L, Mattson JD, Chen T, Smith K, et al. IL-23 promotes tumour incidence and growth. Nature. 2006;442(7101):461-5.
175. Yan J, Smyth MJ, Teng MWL. Interleukin (IL)-12 and IL-23 and Their Conflicting Roles in Cancer. Cold Spring Harb Perspect Biol. 2018;10(7).

176. Grivennikov SI, Wang K, Mucida D, Stewart CA, Schnabl B, Jauch D, et al. Adenoma-linked barrier defects and microbial products drive IL-23/IL-17-mediated tumour growth. Nature. 2012;491(7423):254-8.
177. Ljujic B, Radosavljevic G, Jovanovic I, Pavlovic S, Zdravkovic N, Milovanovic M, et al. Elevated serum level of IL-23 correlates with expression of VEGF in human colorectal carcinoma. Arch Med Res. 2010;41(3):182-9.
178. Zhang L, Li J, Li L, Zhang J, Wang X, Yang C, et al. IL-23 selectively promotes the metastasis of colorectal carcinoma cells with impaired Socs3 expression via the STAT5 pathway. Carcinogenesis. 2014;35(6):1330-40.
179. Calcinotto A, Spataro C, Zagato E, Di Mitri D, Gil V, Crespo M, et al. IL-23 secreted by myeloid cells drives castration-resistant prostate cancer. Nature. 2018;559(7714):363-9.
180. Hu J, Yuan X, Belladonna ML, Ong JM, Wachsmann-Hogiu S, Farkas DL, et al. Induction of potent antitumor immunity by intratumoral injection of interleukin 23-transduced dendritic cells. Cancer research. 2006;66(17):8887-96.
181. Yuan X, Hu J, Belladonna ML, Black KL, Yu JS. Interleukin-23-expressing bone marrow-derived neural stem-like cells exhibit antitumor activity against intracranial glioma. Cancer research. 2006;66(5):2630-8.
182. Overwijk WW, de Visser KE, Tirion FH, de Jong LA, Pols TW, van der Velden YU, et al. Immunological and antitumor effects of IL-23 as a cancer vaccine adjuvant. Journal of immunology. 2006;176(9):5213-22.
183. Fukuda M, Ehara M, Suzuki S, Ohmori Y, Sakashita H. IL-23 promotes growth and proliferation in human squamous cell carcinoma of the oral cavity. Int J Oncol. 2010;36(6):1355-65.
184. Baird AM, Leonard J, Naicker KM, Kilmartin L, O'Byrne KJ, Gray SG. IL-23 is pro-proliferative, epigenetically regulated and modulated by chemotherapy in non-small cell lung cancer. Lung Cancer. 2013;79(1):83-90.
185. Wang D, Xiang T, Zhao Z, Lin K, Yin P, Jiang L, et al. Autocrine interleukin-23 promotes self-renewal of CD133+ ovarian cancer stem-like cells. Oncotarget. 2016;7(46):76006-20.
186. Chen D, Li W, Liu S, Su Y, Han G, Xu C, et al. Interleukin-23 promotes the epithelial-mesenchymal transition of oesophageal carcinoma cells via the Wnt/beta-catenin pathway. Sci Rep. 2015;5:8604.
187. Xu X, Yang C, Chen J, Liu J, Li P, Shi Y, et al. Interleukin-23 promotes the migration and invasion of gastric cancer cells by inducing epithelial-to-mesenchymal transition via the STAT3 pathway. Biochem Biophys Res Commun. 2018;499(2):273-8.
188. Li J, Lau G, Chen L, Yuan YF, Huang J, Luk JM, et al. Interleukin 23 promotes hepatocellular carcinoma metastasis via NF-kappa B induced matrix metalloproteinase 9 expression. PLoS One. 2012;7(9):e46264.
189. Teng MW, Bowman EP, McElwee JJ, Smyth MJ, Casanova JL, Cooper AM, et al. IL-12 and IL-23 cytokines: from discovery to targeted therapies for immune-mediated inflammatory diseases. Nature medicine. 2015;21(7):719-29.
190. Teng MW, Andrews DM, McLaughlin N, von Scheidt B, Ngiow SF, Moller A, et al. IL-23 suppresses innate immune response independently of IL-17A during carcinogenesis and metastasis. Proc Natl Acad Sci U S A. 2010;107(18):8328-33.
191. Nie W, Yu T, Sang Y, Gao X. Tumor-promoting effect of IL-23 in mammary cancer mediated by infiltration of M2 macrophages and neutrophils in tumor microenvironment. Biochem Biophys Res Commun. 2017;482(4):1400-6.
192. Kortylewski M, Xin H, Kujawski M, Lee H, Liu Y, Harris T, et al. Regulation of the IL-23 and IL-12 balance by Stat3 signaling in the tumor microenvironment. Cancer cell. 2009;15(2):114-23.
193. Koh J, Kim HY, Lee Y, Park IK, Kang CH, Kim YT, et al. IL-23-producing human lung cancer cells promote tumor growth via conversion of innate lymphoid cell 1 (ILC1) into ILC3. Clin Cancer Res. 2019.
194. Ngiow SF, Teng MW, Smyth MJ. A balance of interleukin-12 and -23 in cancer. Trends Immunol. 2013;34(11):548-55.
195. Teng MW, Vesely MD, Duret H, McLaughlin N, Towne JE, Schreiber RD, et al. Opposing roles for IL-23 and IL-12 in maintaining occult cancer in an equilibrium state. Cancer research. 2012;72(16):3987-96.

196. Walch-Ruckheim B, Stroder R, Theobald L, Pahne-Zeppenfeld J, Hegde S, Kim YJ, et al. Cervical cancer-instructed stromal fibroblasts enhance IL-23 expression in dendritic cells to support expansion of Th17 cells. Cancer research. 2019.
197. von Scheidt B, Leung PS, Yong MC, Zhang Y, Towne JE, Smyth MJ, et al. Combined anti-CD40 and anti-IL-23 monoclonal antibody therapy effectively suppresses tumor growth and metastases. Cancer research. 2014;74(9):2412-21.
198. Teng MW, von Scheidt B, Duret H, Towne JE, Smyth MJ. Anti-IL-23 monoclonal antibody synergizes in combination with targeted therapies or IL-2 to suppress tumor growth and metastases. Cancer research. 2011;71(6):2077-86.
199. Smyth MJ, Teng MW. Targeting the IL-12/IL-23 axis: An alternative approach to removing tumor induced immune suppression. Oncoimmunology. 2014;3:e28964.
200. McGeachy MJ, Cua DJ, Gaffen SL. The IL-17 Family of Cytokines in Health and Disease. Immunity. 2019;50(4):892-906.
201. Amatya N, Garg AV, Gaffen SL. IL-17 Signaling: The Yin and the Yang. Trends Immunol. 2017;38(5):310-22.
202. Iwakura Y, Ishigame H, Saijo S, Nakae S. Functional specialization of interleukin-17 family members. Immunity. 2011;34(2):149-62.
203. Yuzhalin AE, Kutikhin AG. Interleukin-17 Superfamily and Cancer. Interleukins in Cancer Biology2015. p. 261-89.
204. Monin L, Gaffen SL. Interleukin 17 Family Cytokines: Signaling Mechanisms, Biological Activities, and Therapeutic Implications. Cold Spring Harb Perspect Biol. 2018;10(4).
205. Liang Y, Pan HF, Ye DQ. Tc17 Cells in Immunity and Systemic Autoimmunity. Int Rev Immunol. 2015;34(4):318-31.
206. Gaffen SL. Structure and signalling in the IL-17 receptor family. Nature reviews Immunology. 2009;9(8):556-67.
207. Su Y, Huang J, Zhao X, Lu H, Wang W, Yang XO, et al. Interleukin-17 receptor D constitutes an alternative receptor for interleukin-17A important in psoriasis-like skin inflammation. Sci Immunol. 2019;4(36).
208. Dong C. Cytokine regulation of Th17 and Tfh cell differentiation. Cytokine. 2008;43(3):279-.
209. Wright JF, Guo Y, Quazi A, Luxenberg DP, Bennett F, Ross JF, et al. Identification of an interleukin 17F/17A heterodimer in activated human CD4+ T cells. J Biol Chem. 2007;282(18):13447-55.
210. Ishigame H, Kakuta S, Nagai T, Kadoki M, Nambu A, Komiyama Y, et al. Differential roles of interleukin-17A and -17F in host defense against mucoepithelial bacterial infection and allergic responses. Immunity. 2009;30(1):108-19.
211. De Luca A, Pariano M, Cellini B, Costantini C, Villella VR, Jose SS, et al. The IL-17F/IL-17RC Axis Promotes Respiratory Allergy in the Proximal Airways. Cell Rep. 2017;20(7):1667-80.
212. Veldhoen M. Interleukin 17 is a chief orchestrator of immunity. Nature immunology. 2017;18(6):612-21.
213. Hasegawa E, Sonoda KH, Shichita T, Morita R, Sekiya T, Kimura A, et al. IL-23-independent induction of IL-17 from gammadeltaT cells and innate lymphoid cells promotes experimental intraocular neovascularization. Journal of immunology. 2013;190(4):1778-87.
214. Lee JS, Tato CM, Joyce-Shaikh B, Gulen MF, Cayatte C, Chen Y, et al. Interleukin-23-Independent IL-17 Production Regulates Intestinal Epithelial Permeability. Immunity. 2015;43(4):727-38.
215. Yoshiga Y, Goto D, Segawa S, Ohnishi Y, Matsumoto I, Ito S, et al. Invariant NKT cells produce IL-17 through IL-23-dependent and -independent pathways with potential modulation of Th17 response in collagen-induced arthritis. Int J Mol Med. 2008;22(3):369-74.
216. Hawkes JE, Yan BY, Chan TC, Krueger JG. Discovery of the IL-23/IL-17 Signaling Pathway and the Treatment of Psoriasis. Journal of immunology. 2018;201(6):1605-13.
217. Qian X, Chen H, Wu X, Hu L, Huang Q, Jin Y. Interleukin-17 acts as double-edged sword in anti-tumor immunity and tumorigenesis. Cytokine. 2017;89:34-44.
218. Wang JT, Li H, Zhang H, Chen YF, Cao YF, Li RC, et al. Intratumoral IL17-producing cells infiltration correlate with antitumor immune contexture and improved response to adjuvant chemotherapy in gastric cancer. Ann Oncol. 2019;30(2):266-73.
219. Martin-Orozco N, Muranski P, Chung Y, Yang XO, Yamazaki T, Lu S, et al. T helper 17 cells promote cytotoxic T cell activation in tumor immunity. Immunity. 2009;31(5):787-98.

220. Ma Y, Aymeric L, Locher C, Mattarollo SR, Delahaye NF, Pereira P, et al. Contribution of IL-17-producing gamma delta T cells to the efficacy of anticancer chemotherapy. The Journal of experimental medicine. 2011;208(3):491-503.
221. Coffelt SB, Kersten K, Doornebal CW, Weiden J, Vrijland K, Hau CS, et al. IL-17-producing gammadelta T cells and neutrophils conspire to promote breast cancer metastasis. Nature. 2015;522(7556):345-8.
222. Benevides L, da Fonseca DM, Donate PB, Tiezzi DG, De Carvalho DD, de Andrade JM, et al. IL17 Promotes Mammary Tumor Progression by Changing the Behavior of Tumor Cells and Eliciting Tumorigenic Neutrophils Recruitment. Cancer research. 2015;75(18):3788-99.
223. He D, Li H, Yusuf N, Elmets CA, Li J, Mountz JD, et al. IL-17 promotes tumor development through the induction of tumor promoting microenvironments at tumor sites and myeloid-derived suppressor cells. Journal of immunology. 2010;184(5):2281-8.
224. Cochaud S, Giustiniani J, Thomas C, Laprevotte E, Garbar C, Savoye AM, et al. IL-17A is produced by breast cancer TILs and promotes chemoresistance and proliferation through ERK1/2. Sci Rep. 2013;3:3456.
225. Wang B, Zhao CH, Sun G, Zhang ZW, Qian BM, Zhu YF, et al. IL-17 induces the proliferation and migration of glioma cells through the activation of PI3K/Akt1/NF-kappaB-p65. Cancer letters. 2019;447:93-104.
226. Wang K, Kim MK, Di Caro G, Wong J, Shalapour S, Wan J, et al. Interleukin-17 receptor a signaling in transformed enterocytes promotes early colorectal tumorigenesis. Immunity. 2014;41(6):1052-63.
227. Zhu X, Mulcahy LA, Mohammed RA, Lee AH, Franks HA, Kilpatrick L, et al. IL-17 expression by breast-cancer-associated macrophages: IL-17 promotes invasiveness of breast cancer cell lines. Breast Cancer Res. 2008;10(6):R95.
228. Jiang YX, Yang SW, Li PA, Luo X, Li ZY, Hao YX, et al. The promotion of the transformation of quiescent gastric cancer stem cells by IL-17 and the underlying mechanisms. Oncogene. 2017;36(9):1256-64.
229. Chung AS, Wu X, Zhuang G, Ngu H, Kasman I, Zhang J, et al. An interleukin-17-mediated paracrine network promotes tumor resistance to anti-angiogenic therapy. Nature medicine. 2013;19(9):1114-23.
230. Numasaki M, Watanabe M, Suzuki T, Takahashi H, Nakamura A, McAllister F, et al. IL-17 enhances the net angiogenic activity and in vivo growth of human non-small cell lung cancer in SCID mice through promoting CXCR-2-dependent angiogenesis. Journal of immunology. 2005;175(9):6177-89.
231. Pan B, Shen J, Cao J, Zhou Y, Shang L, Jin S, et al. Interleukin-17 promotes angiogenesis by stimulating VEGF production of cancer cells via the STAT3/GIV signaling pathway in non-small-cell lung cancer. Sci Rep. 2015;5:16053.
232. Li J, Lau GK, Chen L, Dong SS, Lan HY, Huang XR, et al. Interleukin 17A promotes hepatocellular carcinoma metastasis via NF-kB induced matrix metalloproteinases 2 and 9 expression. PLoS One. 2011;6(7):e21816.
233. Li Q, Han Y, Fei G, Guo Z, Ren T, Liu Z. IL-17 promoted metastasis of non-small-cell lung cancer cells. Immunol Lett. 2012;148(2):144-50.
234. Li H, Chen J, Huang A, Stinson J, Heldens S, Foster J, et al. Cloning and characterization of IL-17B and IL-17C, two new members of the IL-17 cytokine family. Proc Natl Acad Sci U S A. 2000;97(2):773-8.
235. Shi Y, Ullrich SJ, Zhang J, Connolly K, Grzegorzewski KJ, Barber MC, et al. A novel cytokine receptor-ligand pair. Identification, molecular characterization, and in vivo immunomodulatory activity. J Biol Chem. 2000;275(25):19167-76.
236. Bie Q, Jin C, Zhang B, Dong H. IL-17B: A new area of study in the IL-17 family. Molecular immunology. 2017;90:50-6.
237. Reynolds JM, Lee YH, Shi Y, Wang X, Angkasekwinai P, Nallaparaju KC, et al. Interleukin-17B Antagonizes Interleukin-25-Mediated Mucosal Inflammation. Immunity. 2015;42(4):692-703.
238. Huang CK, Yang CY, Jeng YM, Chen CL, Wu HH, Chang YC, et al. Autocrine/paracrine mechanism of interleukin-17B receptor promotes breast tumorigenesis through NF-kappaB-mediated antiapoptotic pathway. Oncogene. 2014;33(23):2968-77.

239. Wu HH, Hwang-Verslues WW, Lee WH, Huang CK, Wei PC, Chen CL, et al. Targeting IL-17B-IL-17RB signaling with an anti-IL-17RB antibody blocks pancreatic cancer metastasis by silencing multiple chemokines. The Journal of experimental medicine. 2015;212(3):333-49.
240. Bie Q, Sun C, Gong A, Li C, Su Z, Zheng D, et al. Non-tumor tissue derived interleukin-17B activates IL-17RB/AKT/beta-catenin pathway to enhance the stemness of gastric cancer. Sci Rep. 2016;6:25447.
241. Bie Q, Zhang B, Sun C, Ji X, Barnie PA, Qi C, et al. IL-17B activated mesenchymal stem cells enhance proliferation and migration of gastric cancer cells. Oncotarget. 2017;8(12):18914-23.
242. Laprevotte E, Cochaud S, du Manoir S, Lapierre M, Dejou C, Philippe M, et al. The IL-17B-IL-17 receptor B pathway promotes resistance to paclitaxel in breast tumors through activation of the ERK1/2 pathway. Oncotarget. 2017;8(69):113360-72.
243. Yang YF, Lee YC, Lo S, Chung YN, Hsieh YC, Chiu WC, et al. A positive feedback loop of IL-17B-IL-17RB activates ERK/beta-catenin to promote lung cancer metastasis. Cancer letters. 2018;422:44-55.
244. Brembilla NC, Senra L, Boehncke WH. The IL-17 Family of Cytokines in Psoriasis: IL-17A and Beyond. Front Immunol. 2018;9:1682.
245. Ramirez-Carrozzi V, Sambandam A, Luis E, Lin Z, Jeet S, Lesch J, et al. IL-17C regulates the innate immune function of epithelial cells in an autocrine manner. Nature immunology. 2011;12(12):1159-66.
246. Song X, Zhu S, Shi P, Liu Y, Shi Y, Levin SD, et al. IL-17RE is the functional receptor for IL-17C and mediates mucosal immunity to infection with intestinal pathogens. Nature immunology. 2011;12(12):1151-8.
247. Song X, Gao H, Lin Y, Yao Y, Zhu S, Wang J, et al. Alterations in the microbiota drive interleukin-17C production from intestinal epithelial cells to promote tumorigenesis. Immunity. 2014;40(1):140-52.
248. Jungnickel C, Schmidt LH, Bittigkoffer L, Wolf L, Wolf A, Ritzmann F, et al. IL-17C mediates the recruitment of tumor-associated neutrophils and lung tumor growth. Oncogene. 2017;36(29):4182-90.
249. Starnes T, Broxmeyer HE, Robertson MJ, Hromas R. Cutting edge: IL-17D, a novel member of the IL-17 family, stimulates cytokine production and inhibits hemopoiesis. Journal of immunology. 2002;169(2):642-6.
250. Saddawi-Konefka R, Seelige R, Gross ET, Levy E, Searles SC, Washington A, Jr., et al. Nrf2 Induces IL-17D to Mediate Tumor and Virus Surveillance. Cell Rep. 2016;16(9):2348-58.
251. O'Sullivan T, Saddawi-Konefka R, Gross E, Tran M, Mayfield SP, Ikeda H, et al. Interleukin-17D mediates tumor rejection through recruitment of natural killer cells. Cell Rep. 2014;7(4):989-98.
252. Rickel EA, Siegel LA, Yoon BR, Rottman JB, Kugler DG, Swart DA, et al. Identification of functional roles for both IL-17RB and IL-17RA in mediating IL-25-induced activities. Journal of immunology. 2008;181(6):4299-310.
253. Lee J, Ho WH, Maruoka M, Corpuz RT, Baldwin DT, Foster JS, et al. IL-17E, a novel proinflammatory ligand for the IL-17 receptor homolog IL-17Rh1. J Biol Chem. 2001;276(2):1660-4.
254. von Moltke J, Ji M, Liang HE, Locksley RM. Tuft-cell-derived IL-25 regulates an intestinal ILC2-epithelial response circuit. Nature. 2016;529(7585):221-5.
255. Cheng D, Xue Z, Yi L, Shi H, Zhang K, Huo X, et al. Epithelial interleukin-25 is a key mediator in Th2-high, corticosteroid-responsive asthma. Am J Respir Crit Care Med. 2014;190(6):639-48.
256. Fort MM, Cheung J, Yen D, Li J, Zurawski SM, Lo S, et al. IL-25 induces IL-4, IL-5, and IL-13 and Th2-associated pathologies in vivo. Immunity. 2001;15(6):985-95.
257. Hurst SD, Muchamuel T, Gorman DM, Gilbert JM, Clifford T, Kwan S, et al. New IL-17 family members promote Th1 or Th2 responses in the lung: in vivo function of the novel cytokine IL-25. Journal of immunology. 2002;169(1):443-53.
258. Beale J, Jayaraman A, Jackson DJ, Macintyre JDR, Edwards MR, Walton RP, et al. Rhinovirus-induced IL-25 in asthma exacerbation drives type 2 immunity and allergic pulmonary inflammation. Sci Transl Med. 2014;6(256):256ra134.
259. Kleinschek MA, Owyang AM, Joyce-Shaikh B, Langrish CL, Chen Y, Gorman DM, et al. IL-25 regulates Th17 function in autoimmune inflammation. The Journal of experimental medicine. 2007;204(1):161-70.

260. Wang WB, Yen ML, Liu KJ, Hsu PJ, Lin MH, Chen PM, et al. Interleukin-25 Mediates Transcriptional Control of PD-L1 via STAT3 in Multipotent Human Mesenchymal Stromal Cells (hMSCs) to Suppress Th17 Responses. Stem Cell Reports. 2015;5(3):392-404.
261. Furuta S, Jeng YM, Zhou L, Huang L, Kuhn I, Bissell MJ, et al. IL-25 causes apoptosis of IL-25R-expressing breast cancer cells without toxicity to nonmalignant cells. Sci Transl Med. 2011;3(78):78ra31.
262. Yin SY, Jian FY, Chen YH, Chien SC, Hsieh MC, Hsiao PW, et al. Induction of IL-25 secretion from tumour-associated fibroblasts suppresses mammary tumour metastasis. Nat Commun. 2016;7:11311.
263. Li J, Liao Y, Ding T, Wang B, Yu X, Chu Y, et al. Tumor-infiltrating macrophages express interleukin-25 and predict a favorable prognosis in patients with gastric cancer after radical resection. Oncotarget. 2016;7(10):11083-93.
264. Thelen TD, Green RM, Ziegler SF. Acute blockade of IL-25 in a colitis associated colon cancer model leads to increased tumor burden. Sci Rep. 2016;6:25643.
265. Jiang Z, Chen J, Du X, Cheng H, Wang X, Dong C. IL-25 blockade inhibits metastasis in breast cancer. Protein Cell. 2017;8(3):191-201.
266. Mombelli S, Cochaud S, Merrouche Y, Garbar C, Antonicelli F, Laprevotte E, et al. IL-17A and its homologs IL-25/IL-17E recruit the c-RAF/S6 kinase pathway and the generation of pro-oncogenic LMW-E in breast cancer cells. Sci Rep. 2015;5:11874.
267. Mollica Poeta V, Massara M, Capucetti A, Bonecchi R. Chemokines and Chemokine Receptors: New Targets for Cancer Immunotherapy. Front Immunol. 2019;10:379.
268. Kryczek I, Wei S, Keller E, Liu R, Zou WP. Stroma-derived factor (SDF-1/CXCL12) and human tumor pathogenesis. Am J Physiol-Cell Ph. 2007;292(3):C987-C95.
269. Smith MC, Luker KE, Garbow JR, Prior JL, Jackson E, Piwnica-Worms D, et al. CXCR4 regulates growth of both primary and metastatic breast cancer. Cancer research. 2004;64(23):8604-12.
270. Scotton CJ, Wilson JL, Scott K, Stamp G, Wilbanks GD, Fricker S, et al. Multiple actions of the chemokine CXCL12 on epithelial tumor cells in human ovarian cancer. Cancer research. 2002;62(20):5930-8.
271. Cioffi M, D'Alterio C, Camerlingo R, Tirino V, Consales C, Riccio A, et al. Identification of a distinct population of CD133(+)CXCR4(+) cancer stem cells in ovarian cancer. Sci Rep. 2015;5:10357.
272. Jung MJ, Rho JK, Kim YM, Jung JE, Jin YB, Ko YG, et al. Upregulation of CXCR4 is functionally crucial for maintenance of stemness in drug-resistant non-small cell lung cancer cells. Oncogene. 2013;32(2):209-21.
273. Muller A, Homey B, Soto H, Ge N, Catron D, Buchanan ME, et al. Involvement of chemokine receptors in breast cancer metastasis. Nature. 2001;410(6824):50-6.
274. Darash-Yahana M, Pikarsky E, Abramovitch R, Zeira E, Pal B, Karplus R, et al. Role of high expression levels of CXCR4 in tumor growth, vascularization, and metastasis. FASEB journal : official publication of the Federation of American Societies for Experimental Biology. 2004;18(11):1240-2.
275. Marchesi F, Monti P, Leone BE, Zerbi A, Vecchi A, Piemonti L, et al. Increased survival, proliferation, and migration in metastatic human pancreatic tumor cells expressing functional CXCR4. Cancer research. 2004;64(22):8420-7.
276. Salcedo R, Oppenheim JJ. Role of chemokines in angiogenesis: CXCL12/SDF-1 and CXCR4 interaction, a key regulator of endothelial cell responses. Microcirculation. 2003;10(3-4):359-70.
277. Kryczek I, Lange A, Mottram P, Alvarez X, Cheng P, Hogan M, et al. CXCL12 and vascular endothelial growth factor synergistically induce neoangiogenesis in human ovarian cancers. Cancer research. 2005;65(2):465-72.
278. Zou W, Machelon V, Coulomb-L'Hermin A, Borvak J, Nome F, Isaeva T, et al. Stromal-derived factor-1 in human tumors recruits and alters the function of plasmacytoid precursor dendritic cells. Nature medicine. 2001;7(12):1339-46.
279. Zou L, Barnett B, Safah H, Larussa VF, Evdemon-Hogan M, Mottram P, et al. Bone marrow is a reservoir for CD4+CD25+ regulatory T cells that traffic through CXCL12/CXCR4 signals. Cancer research. 2004;64(22):8451-5.
280. Mattern A, Zellmann T, Beck-Sickinger AG. Processing, signaling, and physiological function of chemerin. IUBMB life. 2014;66(1):19-26.

281. Goralski KB, McCarthy TC, Hanniman EA, Zabel BA, Butcher EC, Parlee SD, et al. Chemerin, a novel adipokine that regulates adipogenesis and adipocyte metabolism. J Biol Chem. 2007;282(38):28175-88.
282. Helfer G, Wu QF. Chemerin: a multifaceted adipokine involved in metabolic disorders. The Journal of endocrinology. 2018;238(2):R79-R94.
283. Roman AA, Parlee SD, Sinal CJ. Chemerin: a potential endocrine link between obesity and type 2 diabetes. Endocrine. 2012;42(2):243-51.
284. Ferland DJ, Watts SW. Chemerin: A comprehensive review elucidating the need for cardiovascular research. Pharmacol Res. 2015;99:351-61.
285. Bondue B, Wittamer V, Parmentier M. Chemerin and its receptors in leukocyte trafficking, inflammation and metabolism. Cytokine & growth factor reviews. 2011;22(5-6):331-8.
286. Zabel BA, Kwitniewski M, Banas M, Zabieglo K, Murzyn K, Cichy J. Chemerin regulation and role in host defense. American journal of clinical and experimental immunology. 2014;3(1):1-19.
287. Kaur J, Adya R, Tan BK, Chen J, Randeva HS. Identification of chemerin receptor (ChemR23) in human endothelial cells: chemerin-induced endothelial angiogenesis. Biochem Biophys Res Commun. 2010;391(4):1762-8.
288. Mariani F, Roncucci L. Chemerin/chemR23 axis in inflammation onset and resolution. Inflammation research : official journal of the European Histamine Research Society [et al]. 2015;64(2):85-95.
289. Zhang J, Jin HC, Zhu AK, Ying RC, Wei W, Zhang FJ. Prognostic significance of plasma chemerin levels in patients with gastric cancer. Peptides. 2014;61:7-11.
290. Erdogan S, Yilmaz FM, Yazici O, Yozgat A, Sezer S, Ozdemir N, et al. Inflammation and chemerin in colorectal cancer. Tumour Biol. 2016;37(5):6337-42.
291. Xu C-H, Yang Y, Wang Y-C, Yan J, Qian L-H. Prognostic significance of serum chemerin levels in patients with non-small cell lung cancer. Oncotarget. 2017;8(14):22483-9.
292. Liu-Chittenden Y, Patel D, Gaskins K, Giordano TJ, Assie G, Bertherat J, et al. Serum RARRES2 Is a Prognostic Marker in Patients With Adrenocortical Carcinoma. J Clin Endocrinol Metab. 2016;101(9):3345-52.
293. Buechler C, Feder S, Haberl EM, Aslanidis C. Chemerin Isoforms and Activity in Obesity. International journal of molecular sciences. 2019;20(5).
294. Wittamer V, Franssen JD, Vulcano M, Mirjolet JF, Le Poul E, Migeotte I, et al. Specific recruitment of antigen-presenting cells by chemerin, a novel processed ligand from human inflammatory fluids. The Journal of experimental medicine. 2003;198(7):977-85.
295. Barnea G, Strapps W, Herrada G, Berman Y, Ong J, Kloss B, et al. The genetic design of signaling cascades to record receptor activation. Proc Natl Acad Sci U S A. 2008;105(1):64-9.
296. Zabel BA, Nakae S, Zuniga L, Kim JY, Ohyama T, Alt C, et al. Mast cell-expressed orphan receptor CCRL2 binds chemerin and is required for optimal induction of IgE-mediated passive cutaneous anaphylaxis. The Journal of experimental medicine. 2008;205(10):2207-20.
297. Yoshimura T, Oppenheim JJ. Chemokine-like receptor 1 (CMKLR1) and chemokine (C-C motif) receptor-like 2 (CCRL2); two multifunctional receptors with unusual properties. Exp Cell Res. 2011;317(5):674-84.
298. Yoshimura T, Oppenheim JJ. Chemerin reveals its chimeric nature. The Journal of experimental medicine. 2008;205(10):2187-90.
299. Shin WJ, Zabel BA, Pachynski RK. Mechanisms and Functions of Chemerin in Cancer: Potential Roles in Therapeutic Intervention. Front Immunol. 2018;9:2772.
300. Yamaguchi Y, Du XY, Zhao L, Morser J, Leung LL. Proteolytic cleavage of chemerin protein is necessary for activation to the active form, Chem157S, which functions as a signaling molecule in glioblastoma. J Biol Chem. 2011;286(45):39510-9.
301. Kumar JD, Holmberg C, Kandola S, Steele I, Hegyi P, Tiszlavicz L, et al. Increased expression of chemerin in squamous esophageal cancer myofibroblasts and role in recruitment of mesenchymal stromal cells. PLoS One. 2014;9(7):e104877.
302. Kumar JD, Kandola S, Tiszlavicz L, Reisz Z, Dockray GJ, Varro A. The role of chemerin and ChemR23 in stimulating the invasion of squamous oesophageal cancer cells. British journal of cancer. 2016;114(10):1152-9.
303. Wang C, Wu WK, Liu X, To KF, Chen GG, Yu J, et al. Increased serum chemerin level promotes cellular invasiveness in gastric cancer: a clinical and experimental study. Peptides. 2014;51:131-8.

304. Wang N, Wang QJ, Feng YY, Shang W, Cai M. Overexpression of chemerin was associated with tumor angiogenesis and poor clinical outcome in squamous cell carcinoma of the oral tongue. Clin Oral Investig. 2014;18(3):997-1004.
305. Tümmler C, Snapkov I, Wickstrom M, Moens U, Ljungblad L, Maria Elfman LH, et al. Inhibition of chemerin/CMKLR1 axis in neuroblastoma cells reduces clonogenicity and cell viability in vitro and impairs tumor growth in vivo. Oncotarget. 2017;8(56):95135-51.
306. Lin W, Chen YL, Jiang L, Chen JK. Reduced expression of chemerin is associated with a poor prognosis and a lowed infiltration of both dendritic cells and natural killer cells in human hepatocellular carcinoma. Clin Lab. 2011;57(11-12):879-85.
307. Lin Y, Yang X, Liu W, Li B, Yin W, Shi Y, et al. Chemerin has a protective role in hepatocellular carcinoma by inhibiting the expression of IL-6 and GM-CSF and MDSC accumulation. Oncogene. 2017;36(25):3599-608.
308. Li JJ, Yin HK, Guan DX, Zhao JS, Feng YX, Deng YZ, et al. Chemerin suppresses hepatocellular carcinoma metastasis through CMKLR1-PTEN-Akt axis. British journal of cancer. 2018;118(10):1337-48.
309. Pachynski RK, Zabel BA, Kohrt HE, Tejeda NM, Monnier J, Swanson CD, et al. The chemoattractant chemerin suppresses melanoma by recruiting natural killer cell antitumor defenses. The Journal of experimental medicine. 2012;209(8):1427-35.
310. Liu-Chittenden Y, Jain M, Gaskins K, Wang S, Merino MJ, Kotian S, et al. RARRES2 functions as a tumor suppressor by promoting beta-catenin phosphorylation/degradation and inhibiting p38 phosphorylation in adrenocortical carcinoma. Oncogene. 2017;36(25):3541-52.
311. Kulig P, Kantyka T, Zabel BA, Banas M, Chyra A, Stefanska A, et al. Regulation of chemerin chemoattractant and antibacterial activity by human cysteine cathepsins. Journal of immunology. 2011;187(3):1403-10.
312. Farsam V, Basu A, Gatzka M, Treiber N, Schneider LA, Mulaw MA, et al. Senescent fibroblast-derived Chemerin promotes squamous cell carcinoma migration. Oncotarget. 2016;7(50):83554-69.
313. Yin F, Xu Z, Wang Z, Yao H, Shen Z, Yu F, et al. Elevated chemokine CC-motif receptor-like 2 (CCRL2) promotes cell migration and invasion in glioblastoma. Biochem Biophys Res Commun. 2012;429(3-4):168-72.
314. Akram IG, Georges R, Hielscher T, Adwan H, Berger MR. The chemokines CCR1 and CCRL2 have a role in colorectal cancer liver metastasis. Tumour Biol. 2015.
315. Wang LP, Cao J, Zhang J, Wang BY, Hu XC, Shao ZM, et al. The human chemokine receptor CCRL2 suppresses chemotaxis and invasion by blocking CCL2-induced phosphorylation of p38 MAPK in human breast cancer cells. Med Oncol. 2015;32(11):254.
316. Marchese A, Docherty JM, Nguyen T, Heiber M, Cheng R, Heng HH, et al. Cloning of human genes encoding novel G protein-coupled receptors. Genomics. 1994;23(3):609-18.
317. Kennedy AJ, Davenport AP. International Union of Basic and Clinical Pharmacology CIII: Chemerin Receptors CMKLR1 (Chemerin1) and GPR1 (Chemerin2) Nomenclature, Pharmacology, and Function. Pharmacol Rev. 2018;70(1):174-96.
318. Shimizu N, Soda Y, Kanbe K, Liu HY, Jinno A, Kitamura T, et al. An orphan G protein-coupled receptor, GPR1, acts as a coreceptor to allow replication of human immunodeficiency virus types 1 and 2 in brain-derived cells. J Virol. 1999;73(6):5231-9.
319. Rourke JL, Muruganandan S, Dranse HJ, McMullen NM, Sinal CJ. Gpr1 is an active chemerin receptor influencing glucose homeostasis in obese mice. The Journal of endocrinology. 2014;222(2):201-15.
320. Karagiannis GS, Weile J, Bader GD, Minta J. Integrative pathway dissection of molecular mechanisms of moxLDL-induced vascular smooth muscle phenotype transformation. BMC Cardiovasc Disord. 2013;13:4.
321. Kumar JD, Aolymat I, Tiszlavicz L, Reisz Z, Garalla HM, Beynon R, et al. Chemerin acts via CMKLR1 and GPR1 to stimulate migration and invasion of gastric cancer cells: putative role of decreased TIMP-1 and TIMP-2. Oncotarget. 2019;10(2):98-112.
322. Wang DZ, Dubois RN. Eicosanoids and cancer. Nature Reviews Cancer. 2010;10(3):181-93.
323. Kalinski P. Regulation of immune responses by prostaglandin E2. Journal of immunology. 2012;188(1):21-8.
324. Liu B, Qu L, Yan S. Cyclooxygenase-2 promotes tumor growth and suppresses tumor immunity. Cancer Cell Int. 2015;15:106.

325. Chizzolini C, Chicheportiche R, Alvarez M, de Rham C, Roux-Lombard P, Ferrari-Lacraz S, et al. Prostaglandin E2 synergistically with interleukin-23 favors human Th17 expansion. Blood. 2008;112(9):3696-703.
326. Taniguchi K, Karin M. NF-kappaB, inflammation, immunity and cancer: coming of age. Nature reviews Immunology. 2018;18(5):309-24.
327. Yu H, Lee H, Herrmann A, Buettner R, Jove R. Revisiting STAT3 signalling in cancer: new and unexpected biological functions. Nature reviews Cancer. 2014;14(11):736-46.
328. Mocsai A, Ruland J, Tybulewicz VL. The SYK tyrosine kinase: a crucial player in diverse biological functions. Nature reviews Immunology. 2010;10(6):387-402.
329. Geahlen RL. Getting Syk: spleen tyrosine kinase as a therapeutic target. Trends in pharmacological sciences. 2014;35(8):414-22.
330. Markham A. Fostamatinib: First Global Approval. Drugs. 2018;78(9):959-63.
331. Krisenko MO, Geahlen RL. Calling in SYK: SYK's dual role as a tumor promoter and tumor suppressor in cancer. Biochim Biophys Acta. 2015;1853(1):254-63.
332. Coopman PJ, Do MT, Barth M, Bowden ET, Hayes AJ, Basyuk E, et al. The Syk tyrosine kinase suppresses malignant growth of human breast cancer cells. Nature. 2000;406(6797):742-7.
333. Larive RM, Urbach S, Poncet J, Jouin P, Mascre G, Sahuquet A, et al. Phosphoproteomic analysis of Syk kinase signaling in human cancer cells reveals its role in cell-cell adhesion. Oncogene. 2009;28(24):2337-47.
334. Shinde A, Hardy SD, Kim D, Akhand SS, Jolly MK, Wang WH, et al. Spleen Tyrosine Kinase-Mediated Autophagy Is Required for Epithelial-Mesenchymal Plasticity and Metastasis in Breast Cancer. Cancer research. 2019;79(8):1831-43.
335. Sun H, Lin DC, Cao Q, Pang B, Gae DD, Lee VKM, et al. Identification of a Novel SYK/c-MYC/MALAT1 Signaling Pathway and Its Potential Therapeutic Value in Ewing Sarcoma. Clin Cancer Res. 2017;23(15):4376-87.
336. Zhang J, Benavente CA, McEvoy J, Flores-Otero J, Ding L, Chen X, et al. A novel retinoblastoma therapy from genomic and epigenetic analyses. Nature. 2012;481(7381):329-34.
337. Yu Y, Gaillard S, Phillip JM, Huang TC, Pinto SM, Tessarollo NG, et al. Inhibition of Spleen Tyrosine Kinase Potentiates Paclitaxel-Induced Cytotoxicity in Ovarian Cancer Cells by Stabilizing Microtubules. Cancer cell. 2015;28(1):82-96.
338. Yu Y, Suryo Rahmanto Y, Lee MH, Wu PH, Phillip JM, Huang CH, et al. Inhibition of ovarian tumor cell invasiveness by targeting SYK in the tyrosine kinase signaling pathway. Oncogene. 2018.
339. Moncayo G, Grzmil M, Smirnova T, Zmarz P, Huber RM, Hynx D, et al. SYK Inhibition Blocks Proliferation and Migration of Glioma Cells, and Modifies the Tumor Microenvironment. Neuro Oncol. 2018.
340. Tümmler C, Dumitriu G, Wickström M, Coopman P, Valkov A, Kogner P, et al. SYK Inhibition Potentiates the Effect of Chemotherapeutic Drugs on Neuroblastoma Cells in Vitro. Cancers (Basel). 2019;11(2):202.
341. Pritchard-Jones K, Pieters R, Reaman GH, Hjorth L, Downie P, Calaminus G, et al. Sustaining innovation and improvement in the treatment of childhood cancer: lessons from high-income countries. Lancet Oncology. 2013;14(3):E95-E103.
342. Murphy MF, Bithell JF, Stiller CA, Kendall GM, O'Neill KA. Childhood and adult cancers: contrasts and commonalities. Maturitas. 2013;76(1):95-8.
343. Vassal G, Schrappe M, Pritchard-Jones K, Arnold F, Bassete L, Biondi A, et al. The SIOPE strategic plan: A European cancer plan for children and adolescents. J Cancer Policy. 2016;8:17-32.
344. Steliarova-Foucher E, Stiller C, Kaatsch P, Berrino F, Coebergh JW, Lacour B, et al. Geographical patterns and time trends of cancer incidence and survival among children and adolescents in Europe since the 1970s (the ACCISproject): an epidemiological study. Lancet. 2004;364(9451):2097-105.
345. Scotting PJ, Walker DA, Perilongo G. Opinion - Childhood solid tumours: a developmental disorder. Nature Reviews Cancer. 2005;5(6):481-8.
346. Grimmer MR, Weiss WA. Childhood tumors of the nervous system as disorders of normal development. Current Opinion in Pediatrics. 2006;18(6):634-8.
347. Grobner SN, Worst BC, Weischenfeldt J, Buchhalter I, Kleinheinz K, Rudneva VA, et al. The landscape of genomic alterations across childhood cancers. Nature. 2018;555(7696):321-+.

348. Ma XT, Liu Y, Liu YL, Alexandrov LB, Edmonson MN, Gawad C, et al. Pan-cancer genome and transcriptome analyses of 1,699 paediatric leukaemias and solid tumours. Nature. 2018;555(7696):371-+.
349. Robison LL, Hudson MM. Survivors of childhood and adolescent cancer: life-long risks and responsibilities. Nature reviews Cancer. 2014;14(1):61-70.
350. Bhakta N, Liu Q, Ness KK, Baassiri M, Eissa H, Yeo F, et al. The cumulative burden of surviving childhood cancer: an initial report from the St Jude Lifetime Cohort Study (SJLIFE). Lancet. 2017;390(10112):2569-82.
351. Brodeur GM. Neuroblastoma: biological insights into a clinical enigma. Nature reviews Cancer. 2003;3(3):203-16.
352. Schwab M, Westermann F, Hero B, Berthold F. Neuroblastoma: biology and molecular and chromosomal pathology. Lancet Oncol. 2003;4(8):472-80.
353. Irwin MS, Park JR. Neuroblastoma: paradigm for precision medicine. Pediatr Clin North Am. 2015;62(1):225-56.
354. London WB, Castleberry RP, Matthay KK, Look AT, Seeger RC, Shimada H, et al. Evidence for an age cutoff greater than 365 days for neuroblastoma risk group stratification in the Children's Oncology Group. Journal of clinical oncology : official journal of the American Society of Clinical Oncology. 2005;23(27):6459-65.
355. Stiller CA, Parkin DM. International variations in the incidence of neuroblastoma. International journal of cancer Journal international du cancer. 1992;52(4):538-43.
356. Gatta G, Ferrari A, Stiller CA, Pastore G, Bisogno G, Trama A, et al. Embryonal cancers in Europe. European journal of cancer. 2012;48(10):1425-33.
357. Matthay KK, Maris JM, Schleiermacher G, Nakagawara A, Mackall CL, Diller L, et al. Neuroblastoma. Nat Rev Dis Primers. 2016;2:16078.
358. Vo KT, Matthay KK, Neuhaus J, London WB, Hero B, Ambros PF, et al. Clinical, biologic, and prognostic differences on the basis of primary tumor site in neuroblastoma: a report from the international neuroblastoma risk group project. Journal of clinical oncology : official journal of the American Society of Clinical Oncology. 2014;32(28):3169-76.
359. DuBois SG, Kalika Y, Lukens JN, Brodeur GM, Seeger RC, Atkinson JB, et al. Metastatic sites in stage IV and IVS neuroblastoma correlate with age, tumor biology, and survival. J Pediatr Hematol Oncol. 1999;21(3):181-9.
360. Spix C, Pastore G, Sankila R, Stiller CA, Steliarova-Foucher E. Neuroblastoma incidence and survival in European children (1978-1997): report from the Automated Childhood Cancer Information System project. European journal of cancer. 2006;42(13):2081-91.
361. Esiashvili N, Goodman M, Ward K, Marcus RB, Jr., Johnstone PA. Neuroblastoma in adults: Incidence and survival analysis based on SEER data. Pediatr Blood Cancer. 2007;49(1):41-6.
362. Nordic Society of Paediatric Haematology and Oncology. NOPHO Annual report 2016. retrieved from: http://www.barnekreftportalen.no/images/Marketing/info/Nyheter/NOPHO%20Annual%20report%202016.pdf. 2016.
363. Berlanga P, Canete A, Castel V. Advances in emerging drugs for the treatment of neuroblastoma. Expert Opin Emerg Drugs. 2017;22(1):63-75.
364. Anderson DJ, Axel R. A bipotential neuroendocrine precursor whose choice of cell fate is determined by NGF and glucocorticoids. Cell. 1986;47(6):1079-90.
365. Anderson DJ, Carnahan JF, Michelsohn A, Patterson PH. Antibody markers identify a common progenitor to sympathetic neurons and chromaffin cells in vivo and reveal the timing of commitment to neuronal differentiation in the sympathoadrenal lineage. J Neurosci. 1991;11(11):3507-19.
366. Tomolonis JA, Agarwal S, Shohet JM. Neuroblastoma pathogenesis: deregulation of embryonic neural crest development. Cell Tissue Res. 2017.
367. Johnsen JI, Dyberg C, Wickstrom M. Neuroblastoma-A Neural Crest Derived Embryonal Malignancy. Front Mol Neurosci. 2019;12:9.
368. Mosse YP, Laudenslager M, Longo L, Cole KA, Wood A, Attiyeh EF, et al. Identification of ALK as a major familial neuroblastoma predisposition gene. Nature. 2008;455(7215):930-5.
369. Ambros PF, Ambros IM, Brodeur GM, Haber M, Khan J, Nakagawara A, et al. International consensus for neuroblastoma molecular diagnostics: report from the International

Neuroblastoma Risk Group (INRG) Biology Committee. British journal of cancer. 2009;100(9):1471-82.
370. Schleiermacher G, Mosseri V, London WB, Maris JM, Brodeur GM, Attiyeh E, et al. Segmental chromosomal alterations have prognostic impact in neuroblastoma: a report from the INRG project. British journal of cancer. 2012;107(8):1418-22.
371. Attiyeh EF, London WB, Mosse YP, Wang Q, Winter C, Khazi D, et al. Chromosome 1p and 11q deletions and outcome in neuroblastoma. The New England journal of medicine. 2005;353(21):2243-53.
372. Bown N, Cotterill S, Lastowska M, O'Neill S, Pearson AD, Plantaz D, et al. Gain of chromosome arm 17q and adverse outcome in patients with neuroblastoma. The New England journal of medicine. 1999;340(25):1954-61.
373. Caren H, Kryh H, Nethander M, Sjoberg RM, Trager C, Nilsson S, et al. High-risk neuroblastoma tumors with 11q-deletion display a poor prognostic, chromosome instability phenotype with later onset. Proc Natl Acad Sci U S A. 2010;107(9):4323-8.
374. Depuydt P, Boeva V, Hocking TD, Cannoodt R, Ambros IM, Ambros PF, et al. Genomic Amplifications and Distal 6q Loss: Novel Markers for Poor Survival in High-risk Neuroblastoma Patients. Journal of the National Cancer Institute. 2018.
375. Brodeur GM, Seeger RC, Schwab M, Varmus HE, Bishop JM. Amplification of N-myc in untreated human neuroblastomas correlates with advanced disease stage. Science. 1984;224(4653):1121-4.
376. Brodeur GM, Seeger RC, Schwab M, Varmus HE, Bishop JM. Amplification of N-myc sequences in primary human neuroblastomas: correlation with advanced disease stage. Prog Clin Biol Res. 1985;175:105-13.
377. Seeger RC, Brodeur GM, Sather H, Dalton A, Siegel SE, Wong KY, et al. Association of multiple copies of the N-myc oncogene with rapid progression of neuroblastomas. The New England journal of medicine. 1985;313(18):1111-6.
378. Kohl NE, Kanda N, Schreck RR, Bruns G, Latt SA, Gilbert F, et al. Transposition and amplification of oncogene-related sequences in human neuroblastomas. Cell. 1983;35(2 Pt 1):359-67.
379. Hogarty MD, Maris JM. PI3King on MYCN to improve neuroblastoma therapeutics. Cancer cell. 2012;21(2):145-7.
380. Huang M, Weiss WA. Neuroblastoma and MYCN. Cold Spring Harb Perspect Med. 2013;3(10):a014415.
381. Ruiz-Perez MV, Henley AB, Arsenian-Henriksson M. The MYCN Protein in Health and Disease. Genes (Basel). 2017;8(4).
382. Pugh TJ, Morozova O, Attiyeh EF, Asgharzadeh S, Wei JS, Auclair D, et al. The genetic landscape of high-risk neuroblastoma. Nat Genet. 2013;45(3):279-84.
383. Cheung NK, Zhang J, Lu C, Parker M, Bahrami A, Tickoo SK, et al. Association of age at diagnosis and genetic mutations in patients with neuroblastoma. JAMA. 2012;307(10):1062-71.
384. Molenaar JJ, Koster J, Zwijnenburg DA, van Sluis P, Valentijn LJ, van der Ploeg I, et al. Sequencing of neuroblastoma identifies chromothripsis and defects in neuritogenesis genes. Nature. 2012;483(7391):589-93.
385. Sausen M, Leary RJ, Jones S, Wu J, Reynolds CP, Liu X, et al. Integrated genomic analyses identify ARID1A and ARID1B alterations in the childhood cancer neuroblastoma. Nat Genet. 2013;45(1):12-7.
386. Schramm A, Koster J, Assenov Y, Althoff K, Peifer M, Mahlow E, et al. Mutational dynamics between primary and relapse neuroblastomas. Nat Genet. 2015;47(8):872-7.
387. Schleiermacher G, Janoueix-Lerosey I, Ribeiro A, Klijanienko J, Couturier J, Pierron G, et al. Accumulation of segmental alterations determines progression in neuroblastoma. Journal of clinical oncology : official journal of the American Society of Clinical Oncology. 2010;28(19):3122-30.
388. Eleveld TF, Oldridge DA, Bernard V, Koster J, Colmet Daage L, Diskin SJ, et al. Relapsed neuroblastomas show frequent RAS-MAPK pathway mutations. Nat Genet. 2015;47(8):864-71.
389. Schleiermacher G, Javanmardi N, Bernard V, Leroy Q, Cappo J, Rio Frio T, et al. Emergence of new ALK mutations at relapse of neuroblastoma. Journal of clinical oncology : official journal of the American Society of Clinical Oncology. 2014;32(25):2727-34.

390. Carr-Wilkinson J, O'Toole K, Wood KM, Challen CC, Baker AG, Board JR, et al. High Frequency of p53/MDM2/p14ARF Pathway Abnormalities in Relapsed Neuroblastoma. Clin Cancer Res. 2010;16(4):1108-18.
391. Hwang WL, Wolfson RL, Niemierko A, Marcus KJ, DuBois SG, Haas-Kogan D. Clinical Impact of Tumor Mutational Burden in Neuroblastoma. Journal of the National Cancer Institute. 2018.
392. Diede SJ. Spontaneous regression of metastatic cancer: learning from neuroblastoma. Nature reviews Cancer. 2014;14(2):71-2.
393. Brodeur GM, Bagatell R. Mechanisms of neuroblastoma regression. Nature reviews Clinical oncology. 2014;11(12):704-13.
394. Brodeur GM. Spontaneous regression of neuroblastoma. Cell Tissue Res. 2018;372(2):277-86.
395. Shimada H, Ambros IM, Dehner LP, Hata J, Joshi VV, Roald B, et al. The International Neuroblastoma Pathology Classification (the Shimada system). Cancer. 1999;86(2):364-72.
396. Peuchmaur M, d'Amore ES, Joshi VV, Hata J, Roald B, Dehner LP, et al. Revision of the International Neuroblastoma Pathology Classification: confirmation of favorable and unfavorable prognostic subsets in ganglioneuroblastoma, nodular. Cancer. 2003;98(10):2274-81.
397. Shimada H, Ambros IM, Dehner LP, Hata J, Joshi VV, Roald B. Terminology and morphologic criteria of neuroblastic tumors: recommendations by the International Neuroblastoma Pathology Committee. Cancer. 1999;86(2):349-63.
398. Borriello L, Seeger RC, Asgharzadeh S, DeClerck YA. More than the genes, the tumor microenvironment in neuroblastoma. Cancer letters. 2015.
399. Martin RF, Beckwith JB. Lymphoid infiltrates in neuroblastomas: their occurrence and prognostic significance. J Pediatr Surg. 1968;3(1):161-4.
400. Lauder I, Aherne W. The significance of lymphocytic infiltration in neuroblastoma. British journal of cancer. 1972;26(4):321-30.
401. Mina M, Boldrini R, Citti A, Romania P, D'Alicandro V, De Ioris M, et al. Tumor-infiltrating T lymphocytes improve clinical outcome of therapy-resistant neuroblastoma. Oncoimmunology. 2015;4(9):e1019981.
402. Layer JP, Kronmuller MT, Quast T, van den Boorn-Konijnenberg D, Effern M, Hinze D, et al. Amplification of N-Myc is associated with a T-cell-poor microenvironment in metastatic neuroblastoma restraining interferon pathway activity and chemokine expression. Oncoimmunology. 2017;6(6):e1320626.
403. Wei JS, Kuznetsov IB, Zhang S, Song YK, Asgharzadeh S, Sindiri S, et al. Clinically Relevant Cytotoxic Immune Cell Signatures and Clonal Expansion of T-Cell Receptors in High-Risk MYCN-Not-Amplified Human Neuroblastoma. Clin Cancer Res. 2018;24(22):5673-84.
404. Carlson LM, De Geer A, Sveinbjornsson B, Orrego A, Martinsson T, Kogner P, et al. The microenvironment of human neuroblastoma supports the activation of tumor-associated T lymphocytes. Oncoimmunology. 2013;2(3):e23618.
405. Vanichapol T, Chutipongtanate S, Anurathapan U, Hongeng S. Immune Escape Mechanisms and Future Prospects for Immunotherapy in Neuroblastoma. BioMed research international. 2018;2018:1812535.
406. Mussai F, Egan S, Hunter S, Webber H, Fisher J, Wheat R, et al. Neuroblastoma Arginase Activity Creates an Immunosuppressive Microenvironment That Impairs Autologous and Engineered Immunity. Cancer research. 2015;75(15):3043-53.
407. Melaiu O, Mina M, Chierici M, Boldrini R, Jurman G, Romania P, et al. PD-L1 Is a Therapeutic Target of the Bromodomain Inhibitor JQ1 and, Combined with HLA Class I, a Promising Prognostic Biomarker in Neuroblastoma. Clin Cancer Res. 2017;23(15):4462-72.
408. Carlson LM, Pahlman S, De Geer A, Kogner P, Levitskaya J. Differentiation induced by physiological and pharmacological stimuli leads to increased antigenicity of human neuroblastoma cells. Cell Res. 2008;18(3):398-411.
409. Bottino C, Dondero A, Bellora F, Moretta L, Locatelli F, Pistoia V, et al. Natural Killer Cells and Neuroblastoma: Tumor Recognition, Escape Mechanisms, and Possible Novel Immunotherapeutic Approaches. Frontiers in Immunology. 2014;5.
410. Brandetti E, Veneziani I, Melaiu O, Pezzolo A, Castellano A, Boldrini R, et al. MYCN is an immunosuppressive oncogene dampening the expression of ligands for NK-cell-activating receptors in human high-risk neuroblastoma. Oncoimmunology. 2017;6(6):e1316439.

411. Semeraro M, Rusakiewicz S, Minard-Colin V, Delahaye NF, Enot D, Vely F, et al. Clinical impact of the NKp30/B7-H6 axis in high-risk neuroblastoma patients. Sci Transl Med. 2015;7(283):283ra55.
412. Asgharzadeh S, Salo JA, Ji L, Oberthuer A, Fischer M, Berthold F, et al. Clinical significance of tumor-associated inflammatory cells in metastatic neuroblastoma. Journal of clinical oncology : official journal of the American Society of Clinical Oncology. 2012;30(28):3525-32.
413. Hashimoto O, Yoshida M, Koma Y, Yanai T, Hasegawa D, Kosaka Y, et al. Collaboration of cancer-associated fibroblasts and tumour-associated macrophages for neuroblastoma development. J Pathol. 2016;240(2):211-23.
414. Song L, Asgharzadeh S, Salo J, Engell K, Wu HW, Sposto R, et al. Valpha24-invariant NKT cells mediate antitumor activity via killing of tumor-associated macrophages. The Journal of clinical investigation. 2009;119(6):1524-36.
415. Hadjidaniel MD, Muthugounder S, Hung LT, Sheard MA, Shirinbak S, Chan RY, et al. Tumor-associated macrophages promote neuroblastoma via STAT3 phosphorylation and up-regulation of c-MYC. Oncotarget. 2017;8(53):91516-29.
416. Santilli G, Piotrowska I, Cantilena S, Chayka O, D'Alicarnasso M, Morgenstern DA, et al. Polyphenon [corrected] E enhances the antitumor immune response in neuroblastoma by inactivating myeloid suppressor cells. Clin Cancer Res. 2013;19(5):1116-25.
417. Mao Y, Eissler N, Blanc KL, Johnsen JI, Kogner P, Kiessling R. Targeting Suppressive Myeloid Cells Potentiates Checkpoint Inhibitors to Control Spontaneous Neuroblastoma. Clin Cancer Res. 2016;22(15):3849-59.
418. Shurin GV, Shurin MR, Bykovskaia S, Shogan J, Lotze MT, Barksdale EM, Jr. Neuroblastoma-derived gangliosides inhibit dendritic cell generation and function. Cancer research. 2001;61(1):363-9.
419. Chen X, Doffek K, Sugg SL, Shilyansky J. Neuroblastoma cells inhibit the immunostimulatory function of dendritic cells. J Pediatr Surg. 2003;38(6):901-5.
420. Kock A, Larsson K, Bergqvist F, Eissler N, Elfman LHM, Raouf J, et al. Inhibition of Microsomal Prostaglandin E Synthase-1 in Cancer-Associated Fibroblasts Suppresses Neuroblastoma Tumor Growth. EBioMedicine. 2018;32:84-92.
421. Larsson K, Kock A, Idborg H, Arsenian Henriksson M, Martinsson T, Johnsen JI, et al. COX/mPGES-1/PGE2 pathway depicts an inflammatory-dependent high-risk neuroblastoma subset. Proc Natl Acad Sci U S A. 2015;112(26):8070-5.
422. Borriello L, Nakata R, Sheard MA, Fernandez GE, Sposto R, Malvar J, et al. Cancer-Associated Fibroblasts Share Characteristics and Protumorigenic Activity with Mesenchymal Stromal Cells. Cancer research. 2017;77(18):5142-57.
423. Di Paolo D, Ambrogio C, Pastorino F, Brignole C, Martinengo C, Carosio R, et al. Selective therapeutic targeting of the anaplastic lymphoma kinase with liposomal siRNA induces apoptosis and inhibits angiogenesis in neuroblastoma. Mol Ther. 2011;19(12):2201-12.
424. Kang J, Rychahou PG, Ishola TA, Mourot JM, Evers BM, Chung DH. N-myc is a novel regulator of PI3K-mediated VEGF expression in neuroblastoma. Oncogene. 2008;27(28):3999-4007.
425. Kim ES, Serur A, Huang J, Manley CA, McCrudden KW, Frischer JS, et al. Potent VEGF blockade causes regression of coopted vessels in a model of neuroblastoma. Proc Natl Acad Sci U S A. 2002;99(17):11399-404.
426. Pezzolo A, Parodi F, Corrias MV, Cinti R, Gambini C, Pistoia V. Tumor origin of endothelial cells in human neuroblastoma. Journal of clinical oncology : official journal of the American Society of Clinical Oncology. 2007;25(4):376-83.
427. Nakata R, Shimada H, Fernandez GE, Fanter R, Fabbri M, Malvar J, et al. Contribution of neuroblastoma-derived exosomes to the production of pro-tumorigenic signals by bone marrow mesenchymal stromal cells. J Extracell Vesicles. 2017;6(1):1332941.
428. Tadeo I, Berbegall AP, Castel V, García-Miguel P, Callaghan R, Påhlman S, et al. Extracellular matrix composition defines an ultra-high-risk group of neuroblastoma within the high-risk patient cohort. British journal of cancer. 2016;115(4):480-9.
429. Ara T, Song L, Shimada H, Keshelava N, Russell HV, Metelitsa LS, et al. Interleukin-6 in the bone marrow microenvironment promotes the growth and survival of neuroblastoma cells. Cancer research. 2009;69(1):329-37.

430. Ara T, Nakata R, Sheard MA, Shimada H, Buettner R, Groshen SG, et al. Critical role of STAT3 in IL-6-mediated drug resistance in human neuroblastoma. Cancer research. 2013;73(13):3852-64.
431. Egler RA, Burlingame SM, Nuchtern JG, Russell HV. Interleukin-6 and soluble interleukin-6 receptor levels as markers of disease extent and prognosis in neuroblastoma. Clin Cancer Res. 2008;14(21):7028-34.
432. Fiebich BL, Mueksch B, Boehringer M, Hull M. Interleukin-1beta induces cyclooxygenase-2 and prostaglandin E(2) synthesis in human neuroblastoma cells: involvement of p38 mitogen-activated protein kinase and nuclear factor-kappaB. J Neurochem. 2000;75(5):2020-8.
433. Johnsen JI, Lindskog M, Ponthan F, Pettersen I, Elfman L, Orrego A, et al. Cyclooxygenase-2 is expressed in neuroblastoma, and nonsteroidal anti-inflammatory drugs induce apoptosis and inhibit tumor growth in vivo. Cancer research. 2004;64(20):7210-5.
434. Johnsen JI, Lindskog M, Ponthan F, Pettersen I, Elfman L, Orrego A, et al. NSAIDs in neuroblastoma therapy. Cancer letters. 2005;228(1-2):195-201.
435. Lau L, Hansford LM, Cheng LS, Hang M, Baruchel S, Kaplan DR, et al. Cyclooxygenase inhibitors modulate the p53/HDM2 pathway and enhance chemotherapy-induced apoptosis in neuroblastoma. Oncogene. 2007;26(13):1920-31.
436. Ponthan F, Wickstrom M, Gleissman H, Fuskevag OM, Segerstrom L, Sveinbjornsson B, et al. Celecoxib prevents neuroblastoma tumor development and potentiates the effect of chemotherapeutic drugs in vitro and in vivo. Clin Cancer Res. 2007;13(3):1036-44.
437. Rasmuson A, Kock A, Fuskevag OM, Kruspig B, Simon-Santamaria J, Gogvadze V, et al. Autocrine prostaglandin E2 signaling promotes tumor cell survival and proliferation in childhood neuroblastoma. PLoS One. 2012;7(1):e29331.
438. Carlson LM, Rasmuson A, Idborg H, Segerstrom L, Jakobsson PJ, Sveinbjornsson B, et al. Low-dose aspirin delays an inflammatory tumor progression in vivo in a transgenic mouse model of neuroblastoma. Carcinogenesis. 2013;34(5):1081-8.
439. Jansen SR, Holman R, Hedemann I, Frankes E, Elzinga CR, Timens W, et al. Prostaglandin E2 promotes MYCN non-amplified neuroblastoma cell survival via beta-catenin stabilization. J Cell Mol Med. 2015;19(1):210-26.
440. Geminder H, Sagi-Assif O, Goldberg L, Meshel T, Rechavi G, Witz IP, et al. A possible role for CXCR4 and its ligand, the CXC chemokine stromal cell-derived factor-1, in the development of bone marrow metastases in neuroblastoma. Journal of immunology. 2001;167(8):4747-57.
441. Russell HV, Hicks J, Okcu MF, Nuchtern JG. CXCR4 expression in neuroblastoma primary tumors is associated with clinical presentation of bone and bone marrow metastases. J Pediatr Surg. 2004;39(10):1506-11.
442. Airoldi I, Raffaghello L, Piovan E, Cocco C, Carlini B, Amadori A, et al. CXCL12 does not attract CXCR4+ human metastatic neuroblastoma cells: clinical implications. Clin Cancer Res. 2006;12(1):77-82.
443. Meier R, Muhlethaler-Mottet A, Flahaut M, Coulon A, Fusco C, Louache F, et al. The chemokine receptor CXCR4 strongly promotes neuroblastoma primary tumour and metastatic growth, but not invasion. PLoS One. 2007;2(10):e1016.
444. Carlisle AJ, Lyttle CA, Carlisle RY, Maris JM. CXCR4 expression heterogeneity in neuroblastoma cells due to ligand-independent regulation. Mol Cancer. 2009;8:126.
445. Ma M, Ye JY, Deng R, Dee CM, Chan GC. Mesenchymal stromal cells may enhance metastasis of neuroblastoma via SDF-1/CXCR4 and SDF-1/CXCR7 signaling. Cancer letters. 2011;312(1):1-10.
446. Liberman J, Sartelet H, Flahaut M, Muhlethaler-Mottet A, Coulon A, Nyalendo C, et al. Involvement of the CXCR7/CXCR4/CXCL12 axis in the malignant progression of human neuroblastoma. PLoS One. 2012;7(8):e43665.
447. Muhlethaler-Mottet A, Liberman J, Ascencao K, Flahaut M, Balmas Bourloud K, Yan P, et al. The CXCR4/CXCR7/CXCL12 Axis Is Involved in a Secondary but Complex Control of Neuroblastoma Metastatic Cell Homing. PLoS One. 2015;10(5):e0125616.
448. Abraham D, Zins K, Sioud M, Lucas T, Schafer R, Stanley ER, et al. Stromal cell-derived CSF-1 blockade prolongs xenograft survival of CSF-1-negative neuroblastoma. International journal of cancer Journal international du cancer. 2010;126(6):1339-52.

449. Eissler N, Mao Y, Brodin D, Reutersward P, Andersson Svahn H, Johnsen JI, et al. Regulation of myeloid cells by activated T cells determines the efficacy of PD-1 blockade. Oncoimmunology. 2016;5(12):e1232222.
450. Webb MW, Sun J, Sheard MA, Liu WY, Wu HW, Jackson JR, et al. Colony stimulating factor 1 receptor blockade improves the efficacy of chemotherapy against human neuroblastoma in the absence of T lymphocytes. International journal of cancer Journal international du cancer. 2018;143(6):1483-93.
451. Goillot E, Combaret V, Ladenstein R, Baubet D, Blay JY, Philip T, et al. Tumor necrosis factor as an autocrine growth factor for neuroblastoma. Cancer research. 1992;52(11):3194-200.
452. Korner M, Tarantino N, Pleskoff O, Lee LM, Debre P. Activation of nuclear factor kappa B in human neuroblastoma cell lines. J Neurochem. 1994;62(5):1716-26.
453. Galenkamp KM, Carriba P, Urresti J, Planells-Ferrer L, Coccia E, Lopez-Soriano J, et al. TNFalpha sensitizes neuroblastoma cells to FasL-, cisplatin- and etoposide-induced cell death by NF-kappaB-mediated expression of Fas. Mol Cancer. 2015;14:62.
454. Dondero A, Pastorino F, Della Chiesa M, Corrias MV, Morandi F, Pistoia V, et al. PD-L1 expression in metastatic neuroblastoma as an additional mechanism for limiting immune surveillance. Oncoimmunology. 2016;5(1):e1064578.
455. Harada K, Ihara F, Takami M, Kamata T, Mise N, Yoshizawa H, et al. Soluble factors derived from neuroblastoma cell lines suppress dendritic cell differentiation and activation. Cancer Sci. 2019.
456. Fultang L, Gamble LD, Gneo L, Berry AM, Egan SA, De Bie F, et al. Macrophage-derived IL-1beta and TNF-alpha regulate arginine metabolism in neuroblastoma. Cancer research. 2018.
457. Brodeur GM, Seeger RC, Barrett A, Berthold F, Castleberry RP, D'Angio G, et al. International criteria for diagnosis, staging, and response to treatment in patients with neuroblastoma. Journal of clinical oncology : official journal of the American Society of Clinical Oncology. 1988;6(12):1874-81.
458. Brodeur GM, Pritchard J, Berthold F, Carlsen NL, Castel V, Castelberry RP, et al. Revisions of the international criteria for neuroblastoma diagnosis, staging, and response to treatment. Journal of clinical oncology : official journal of the American Society of Clinical Oncology. 1993;11(8):1466-77.
459. Cohn SL, Pearson AD, London WB, Monclair T, Ambros PF, Brodeur GM, et al. The International Neuroblastoma Risk Group (INRG) classification system: an INRG Task Force report. Journal of clinical oncology : official journal of the American Society of Clinical Oncology. 2009;27(2):289-97.
460. Monclair T, Brodeur GM, Ambros PF, Brisse HJ, Cecchetto G, Holmes K, et al. The International Neuroblastoma Risk Group (INRG) staging system: an INRG Task Force report. Journal of clinical oncology : official journal of the American Society of Clinical Oncology. 2009;27(2):298-303.
461. Tolbert VP, Matthay KK. Neuroblastoma: clinical and biological approach to risk stratification and treatment. Cell Tissue Res. 2018;372(2):195-209.
462. Hero B, Simon T, Spitz R, Ernestus K, Gnekow AK, Scheel-Walter H-G, et al. Localized Infant Neuroblastomas Often Show Spontaneous Regression: Results of the Prospective Trials NB95-S and NB97. 2008;26(9):1504-10.
463. Nuchtern JG, London WB, Barnewolt CE, Naranjo A, McGrady PW, Geiger JD, et al. A prospective study of expectant observation as primary therapy for neuroblastoma in young infants: a Children's Oncology Group study. Ann Surg. 2012;256(4):573-80.
464. Baker DL, Schmidt ML, Cohn SL, Maris JM, London WB, Buxton A, et al. Outcome after reduced chemotherapy for intermediate-risk neuroblastoma. The New England journal of medicine. 2010;363(14):1313-23.
465. Rubie H, De Bernardi B, Gerrard M, Canete A, Ladenstein R, Couturier J, et al. Excellent outcome with reduced treatment in infants with nonmetastatic and unresectable neuroblastoma without MYCN amplification: results of the prospective INES 99.1. Journal of clinical oncology : official journal of the American Society of Clinical Oncology. 2011;29(4):449-55.
466. Strother DR, London WB, Schmidt ML, Brodeur GM, Shimada H, Thorner P, et al. Outcome after surgery alone or with restricted use of chemotherapy for patients with low-risk

neuroblastoma: results of Children's Oncology Group study P9641. Journal of clinical oncology : official journal of the American Society of Clinical Oncology. 2012;30(15):1842-8.
467. Pinto NR, Applebaum MA, Volchenboum SL, Matthay KK, London WB, Ambros PF, et al. Advances in Risk Classification and Treatment Strategies for Neuroblastoma. Journal of clinical oncology : official journal of the American Society of Clinical Oncology. 2015;33(27):3008-17.
468. Smith V, Foster J. High-Risk Neuroblastoma Treatment Review. Children (Basel). 2018;5(9).
469. Wilson JS, Gains JE, Moroz V, Wheatley K, Gaze MN. A systematic review of 131I-meta iodobenzylguanidine molecular radiotherapy for neuroblastoma. European journal of cancer. 2014;50(4):801-15.
470. Johnsen JI, Dyberg C, Fransson S, Wickstrom M. Molecular mechanisms and therapeutic targets in neuroblastoma. Pharmacol Res. 2018;131:164-76.
471. Greengard EG. Molecularly Targeted Therapy for Neuroblastoma. Children (Basel). 2018;5(10).
472. Yu AL, Gilman AL, Ozkaynak MF, London WB, Kreissman SG, Chen HX, et al. Anti-GD2 antibody with GM-CSF, interleukin-2, and isotretinoin for neuroblastoma. The New England journal of medicine. 2010;363(14):1324-34.
473. Talleur AC, Triplett BM, Federico S, Mamcarz E, Janssen W, Wu J, et al. Consolidation Therapy for Newly Diagnosed Pediatric Patients with High-Risk Neuroblastoma Using Busulfan/Melphalan, Autologous Hematopoietic Cell Transplantation, Anti-GD2 Antibody, Granulocyte-Macrophage Colony-Stimulating Factor, Interleukin-2, and Haploidentical Natural Killer Cells. Biol Blood Marrow Transplant. 2017;23(11):1910-7.
474. Sait S, Modak S. Anti-GD2 immunotherapy for neuroblastoma. Expert Rev Anticancer Ther. 2017;17(10):889-904.
475. Federico SM, McCarville MB, Shulkin BL, Sondel PM, Hank JA, Hutson P, et al. A Pilot Trial of Humanized Anti-GD2 Monoclonal Antibody (hu14.18K322A) with Chemotherapy and Natural Killer Cells in Children with Recurrent/Refractory Neuroblastoma. Clin Cancer Res. 2017;23(21):6441-9.
476. Mody R, Naranjo A, Van Ryn C, Yu AL, London WB, Shulkin BL, et al. Irinotecan-temozolomide with temsirolimus or dinutuximab in children with refractory or relapsed neuroblastoma (COG ANBL1221): an open-label, randomised, phase 2 trial. Lancet Oncol. 2017;18(7):946-57.
477. Siebert N, Zumpe M, Juttner M, Troschke-Meurer S, Lode HN. PD-1 blockade augments anti-neuroblastoma immune response induced by anti-GD2 antibody ch14.18/CHO. Oncoimmunology. 2017;6(10):e1343775.
478. Mueller I, Ehlert K, Endres S, Pill L, Siebert N, Kietz S, et al. Tolerability, response and outcome of high-risk neuroblastoma patients treated with long-term infusion of anti-GD2 antibody ch14.18/CHO. MAbs. 2018;10(1):55-61.
479. Wagner LM, Adams VR. Targeting the PD-1 pathway in pediatric solid tumors and brain tumors. Onco Targets Ther. 2017;10:2097-106.
480. Heczey A, Louis CU, Savoldo B, Dakhova O, Durett A, Grilley B, et al. CAR T Cells Administered in Combination with Lymphodepletion and PD-1 Inhibition to Patients with Neuroblastoma. Mol Ther. 2017;25(9):2214-24.
481. Kanold J, Paillard C, Tchirkov A, Lang P, Kelly A, Halle P, et al. NK cell immunotherapy for high-risk neuroblastoma relapse after haploidentical HSCT. Pediatr Blood Cancer. 2012;59(4):739-42.
482. Merchant MS, Wright M, Baird K, Wexler LH, Rodriguez-Galindo C, Bernstein D, et al. Phase I Clinical Trial of Ipilimumab in Pediatric Patients with Advanced Solid Tumors. Clin Cancer Res. 2016;22(6):1364-70.
483. Walker AJ, Majzner RG, Zhang L, Wanhainen K, Long AH, Nguyen SM, et al. Tumor Antigen and Receptor Densities Regulate Efficacy of a Chimeric Antigen Receptor Targeting Anaplastic Lymphoma Kinase. Mol Ther. 2017;25(9):2189-201.
484. Parihar R, Rivas C, Huynh M, Omer B, Lapteva N, Metelitsa LS, et al. NK Cells Expressing a Chimeric Activating Receptor Eliminate MDSCs and Rescue Impaired CAR-T Cell Activity against Solid Tumors. Cancer Immunol Res. 2019.
485. Wu HW, Sheard MA, Malvar J, Fernandez GE, DeClerck YA, Blavier L, et al. Anti-CD105 Antibody Eliminates Tumor Microenvironment Cells and Enhances Anti-GD2 Antibody Immunotherapy of Neuroblastoma with Activated Natural Killer Cells. Clin Cancer Res. 2019.
486. Harenza JL, Diamond MA, Adams RN, Song MM, Davidson HL, Hart LS, et al. Transcriptomic profiling of 39 commonly-used neuroblastoma cell lines. Sci Data. 2017;4:170033.

487. Kuhlmann I. The prophylactic use of antibiotics in cell culture. Cytotechnology. 1995;19(2):95-105.
488. Ryu AH, Eckalbar WL, Kreimer A, Yosef N, Ahituv N. Use antibiotics in cell culture with caution: genome-wide identification of antibiotic-induced changes in gene expression and regulation. Sci Rep. 2017;7(1):7533.
489. Thermo Fisher Scientific Inc. Cell Culture Basics Handbook 2016 [Available from: thermofisher.com/gibcoeducation.
490. Tamassia N, Arruda-Silva F, Calzetti F, Lonardi S, Gasperini S, Gardiman E, et al. A Reappraisal on the Potential Ability of Human Neutrophils to Express and Produce IL-17 Family Members In Vitro: Failure to Reproducibly Detect It. Front Immunol. 2018;9:795.
491. Tamarozzi F, Wright HL, Thomas HB, Edwards SW, Taylor MJ. A lack of confirmation with alternative assays questions the validity of IL-17A expression in human neutrophils using immunohistochemistry. Immunol Lett. 2014;162(2 Pt B):194-8.
492. Baker M. Reproducibility crisis: Blame it on the antibodies. Nature. 2015;521(7552):274-6.
493. Uhlen M, Fagerberg L, Hallstrom BM, Lindskog C, Oksvold P, Mardinoglu A, et al. Proteomics. Tissue-based map of the human proteome. Science. 2015;347(6220):1260419.
494. Uhlen M, Bandrowski A, Carr S, Edwards A, Ellenberg J, Lundberg E, et al. A proposal for validation of antibodies. Nature methods. 2016;13(10):823-7.
495. Voskuil JL. The challenges with the validation of research antibodies. F1000Res. 2017;6:161.
496. Janes KA. An analysis of critical factors for quantitative immunoblotting. Sci Signal. 2015;8(371):rs2.
497. Leybaert L, Sanderson MJ. Intercellular Ca(2+) waves: mechanisms and function. Physiol Rev. 2012;92(3):1359-92.
498. Mosmann T. Rapid colorimetric assay for cellular growth and survival: application to proliferation and cytotoxicity assays. J Immunol Methods. 1983;65(1-2):55-63.
499. Chaitanya GV, Steven AJ, Babu PP. PARP-1 cleavage fragments: signatures of cell-death proteases in neurodegeneration. Cell communication and signaling : CCS. 2010;8:31.
500. Liang CC, Park AY, Guan JL. In vitro scratch assay: a convenient and inexpensive method for analysis of cell migration in vitro. Nature protocols. 2007;2(2):329-33.
501. Adli M. The CRISPR tool kit for genome editing and beyond. Nat Commun. 2018;9(1):1911.
502. Flanagan SP. 'Nude', a new hairless gene with pleiotropic effects in the mouse. Genet Res. 1966;8(3):295-309.
503. Nehls M, Pfeifer D, Schorpp M, Hedrich H, Boehm T. New member of the winged-helix protein family disrupted in mouse and rat nude mutations. Nature. 1994;372(6501):103-7.
504. Kaestner KH, Knochel W, Martinez DE. Unified nomenclature for the winged helix/forkhead transcription factors. Genes Dev. 2000;14(2):142-6.
505. Weiss WA, Aldape K, Mohapatra G, Feuerstein BG, Bishop JM. Targeted expression of MYCN causes neuroblastoma in transgenic mice. EMBO J. 1997;16(11):2985-95.
506. Teitz T, Inoue M, Valentine MB, Zhu K, Rehg JE, Zhao W, et al. Th-MYCN mice with caspase-8 deficiency develop advanced neuroblastoma with bone marrow metastasis. Cancer research. 2013;73(13):4086-97.
507. Berry T, Luther W, Bhatnagar N, Jamin Y, Poon E, Sanda T, et al. The ALK(F1174L) mutation potentiates the oncogenic activity of MYCN in neuroblastoma. Cancer cell. 2012;22(1):117-30.
508. Heukamp LC, Thor T, Schramm A, De Preter K, Kumps C, De Wilde B, et al. Targeted expression of mutated ALK induces neuroblastoma in transgenic mice. Sci Transl Med. 2012;4(141):141ra91.
509. Iwakura H, Ariyasu H, Kanamoto N, Hosoda K, Nakao K, Kangawa K, et al. Establishment of a novel neuroblastoma mouse model. Int J Oncol. 2008;33(6):1195-9.
510. Friedman DN, Henderson TO. Late Effects and Survivorship Issues in Patients with Neuroblastoma. Children (Basel). 2018;5(8).
511. Sabnis AJ, Bivona TG. Principles of Resistance to Targeted Cancer Therapy: Lessons from Basic and Translational Cancer Biology. Trends in molecular medicine. 2019;25(3):185-97.
512. DuBois SG, Mosse YP, Fox E, Kudgus RA, Reid JM, McGovern R, et al. Phase II Trial of Alisertib in Combination with Irinotecan and Temozolomide for Patients with Relapsed or Refractory Neuroblastoma. Clin Cancer Res. 2018;24(24):6142-9.

513. Guan J, Fransson S, Siaw JT, Treis D, Van den Eynden J, Chand D, et al. Clinical response of the novel activating ALK-I1171T mutation in neuroblastoma to the ALK inhibitor ceritinib. Cold Spring Harb Mol Case Stud. 2018;4(4).
514. Sun S, Xue D, Chen Z, Ou-Yang Y, Zhang J, Mai J, et al. R406 elicits anti-Warburg effect via Syk-dependent and -independent mechanisms to trigger apoptosis in glioma stem cells. Cell death & disease. 2019;10(5):358.
515. Cash JL, Christian AR, Greaves DR. Chemerin peptides promote phagocytosis in a ChemR23- and Syk-dependent manner. Journal of immunology. 2010;184(9):5315-24.
516. Torres-Hernandez A, Wang W, Nikiforov Y, Tejada K, Torres L, Kalabin A, et al. Targeting SYK signaling in myeloid cells protects against liver fibrosis and hepatocarcinogenesis. Oncogene. 2019.
517. Ghotra VP, He S, van der Horst G, Nijhoff S, de Bont H, Lekkerkerker A, et al. SYK is a candidate kinase target for the treatment of advanced prostate cancer. Cancer research. 2015;75(1):230-40.
518. Pachynski RK, Wang P, Salazar N, Zheng Y, Nease L, Rosalez J, et al. Chemerin Suppresses Breast Cancer Growth by Recruiting Immune Effector Cells Into the Tumor Microenvironment. Front Immunol. 2019;10:983.
519. Nakamura N, Naruse K, Kobayashi Y, Miyabe M, Saiki T, Enomoto A, et al. Chemerin promotes angiogenesis in vivo. Physiol Rep. 2018;6(24):e13962.
520. Fultang L, Gamble LD, Gneo L, Berry AM, Egan SA, De Bie F, et al. Macrophage-Derived IL1beta and TNFalpha Regulate Arginine Metabolism in Neuroblastoma. Cancer research. 2019;79(3):611-24.
521. Rouvier E, Luciani MF, Mattei MG, Denizot F, Golstein P. CTLA-8, cloned from an activated T cell, bearing AU-rich messenger RNA instability sequences, and homologous to a herpesvirus saimiri gene. Journal of immunology. 1993;150(12):5445-56.
522. Yao Z, Painter SL, Fanslow WC, Ulrich D, Macduff BM, Spriggs MK, et al. Human IL-17: a novel cytokine derived from T cells. Journal of immunology. 1995;155(12):5483-6.
523. Barilla RM, Diskin B, Caso RC, Lee KB, Mohan N, Buttar C, et al. Specialized dendritic cells induce tumor-promoting IL-10(+)IL-17(+) FoxP3(neg) regulatory CD4(+) T cells in pancreatic carcinoma. Nat Commun. 2019;10(1):1424.
524. Oliveira LM, Teixeira FME, Sato MN. Impact of Retinoic Acid on Immune Cells and Inflammatory Diseases. Mediators Inflamm. 2018;2018:3067126.
525. Vertuani S, De Geer A, Levitsky V, Kogner P, Kiessling R, Levitskaya J. Retinoids act as multistep modulators of the major histocompatibility class I presentation pathway and sensitize neuroblastomas to cytotoxic lymphocytes. Cancer research. 2003;63(22):8006-13.
526. Boniface K, Bak-Jensen KS, Li Y, Blumenschein WM, McGeachy MJ, McClanahan TK, et al. Prostaglandin E2 regulates Th17 cell differentiation and function through cyclic AMP and EP2/EP4 receptor signaling. The Journal of experimental medicine. 2009;206(3):535-48.
527. Dejani NN, Orlando AB, Nino VE, Penteado LA, Verdan FF, Bazzano JMR, et al. Intestinal host defense outcome is dictated by PGE2 production during efferocytosis of infected cells. Proc Natl Acad Sci U S A. 2018;115(36):E8469-E78.
528. Napolitani G, Acosta-Rodriguez EV, Lanzavecchia A, Sallusto F. Prostaglandin E2 enhances Th17 responses via modulation of IL-17 and IFN-gamma production by memory CD4+ T cells. Eur J Immunol. 2009;39(5):1301-12.
529. Yao C, Sakata D, Esaki Y, Li Y, Matsuoka T, Kuroiwa K, et al. Prostaglandin E2-EP4 signaling promotes immune inflammation through Th1 cell differentiation and Th17 cell expansion. Nature medicine. 2009;15(6):633-40.
530. Li Q, Liu L, Zhang Q, Liu S, Ge D, You Z. Interleukin-17 Indirectly Promotes M2 Macrophage Differentiation through Stimulation of COX-2/PGE2 Pathway in the Cancer Cells. Cancer Res Treat. 2014;46(3):297-306.
531. Kocieda VP, Adhikary S, Emig F, Yen JH, Toscano MG, Ganea D. Prostaglandin E2-induced IL-23p19 subunit is regulated by cAMP-responsive element-binding protein and C/AATT enhancer-binding protein beta in bone marrow-derived dendritic cells. J Biol Chem. 2012;287(44):36922-35.
532. Qian X, Gu L, Ning H, Zhang Y, Hsueh EC, Fu M, et al. Increased Th17 cells in the tumor microenvironment is mediated by IL-23 via tumor-secreted prostaglandin E2. Journal of immunology. 2013;190(11):5894-902.

533. Schirmer C, Klein C, von Bergen M, Simon JC, Saalbach A. Human fibroblasts support the expansion of IL-17-producing T cells via up-regulation of IL-23 production by dendritic cells. Blood. 2010;116(10):1715-25.
534. Sheibanie AF, Tadmori I, Jing H, Vassiliou E, Ganea D. Prostaglandin E2 induces IL-23 production in bone marrow-derived dendritic cells. FASEB journal : official publication of the Federation of American Societies for Experimental Biology. 2004;18(11):1318-20.
535. Wang S, Ma Y, Wang X, Jiang J, Zhang C, Wang X, et al. IL-17A Increases Multiple Myeloma Cell Viability by Positively Regulating Syk Expression. Transl Oncol. 2019;12(8):1086-91.
536. Wu NL, Huang DY, Tsou HN, Lin YC, Lin WW. Syk mediates IL-17-induced CCL20 expression by targeting Act1-dependent K63-linked ubiquitination of TRAF6. J Invest Dermatol. 2015;135(2):490-8.
537. Fisher JP, Flutter B, Wesemann F, Frosch J, Rossig C, Gustafsson K, et al. Effective combination treatment of GD2-expressing neuroblastoma and Ewing's sarcoma using anti-GD2 ch14.18/CHO antibody with Vgamma9Vdelta2+ gammadeltaT cells. Oncoimmunology. 2016;5(1):e1025194.
538. Fisher JP, Yan M, Heuijerjans J, Carter L, Abolhassani A, Frosch J, et al. Neuroblastoma killing properties of Vdelta2 and Vdelta2-negative gammadeltaT cells following expansion by artificial antigen-presenting cells. Clin Cancer Res. 2014;20(22):5720-32.
539. Di Carlo E, Bocca P, Emionite L, Cilli M, Cipollone G, Morandi F, et al. Mechanisms of the antitumor activity of human Vgamma9Vdelta2 T cells in combination with zoledronic acid in a preclinical model of neuroblastoma. Mol Ther. 2013;21(5):1034-43.
540. Zoine JT, Knight KA, Fleischer LC, Sutton KS, Goldsmith KC, Doering CB, et al. Ex vivo expanded patient-derived γδ T-cell immunotherapy enhances neuroblastoma tumor regression in a murine model. OncoImmunology. 2019;8(8):1593804.
541. Capsomidis A, Benthall G, Van Acker HH, Fisher J, Kramer AM, Abeln Z, et al. Chimeric Antigen Receptor-Engineered Human Gamma Delta T Cells: Enhanced Cytotoxicity with Retention of Cross Presentation. Mol Ther. 2018;26(2):354-65.
542. Pressey JG, Adams J, Harkins L, Kelly D, You Z, Lamb LS, Jr. In vivo expansion and activation of gammadelta T cells as immunotherapy for refractory neuroblastoma: A phase 1 study. Medicine (Baltimore). 2016;95(39):e4909.
543. Peng T, Chanthaphavong RS, Sun S, Trigilio JA, Phasouk K, Jin L, et al. Keratinocytes produce IL-17c to protect peripheral nervous systems during human HSV-2 reactivation. The Journal of experimental medicine. 2017;214(8):2315-29.
544. Akimzhanov AM, Yang XO, Dong C. Chromatin remodeling of interleukin-17 (IL-17)-IL-17F cytokine gene locus during inflammatory helper T cell differentiation. J Biol Chem. 2007;282(9):5969-72.
545. Lauenborg B, Litvinov IV, Zhou Y, Willerslev-Olsen A, Bonefeld CM, Nastasi C, et al. Malignant T cells activate endothelial cells via IL-17 F. Blood Cancer J. 2017;7(7):e586.
546. Maxwell JR, Zhang Y, Brown WA, Smith CL, Byrne FR, Fiorino M, et al. Differential Roles for Interleukin-23 and Interleukin-17 in Intestinal Immunoregulation. Immunity. 2015;43(4):739-50.
547. Olin A, Henckel E, Chen Y, Lakshmikanth T, Pou C, Mikes J, et al. Stereotypic Immune System Development in Newborn Children. Cell. 2018;174(5):1277-92 e14.
548. Zhang X, Zhivaki D, Lo-Man R. Unique aspects of the perinatal immune system. Nature reviews Immunology. 2017;17(8):495-507.
549. Vermijlen D, Prinz I. Ontogeny of Innate T Lymphocytes - Some Innate Lymphocytes are More Innate than Others. Front Immunol. 2014;5:486.
550. Gibbons DL, Haque SF, Silberzahn T, Hamilton K, Langford C, Ellis P, et al. Neonates harbour highly active gammadelta T cells with selective impairments in preterm infants. Eur J Immunol. 2009;39(7):1794-806.
551. Simon AK, Hollander GA, McMichael A. Evolution of the immune system in humans from infancy to old age. Proc Biol Sci. 2015;282(1821):20143085.
552. Goriely S, Van Lint C, Dadkhah R, Libin M, De Wit D, Demonte D, et al. A defect in nucleosome remodeling prevents IL-12(p35) gene transcription in neonatal dendritic cells. The Journal of experimental medicine. 2004;199(7):1011-6.

553. Goriely S, Vincart B, Stordeur P, Vekemans J, Willems F, Goldman M, et al. Deficient IL-12(p35) gene expression by dendritic cells derived from neonatal monocytes. Journal of immunology. 2001;166(3):2141-6.
554. Kollmann TR, Crabtree J, Rein-Weston A, Blimkie D, Thommai F, Wang XY, et al. Neonatal innate TLR-mediated responses are distinct from those of adults. Journal of immunology. 2009;183(11):7150-60.
555. Vanden Eijnden S, Goriely S, De Wit D, Goldman M, Willems F. Preferential production of the IL-12(p40)/IL-23(p19) heterodimer by dendritic cells from human newborns. Eur J Immunol. 2006;36(1):21-6.
556. Davidoff AM, Kimbrough SA, Ng CY, Shochat SJ, Vanin EF. Neuroblastoma regression and immunity induced by transgenic expression of interleukin-12. J Pediatr Surg. 1999;34(5):902-6; discussion 6-7.
557. Lode HN, Dreier T, Xiang R, Varki NM, Kang AS, Reisfeld RA. Gene therapy with a single chain interleukin 12 fusion protein induces T cell-dependent protective immunity in a syngeneic model of murine neuroblastoma. Proc Natl Acad Sci U S A. 1998;95(5):2475-80.
558. Siapati KE, Barker S, Kinnon C, Michalski A, Anderson R, Brickell P, et al. Improved antitumour immunity in murine neuroblastoma using a combination of IL-2 and IL-12. British journal of cancer. 2003;88(10):1641-8.

PAPER I

www.impactjournals.com/oncotarget/ Oncotarget, 2017, Vol. 8, (No. 56), pp: 95135-95151

Research Paper

Inhibition of chemerin/CMKLR1 axis in neuroblastoma cells reduces clonogenicity and cell viability *in vitro* and impairs tumor growth *in vivo*

Conny Tümmler[1], Igor Snapkov[1], Malin Wickström[2], Ugo Moens[1], Linda Ljungblad[2], Lotta Helena Maria Elfman[2], Jan-Olof Winberg[3], Per Kogner[2], John Inge Johnsen[2] and Baldur Sveinbjørnsson[1,2]

[1]Molecular Inflammation Research Group, Department of Medical Biology, Faculty of Health Science, University of Tromsø, Tromsø, Norway

[2]Childhood Cancer Research Unit, Department of Women's and Children's Health, Karolinska Institutet, Stockholm, Sweden

[3]Tumor Biology Research Group, Department of Medical Biology, Faculty of Health Science, University of Tromsø, Tromsø, Norway

Correspondence to: *Conny Tümmler,* ***email:*** *conny.tummler@uit.no*

Keywords: *pediatric cancer; neuroblastoma; inflammation; GPCR; chemerin*

Received: *December 10, 2016* ***Accepted:*** *July 06, 2017* ***Published:*** *July 27, 2017*

ABSTRACT

Pro-inflammatory cells, cytokines, and chemokines are essential in promoting a tumor supporting microenvironment. Chemerin is a chemotactic protein and a natural ligand for the receptors CMKLR1, GPR1, and CCRL2. The chemerin/CMKLR1 axis is involved in immunity and inflammation, and it has also been implicated in obesity and cancer.

In neuroblastoma, a childhood tumor of the peripheral nervous system we identified correlations between high *CMKLR1* and *GPR1* expression and reduced overall survival probability. CMKLR1, GPR1, and chemerin RNA and protein were detected in neuroblastoma cell lines and neuroblastoma primary tumor tissue. Chemerin induced calcium mobilization, increased MMP-2 synthesis as well as MAP-kinase- and Akt-mediated signaling in neuroblastoma cells. Stimulation of neuroblastoma cells with serum, TNFα or IL-1β increased chemerin secretion. The small molecule CMKLR1 antagonist α-NETA reduced the clonogenicity and viability of neuroblastoma cell lines indicating the chemerin/CMKLR1 axis as a promoting factor in neuroblastoma tumorigenesis. Furthermore, nude mice carrying neuroblastoma SK-N-AS cells as xenografts showed impaired tumor growth when treated daily with α-NETA from day 1 after tumor cell injection.

This study demonstrates the potential of the chemerin/CMKLR1 axis as a prognostic factor and possible therapeutic target in neuroblastoma.

INTRODUCTION

Neuroblastoma is a malignancy of the sympathetic nervous system occurring in early childhood and accounting for 7% of all pediatric cancers [1]. While the prognosis for low and intermediate risk neuroblastoma patients is favorable, the long-term event-free survival rate for high-risk patients remains less than 50%, despite intensive treatment [1, 2].

Chronic inflammation is an important modulator of the tumor microenvironment (TME). Pro-inflammatory cells, cytokines, and chemokines present in the TME promote tumor development, progression, and metastasis in various cancers [3, 4]. Recently, a subset of high-risk, therapy-resistant neuroblastomas was demonstrated to be inflammation-driven indicating the importance of inflammation in neuroblastoma [5]. A thorough understanding of the neuroblastoma TME and the

inflammatory processes involved in tumorigenesis may lead to new therapy approaches and the discovery of novel prognostic markers [6–9].

Chemerin (also known as TIG-2 or RARRES2) is an adipokine and chemoattractant factor associated with obesity, inflammatory diseases and cancer [10–20]. Synthesized as a 163 amino acid preproprotein, this chemerin precursor is N-terminally cleaved and secreted as prochemerin with low activity. Following secretion, prochemerin can be C-terminally cleaved by a variety of extracellular proteases, resulting in several chemerin isoforms with varying length, receptor affinity, and biological activity [21]. Proteases associated with inflammation such as cathepsin G and neutrophil elastase respectively cleave prochemerin into chemerin 21-156 and 21-157. These are the most active forms, whereas prochemerin processed with mast cell chymase or protease 3 results in the inactive or low activity chemerin 21-154 and 21-155 variants, respectively [22, 23]. During inflammation initiation, maintenance and resolution the different chemerin isoforms may exert pro- and/or anti-inflammatory functions [24, 25]. Chemerin is a natural ligand for the G-protein-coupled receptors CMKLR1 (or ChemR23), GPR1, and CCRL2. CMKLR1 is expressed by different cell types including macrophages as well as immature dendritic cells and mediates the majority of the described chemerin functions [10, 24, 26–29]. Besides the involvement in various inflammatory diseases, the chemerin/CMKLR1 axis has been shown to play a role in different malignancies. While there is evidence that chemerin and CMKLR1 support tumorigenesis in glioblastoma, gastric cancer, squamous esophageal cancer and squamous cell carcinoma of the oral tongue [16-18, 20], an anti-tumorigenic effect has been suggested in melanoma, hepatocellular carcinoma and non-small cell lung cancer [15, 30, 31].

GPR1 functions are so far less understood, but it has recently been found to contribute to the regulation of glucose homeostasis in obese mice [32]. At present, no active signaling has been detected following chemerin binding to CCRL2. However, CCRL2 is known to increase local chemerin concentrations [33] and its expression has been linked to rheumatoid arthritis and liver metastasis in colorectal cancer [34, 35]. The aim of the present study was to investigate the functional significance of chemerin, CMKLR1 and GPR1 in the neuroblastoma microenvironment and assess their potential as prognostic factors and therapeutic targets.

RESULTS

High *CMKLR1* and *GPR1* expression predict poor overall survival probability in neuroblastoma

To investigate *CMKLR1* and *GPR1* gene expression in neuroblastoma we used the publically available R2: Genomics analysis and visualization platform http://r2.amc.nl. Examining two neuroblastoma gene expression cohorts, we found a correlation between high expression of *CMKLR1* (Figure 1A and 1B) and *GPR1* (Figure 1D and 1E) and a decrease in overall survival probability. Furthermore, *CMKLR1* expression was higher in neuroblastoma cohorts compared to benign neurofibroma and neural crest cells (Figure 1C). However, no difference was found comparing *GPR1* expression in the different cohorts (Figure 1F).

Additionally, we observed that expression of chemerin receptor *CCRL2* was elevated in the neuroblastoma cohorts compared to neurofibroma and neural crest, and that high expression of *CCRL2* correlated with a poor survival prognosis (Supplementary Figure 1D-1F). While chemerin (*RARRES2*) expression was higher in the neuroblastoma cohorts compared to the neural crest, no difference was seen in comparison with benign neurofibroma. Furthermore, no clear correlation between high expression of *RARRES2* and a decrease in overall survival probability was apparent due to conflicting results in the selected data sets (Supplementary Figure 1A-1C).

Neuroblastoma cell lines express chemerin, CMKLR1 and GPR1

We examined different neuroblastoma cell lines for the expression of CMKLR1, GPR1 and chemerin. Using RT-PCR (Figure 2A) and western blot (Figure 2B) we demonstrated expression of CMKLR1, GPR1 and chemerin mRNA and protein at varying levels in all neuroblastoma cell lines tested. No correlation was apparent between CMKLR1, GPR1 or chemerin expression levels and specific cell line characteristics such as *MYCN* amplification, 1p deletion, 11q deletion or multi-drug resistance phenotype.

HepG2 cells were included in the western blots as a positive control. They are known to express and secrete chemerin and several antibody suppliers recommended them as a control cell line for CMKLR1.

Furthermore, we examined the expression levels of *RARRES2* (chemerin), *CMKLR1* and *GPR1* in a panel of neuroblastoma cell lines using the publically available R2: Genomics analysis and visualization platform http://r2.amc.nl. We observed that all three genes are expressed at varying levels in the neuroblastoma cell lines included in this panel (Supplementary Figure 2A-2C). In addition we compared their expression to known neuroblastoma promoting cytokines, chemokines, growth factors and their receptors and found *GPR1* and *CMKLR1* expression in the range of *FPR1*, *IL6R* and *PDGFRA*. While *RARRES2* (chemerin) expression is lower than *VEGFA*, it is comparable to *CCL2* and *CCL5* expression (Supplementary Figure 2D and 2E).

Immunofluorescence staining demonstrated the cellular distribution of CMKLR1 (Figure 2C) and GPR1 (Figure 2D) in the neuroblastoma cell line SH-SY5Y. Both receptors were localized at the cell membrane

and in the cytoplasm. Comparable staining pattern for CMKLR1 was observed in other neuroblastoma cell lines using additional primary antibodies for confirmation (Supplementary Figure 3A and 3B). No apparent staining was observed in cells incubated with an isotype control antibody instead of the primary antibody (Supplementary Figure 3C).

TNFα, IL-1β and serum increase chemerin secretion in neuroblastoma cells

To investigate the effect of the pro-inflammatory cytokines TNFα and IL-1β as well as serum components on chemerin expression and secretion, chemerin concentrations were measured by ELISA. Exposure to IL-1β, TNFα as well as 10% serum for 24h increased the level of chemerin in the supernatant of SK-N-AS cells (Figure 2E).

CMKLR1, GPR1 and chemerin are expressed in neuroblastoma primary tumors

To confirm the presence of CMKLR1, GPR1 and chemerin in neuroblastoma primary tumors, IHC and IF-P were performed. A total of 27 neuroblastoma tissue samples from all clinical stages and biological subsets [36] were stained with antibodies detecting chemerin, CMKLR1 and GPR1. All tumor samples investigated demonstrated a significant expression of chemerin and its receptors. Figure 3 presents a representative labeling with CMKLR1 (Figure 3A), GPR1 (Figure 3B) and chemerin (Figure 3C) specific antibodies showing a clear staining of both the receptors and chemerin in neuroblastoma primary tumors. Fluorescence labeling of CMKLR1 (green) and chemerin (red) displayed the membranous and cytoplasmic localization of CMKLR1 whereas chemerin was detected both in intra- and extracellular compartments (Figure

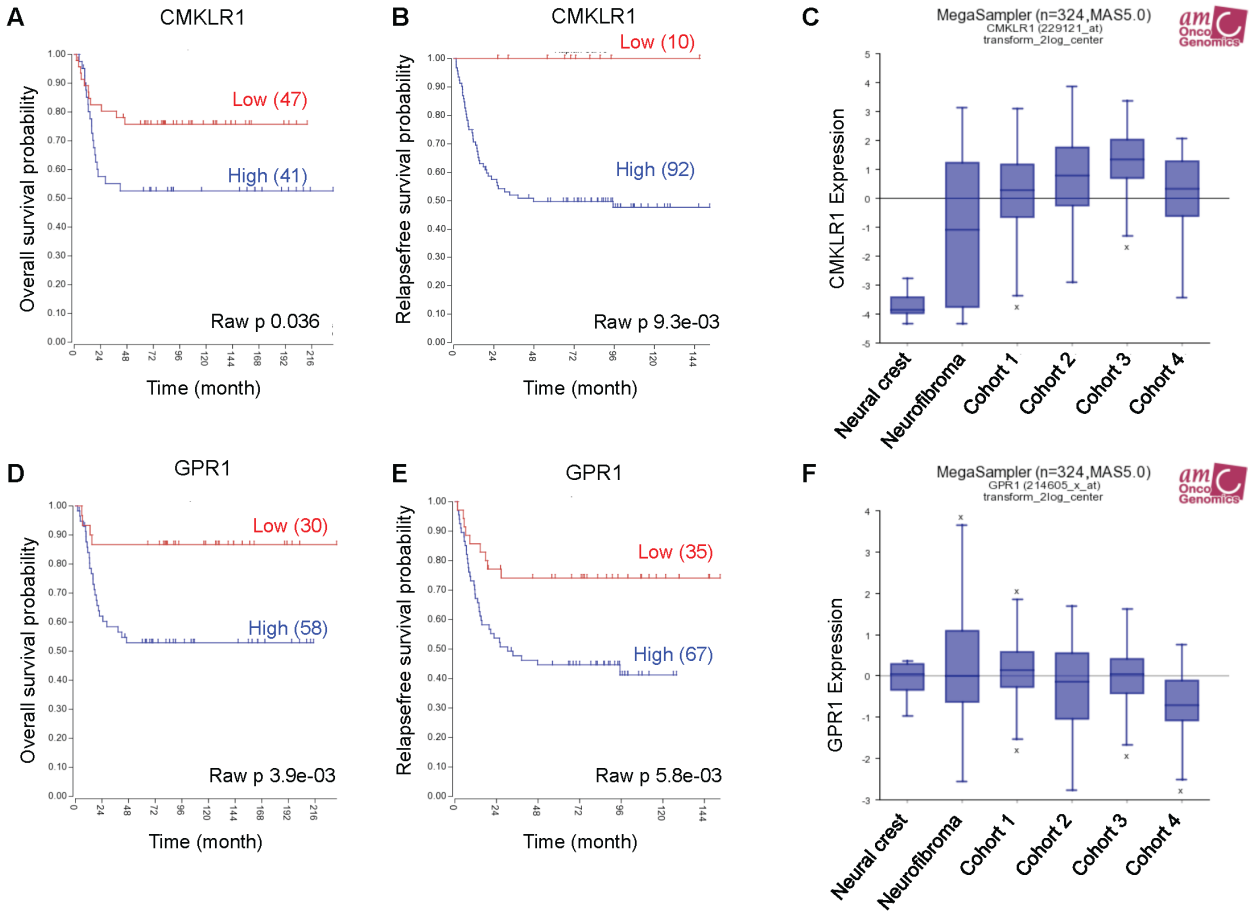

Figure 1: High *CMKLR1* and *GPR1* expression predicts poor survival in neuroblastoma patients. Expression data was analyzed using the R2 database http://r2.amc.nl. Kaplan-Meier survival estimates were used to evaluate the prognostic value of *CMKLR1* **(A, B)** and *GPR1* **(D, E)** expression in two patient data sets (A and D: Versteeg n=88; B and E: Seeger n=102). The Kaplan-Meier scanning tool was used to determine the CMKLR1 and GPR1 mRNA expression in neuroblastoma. All expression data were scanned to find the most optimal cut-off between high and low gene expression and the log-rank test that gave the lowest p-value was calculated to search for significant differences between tumor samples expressing high and low CMKLR1 and GPR1 mRNA levels, respectively. The expression of *CMKLR1* **(C)** and *GPR1* **(F)** was compared between neural crest (Etchevers n=5), benign neurofibroma (Miller n=86) and 4 neuroblastoma cohorts (cohort 1: Versteeg n=88, cohort 2: Delattre n=64, cohort 3: Hiyama n=51, cohort 4: Lastowska n=30).

3D-3F) indicating chemerin secretion in neuroblastoma primary tumor tissue. For both, IHC and IF-P, no apparent staining was observed in sections incubated with isotype control antibodies instead of the primary antibodies (Supplementary Figure 3D-3F).

Chemerin induces calcium mobilization and promotes MAPK and Akt signaling in neuroblastoma cell lines

Chemerin has been previously shown to stimulate intracellular calcium mobilization in immature DCs and macrophages as well as MAPK and Akt signaling in human chondrocytes and endothelial cells through CMKLR1 [14, 24, 37]. GPR1-mediated calcium mobilization and ERK1/2 phosphorylation following chemerin binding has been demonstrated to be much weaker [38, 39]. Recently, both CMKLR1 and GPR1 were found to signal through the RhoA/Rock pathway in HEK293A and gastric carcinoma cells [40].

To determine the effect of chemerin in neuroblastoma, we studied calcium mobilization, MAPK, and Akt signaling in neuroblastoma cell lines. Chemerin stimulation caused a rapid, but transient increase in intracellular calcium in SK-N-SH cells (Figure 4A and 4B) in comparison to vehicle treatment. Furthermore, prior incubation with the calcium chelator EDTA showed no inhibitory effect (Figure 4B) indicating calcium release from intracellular compartments.

The addition of chemerin to SK-N-AS cells induced a rapid and dose-dependent phosphorylation of MEK1/2, ERK1/2 and Akt (Figure 4C) indicating the activation of MAPK and Akt signaling. Similar phosphorylation patterns were observed in SK-N-BE(2) cells (data not shown).

Chemerin increases MMP-2 synthesis in neuroblastoma cells

Chemerin is known to stimulate MMP-2 and MMP-9 expression and activity [37, 41]. Using real-time zymography, we could follow the degradation of gelatin by MMP-2 and MMP-9 in real-time. We observed a dose-dependent increase in MMP-2 synthesis in both SK-N-

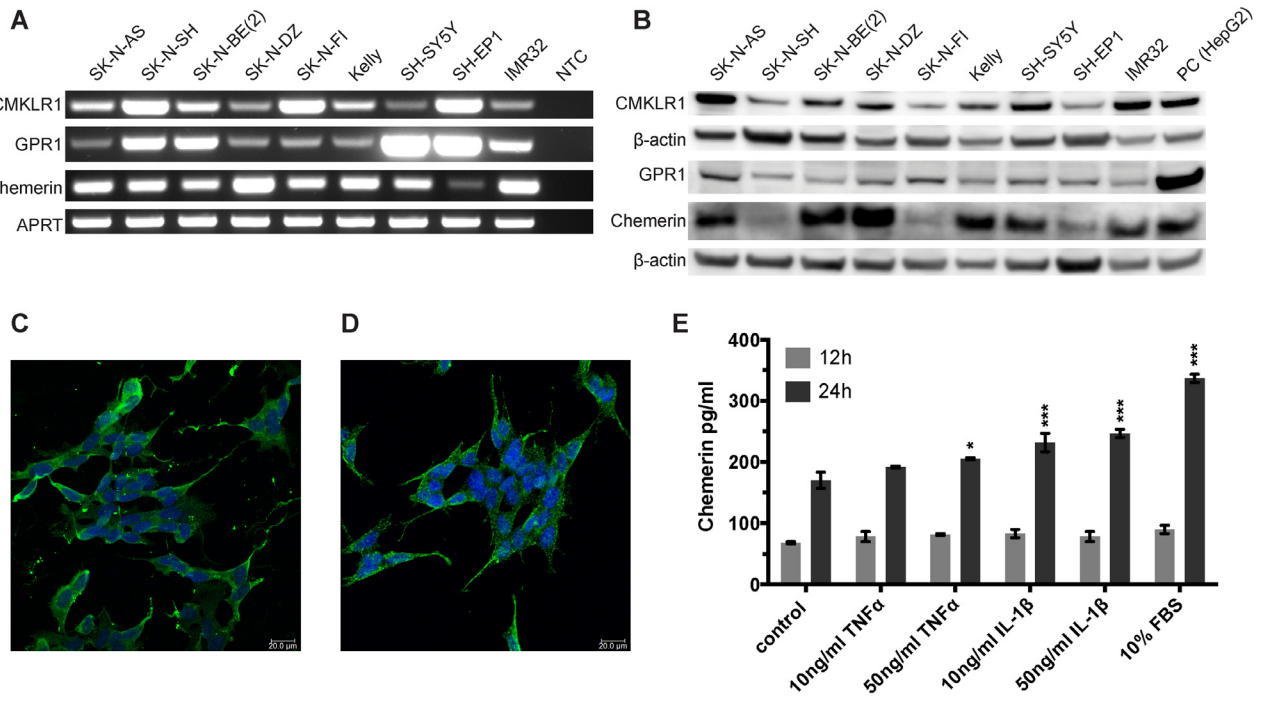

Figure 2: CMKLR1, GPR1 and chemerin are expressed in neuroblastoma cell lines and TNFα, IL-1β, and serum stimulate chemerin secretion. (A) RT-PCR analysis demonstrating the expression of chemerin, CMKLR1 and GPR1 mRNA in all neuroblastoma cell lines investigated. NTC, no template control. The expression of chemerin, CMKLR1, and GPR1 protein was confirmed by western blot **(B)**. HepG2 cells were used as a positive control. The images are representative of three independent experiments. Immunofluorescence labeling shows the presence of CMKLR1 **(C)** and GPR1 **(D)** in SH-SY5Y cells (green). The nuclei (blue) were stained with Hoechst 33342, scale bar 20μm. **(E)** Chemerin concentrations were measured in cell supernatants of SK-N-AS cells after treatment with 10 or 50ng/ml TNFα, IL-1β or 10% FBS for 12 or 24h, respectively. The supernatants of 10 independent samples were pooled and concentrated 10x prior to ELISA measurement. The standards and samples were measured in duplicates and the data is presented as mean and range. Statistical analysis was performed using a two-way ANOVA $P<0.001$ for both stimulation and incubation time followed by Dunnett's post-test control vs. treatment * $P<0.05$, *** $P<0.001$.

AS and to a lesser extent in SK-N-BE(2) cells after 6, 12, 24 and 48h stimulation with active chemerin (Figure 5). No effect on MMP-9 synthesis was observed under these conditions.

CMKLR1 inhibition reduces the cell viability and clonogenicity of neuroblastoma cells

The effect of CMKLR1 inhibition on neuroblastoma cell lines was studied using the recently described CMKLR1 inhibitor α-NETA [42]. Increasing concentrations of α-NETA reduced the cell viability of four neuroblastoma cells lines after 72h of treatment with IC_{50} values ranging between 3.87-7.49μM (Figure 6A and 6B). No effect (IC_{50} values >10μM) was observed on human fibroblasts (MRC-5) and endothelial cells (HUVEC). A dose-dependent inhibition of clonogenicity was observed in SK-N-BE(2) cells (Figure 6C) as well as SK-N-AS, SK-N-DZ, and SH-SY5Y cells (Figure 6D). The colony forming ability was completely inhibited using 5μM α-NETA.

Early and prolonged CMKLR1 inhibition impairs neuroblastoma growth *in vivo*

The therapeutic effect of CMKLR1 inhibition was examined in a SK-N-AS xenograft model. A significant prolongation (p=0.015, Log rank test) of survival (defined as time needed for the animals to grow a macroscopic tumor with a volume >1.5ml) was observed in the pre-treatment group, where the animals were treated s.c. with α-NETA continuously from day 1 after tumor cell injection, compared to the control group (Figure 7). In addition, when comparing tumor growth rates for individual tumors, the tumors from the pre-treated mice grew significantly slower than the tumors in the control group (p=0.0061, one way ANOVA with Bonferroni post-test, control vs. pre-treatment p=0.049, Supplementary Figure 4). However, no effect was seen in the treatment group, where α-NETA s.c. injections were initiated after the tumor reached a volume of ≥ 0.15ml, compared to the control group. No signs of toxicity were observed at the used concentrations of α-NETA. In the pre-treatment

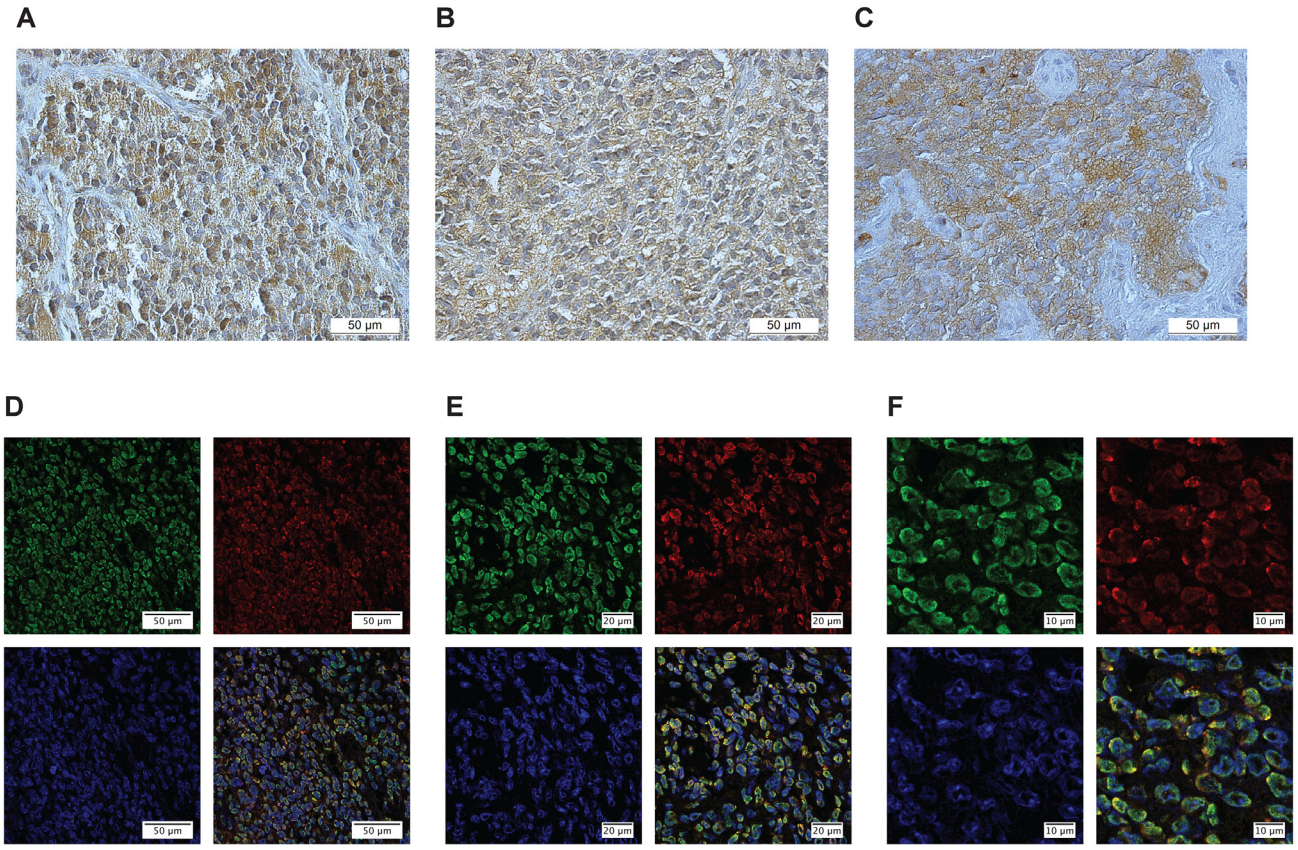

Figure 3: CMKLR1, GPR1 and chemerin are expressed in neuroblastoma primary tumors. Immunoperoxidase staining demonstrates specific expression of **(A)** CMKLR1, **(B)** GPR1 and **(C)** chemerin in neuroblastoma primary tumor tissue. Immunofluorescence labeling **(D-F)** displays CMKLR1 (green) and chemerin (red) localization in neuroblastoma tissue. The nuclei were stained with DAPI (blue). (E and F) are higher magnifications of (D) to illustrate the colocalization of CMKLR1 and chemerin. The displayed images are representative stainings from a panel of neuroblastoma tumors.

group, a hardening of the skin was seen at the later stages of the experiment probably due to the daily s.c. injection over a prolonged period. All mice gained weight over the course of the experiment.

DISCUSSION

Neuroblastoma is a malignancy with only a few identified key genetic events. Besides amplification of the *MYCN* oncogene (in approximately 20% of neuroblastomas), *ALK* mutations and amplifications occur in 9% and 2-3%, respectively. Other affected genes include *ODC, NTRK2/TrkB, FOXR1, PTPN11, ATRX, CADM1*, and *ARID1A/B* [2, 43]. For the discovery of potential new therapeutic targets, understanding of the neuroblastoma TME is of great importance. Chemokines and chemoattractant factors are essential regulators of cell trafficking during immune response and inflammation. Furthermore, they are involved in all stages of cancer development: tumor establishment, neovascularization, and metastasis [44, 45].

Several chemokine receptors and their ligands have been identified as contributors to neuroblastoma angiogenesis, metastasis, and communication between tumor cells and cells of the TME [6, 46]. CMKLR1 is a chemoattractant receptor present on immune cells such as immature DCs, macrophages and NK cells [47]. Recently, CMKLR1 was found to be expressed in a subset of myeloid-derived suppressor cells (MDSCs) in hepatocellular carcinoma [48].

Chemerin, a ligand for CMKLR1 possesses a wide variety of characteristics attributed to tumor growth such as chemotaxis and cell adhesion, as well as cell survival and proliferation [21, 41, 47]. In ECs, CMKLR1 was

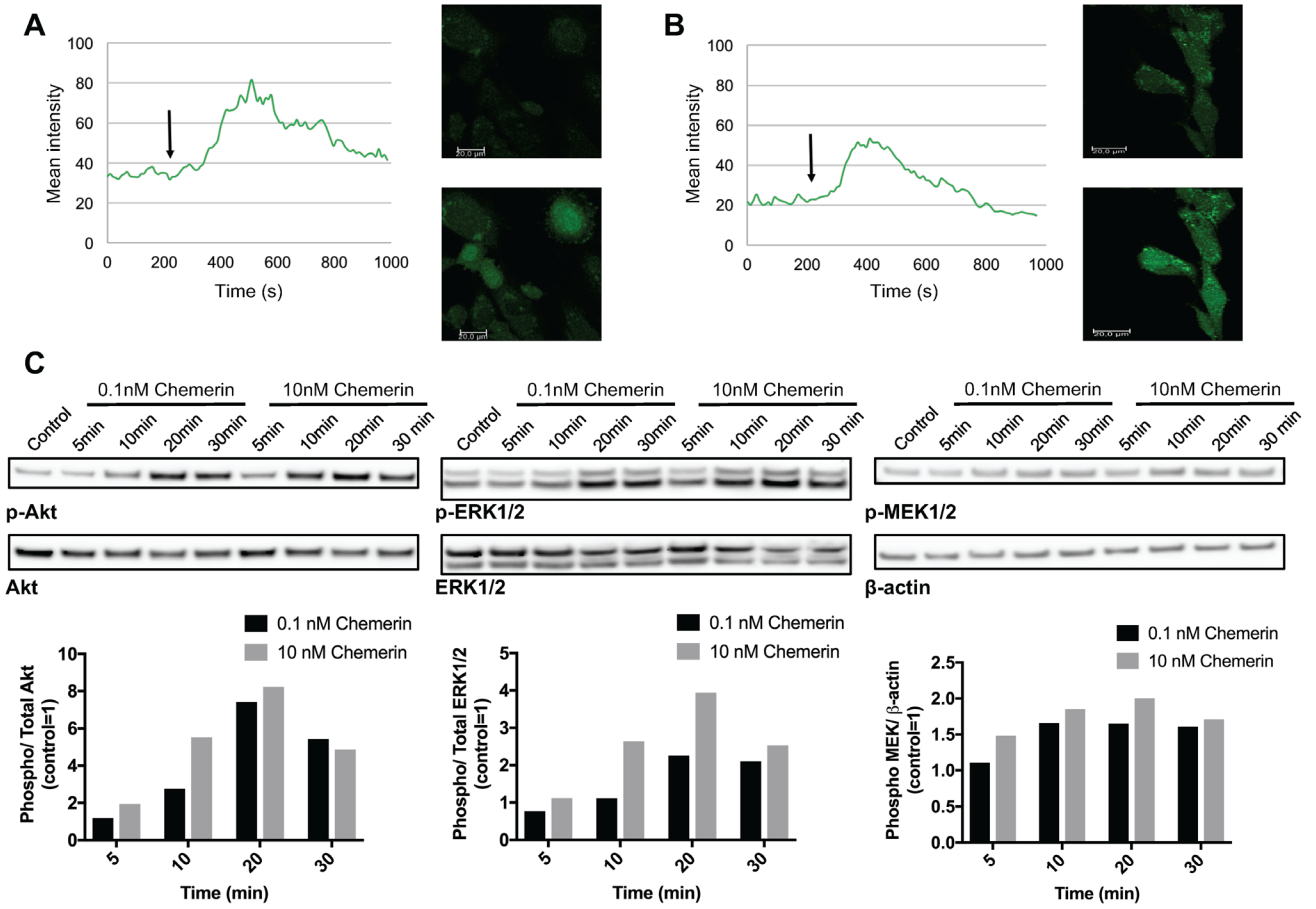

Figure 4: Chemerin induces intracellular calcium mobilization and stimulates MAPK and Akt signaling in neuroblastoma cells. Intracellular calcium mobilization was measured in SK-N-SH cells with confocal laser scanning microscopy following the stimulation with 10nM chemerin without **(A)** and with **(B)** the prior addition of the calcium chelator EDTA. The arrow indicates the time point when chemerin was added. **(C)** Chemerin stimulates the phosphorylation of Akt, ERK1/2 and MEK1/2 in SK-N-AS cells in a dose-dependent manner. The cells were serum-starved for 24h prior to stimulation and samples were taken 5, 10, 20 and 30min after stimulation. Densitometric analysis of the protein bands was performed and the ratios between p-ERK1/2 and total ERK1/2, p-Akt and total Akt as well as p-MEK1/2 and β-actin were calculated. The values are displayed relative to the control=1. The experiments were performed three times with similar results.

found to be upregulated by the pro-inflammatory cytokines TNFα, IL-1β and IL-6. Furthermore, chemerin stimulation induced MMP production and angiogenesis [37]. Recent work by Chua et al. demonstrates that hypoxia promotes chemerin expression in human coronary artery endothelial cells as well as migration and tube formation, supporting previous findings on the role of chemerin in angiogenesis [49]. However, the function of the chemerin/CMKLR1 axis in malignancies is probably tumor specific as both tumor promoting and tumor suppressing roles have been reported [15-18, 20, 30, 31].

In the present study, we investigated the role of chemerin and its receptors CMKLR1 and GPR1 in neuroblastoma tumorigenesis. Using publically available gene expression datasets (http://r2.amc.nl) we observed that high *CMKLR1* and *GPR1* expression correlates with a reduced overall survival probability in the two datasets we examined. We did not find any relationship between genetic characteristics of neuroblastoma, such as MYCN expression, and CMKLR1, GPR1 or chemerin expression. Our findings indicate that CMKLR1 and/or GPR1 could potentially be used as independent prognostic factors.

Tumor-associated macrophages (TAMs) have been shown to promote neuroblastoma tumorigenesis [6], and CMKLR1 expression in macrophages can be stimulated by mammary and lung carcinoma cells [50]. Asgharzadeh et al. [7] described the prognostic value of a TAM gene expression signature (*CD33, CD16, IL6R, IL10, FCGR3*) in metastatic neuroblastoma. Examining publically available neuroblastoma gene expression datasets (R2: Genomics Analysis and Visualization Platform http://r2.amc.nl) we observed a significant correlation between expression of CMKLR1 and the TAM markers (Supplementary Figure 5). IHC labeling of the macrophage marker CD68 as well as double IF-P staining of CD68 and CMKLR1 in neuroblastoma tissue demonstrated that while the majority of CMKLR1 is expressed by the tumors cells, $CD68^{+}$ cells in the TME also express CMKLR1 (Supplementary Figure 6).

Additionally, CMKLR1 is expressed at high levels in monocytic MDSCs in hepatocellular carcinoma [48]. Therefore, the expression of CMKLR1 on tumor promoting immune cells could also play a significant role in the tumorigenesis process.

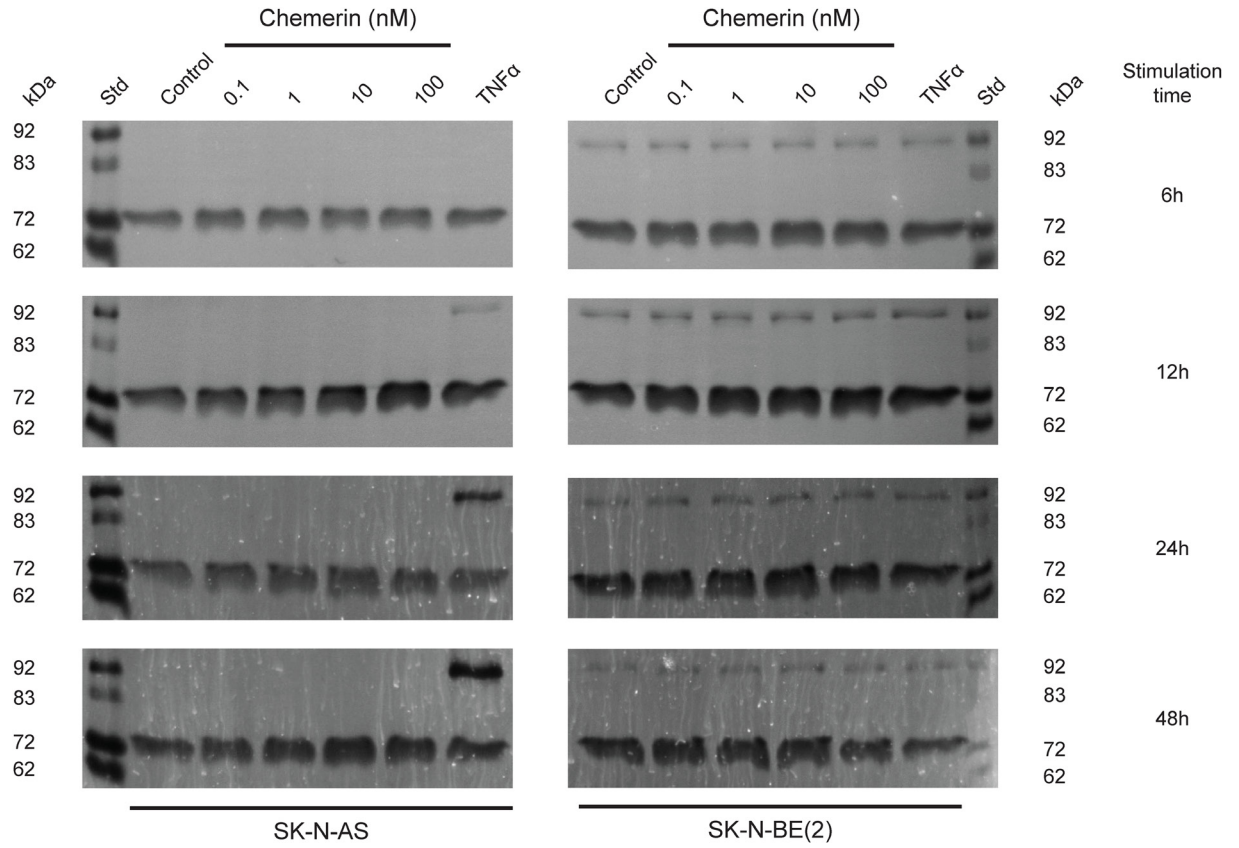

Figure 5: Chemerin stimulates MMP-2 synthesis in neuroblastoma cells. Typical real-time gelatin zymography of supernatants from SK-N-AS and SK-N-BE(2) cells untreated (control) or treated with increasing concentrations of chemerin (0.1-100 nM) or TNFα (10 ng/ml) for 6h, 12h, 24h and 48h. Prior to stimulation, the cells were serum-starved for 24h. For each zymogram the supernatants of three independent samples were pooled and analyzed. The shown zymograms were taken after optimal incubation time (for SK-N-AS 15h, 10h, 13h and 13h and for SK-N-BE(2) 15h, 10h, 5h and 4h) in assay buffer after the removal of SDS from the gels. The standard (st) comprised a mixture of proMMP-9 monomer (92 kDa), active MMP-9 (83 kDa), proMMP-2 (72 kDa) and active MMP-2 (62 kDa).

A recent study demonstrated that chemerin secreted by esophageal squamous cancer-associated myofibroblasts stimulates the migration of cancer cells, indicating a role in invasion. Blockage of the chemerin/CMKLR1 axis inhibited invasion [41]. In addition, Kaur et al. determined a mitogenic effect of chemerin on human macro- and microvascular endothelial cells through activation of CMKLR1 [37]. Therefore, a potential role of chemerin/CMKLR1 in neuroblastoma angiogenesis could be hypothesized. Collectively, these findings indicate that targeting CMKLR1 expressed on stromal cells in addition to the tumor cells could be of therapeutic interest.

In the present study, active chemerin induced both calcium mobilization and the activation of MAPK and Akt signaling. PI3K/Akt- and MAPK-mediated signaling are known to contribute to neuroblastoma tumorigenesis [51–54]. Furthermore, we demonstrated that the pro-inflammatory cytokines TNFα and IL-1β as well as serum components stimulate chemerin secretion by neuroblastoma cells. Both cytokines have been previously found to regulate CMKLR1 and chemerin expression in human endothelial cells, keratinocytes (IL-1β), and other cell types [37, 55]. Additionally, we observed that chemerin stimulated MMP-2 synthesis in a dose-dependent manner. MMP-2 is a member of the matrix metalloproteinase family with important functions in tumorigenesis. Through processing of extracellular matrix and non-matrix proteins, MMP-2, and other members of the MMP family, contribute to cell invasion, metastasis and neovascularization [56]. Increased MMP-2 expression in neuroblastoma has been associated with increased angiogenesis, advanced stage, and poor clinical outcome [57, 58]. Our results indicate that chemerin may contribute to an increased MMP-2 synthesis in neuroblastoma.

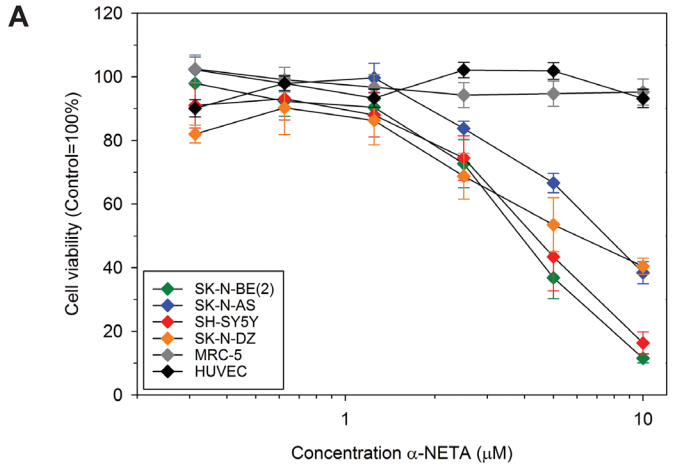

B

Cell line	IC_{50} with 95% confidence interval
SK-N-BE(2)	3.87μM (3.45 – 4.34)
SK-N-AS	7.49μM (6.64 – 8.60)
SK-N-DZ	6.50μM (4.71 – 10.5)
SH-SY5Y	4.26μM (3.54 – 5.14)
HUVEC	>10μM
MRC-5	>10μM

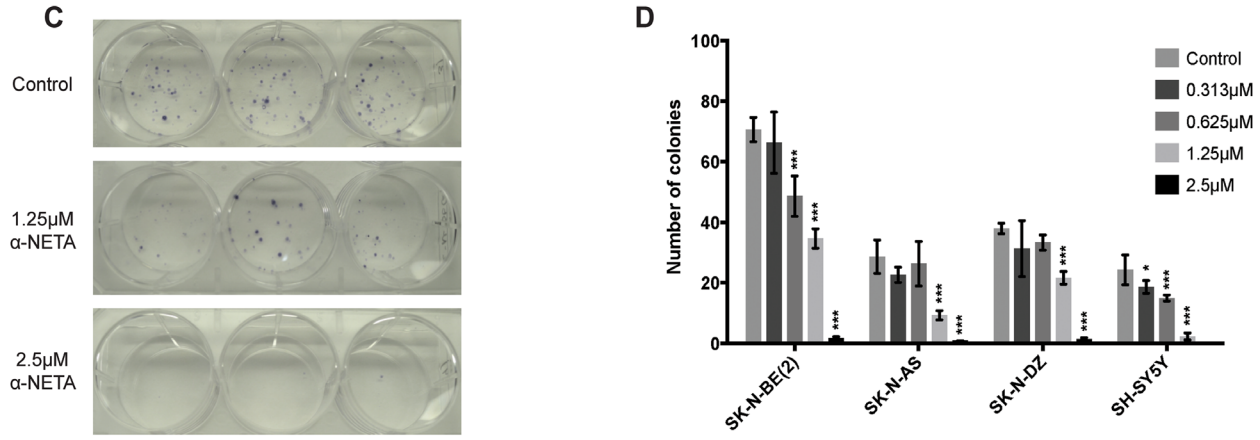

Figure 6: The CMKLR1 antagonist α-NETA reduces the cell viability and clonogenicity of neuroblastoma cell lines. Cell viability was determined after 72h of incubation with α-NETA (0.313-10μM). A dose-dependent decrease in cell viability was observed in the neuroblastoma cell lines but not in MRC-5 and HUVEC cells **(A)**. Data is presented as mean ± SEM from three experiments. The IC_{50} values are given with 95% confidence intervals in **(B)**. The mean of log IC_{50}s in neuroblastoma cell lines was significantly lower than the hypothetical log IC_{50} of the investigated normal cell lines (one sample t-test, p=0.029; means: 0.726 vs 1). The CMKLR1 antagonist α-NETA reduces the clonogenicity of SK-N-BE(2) cells (**C**; 1.25 and 2.5μM, n=3) and other neuroblastoma cell lines (**D**; 0.313-2.5μM, n=3) in a dose-dependent manner after 72h treatment. Data is presented as mean ± SD from a representative experiment. The experiment was repeated twice more with similar results. Statistical testing was performed using a two-way ANOVA P<0.001 for both stimulation and between cell lines followed by Dunnett's post-test control vs. treatment * P<0.05, *** P<0.001.

In our work, we observed that α-NETA, a small molecule inhibitor for CMKLR1, reduced the cell viability and clonogenicity of neuroblastoma cell lines. Initially identified as a choline acetyltransferase inhibitor, α-NETA was recently found to be a more potent inhibitor of CMKLR1 [42]. In an *in vivo* xenograft study, we observed that continuous, long-term treatment with α-NETA resulted in impaired tumor growth. However, no effect was observed when α-NETA injections were initiated after the tumor had reached a volume of 0.15ml. These results indicate that CMKLR1 function might be of greater importance during the early stages of tumor growth as well as tumor recurrence and relapse in neuroblastoma patients. However, SK-N-AS xenograft tumors grow very fast once the tumor has been established therefore providing only a narrow treatment window. In order to achieve a significant effect, a longer treatment window as given in the pre-treatment group might be necessary. The results from the *in vitro* studies indicate a role of CMKLR1 during clone formation. Inhibiting CMKLR1 at a stage where the tumor has reached a certain size might therefore have a smaller impact. Since α-NETA has only recently been described as a CMKLR1 inhibitor, potential off-target effects are not fully studied. Concerning bioavailability and stability of α-NETA *in vivo* only limited data is available, hampering dose estimation. Hence, the concentration used in this study might have been too low to sufficiently abrogate CMKLR1 function in established tumors. Further studies are therefore necessary to determine the appropriate concentrations for α-NETA *in vivo*. Additionally, the results should be confirmed using *CMKLR1* knockout neuroblastoma cell lines. Although we made several attempts to knock down/out CMKLR1 in neuroblastoma cell lines using both shRNA and the CRISPR/Cas9 system, we have established to date only one SK-N-AS cell line with a marked CMKLR1 downregulation (Supplementary Figure 7). Since this cell line grows very slowly and is unable to form distinct colonies in clonogenicity assays we have been unable to utilize it in functional *in vitro* or *in vivo* studies. While these findings, taken together with the results from the inhibitor studies, indicate that CMKLR1 may contribute to colony formation and tumorigenesis we have been unable to confirm these findings with additional knock down clones.

GPR1 is an additional active chemerin receptor expressed in the central nervous system, skeletal muscle, and adipose tissue [47]. In this work, we also demonstrate the expression of GPR1 mRNA and protein in neuroblastoma cell lines and primary tumor tissue. While most of the known chemerin functions have been connected to CMKLR1-mediated signaling, we cannot exclude that chemerin mediated signaling in neuroblastoma cell lines is not at least partly mediated by GPR1. However, GPR1 mediated calcium mobilization and ERK1/2 phosphorylation has been demonstrated to be much weaker compared to CMKLR1 [38, 39]. Recently, chemerin was found to activate RhoA/Rock signaling through CMKLR1 and GPR1 [40]. The Rho/Rock pathway is involved in actin rearrangement, hence suggesting a potential role of the chemerin/CMKLR1/GPR1 axis in migration and metastasis.

CCRL2, the third known chemerin receptor is present on myeloid cells, mast cells and CD34+ bone marrow precursors [47]. While not actively signaling, it was found

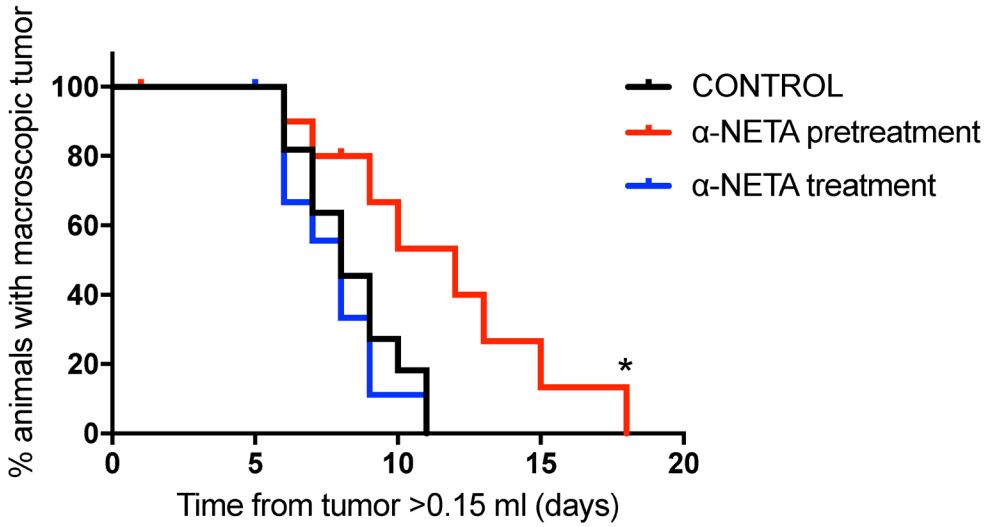

Figure 7: Early and prolonged CMKLR1 inhibition with α-NETA impairs tumor growth *in vivo*. Kaplan-Meier survival plots of nude mice (n=11 in control group and in pre-treatment group, n=10 in treatment group) injected daily s.c. with 20mg/kg α-NETA after the tumor reached 0.15ml (treatment group), 10mg/kg α-NETA from the day after tumor cell injection and 20mg/kg when the tumor reached 0.15ml (pre-treatment group) or 10% Captisol® (control group). Survival, defined as time needed for the animals to grow a macroscopic tumor (volume >1.5ml), was significantly prolonged in the pre-treatment group (log rank test P=0.015, control vs. pre-treatment P= 0.019 and control vs. treatment P=0.51).

Table 1: Antibodies used in the study

Antibody	Application	Source
Anti-ChemR23	WB, IHC	#STJ92262, St John's Laboratory
Anti-Human ChemR23	IF-P, ICC	#MAB362, R&D Systems
Anti-GPCR GPR1	WB	#ab157209, abcam
Anti-GPCR GPR1	ICC	#ab121315, abcam
Anti-GPCR GPR1	IHC	#ab188977, abcam
Anti-TIG2 Antibody (K-15)	WB, IF-P	#sc-47482, Santa Cruz Biotechnology
Anti-Human Chemerin	IHC	#MAB2324, R&D Systems
Anti-beta Actin	WB	#ab8227, abcam
Anti-p44/42 MAPK (Erk1/2)	WB	#4695, Cell Signaling Technology
Anti-Phospho-p44/42 MAPK (Erk1/2) (Thr202/Tyr204)	WB	#4370, Cell Signaling Technology
Anti-Akt	WB	#9272, Cell Signaling Technology
Anti-Phospho-Akt (Ser473) (D9E)	WB	#4060, Cell Signaling Technology
Anti-Phospho-MEK1/2 (Ser217/221)	WB	#9121, Cell Signaling Technology
Goat Anti-Rabbit IgG H&L (HRP)	WB	#ab6721, abcam
Swine Anti-Goat Ig's, HRP	WB	#ACI0404, Thermo Fisher Scientific
Goat anti-Rabbit IgG (H+L), Alexa Fluor 488	ICC	# A-11008, Thermo Fisher Scientific
Donkey anti-Goat IgG (H+L), Alexa Fluor 594	IF-P	#A-11058, Thermo Fisher Scientific
Rabbit anti-Mouse IgG (H+L), Alexa Fluor 488	IF-P	# A-11059, Thermo Fisher Scientific

to increase local chemerin levels suggesting that CCRL2 presents chemerin to CMKLR1 or GPR1 on neighboring cells [33]. Akram et al. recently identified a role of CCRL2 in colorectal cancer liver metastases [35]. Although we were able to detect CCRL2 mRNA in neuroblastoma cell lines (data not shown), the role of CCRL2 in neuroblastoma was not addressed in the present study.

Our results demonstrate, for the first time, the presence of a fully active and functional chemerin/CMKLR1 axis in childhood neuroblastoma. Neuroblastoma cells produce chemerin that can promote survival in an autocrine manner. Inhibition of the chemerin/CMKLR1 axis impaired neuroblastoma cell growth *in vitro* and *in vivo*. Our findings provide new insight into the pathobiology of neuroblastoma. Pharmacological interventions targeting the chemerin/CMKLR1 signaling pathway may be an important adjuvant therapy for children with neuroblastoma, but further preclinical *in vivo* studies are warranted.

MATERIALS AND METHODS

Microarray gene expression analysis

Gene expression analysis was performed using the publicly available R2: Genomics Analysis and Visualization Platform (http://r2.amc.nl).

Antibodies and reagents

The antibodies used in this study are listed in Table 1. Recombinant human IL-1β was purchased from Cell Guidance Systems Ltd. (Cambridge, UK). Recombinant human TNFα and chemerin were obtained from R&D Systems, Inc. (Minneapolis, USA) and α-NETA was from Santa Cruz Biotechnology, Inc. (Dallas, USA).

Cell lines and human tissue samples

The human neuroblastoma cell lines SK-N-AS, SK-N-SH, SK-N-DZ, SK-N-FI, SH-EP1, Kelly, SH-SY5Y, and IMR-32 as well as the hepatocellular carcinoma cell line HepG2 were purchased from the ATCC (American Type Culture Collection), and SK-N-BE(2) cells were bought from DSMZ (Deutsche Sammlung von Mikroorganismen und Zellkulturen). The cells were cultivated in RPMI-1640 medium containing L-glutamine and sodium bicarbonate (Sigma-Aldrich Norway AS, Oslo, Norway) supplemented with 10% heat-inactivated FBS (Thermo Fisher Scientific Inc.) at 37°C in humidified air with 5% CO_2. The human fibroblast cell line MRC-5 and human umbilical vein endothelial cells (HUVEC) were purchased from the ATCC and cultivated in EGM-2 BulletKit with 2% FBS (Lonza, Basel, Switzerland)

and MEM supplemented with 2mM L-glutamine, 1% non-essential amino acids and 10% FBS, respectively. Mycoplasma tests were regularly performed using the MycoAlert™ PLUS Mycoplasma Detection Kit (Lonza, Basel, Switzerland).

Neuroblastoma tumor tissue was obtained from the Karolinska University Hospital according to the ethical approval from the Stockholm Regional Ethical Review Board and the Karolinska University Hospital Research Ethics Committee (approval ID 2009/1369-31/1 and 03-736). Informed consent (written or verbal) was provided by the parents or guardians for the use of tumor samples in research. Samples were collected during surgery, snap-frozen in liquid nitrogen and stored at -80°C until further use. Twenty-seven neuroblastoma samples derived from children of different ages and all clinical stages, including different biological subsets [36] were analyzed.

RNA isolation and reverse transcriptase PCR

Total RNA was isolated using the RNeasy® Mini Kit (Qiagen Norge, Oslo, Norway) according to the provided manual. The RNA quantity and quality was determined using the NanoDrop 1000 (Thermo Fisher Scientific Inc.). One µg RNA was used for cDNA synthesis with the iScript™ cDNA Synthesis Kit (Bio-Rad Laboratories AB, Oslo, Norway). PCR was performed in a 25µl reaction mix containing 2µl cDNA, 12.5µl AccuStart™ II GelTrack PCR SuperMix (Quanta Biosciences, Gaithersburg, USA), 400 nM of each primer and 10.1µl of ultra-pure H_2O (Biochrom GmbH, Berlin, Germany). The PCR run was performed in a T100™ Thermal Cycler (Bio-Rad Laboratories AB, Oslo, Norway) as follows: 2min at 94°C and 35 cycles of 94°C for 20s, 62°C for 30s and 72°C for 90s. The sequences for the PCR primers were the following: APRT (housekeeping) 5'-CCCGAGGCTTCCTCTTTGGC-3' (sense) and 5'-CTCCCTGCCCTTAAGCGAGG-3' (antisense) [59], CMKLR1 5'-GCCAACCTGCATGGGAAAATA-3' (sense) and 5'-GTGAGGTAGCAAGCTGTGATG-3' (antisense), GPR1 5'-CAATCTAGCCATTGCGG ATTTCA-3' (sense) and 5'-CCGATGAGATA AGACAGGATGGA-3' (antisense), chemerin 5'-AGAAACCCGAGTG CAAAGTCA-3' (sense) and 5'-AGAACTTGGGTCTCTATGGGG-3' (antisense) (Primer bank ID 215272316c3, 148228828c3 and 218931208c1 http://pga.mgh.harvard.edu/primerbank/index.html).

PCR products were analyzed by gel electrophoresis. The 1.8% SeaKem® LE Agarose gel (Lonza) was stained with GelRed™ (Biotium, Inc., Hayward, USA) and visualized under UV light in the BioDoc-It™ Imaging System (UVP, LLC, Upland, USA). The PCR results for CMKLR1, GPR1 and chemerin were confirmed with a second, independent primer set (data not shown).

Western blot

Cultured cells were washed briefly with phosphate-buffered saline (PBS, Biochrom GmbH) and harvested in RIPA Lysis and Extraction Buffer containing Halt™ Protease and Phosphatase Inhibitor Cocktail (Thermo Fisher Scientific Inc.). Following sonication, the protein concentration was determined using a Protein Quantification Assay (MACHEREY-NAGEL GmbH & Co. KG, Düren, Germany). The protein lysates were supplemented with NuPAGE® LDS Sample Buffer (4X) (Thermo Fisher Scientific Inc.) as well as 100mM DTT (Sigma-Aldrich Norway AS) and incubated for 10min at 70°C. Equal amounts of protein were separated on NuPAGE™ Novex™ 4-12% Bis-Tris Protein Gels (Thermo Fisher Scientific Inc.) and transferred onto a 0.45µm PVDF Membrane (Merck Life Science AS, Oslo, Norway) according to the XCell SureLock Mini-Cell technical guide (Thermo Fisher Scientific Inc.). The membranes were blocked in TBS-T (Tris-buffered saline (TBS) with 0.1% Tween-20; Sigma-Aldrich Norway AS) containing 5% (w/v) skimmed milk powder. Incubation with the primary antibody was performed overnight at 4°C according to antibody supplier recommendation in either blocking buffer or 5% BSA (AppliChem, Darmstadt, Germany) in TBS-T. Following three washes in TBS-T, the membranes were incubated in the appropriate secondary antibody solution for 1h at room temperature. After four washes, detection and visualization were performed using SuperSignal™ West Pico Chemiluminescent Substrate (Thermo Fisher Scientific Inc.) and the ImageQuant LAS 4000 imager (GE Healthcare, Oslo, Norway). MagicMark™ XP Western Protein Standard (Thermo Fisher Scientific Inc.) was used to estimate the molecular mass of the detected proteins. Densitometry was performed using Fiji software [60].

ICC

For immunocytochemistry, cells were grown on 8-well µ-Slide (ibidi GmbH, Munich, Germany) for 24h. Cells were then rinsed briefly with PBS and fixed with 4% formaldehyde for 20min. After three washes with PBS, unspecific binding sites were blocked with 1% BSA in PBS containing 0.3% Triton-X-100 (Sigma-Aldrich Norway AS) for 45min. The cells were incubated with primary antibodies diluted in blocking solution at 4°C overnight. After three washes with PBS, the cells were incubated with the secondary antibodies diluted in blocking solution for 1h at room temperature, protected from light. Following three washes with PBS, the nuclei were stained with Hoechst 33342 (ImmunoChemistry Technologies, LLC, Bloomington, USA) for 10min. The cells were washed 2x with PBS and covered with Mounting Medium for fluorescence microscopy (ibidi GmbH). The cells were subsequently examined with a Leica TCS SP5 or Zeiss LSM780 confocal microscope.

IHC

Formalin-fixed and paraffin-embedded tissue sections were deparaffinized in xylene and graded alcohols, hydrated and washed in PBS. After antigen retrieval in a sodium citrate buffer (pH 6) in a microwave oven, the endogenous peroxidase was blocked by 0.3% H_2O_2 for 15min. Sections were incubated overnight at 4°C with the primary antibody. As a secondary antibody, the anti-rabbit-HRP SuperPicTure Polymer detection kit (87-9663, Zymed-Invitrogen, San Francisco, USA) or anti-mouse EnVision-HRP (Dako, Agilent Technologies, Inc., Santa Clara, USA) was used. A matched isotype control was used as a control for nonspecific background staining.

For immunofluorescence histology studies (IF-P), the sections were treated as described above and stained sequentially with the primary and secondary antibody sets. Alexa Fluor® 488 and Alexa Fluor® 594 conjugated secondary antibodies were used to visualize positive staining.

The fluorescence labeled tissue sections were examined using the Zeiss LSM780 confocal microscope and the immunoperoxidase stained sections using the Leica DMI6000B microscope.

Calcium mobilization assay

SK-N-SH cells were seeded into an 8-well µ-Slide (ibidi GmbH) and incubated overnight in RPMI containing 10% FBS. The following day the cells were washed and preloaded with 20µM Cal-520 (AATBio, Sunnyvale, USA) in Hanks' Buffer with 20mM Hepes (HHBS) with 0.04% Pluronic® F-127 (AATBio). After 90min of incubation at 37°C, the dye solution was replaced with HHBS and the cells were subsequently examined with a Leica TCS SP5 confocal microscope in the presence or absence 2mM EDTA. Before the addition of 10nM of chemerin, a baseline measurement was taken. Images were then obtained and analyzed using the Leica LAS AF software.

Stimulation of cells with chemerin

Cells were seeded in 35mm cell culture dishes (Corning, Corning, USA) and incubated overnight in complete growth medium. The cells were serum starved for 24h prior to stimulation with recombinant human chemerin (0.1-10 nM) for 5, 10, 20 and 30min.

Chemerin ELISA

SK-N-AS cells were seeded in 96-well culture plates. The following day, the medium was removed and the cells were serum starved (0.1% FBS) overnight. The cells were then stimulated with either 10% FBS or 10 ng/ml, 50 ng/ml TNFα, or IL-1β in serum reduced medium (0.1% FBS) for 12 and 24h. After incubation, supernatants from 10 parallels were pooled and spun for 5min at 200xg to pellet floating cells. The cell supernatant was concentrated 10x using Amicon Ultra-0.5 Centrifugal Filter Unit (Merck Life Science AS). The chemerin quantity was assayed by ELISA according to the manufacturer's instructions (Human Chemerin Quantikine ELISA, R&D Systems, Inc).

Real-time zymography

SK-N-AS and SK-N-BE(2) cells were seeded in 96-well plates (Corning, Corning, USA) and left to attach overnight. The medium was replaced with Opti-MEM and the cells were serum-starved for 24h. The cells were thereafter exposed to chemerin (0.1-100 nM) for 6, 12, 24 and 48h, using Opti-MEM serum-free medium. TNFα (10ng/ml) was used as a positive control. After the incubation, the medium from three independent samples was pooled, centrifuged at 200xg for 5min at 4°C, and made 10 and 100mM with respect to $CaCl_2$ and Hepes (pH 7.5). Undiluted samples were analyzed for the expression of gelatin degrading enzymes using real-time zymography. Zymography was performed as described previously [61] with the exception that 0.1% (w/v) 2-methoxy-2,4-diphenyl-3(2H)-furanone (MDPF)-fluorescent labeled gelatin was incorporated in the 7.5 % SDS-PAGE separating gel instead of 0.1% (w/v) unlabeled gelatin. Gelatin (Sigma-Aldrich Norway AS) was labeled with the fluorescent dye 2-methoxy-2,4-diphenyl-3(2H)-furanone (Sigma-Aldrich Norway AS) to give MDPF-gelatin as described previously [62]. The main difference between normal gelatin zymography and real-time gelatin zymography is that in real-time zymography the gel is not stained and hence it is possible to follow the degradation of the gelatin in real time without staining. In the present work, each gel was monitored continuously and a picture of the gel was taken approximately every second hour for fifteen hours or more. Gelatinase activity was evident as dark bands against the un-degraded fluorescent background.

Cell viability assay

A colorimetric 3-(4,5-dimethylthiazol-2-yl)-2,5-diphenyltetrazolium bromide (MTT) viability assay [63] was employed to assess the effect of α-NETA on the viability of neuroblastoma cell lines as well as MRC-5 and HUVEC. The cells were seeded in 96-well plates in full growth media. After 24h the cells were washed once with Opti-MEM (Thermo Fisher Scientific Inc.) before being incubated with 313nM-10µM α-NETA (dissolved in dimethylsulfoxide, DMSO) in Opti-MEM for 72h. Control cells received DMSO corresponding to the highest concentration present in the α-NETA treated cells. The MTT solution (20µl of 5mg MTT, Sigma-Aldrich Norway AS, per ml phosphate buffered saline) was added to each well. After 2-3h additional incubation 150µl of solution were

carefully removed from each well and 100µl isopropanol containing 0.04M HCl were added and mixed thoroughly. To further facilitate formazan crystal solubilizing, the plates were placed on an orbital shaker for 1h at room temperature. The absorbance was measured with a CLARIOstar plate reader (BMG LABTECH, Ortenberg, Germany) at 590 nm. The experiment was repeated three times with at least three parallels per treatment and the cell viability was calculated as the ratio of the mean OD of treated cells over vehicle treated control cells (100% living cells). The IC_{50}s were calculated from log concentration curves using non-linear regression analysis in GraphPad Prism.

Clonogenic assay

SK-N-AS, SK-N-BE(2), SK-N-DZ, and SH-SY5Y cells were seeded in 6 well plates and allowed to attach to the surface overnight. The cells were washed and the medium was replaced with Opti-MEM containing 313 nM-5µM α-NETA dissolved in DMSO. The control cells received DMSO corresponding to the highest concentration present in the α-NETA treated cells. After 72h the medium was replaced with regular growth medium containing 10% FBS. When the cell colonies reached ≥ 50 cells, the plates were briefly rinsed with PBS (Thermo Fisher Scientific Inc.), fixed in 4% formaldehyde (Merck Life Science AS), and stained with Giemsa (Merck Life Science AS). Colonies containing at least 50 cells were counted.

In vivo xenograft study

All animal experiments were approved by the local ethical committee (approval ID: N231/14) appointed by the Swedish Board of Agriculture and conducted in accordance with the local guidelines and the European Directive 2010/63/EU.

Female, immunodeficient nude mice (NMRI-nu/nu, Taconic) were used for the xenograft studies. The animals were housed in cages containing 2–6 mice with ad libitum access to food and sterile water. The cages contained environmental enrichment (a house, nest material and gnawing sticks) and the mice were kept on a 12h day/night cycle.

Each mouse was anaesthetized (Isoflurane 4% induction and 2% maintenance) and injected subcutaneously (s.c.) on the right flank with $1x10^7$ SK-N-AS cells. After 24h, 11 animals were randomly selected for the pre-treatment group and received 10 mg/kg α-NETA s.c. daily. α-NETA was dissolved in 10% Captisol® (Ligand Pharmaceuticals, Inc., La Jolla, USA). The mice were weighed and tumors were measured every other day. The tumor volume was calculated with the following formula: length × $(width)^2$ × 0.44. When tumors reached a volume of ≥ 0.15ml the mice were randomized to either treatment group (20 mg/kg α-NETA, daily s.c. injections, n=11 in pre-treatment group and n=10 in treatment group) or control group (vehicle, daily s.c. injections, n=11). When the tumors from the pre-treatment group were ≥ 0.15ml the α-NETA dose was increased to 20 mg/kg.

The mice were closely monitored for weight loss and other signs of toxicity. In accordance with the ethical guidelines the animals were sacrificed when tumors reached a volume of 2ml, or a diameter over 2cm, and the tumors were resected. Hence, survival was defined as time needed for the animals to grow a macroscopic tumor (volume >1.5ml). Smaller parts of the tumors were fixed in formaldehyde or frozen.

Tumor volume growth was analyzed using rate-based comparison. By fitting each tumor's growth curve to an exponential model (by correlating the logarithm of the tumor volume measurements to the time), the slope, as an estimate for the tumor growth, for each tumor's growth could be determined [64].

Statistics

SigmaPlot and GraphPad Prism software was used for the statistical analysis and the graphs. Differences between several groups were assessed with one-way ANOVA and Bonferroni post-test or two-way ANOVA and Dunnett's post-test. One sample t-test was used to compare differences between one group and a hypothetical mean. The survival analysis on tumor growth *in vivo* was performed using the Kaplan-Meier method and statistical differences between groups were performed using log-rank test.

Abbreviations

CCRL2, C-C chemokine receptor-like 2; CMKLR1, chemokine-like receptor 1; GPR1, G-protein-coupled receptor 1; TME, tumor microenvironment; α-NETA, 2-(α-naphthoyl) ethyltrimethylammonium iodide; MMP, matrix metalloproteases; ICC, Immunocytochemistry; IHC, immunohistochemistry; IF-P, immunofluorescence on paraffin-embedded samples.

Author contributions

Conception and design: C.T., B.S., U.M., I.S., M.W., J.I.J., J.O.W., L.L., P.K. Acquisition of data: C.T., I.S., B.S., M.W., L.L., L.H.M.E., J.O.W., Analysis and interpretation of data: C.T., B.S., U.M., I.S., M.W., J.I.J., J.O.W., L.L., L.H.M.E., P.K., Writing and review of manuscript: C.T., B.S., U.M., I.S., M.W., J.I.J., J.O.W., L.L., L.H.M.E., P.K.

ACKNOWLEDGMENTS

We thank Eli Berg for her excellent support with the Zymography experiments and Joe Hurley for proofreading.

CONFLICTS OF INTEREST

The authors declare no conflicts of interest.

FUNDING

This study was funded with grants from the University of Tromsø, Northern Regional Health Authority (SFP996-11), Erna and Olav Aakre Foundation for Cancer Research (A20310), Tromsø, Norway as well as The Swedish Children's Cancer Foundation, Swedish Foundation for Strategic Research http://nnbcr.se/, Swedish Cancer Society and Swedish Research Council.

REFERENCES

1. Park JR, Bagatell R, London WB, Maris JM, Cohn SL, Mattay KK, Hogarty M; COG Neuroblastoma Committee. Children's Oncology Group's 2013 blueprint for research: neuroblastoma. Pediatr Blood Cancer. 2013; 60: 985-93. http://doi.org/10.1002/pbc.24433.
2. Matthay KK, Maris JM, Schleiermacher G, Nakagawara A, Mackall CL, Diller L, Weiss WA. Neuroblastoma. Nat Rev Dis Primers. 2016; 2: 16078. http://doi.org/10.1038/nrdp.2016.78.
3. Hanahan D, Weinberg RA. Hallmarks of cancer: the next generation. Cell. 2011; 144: 646-74. http://doi.org/10.1016/j.cell.2011.02.013.
4. Mantovani A, Allavena P, Sica A, Balkwill F. Cancer-related inflammation. Nature. 2008; 454: 436-44. http://doi.org/10.1038/nature07205.
5. Larsson K, Kock A, Idborg H, Arsenian Henriksson M, Martinsson T, Johnsen JI, Korotkova M, Kogner P, Jakobsson PJ. COX/mPGES-1/PGE2 pathway depicts an inflammatory-dependent high-risk neuroblastoma subset. Proc Natl Acad Sci U S A. 2015; 112: 8070-5. http://doi.org/10.1073/pnas.1424355112.
6. Borriello L, Seeger RC, Asgharzadeh S, DeClerck YA. More than the genes, the tumor microenvironment in neuroblastoma. Cancer Lett. 2015. http://doi.org/10.1016/j.canlet.2015.11.017.
7. Asgharzadeh S, Salo JA, Ji L, Oberthuer A, Fischer M, Berthold F, Hadjidaniel M, Liu CW, Metelitsa LS, Pique-Regi R, Wakamatsu P, Villablanca JG, Kreissman SG, et al. Clinical significance of tumor-associated inflammatory cells in metastatic neuroblastoma. J Clin Oncol. 2012; 30: 3525-32. http://doi.org/10.1200/JCO.2011.40.9169.
8. Carlson LM, Rasmuson A, Idborg H, Segerstrom L, Jakobsson PJ, Sveinbjornsson B, Kogner P. Low-dose aspirin delays an inflammatory tumor progression *in vivo* in a transgenic mouse model of neuroblastoma. Carcinogenesis. 2013; 34: 1081-8. http://doi.org/10.1093/carcin/bgt009.
9. Johnsen JI, Lindskog M, Ponthan F, Pettersen I, Elfman L, Orrego A, Sveinbjornsson B, Kogner P. NSAIDs in neuroblastoma therapy. Cancer Lett. 2005; 228: 195-201. http://doi.org/10.1016/j.canlet.2005.01.058.
10. Goralski KB, McCarthy TC, Hanniman EA, Zabel BA, Butcher EC, Parlee SD, Muruganandan S, Sinal CJ. Chemerin, a novel adipokine that regulates adipogenesis and adipocyte metabolism. J Biol Chem. 2007; 282: 28175-88. http://doi.org/10.1074/jbc.M700793200.
11. Landgraf K, Friebe D, Ullrich T, Kratzsch J, Dittrich K, Herberth G, Adams V, Kiess W, Erbs S, Korner A. Chemerin as a mediator between obesity and vascular inflammation in children. J Clin Endocrinol Metab. 2012; 97: E556-64. http://doi.org/10.1210/jc.2011-2937.
12. Kulig P, Kantyka T, Zabel BA, Banas M, Chyra A, Stefanska A, Tu H, Allen SJ, Handel TM, Kozik A, Potempa J, Butcher EC, Cichy J. Regulation of chemerin chemoattractant and antibacterial activity by human cysteine cathepsins. J Immunol. 2011; 187: 1403-10. http://doi.org/10.4049/jimmunol.1002352.
13. Schultz S, Saalbach A, Heiker JT, Meier R, Zellmann T, Simon JC, Beck-Sickinger AG. Proteolytic activation of prochemerin by kallikrein 7 breaks an ionic linkage and results in C-terminal rearrangement. Biochem J. 2013; 452: 271-80. http://doi.org/10.1042/BJ20121880.
14. Berg V, Sveinbjornsson B, Bendiksen S, Brox J, Meknas K, Figenschau Y. Human articular chondrocytes express ChemR23 and chemerin; ChemR23 promotes inflammatory signalling upon binding the ligand chemerin(21-157). Arthritis Res Ther. 2010; 12: R228. http://doi.org/10.1186/ar3215.
15. Pachynski RK, Zabel BA, Kohrt HE, Tejeda NM, Monnier J, Swanson CD, Holzer AK, Gentles AJ, Sperinde GV, Edalati A, Hadeiba HA, Alizadeh AA, Butcher EC. The chemoattractant chemerin suppresses melanoma by recruiting natural killer cell antitumor defenses. J Exp Med. 2012; 209: 1427-35. http://doi.org/10.1084/jem.20112124.
16. Wang N, Wang QJ, Feng YY, Shang W, Cai M. Overexpression of chemerin was associated with tumor angiogenesis and poor clinical outcome in squamous cell carcinoma of the oral tongue. Clin Oral Investig. 2014; 18: 997-1004. http://doi.org/10.1007/s00784-013-1046-8.
17. Kumar JD, Holmberg C, Kandola S, Steele I, Hegyi P, Tiszlavicz L, Jenkins R, Beynon RJ, Peeney D, Giger OT, Alqahtani A, Wang TC, Charvat TT, et al. Increased expression of chemerin in squamous esophageal cancer myofibroblasts and role in recruitment of mesenchymal stromal cells. PLoS One. 2014; 9: e104877. http://doi.org/10.1371/journal.pone.0104877.
18. Wang C, Wu WK, Liu X, To KF, Chen GG, Yu J, Ng EK. Increased serum chemerin level promotes cellular invasiveness in gastric cancer: a clinical and experimental study. Peptides. 2014; 51: 131-8. http://doi.org/10.1016/j.peptides.2013.10.009.

19. Lande R, Gafa V, Serafini B, Giacomini E, Visconti A, Remoli ME, Severa M, Parmentier M, Ristori G, Salvetti M, Aloisi F, Coccia EM. Plasmacytoid dendritic cells in multiple sclerosis: intracerebral recruitment and impaired maturation in response to interferon-beta. J Neuropathol Exp Neurol. 2008; 67: 388-401. http://doi.org/10.1097/NEN.0b013e31816fc975.

20. Yamaguchi Y, Du XY, Zhao L, Morser J, Leung LL. Proteolytic cleavage of chemerin protein is necessary for activation to the active form, Chem157S, which functions as a signaling molecule in glioblastoma. J Biol Chem. 2011; 286: 39510-9. http://doi.org/10.1074/jbc.M111.258921.

21. Mattern A, Zellmann T, Beck-Sickinger AG. Processing, signaling, and physiological function of chemerin. IUBMB Life. 2014; 66: 19-26. http://doi.org/10.1002/iub.1242.

22. Zabel BA, Allen SJ, Kulig P, Allen JA, Cichy J, Handel TM, Butcher EC. Chemerin activation by serine proteases of the coagulation, fibrinolytic, and inflammatory cascades. J Biol Chem. 2005; 280: 34661-6. http://doi.org/10.1074/jbc.M504868200.

23. Guillabert A, Wittamer V, Bondue B, Godot V, Imbault V, Parmentier M, Communi D. Role of neutrophil proteinase 3 and mast cell chymase in chemerin proteolytic regulation. J Leukoc Biol. 2008; 84: 1530-8. http://doi.org/10.1189/jlb.0508322.

24. Wittamer V, Franssen JD, Vulcano M, Mirjolet JF, Le Poul E, Migeotte I, Brezillon S, Tyldesley R, Blanpain C, Detheux M, Mantovani A, Sozzani S, Vassart G, et al. Specific recruitment of antigen-presenting cells by chemerin, a novel processed ligand from human inflammatory fluids. J Exp Med. 2003; 198: 977-85. http://doi.org/10.1084/jem.20030382.

25. Luangsay S, Wittamer V, Bondue B, De Henau O, Rouger L, Brait M, Franssen JD, de Nadai P, Huaux F, Parmentier M. Mouse ChemR23 is expressed in dendritic cell subsets and macrophages, and mediates an anti-inflammatory activity of chemerin in a lung disease model. J Immunol. 2009; 183: 6489-99. http://doi.org/10.4049/jimmunol.0901037.

26. Zabel BA, Ohyama T, Zuniga L, Kim JY, Johnston B, Allen SJ, Guido DG, Handel TM, Butcher EC. Chemokine-like receptor 1 expression by macrophages *in vivo*: regulation by TGF-beta and TLR ligands. Exp Hematol. 2006; 34: 1106-14. http://doi.org/10.1016/j.exphem.2006.03.011.

27. Parolini S, Santoro A, Marcenaro E, Luini W, Massardi L, Facchetti F, Communi D, Parmentier M, Majorana A, Sironi M, Tabellini G, Moretta A, Sozzani S. The role of chemerin in the colocalization of NK and dendritic cell subsets into inflamed tissues. Blood. 2007; 109: 3625-32. http://doi.org/10.1182/blood-2006-08-038844.

28. Zabel BA, Silverio AM, Butcher EC. Chemokine-like receptor 1 expression and chemerin-directed chemotaxis distinguish plasmacytoid from myeloid dendritic cells in human blood. J Immunol. 2005; 174: 244-51.

29. Sell H, Laurencikiene J, Taube A, Eckardt K, Cramer A, Horrighs A, Arner P, Eckel J. Chemerin is a novel adipocyte-derived factor inducing insulin resistance in primary human skeletal muscle cells. Diabetes. 2009; 58: 2731-40. http://doi.org/10.2337/db09-0277.

30. Imai K, Takai K, Hanai T, Shiraki M, Suzuki Y, Hayashi H, Naiki T, Nishigaki Y, Tomita E, Shimizu M, Moriwaki H. Impact of serum chemerin levels on liver functional reserves and platelet counts in patients with hepatocellular carcinoma. Int J Mol Sci. 2014; 15: 11294-306. http://doi.org/10.3390/ijms150711294.

31. Zhao S, Li C, Ye YB, Peng F, Chen Q. Expression of chemerin correlates with a favorable prognosis in patients with non-small cell lung cancer. Lab Med. 2011; 42: 553-7. http://doi.org/10.1309/lmww79nits6zadpt.

32. Rourke JL, Muruganandan S, Dranse HJ, McMullen NM, Sinal CJ. Gpr1 is an active chemerin receptor influencing glucose homeostasis in obese mice. J Endocrinol. 2014; 222: 201-15. http://doi.org/10.1530/JOE-14-0069.

33. Zabel BA, Nakae S, Zuniga L, Kim JY, Ohyama T, Alt C, Pan J, Suto H, Soler D, Allen SJ, Handel TM, Song CH, Galli SJ, et al. Mast cell-expressed orphan receptor CCRL2 binds chemerin and is required for optimal induction of IgE-mediated passive cutaneous anaphylaxis. J Exp Med. 2008; 205: 2207-20. http://doi.org/10.1084/jem.20080300.

34. Galligan CL, Matsuyama W, Matsukawa A, Mizuta H, Hodge DR, Howard OM, Yoshimura T. Up-regulated expression and activation of the orphan chemokine receptor, CCRL2, in rheumatoid arthritis. Arthritis Rheum. 2004; 50: 1806-14. http://doi.org/10.1002/art.20275.

35. Akram IG, Georges R, Hielscher T, Adwan H, Berger MR. The chemokines CCR1 and CCRL2 have a role in colorectal cancer liver metastasis. Tumour Biol. 2015. http://doi.org/10.1007/s13277-015-4089-4.

36. Sveinbjornsson B, Rasmuson A, Baryawno N, Wan M, Pettersen I, Ponthan F, Orrego A, Haeggstrom JZ, Johnsen JI, Kogner P. Expression of enzymes and receptors of the leukotriene pathway in human neuroblastoma promotes tumor survival and provides a target for therapy. FASEB J. 2008; 22: 3525-36. http://doi.org/10.1096/fj.07-103457.

37. Kaur J, Adya R, Tan BK, Chen J, Randeva HS. Identification of chemerin receptor (ChemR23) in human endothelial cells: chemerin-induced endothelial angiogenesis. Biochem Biophys Res Commun. 2010; 391: 1762-8. http://doi.org/10.1016/j.bbrc.2009.12.150.

38. Barnea G, Strapps W, Herrada G, Berman Y, Ong J, Kloss B, Axel R, Lee KJ. The genetic design of signaling cascades to record receptor activation. Proc Natl Acad Sci U S A. 2008; 105: 64-9. http://doi.org/10.1073/pnas.0710487105.

39. De Henau O, Degroot GN, Imbault V, Robert V, De Poorter C, McHeik S, Gales C, Parmentier M, Springael JY. Signaling properties of chemerin receptors CMKLR1, GPR1 and CCRL2. PLoS One. 2016; 11: e0164179. http://doi.org/10.1371/journal.pone.0164179.

40. Rourke JL, Dranse HJ, Sinal CJ. CMKLR1 and GPR1 mediate chemerin signaling through the RhoA/ROCK

pathway. Mol Cell Endocrinol. 2015; 417: 36-51. http://doi.org/10.1016/j.mce.2015.09.002.

41. Kumar JD, Kandola S, Tiszlavicz L, Reisz Z, Dockray GJ, Varro A. The role of chemerin and ChemR23 in stimulating the invasion of squamous oesophageal cancer cells. Br J Cancer. 2016; 114: 1152-9. http://doi.org/10.1038/bjc.2016.93.

42. Graham KL, Zhang JV, Lewen S, Burke TM, Dang T, Zoudilova M, Sobel RA, Butcher EC, Zabel BA. A novel CMKLR1 small molecule antagonist suppresses CNS autoimmune inflammatory disease. PLoS One. 2014; 9: e112925. http://doi.org/10.1371/journal.pone.0112925.

43. Brodeur GM, Iyer R, Croucher JL, Zhuang T, Higashi M, Kolla V. Therapeutic targets for neuroblastomas. Expert Opin Ther Targets. 2014; 18: 277-92. http://doi.org/10.1517/14728222.2014.867946.

44. Chow MT, Luster AD. Chemokines in cancer. Cancer Immunol Res. 2014; 2: 1125-31. http://doi.org/10.1158/2326-6066.CIR-14-0160.

45. Zhou J, Xiang Y, Yoshimura T, Chen K, Gong W, Huang J, Zhou Y, Yao X, Bian X, Wang JM. The role of chemoattractant receptors in shaping the tumor microenvironment. Biomed Res Int. 2014; 2014: 751392. http://doi.org/10.1155/2014/751392.

46. Gross N, Meier R. Chemokines in neuroectodermal cancers: the crucial growth signal from the soil. Semin Cancer Biol. 2009; 19: 103-10. http://doi.org/10.1016/j.semcancer.2008.10.009.

47. Bondue B, Wittamer V, Parmentier M. Chemerin and its receptors in leukocyte trafficking, inflammation and metabolism. Cytokine Growth Factor Rev. 2011; 22: 331-8. http://doi.org/10.1016/j.cytogfr.2011.11.004.

48. Zhao W, Xu Y, Xu J, Wu D, Zhao B, Yin Z, Wang X. Subsets of myeloid-derived suppressor cells in hepatocellular carcinoma express chemokines and chemokine receptors differentially. Int Immunopharmacol. 2015; 26: 314-21. http://doi.org/10.1016/j.intimp.2015.04.010.

49. Chua SK, Shyu KG, Lin YF, Lo HM, Wang BW, Chang H, Lien LM. Tumor necrosis factor-alpha and the ERK pathway drive chemerin expression in response to hypoxia in cultured human coronary artery endothelial cells. PLoS One. 2016; 11: e0165613. http://doi.org/10.1371/journal.pone.0165613.

50. Rama D, Esendagli G, Guc D. Expression of chemokine-like receptor 1 (CMKLR1) on J744A.1 macrophages co-cultured with fibroblast and/or tumor cells: modeling the influence of microenvironment. Cell Immunol. 2011; 271: 134-40. http://doi.org/10.1016/j.cellimm.2011.06.016.

51. Singh A, Ruan Y, Tippett T, Narendran A. Targeted inhibition of MEK1 by cobimetinib leads to differentiation and apoptosis in neuroblastoma cells. J Exp Clin Cancer Res. 2015; 34: 104. http://doi.org/10.1186/s13046-015-0222-x.

52. Vieira GC, Chockalingam S, Melegh Z, Greenhough A, Malik S, Szemes M, Park JH, Kaidi A, Zhou L, Catchpoole D, Morgan R, Bates DO, Gabb PD, et al. LGR5 regulates pro-survival MEK/ERK and proliferative Wnt/beta-catenin signalling in neuroblastoma. Oncotarget. 2015; 6: 40053-67. http://doi.org/10.18632/oncotarget.5548.

53. Johnsen JI, Segerstrom L, Orrego A, Elfman L, Henriksson M, Kagedal B, Eksborg S, Sveinbjornsson B, Kogner P. Inhibitors of mammalian target of rapamycin downregulate MYCN protein expression and inhibit neuroblastoma growth *in vitro* and *in vivo*. Oncogene. 2008; 27: 2910-22. http://doi.org/10.1038/sj.onc.1210938.

54. King D, Yeomanson D, Bryant HE. PI3King the lock: targeting the PI3K/Akt/mTOR pathway as a novel therapeutic strategy in neuroblastoma. J Pediatr Hematol Oncol. 2015; 37: 245-51. http://doi.org/10.1097/MPH.0000000000000329.

55. Banas M, Zegar A, Kwitniewski M, Zabieglo K, Marczynska J, Kapinska-Mrowiecka M, LaJevic M, Zabel BA, Cichy J. The expression and regulation of chemerin in the epidermis. PLoS One. 2015; 10: e0117830. http://doi.org/10.1371/journal.pone.0117830.

56. Hadler-Olsen E, Winberg JO, Uhlin-Hansen L. Matrix metalloproteinases in cancer: their value as diagnostic and prognostic markers and therapeutic targets. Tumour Biol. 2013; 34: 2041-51. http://doi.org/10.1007/s13277-013-0842-8.

57. Ribatti D, Surico G, Vacca A, De Leonardis F, Lastilla G, Montaldo PG, Rigillo N, Ponzoni M. Angiogenesis extent and expression of matrix metalloproteinase-2 and -9 correlate with progression in human neuroblastoma. Life Sci. 2001; 68: 1161-8.

58. Ara T, Fukuzawa M, Kusafuka T, Komoto Y, Oue T, Inoue M, Okada A. Immunohistochemical expression of MMP-2, MMP-9, and TIMP-2 in neuroblastoma: association with tumor progression and clinical outcome. J Pediatr Surg. 1998; 33: 1272-8.

59. Figenschau Y, Knutsen G, Shahazeydi S, Johansen O, Sveinbjornsson B. Human articular chondrocytes express functional leptin receptors. Biochem Biophys Res Commun. 2001; 287: 190-7. http://doi.org/10.1006/bbrc.2001.5543.

60. Schindelin J, Arganda-Carreras I, Frise E, Kaynig V, Longair M, Pietzsch T, Preibisch S, Rueden C, Saalfeld S, Schmid B, Tinevez JY, White DJ, Hartenstein V, et al. Fiji: an open-source platform for biological-image analysis. Nat Methods. 2012; 9: 676-82. http://doi.org/10.1038/nmeth.2019.

61. Malla N, Berg E, Uhlin-Hansen L, Winberg JO. Interaction of pro-matrix metalloproteinase-9/proteoglycan heteromer with gelatin and collagen. J Biol Chem. 2008; 283: 13652-65. http://doi.org/10.1074/jbc.M709140200.

62. Mathisen B, Lindstad RI, Hansen J, El-Gewely SA, Maelandsmo GM, Hovig E, Fodstad O, Loennechen T, Winberg JO. S100A4 regulates membrane induced

activation of matrix metalloproteinase-2 in osteosarcoma cells. Clin Exp Metastasis. 2003; 20: 701-11.

63. Mosmann T. Rapid colorimetric assay for cellular growth and survival: application to proliferation and cytotoxicity assays. J Immunol Methods. 1983; 65: 55-63.

64. Hather G, Liu R, Bandi S, Mettetal J, Manfredi M, Shyu WC, Donelan J, Chakravarty A. Growth rate analysis and efficient experimental design for tumor xenograft studies. Cancer Inform. 2014; 13: 65-72. http://doi.org/10.4137/CIN.S13974.

Inhibition of chemerin/CMKLR1 axis in neuroblastoma cells reduces clonogenicity and cell viability *in vitro* and impairs tumor growth *in vivo*

SUPPLMENTARY MATERIALS

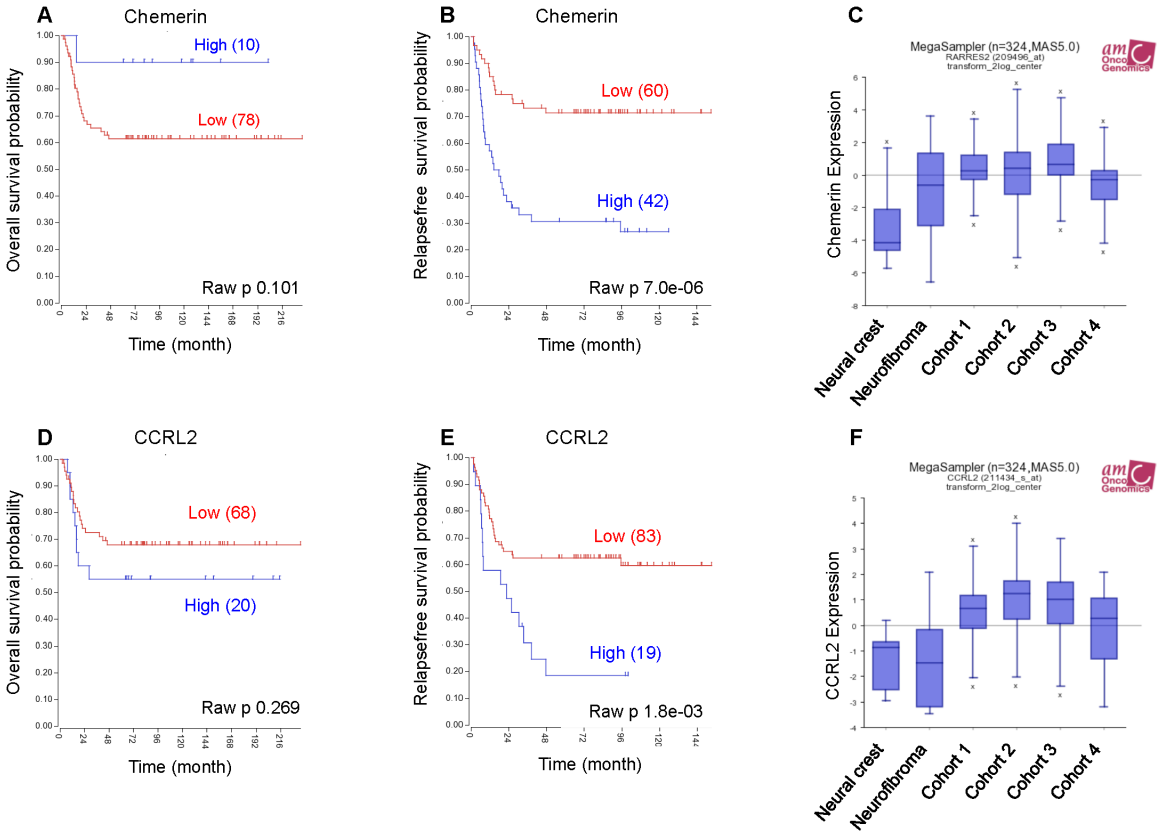

Supplementary Figure 1: Expression data was analyzed using the R2 database http://r2.amc.nl. Kaplan-Meier survival estimates were used to evaluate the prognostic value of *RARRES2* (chemerin) **(A, B)** and *CCRL2* **(D, E)** expression in two patient data sets (A and D: Versteeg n=88; B and E: Seeger n=102). The Kaplan-Meier scanning tool was used to determine the RARRES2 (chemerin) and CCRL2 mRNA expression in neuroblastoma. All expression data were scanned to find the most optimal cut-off between high and low gene expression and the log-rank test that gave the lowest p-value was calculated to search for significant differences between tumor samples expressing high and low RARRES2 (chemerin) and CCRL2 mRNA levels, respectively. The expression of *RARRES2* (chemerin) **(C)** and *CCRL2* **(F)** was compared between neural crest (Etchevers n=5), benign neurofibroma (Miller n=86) and 4 neuroblastoma cohorts (cohort 1: Versteeg n=88, cohort 2: Delattre n=64, cohort 3: Hiyama n=51, cohort 4: Lastowska n=30).

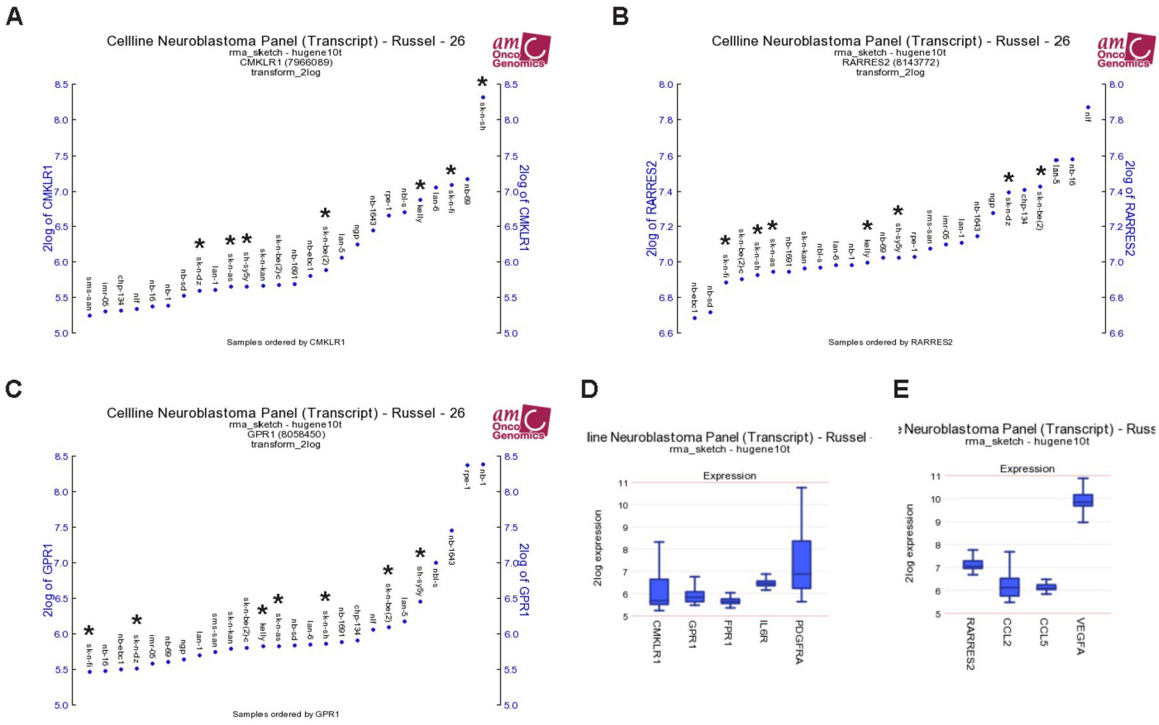

Supplementary Figure 2: *CMKLR1* **(A),** *RARRES2* **(B)** and *GPR1* **(C)** expression was analyzed using the Russel neuroblastoma cell line panel (transcript) in the R2 database http://r2.amc.nl. Cell lines used in this study were marked with an asterisk. The expression of *CMKLR1* and *GPR1* was compared to the previously in neuroblastoma cell lines described receptors *FPR1*, *IL6R* and *PDGFRA* **(D)**. Chemerin expression was compared to *CCL2*, *CCL5* and *VEGFA* **(E)**.

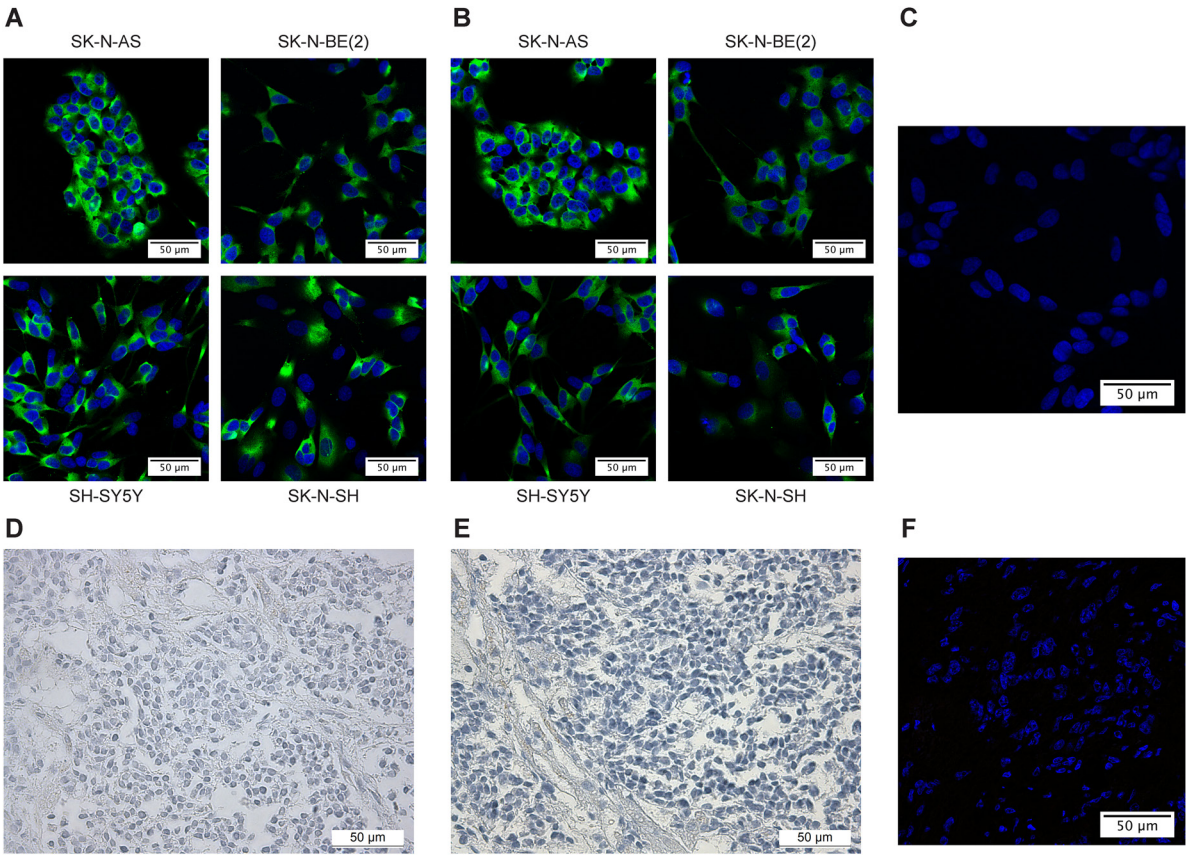

Supplementary Figure 3: Immunofluorescence CMKLR1 staining using SK-N-AS, SK-N-BE(2), SH-SY5Y and SK-N-SH cells and two different antibodies: STJ92262 from St. John's laboratory **(A)** and LS-B12924 from LSBio **(B)**. The used secondary antibody was Goat anti-Rabbit IgG (H+L), Alexa Fluor 488 (A-11008, Thermo Fisher Scientific) and the nuclei were stained with Hoechst 33342 (ImmunoChemistry Technologies). Isotype control staining for IF and IHC. **(C)** SH-SY5Y cells were incubated with rabbit isotype antibody instead of primary antibody. Immunoperoxidase labeled tissue sections where the primary antibodies were replaced with rabbit **(D)** or mouse **(E)** isotype antibodies. Neuroblastoma tissue sections were incubated with mouse and goat isotype antibodies prior to fluorescence staining **(F)**.

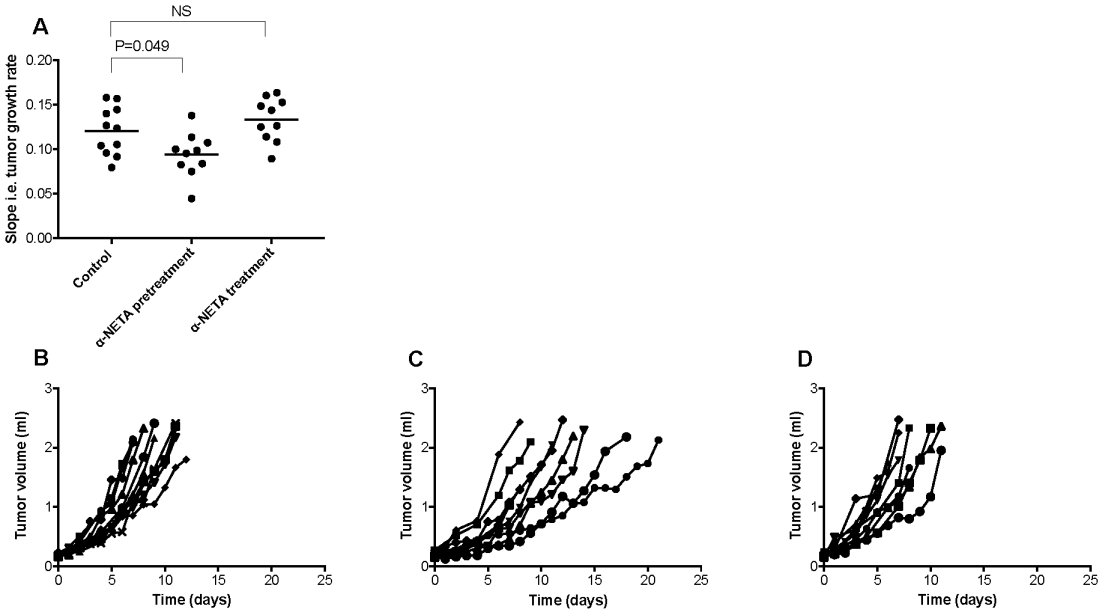

Supplementary Figure 4: The tumor growth rate in neuroblastoma bearing mice was significantly lower in the α-NETA pre-treatment group compared to the control group (one-way ANOVA P=0.0061, Bonferroni post-test, control vs. pre-treatment P=0.049). Growth rate in the different treatment groups was illustrated as the slope from curves over individual mice log tumor volume versus time. Goodness of curve fitting was assessed with R^2 (R^2 mean 0.97; range 0.875-0.999). The line represents mean slope in each treatment group **(A)**. Individual tumor growth in **(B)** control mice (daily s.c. injections with 10% Captisol®), **(C)** pre-treatment group (daily s.c. injections with 10 mg/kg α-NETA from the day after tumor cell injection and 20 mg/kg when the tumor reached 0.15ml) and **(D)** treatment group (daily s.c. injections with 20 mg/kg α-NETA after the tumor reached 0.15ml).

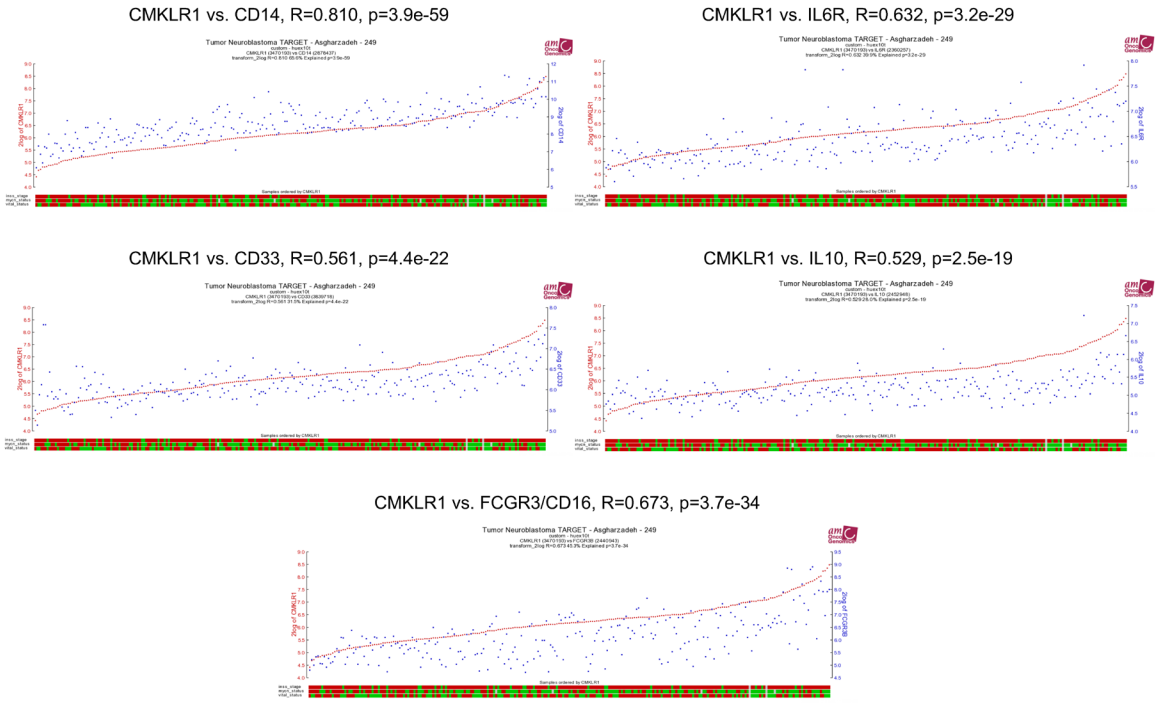

Supplementary Figure 5: Expression data was analyzed using the R2 database http://r2.amc.nl. The Asgharzadeh neuroblastoma cohort n=249 was used to correlate the expression of previously identified TAM markers (*CD33, CD14, IL6R, IL10, FCGR3*) to *CMKLR1* expression.

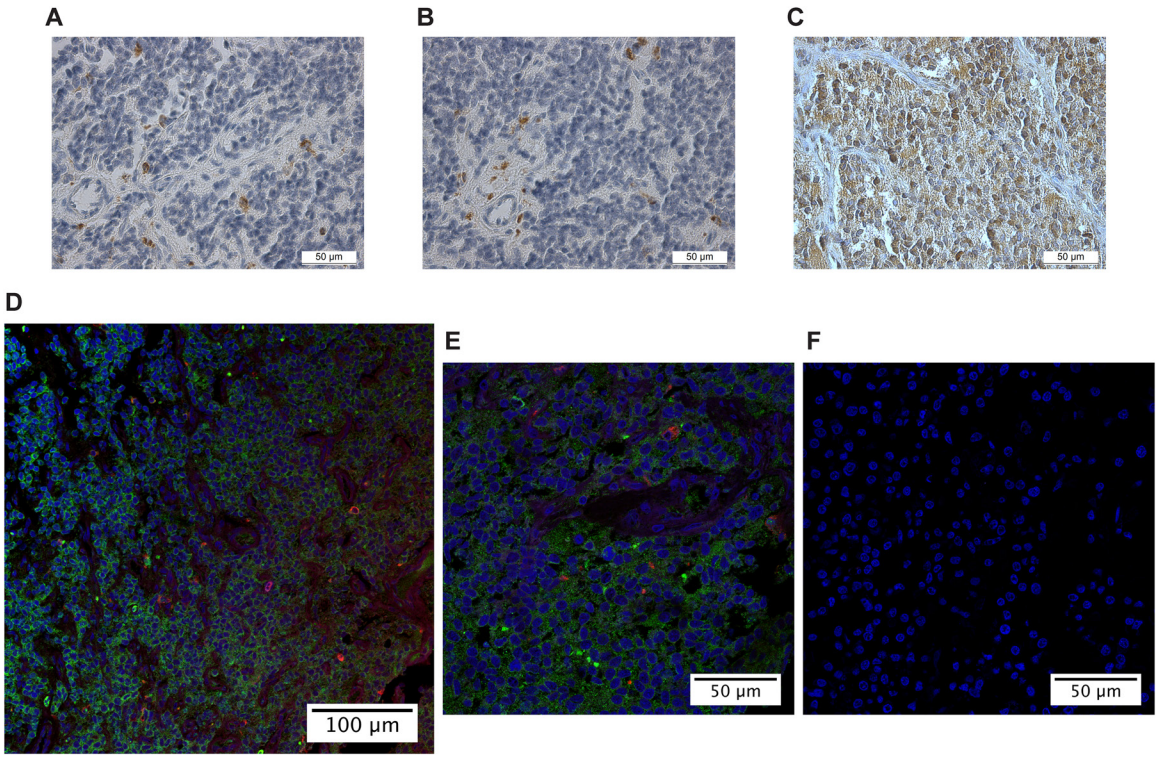

Supplementary Figure 6: Immunoperoxidase staining of the macrophage marker CD68 using M0814 from Dako **(A, B)** and CMKLR1 using STJ92262 from St. John's laboratory **(C)** in neuroblastoma primary tumor tissue demonstrates while the majority of cells in the TME are positive for CMKLR1 only few are positive for CD68. Double immunofluorescence labeling **(D, E)** of CMKLR1 (green) and CD68 (red) confirms this observation. The used secondary antibodies were Goat anti-Rabbit IgG (H+L), Alexa Fluor 488 (A-11008, Thermo Fisher Scientific) and Donkey anti-Mouse IgG (H+L), Alexa Fluor 594 (A-21203, Thermo Fisher Scientific). The nuclei were stained with DAPI (blue). Isotype control staining is displayed in panel **(F)**.

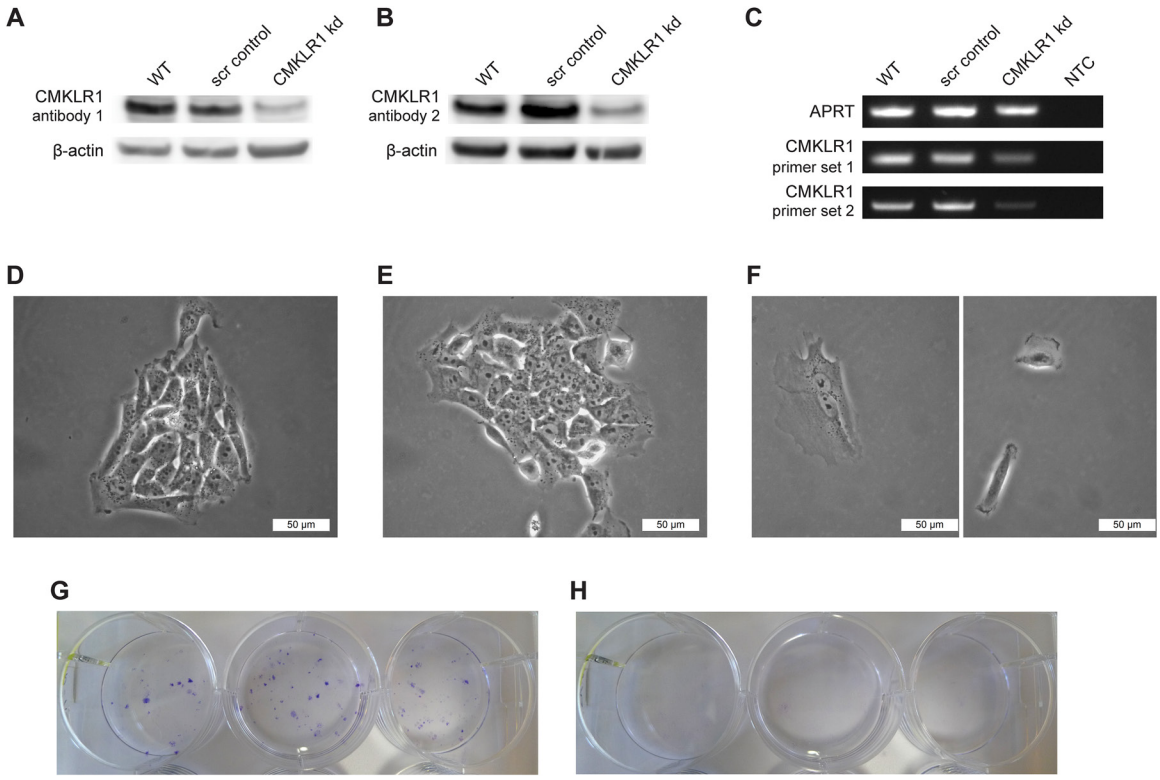

Supplementary Figure 7: SK-N-AS cells were transfected with sgRNA/Cas9 targeting all variants for human CMKLR1 or scrambled sgRNA control plasmids (GeneCopoeia, Inc., Rockville, USA) using jetPRIME® transfection reagent (Polyplus-transfection®, Illkirch, France) according to the provided manual. Forty-eight hours post transfection the cells were seeded as single cells into 96-well plates. After clonal expansion, the clones were screened for CMKLR1 expression using western blot and RT-PCR. Western blot of SK-N-AS wild-type (wt), scramble control (scr control) and CMKLR1 knockdown (CMKLR1 kd) using two different antibodies targeting CMKLR1 (**A**, STJ92262, St. John's laboratory and **(B)** ab64881, abcam) showing a clear reduction in CMKLR1 protein in the knockdown clone. RT-PCR analysis demonstrating a downregulation of CMKLR1 transcripts using two different primer sets **(C)**. In clonogenicity assays **(D-H)** slower growth and the formation of indistinct colonies was observed in CMKLR1 knockdown cells. While small but distinct colonies were observed 6 days after cell seeding in the wild-type **(D)** and scramble control **(E)** the CMKLR1 knock down cells multiplied slower and were only loosely connected **(F)**. After completion of the assays macroscopic colonies were observed in the scramble control **(G)** but not the CMKLR1 knockdown cells **(H)**.

PAPER II

cancers

MDPI

Article

SYK Inhibition Potentiates the Effect of Chemotherapeutic Drugs on Neuroblastoma Cells In Vitro

Conny Tümmler [1,*], Gianina Dumitriu [1], Malin Wickström [2], Peter Coopman [3], Andrey Valkov [4], Per Kogner [2], John Inge Johnsen [2], Ugo Moens [1] and Baldur Sveinbjörnsson [1,2]

1 Molecular Inflammation Research Group, Department of Medical Biology, Faculty of Health Sciences, UiT The Arctic University of Norway, Hansine Hansens veg 18, 9019 Tromsø, Norway; gianina.dumitriu@uit.no (G.D.); ugo.moens@uit.no (U.M.); baldur.sveinbjornsson@uit.no (B.S.)

2 Childhood Cancer Research Unit, Department of Women's and Children's Health, Karolinska Institutet, Tomtebodav 18A, 17177 Stockholm, Sweden; Malin.Wickstrom@ki.se (M.W.); Per.Kogner@ki.se (P.K.); John.Inge.Johnsen@ki.se (J.I.J.)

3 IRCM, Inserm U1194, Université Montpellier, ICM, Institut régional du Cancer Montpellier, Campus Val d'Aurelle, 208 Rue des Apothicaires, 34298 Montpellier CEDEX 5, France; peter.coopman@inserm.fr

4 Department of Clinical Pathology, University Hospital of Northern Norway, Sykehusveien 38, 9019 Tromsø, Norway; andrej.yurjevic.valkov@unn.no

* Correspondence: conny.tummler@uit.no; Tel.: +47-776-44655

Received: 17 December 2018; Accepted: 6 February 2019; Published: 10 February 2019

Abstract: Neuroblastoma is a malignancy arising from the developing sympathetic nervous system and the most common and deadly cancer of infancy. New therapies are needed to improve the prognosis for high-risk patients and to reduce toxicity and late effects. Spleen tyrosine kinase (SYK) has previously been identified as a promising drug target in various inflammatory diseases and cancers but has so far not been extensively studied as a potential therapeutic target in neuroblastoma. In this study, we observed elevated *SYK* gene expression in neuroblastoma compared to neural crest and benign neurofibroma. While SYK protein was detected in the majority of examined neuroblastoma tissues it was less frequently observed in neuroblastoma cell lines. Depletion of SYK by siRNA and the use of small molecule SYK inhibitors significantly reduced the cell viability of neuroblastoma cell lines expressing SYK protein. Moreover, SYK inhibition decreased ERK1/2 and Akt phosphorylation. The SYK inhibitor BAY 61-3606 enhanced the effect of different chemotherapeutic drugs. Transient expression of a constitutive active SYK variant increased the viability of neuroblastoma cells independent of endogenous SYK levels. Collectively, our findings suggest that targeting SYK in combination with conventional chemotherapy should be further evaluated as a treatment option in neuroblastoma.

Keywords: pediatric cancer; neuroblastoma; tyrosine kinase; combination therapy

1. Introduction

Tyrosine kinases are important mediators of cellular functions such as proliferation, differentiation, metabolism, and survival. As tyrosine kinases are frequently deregulated in e.g. inflammatory diseases and cancer they are among the most attractive drug targets [1–3]. Spleen tyrosine kinase (SYK) is a 72 kDa non-receptor tyrosine kinase consisting of two SRC homology 2 (SH2) domains and a kinase domain joined by two linker regions, interdomains A and B [4]. A shorter SYK splice variant lacking 23 amino acids in the linker region B (SYK(S) or SYK B) has also been described in various cell types [5–7].

SYK is a multifunctional protein. It mediates inflammatory responses by linking immune cell receptors to various intracellular signaling networks and exhibits, for example, a pivotal role in B-cell development [4,8,9]. Among its various functions, SYK promotes, in concert with PKCδ, the expression of anti-apoptotic Mcl-1 in B-cell chronic lymphocytic leukemia (CLL) [10] and regulates actin filament assembly and dynamics through phosphorylation of cortactin and cofilin in ovarian cancer, thereby promoting migration and invasion [11]. Furthermore, phosphorylated SYK has been observed in specific cell types and areas of the developing nervous system and diverse functions have been described [12–14].

Widely expressed in hematopoietic cells [15,16], SYK is a promising therapeutic target in inflammatory diseases (including rheumatoid arthritis, allergies, systemic lupus erythematosus, and chronic immune thrombocytopenia) [17–19] as well as in different hematological malignancies such as CLL [10,20,21], non-Hodgkin lymphoma [22], and acute myeloid leukemia (AML) [23].

However, SYK expression is not restricted to hematopoietic cells and its presence has been described, among others, in epithelial, endothelial, and neuronal cells as well as in different solid tumors [24,25]. The role of SYK in the tumorigenesis of both hematological and solid malignancies is highly complex, tumor-specific and cell type-dependent, as both tumor promoting and suppressing functions have been described [25].

A tumor-suppressing role for SYK has been demonstrated in e.g. breast cancer [26], pancreatic cancer [27], melanoma [28], hepatocellular carcinoma [29] as well as childhood pro-B-ALL [30]. In contrast, SYK has been shown to be pro-tumorigenic in prostate cancer [31], small-cell lung cancer [32], ovarian cancer [11,33], glioma [34], pediatric retinoblastoma [35], and Ewing sarcoma [36].

Of note, distinct functions of the two SYK splice variants have also been demonstrated. While the longer SYK variant suppressed breast cancer invasiveness, the shorter variant SYK B did not [37].

Neuroblastoma is a malignancy of early childhood with 90% of patients diagnosed below the age of 10 [38]. Worldwide, neuroblastoma accounts for 12.5% of cancer cases in children of age 0 to 4 years [39]. Arising from the developing sympathetic nervous system, the majority of primary tumors occur in the adrenal gland [38]. About 50% of neuroblastomas are classified as low- and very-low-risk with a very good prognosis and receive minimum therapy [38]. In contrast, the treatment of high-risk neuroblastomas remains a challenge. Despite intensive therapy, about 50% of patients are refractory to first-line treatment or relapse within two years [40].

With the increasing understanding of neuroblastoma biology and the identification of druggable protein kinase targets such as ALK and Aurora A kinase as well as the MAPK and PI3K/mTOR/Akt signaling pathways targeted therapies, both alone and in combination with conventional drugs, provide new promising treatment options [41]. The aim of the present study was to investigate the expression of SYK in neuroblastoma tumor tissues as well as neuroblastoma cell lines and to evaluate its use as a potential therapeutic target.

2. Results

2.1. SYK Is Expressed in Neuroblastoma Tissue

We examined *SYK* gene expression using the publicly available R2: Genomics analysis and visualization platform (http://r2.amc.nl) and observed that *SYK* expression was higher in four different neuroblastoma cohorts compared to neural crest cells and benign neurofibroma (Figure 1A).

Furthermore, we evaluated the presence of SYK protein in neuroblastoma and ganglioneuroma using immunohistochemistry (IHC). Supplementary Table S1 displays the clinical features of the neuroblastoma tumors used in this study. SYK was present at varying levels in 40 out of 42 neuroblastomas and 3 out of 3 ganglioneuromas (Table 1). Figure 1B,C display a representative staining of SYK in non-*MYCN*-amplified and *MYCN*-amplified tumors, respectively. In both, the cytoplasm and the nucleus, a positive SYK staining was observed. SYK-positive tumor cells were present in 31 out of 32 non-*MYCN*-amplified neuroblastomas and in 9 out of 10 *MYCN*-amplified tumors (Table 1).

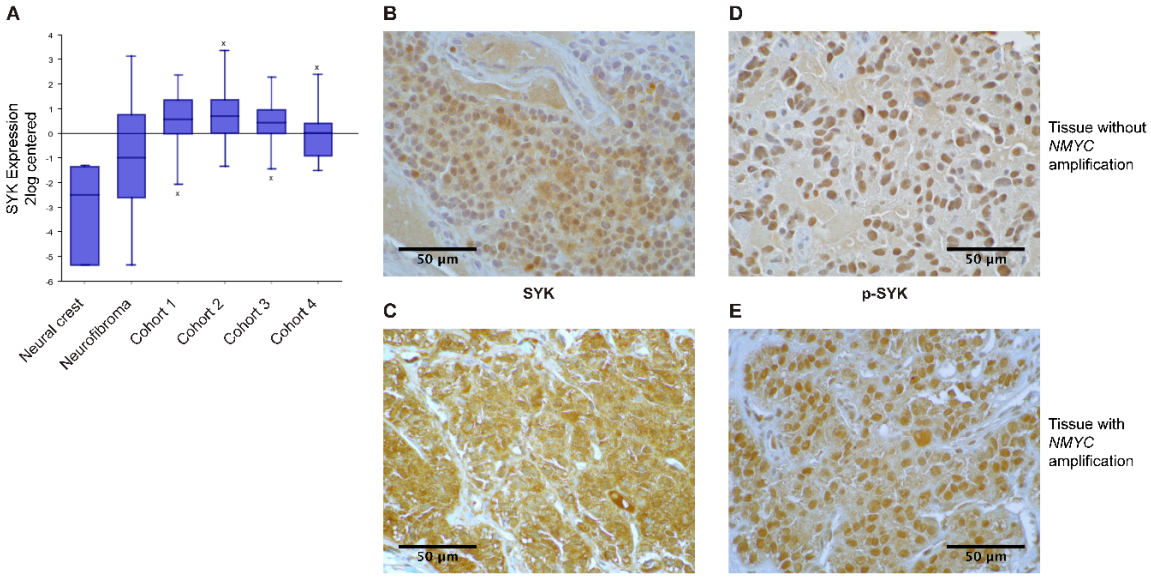

Figure 1. SYK is expressed in neuroblastoma tissue. Gene expression data were analyzed using the R2 database http://r2.amc.nl. (**A**) The expression of *SYK* was compared between neural crest (Etchevers n = 5), benign neurofibroma (Miller n = 86) and 4 neuroblastoma cohorts (cohort 1: Versteeg n = 88, cohort 2: Delattre n = 64, cohort 3: Hiyama n = 51, cohort 4: Lastowska n = 30). The presence of SYK protein (**B**,**C**) and phosphorylation at Tyr525 (**D**,**E**) were determined in neuroblastoma primary tissue using immunoperoxidase staining. (**B**,**D**) display a staining of a non-*MYCN*-amplified tumor and (**C**,**E**) show a *MYCN*-amplified tumor. Images were captured at a magnification of 900×. The displayed images are representative stainings from a panel of neuroblastoma tumors.

Table 1. Presence of SYK and p-SYK (Tyr525) in neuroblastoma tumor tissue.

Neuroblastoma Subgroups	SYK Positive (Sections Examined)	p-SYK Positive (Sections Examined)
Neuroblastoma	40 (42)	38 (40)
Non-*MYCN*-amplified	31 (32)	29 (31)
MYCN amplified	9 (10)	9 (9)
* Treated tissue	11 (13)	10 (11)
* Untreated tissue	26 (26)	25 (26)
Ganglioneuroma	3 (3)	3 (3)

* For three tumor tissue samples the information concerning prior treatment was unavailable.

Using Fisher's exact test we determined that there was no significant difference in the presence of SYK protein between *MYCN*-amplified and non-amplified tumors ($p = 0.4239$). However, examining different neuroblastoma datasets in the R2: Genomics analysis and visualization platform, we observed a significant negative correlation between *MYCN* and *SYK* expression (Supplementary Figure S1A displaying a representative dataset). In contrast, we found a significant positive correlation between *SYK* and *MYC* expression (Supplementary Figure S1B). Furthermore, we evaluated whether there was a difference in the presence of SYK in tumors that were treated with chemotherapy prior to surgery compared to untreated tumors. All 26 untreated tumor samples and 11 out of 13 treated tumor samples were SYK-positive. This difference was however not significant (Fisher's exact test $p = 0.1053$). Of note, surgery was performed after at least 10–14 days of washout. Hence, no acute chemotherapy-induced regulation of genes should be expected.

Additionally, the presence of SYK phosphorylated at Tyr525, located within the activation loop of the kinase domain, was examined as an indication for active SYK [8,42]. Figure 1D,E display a representative staining of p-SYK in non-*MYCN*-amplified and *MYCN*-amplified tumors. A strong nuclear staining, as well as some cytoplasmic staining, was observed. Phospho-SYK was present in

29 out of 31 non-*MYCN*-amplified tumors, 9 out of 9 *MYCN*-amplified tumors, 25 out of 26 untreated tumors, and 10 out of 11 treated tumors (Table 1).

Examples for SYK- and p-SYK-negative tumors are displayed in Supplementary Figures S2A and S2B. To ensure the specificity of the labeling, a corresponding isotype control antibody was used instead of the primary antibodies with which no apparent staining was observed (Supplementary Figure S2C).

2.2. SYK mRNA and to a Lesser Extend SYK Protein Are Present in Neuroblastoma Cell Lines

Using RT-PCR, western blot and immunocytochemistry (ICC) we examined the presence of *SYK* mRNA and protein in neuroblastoma cell lines. The majority of the neuroblastoma cell lines express *SYK* mRNA at varying levels (Figure 2A). However, SYK protein was detected by western blotting in only two of 10 neuroblastoma cell lines, even after long exposure times (Figure 2B). Interestingly, we noticed that the cell lines with absent or very low *SYK* mRNA levels are *MYCN*-amplified cell lines (SK-N-BE(2), SK-N-DZ, Kelly and IMR-32).

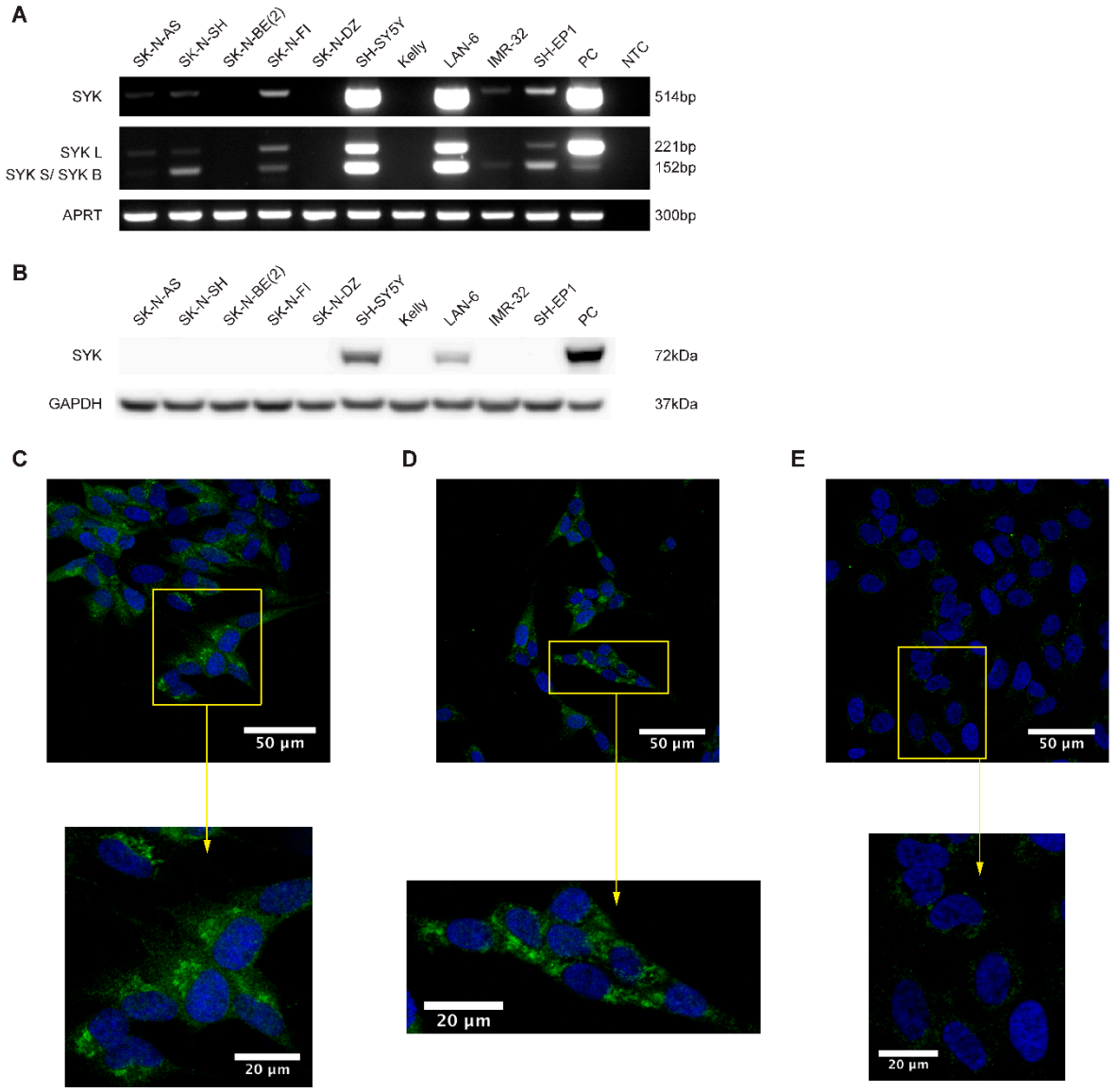

Figure 2. *Cont.*

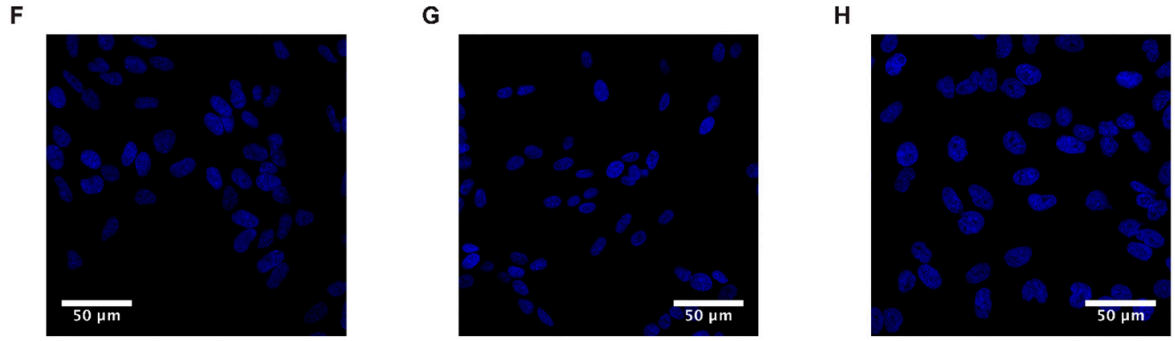

Figure 2. *SYK* mRNA and to a lesser extend SYK protein are expressed in neuroblastoma cell lines. (**A**) RT-PCR analysis demonstrating the expression of both *SYK* mRNA variants in different neuroblastoma cell lines. U937 cells were used as a positive control (PC). NTC, no template control. (**B**) Expression of SYK protein was determined by western blot. THP-1 cells were used as a positive control. Immunofluorescence labeling of SYK (green) in SH-SY5Y (**C**), LAN-6 (**D**) and SK-N-BE(2) cells (**E**). The nuclei (blue) were stained with Hoechst 33342. Panels (**F–H)** display isotype controls for SH-SY5Y (**F**), LAN-6 (**G**) and SK-N-BE(2) cells (**H**).

The shorter SYK splice variant SYK B has previously been detected in different cell types [5–7,37]. We observed that SH-SY5Y, LAN-6 and SK-N-FI cells concomitantly express both splice variants of *SYK* mRNA at similar levels whereas SH-EP1, SK-N-SH, and IMR-32 exhibit predominantly the short SYK B variant. The monocytic cell lines U937 and THP-1 with known SYK expression were used as positive controls for RT-PCR and western blot, respectively [43].

ICC was used to confirm the presence of SYK protein in SH-SY5Y and LAN-6 cells. A clear SYK labeling was observed in the cytoplasm of SH-SY5Y (Figure 2C) and LAN-6 cells (Figure 2D). The SYK signal appears to be localized mainly in the cytoplasm, with an increased intensity in patch-like structures. However, a faint staining was also observed in SK-N-BE(2) cells (Figure 2E). This could most likely be attributed to some moderate non-specific binding of the antibody. No staining was apparent in cells incubated with an isotype control antibody (Figure 2F–H).

2.3. SYK Is Phosphorylated in Neuroblastoma Cell Lines

SYK activity is tightly controlled by its (auto)phosphorylation and important regulatory functions are associated with particular tyrosine residues, such as tyrosine 323, 352, 525, and 526 [8]. To determine whether SYK exhibits basic activity in neuroblastoma cell lines, we performed SYK immunoprecipitation followed by western blot with different phosphotyrosine-specific SYK antibodies in SH-SY5Y cell lysates and THP-1 cells, serving as a positive control. We detected phosphorylation of tyrosine 352 and tyrosine 323 in both cell types (Figure 3A).

The presence of phosphorylated tyrosine 525/526 was examined by immunocytochemistry. Phospho-525/526 SYK was detected in the cytoplasm and close to the cell membrane in both SH-SY5Y cells (Figure 3B) and LAN-6 cells (Figure 3C). A weak nuclear staining was also noticeable. Variations in staining intensity were observed among the cells. As no prior synchronization or stimulation of the cells was performed, this may be attributed to the dynamic regulation of SYK-phosphorylation [8]. A very weak staining, most probably caused by non-specific background binding of the antibody, was observed in SK-N-BE(2) cells (Figure 3D) with no apparent SYK expression (Figure 2A,B).

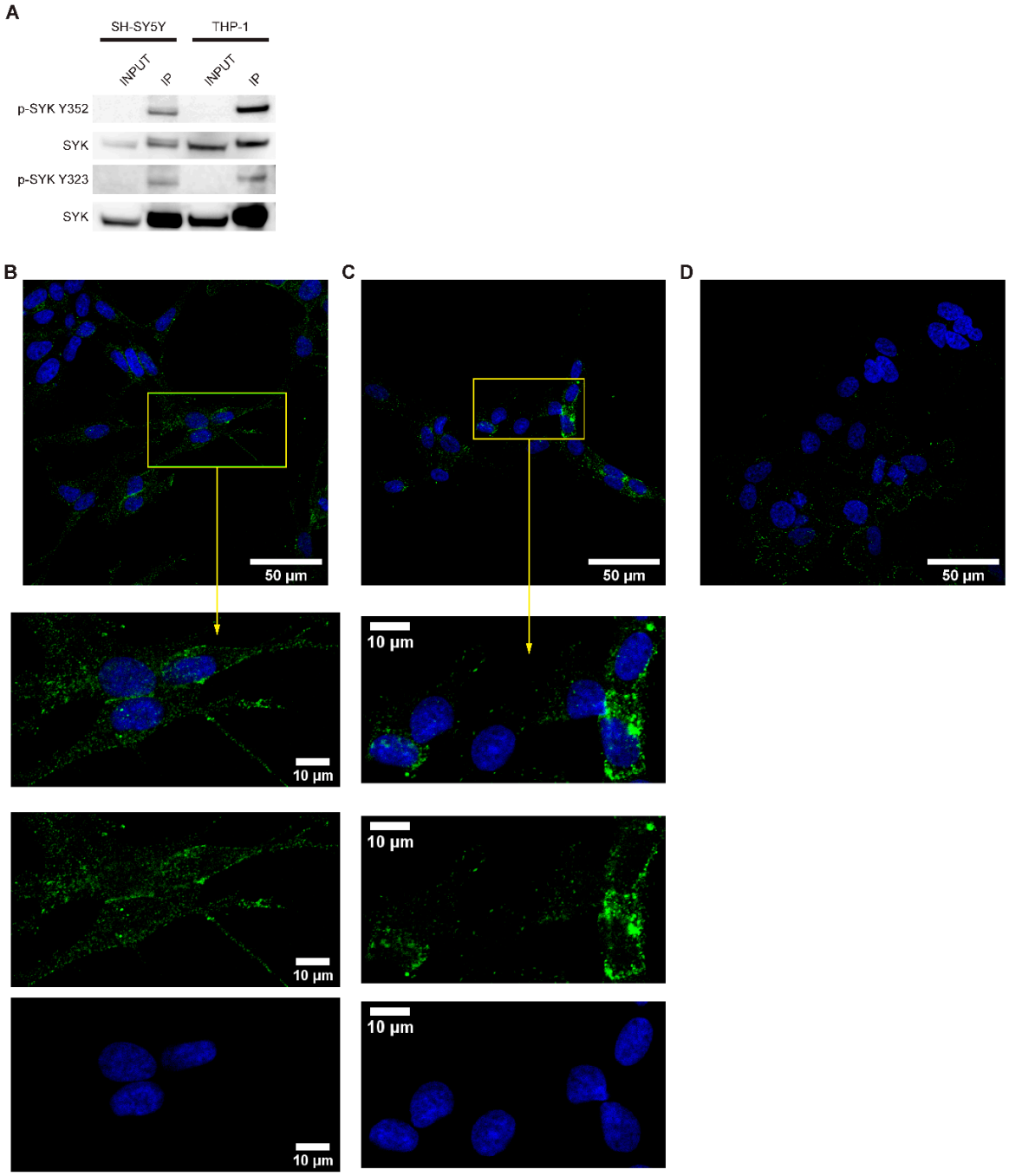

Figure 3. SYK is phosphorylated in neuroblastoma cell lines. (**A**) Immunoprecipitation with a SYK specific antibody was performed followed by western blot using antibodies against the SYK Tyr352 and Tyr323 phosphorylation residues. THP-1 cells were used as a positive control. Immunofluorescence labeling of p-SYK (Tyr525/526) in SH-SY5Y (**B**) and LAN-6 cells (**C**). SK-N-BE(2) cells (**D**) served as a negative control. The nuclei (blue) were stained with Hoechst 33342.

2.4. Downregulation of SYK Reduces the Cell Viability of SYK Expressing Neuroblastoma Cell Lines

Using siRNA, we assessed the consequences of SYK knockdown on the cell viability of SYK-positive SH-SY5Y and LAN-6 as well as SK-N-BE(2) cells that show no apparent SYK expression. In SH-SY5Y and LAN-6, but not SK-N-BE(2) cells, we observed a significant decrease in cell viability 72 h post-transfection with two different SYK targeting siRNAs compared to scramble control siRNA (scr.) (Figure 4A). The decreased cell viability corresponded to reduced SYK protein levels in SH-SY5Y

and LAN-6 cells (Figure 4B). Using densitometry, we calculated the downregulation of SYK protein. In SH-SY5Y cells the downregulation was approximately 5-fold with 18.1% (siRNA 1) and 21.3% (siRNA 2) of SYK protein remaining compared to the scrambled siRNA control (=100%). In LAN-6 cell the downregulation was less effective with 45.2% (siRNA 1) and 40.7% (siRNA 2) remaining SYK protein compared to the scrambled siRNA control.

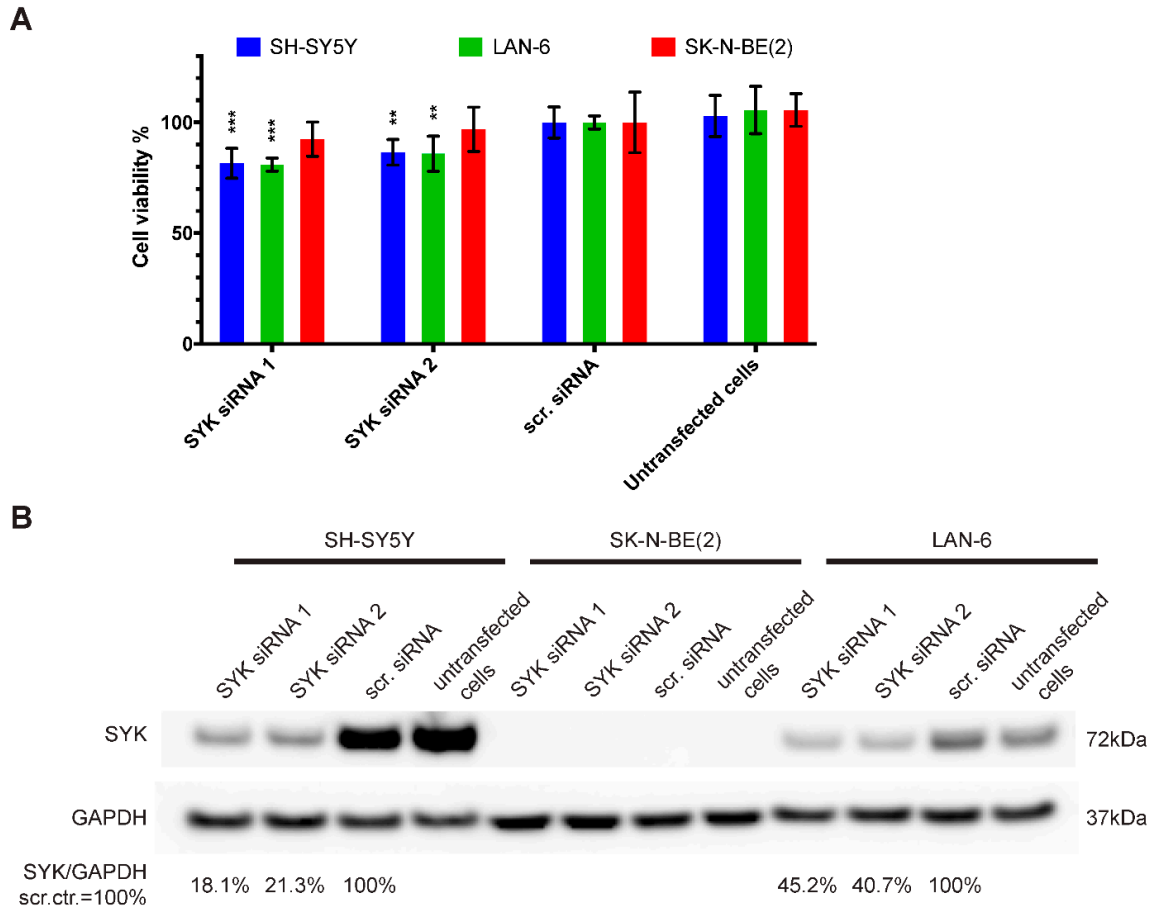

Figure 4. SYK downregulation reduces the cell viability of SYK expressing neuroblastoma cell lines. SYK-positive SH-SY5Y and LAN-6 cells, as well as SYK-negative SK-N-BE(2) cells, were transfected with 5 pmol SYK specific or scrambled (scr.) siRNA. The medium was replaced after 4 h. After 72 h, the cell viability was evaluated by MTT assay (**A**). The scr. control was set as 100% viable cells. Data are presented as mean ± SD from three independent experiments. Statistical comparisons were made using two-way ANOVA and a significant effect was observed for the siRNA treatment $p < 0.001$ and between cell lines $p = 0.003$. The Dunnett's multiple comparison test was used to evaluate the difference between scr. siRNA vs. SYK specific siRNA: ** $p < 0.01$, *** $p < 0.001$. (**B**) SYK expression levels were determined by western blot.

2.5. SYK Activity Inhibition Decreases the Cell Viability of Neuroblastoma Cells

Four commercially available, pharmacological SYK inhibitors were used to evaluate the effect of SYK catalytic inhibition on the cell viability of SYK-positive SH-SY5Y and SYK-negative SK-N-BE(2) cells. Figure 5 displays the cell viability (MTT assay) after 48 h incubation with the SYK inhibitors BAY 61-3606 (Figure 5A), R406 (Figure 5B), PRT062607 (=P505-15; Figure 5C) and GS-9973 (=entospletinib; Figure 5D). The results of 24 h incubation with these inhibitors are shown in Supplementary Figure S3 and comparable tendencies could be observed. A statistically significant difference (control vs. treatment) in the cell viability of SH-SY5Y and SK-N-BE(2) cells was observed upon exposure to multiple inhibitor concentrations (marked by asterisks in the graphs). SH-SY5Y cells expressing high

SYK levels were significantly more sensitive to the SYK inhibitors in comparison to SK-N-BE(2) cells expressing very low or no SYK (Figure 5). All four inhibitors significantly reduced the cell viability of both cell lines in a dose-dependent matter suggesting that at higher inhibitor concentrations the decrease in cell viability of SK-N-BE(2) is SYK-independent and caused by off-target effects.

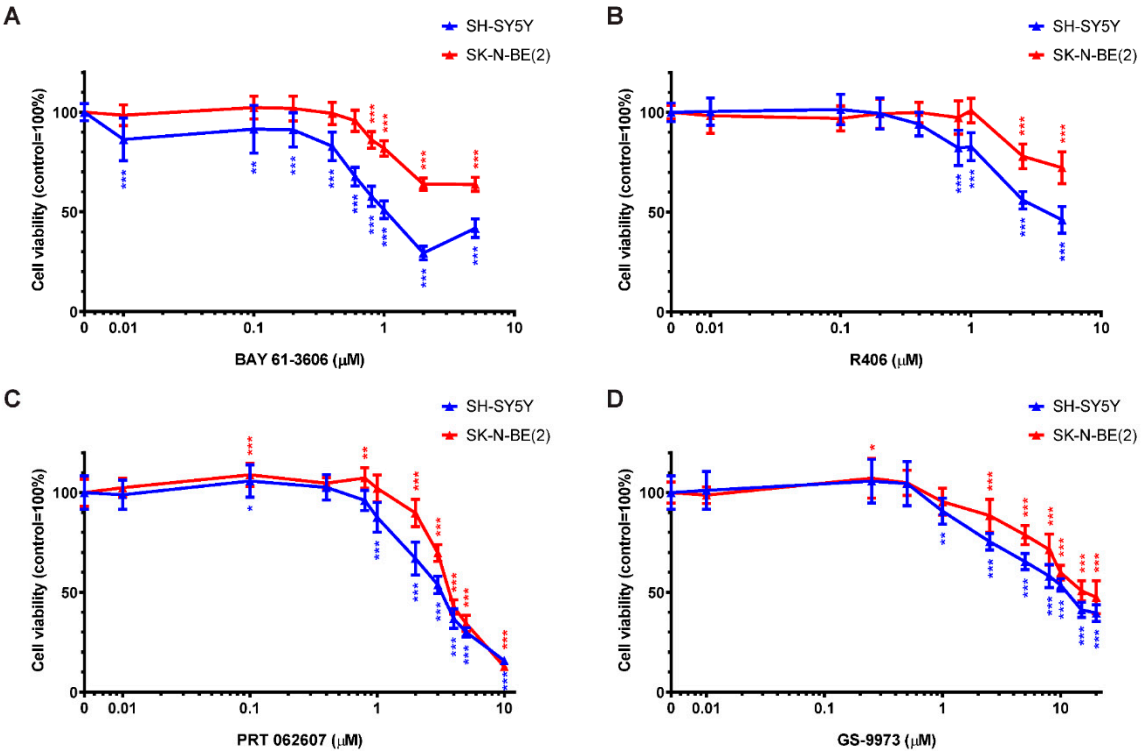

Figure 5. Inhibition of SYK decreases the cell viability of neuroblastoma cells. Cell viability was measured in SH-SY5Y and SK-N-BE(2) cells by MTT assay after 48 h incubation with increasing concentrations of the SYK inhibitors BAY 61-3606 (**A**) R406 (**B**) PRT062607 (**C**) GS-9973 (**D**). The control was set as 100% viable cells. Data are presented as mean ± SD from three independent experiments. Using two-way ANOVA, a significant difference between cell lines and a significant effect of the inhibitor $p < 0.001$ was seen. Dunnett's multiple comparison test was used to evaluate the difference between vehicle treated control cells and the various inhibitor concentrations: * $p < 0.05$ ** $p < 0.01$ *** $p < 0.001$.

Considering only inhibitor concentrations that impaired the cell viability of SH-SY5Y but not SK-N-BE(2) cells after 48 h of treatment, the concentration ranges were more narrow: 0.01–0.6 μM for BAY 61-3606, 0.8–1 μM for R406, and 1 μM for both PRT062607 and GS-9973. Because BAY 61-3606 displayed the most prominent differences between the two cell lines, it was used in subsequent experiments.

2.6. Inhibition of SYK Activity Reduces ERK1/2 and Akt Phosphorylation in Neuroblastoma Cells

Active SYK is known to affect various downstream targets including MAPK, PI3K/Akt and NFκB signaling pathways [4,8,36]. Hence, we evaluated the consequences of SYK inhibition on ERK1/2 and Akt phosphorylation under the same experimental conditions used for the cell viability studies. As compared to vehicle alone, a significant and lasting reduction of ERK1/2 phosphorylation (Figure 6A,B) and Akt phosphorylation (Figure 6A,C) was observed for three out of four inhibitors (BAY 61-3606, R406, and PRT062607) after 4 h and 24 h. In contrast, GS-9973 treatment did not affect ERK1/2 or Akt phosphorylation at the investigated time points.

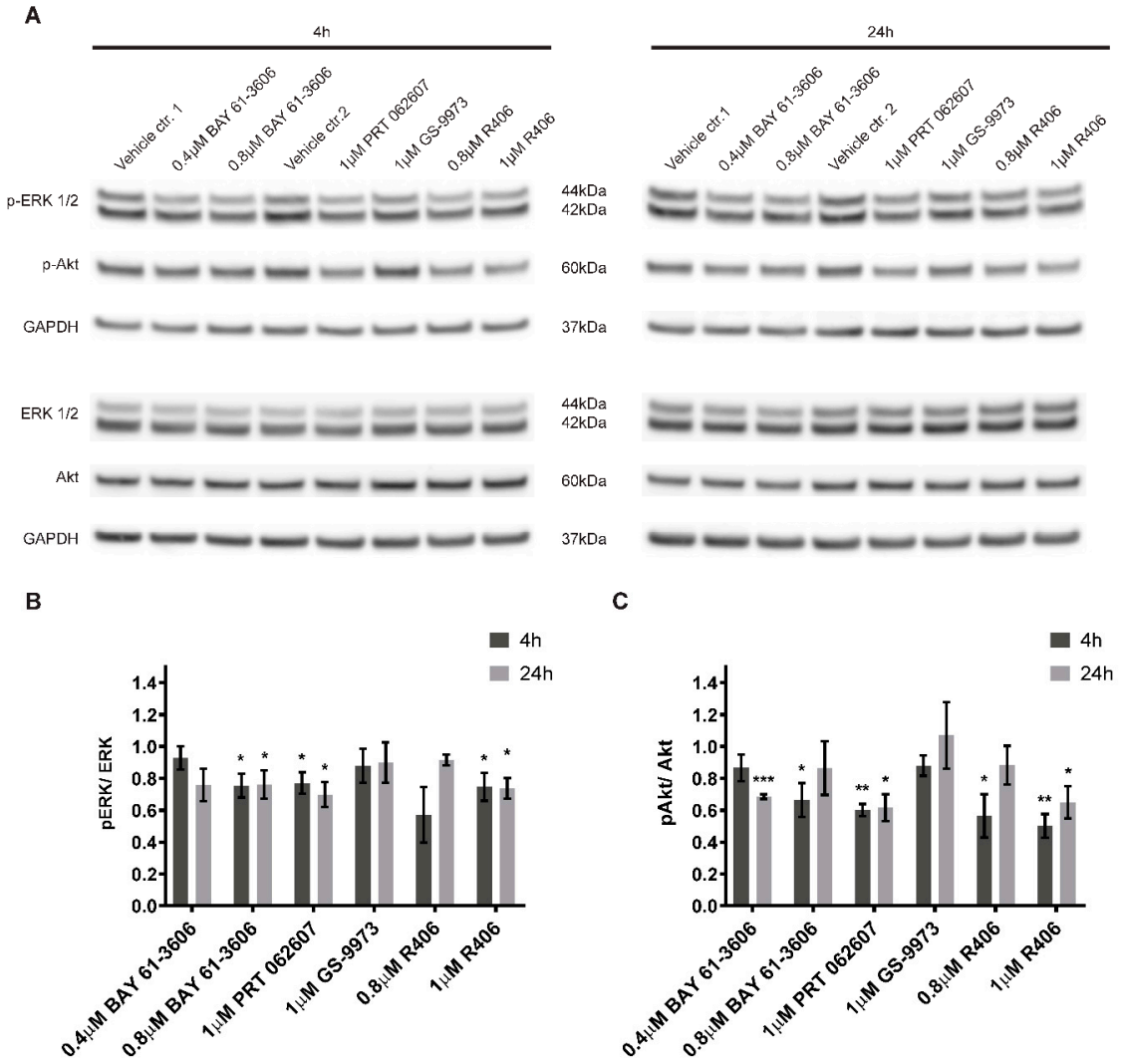

Figure 6. SYK inhibition decreases ERK1/2 and Akt phosphorylation. SYK inhibitors BAY 61-3606, R406, and PRT062607 reduce the phosphorylation of ERK1/2 and Akt in SH-SY5Y cells after a 4 or 24 h treatment (**A**). Control cells were treated with the corresponding vehicles (water = vehicle control 1 and DMSO = vehicle control 2). Densitometric analysis of the protein bands was performed. Phosphorylated and total protein were normalized to their respective GAPDH loading controls and the ratios between normalized p-ERK1/2 and ERK as well as normalized p-Akt and Akt were calculated. The values are displayed as mean ± SD relative to the vehicle control = 1 (**B** and **C**). The results are based on three independent experiments. One sample t-test (two-tailed) was performed to compare the vehicle (theoretical mean = 1) vs. inhibitor treatment: * $p < 0.05$ ** $p < 0.01$ *** $p < 0.001$.

2.7. The Selective SYK Inhibitor BAY 61-3606 Enhances the Effect of Chemotherapeutic Drugs on Neuroblastoma Cells

To determine whether SYK inhibition could increase the efficacy of chemotherapeutic agents to inhibit neuroblastoma cell growth, we combined BAY 61-3606 with the drugs paclitaxel, cisplatin, doxorubicin, and temozolomide, respectively. We investigated the effect of single vs. combined treatment on PARP cleavage (indicating apoptosis) and cell viability (MTT assay) in SYK-positive SH-SY5Y and SYK-negative SK-N-BE(2) cells (Figure 7A and Table 2). After 24 h, we observed an increase in cleaved PARP in SH-SY5Y cells for the combination of 0.4 μM BAY 61-3606 with paclitaxel, cisplatin, and temozolomide compared to single drug treatment (Figure 7A). For the combination of 0.4 μM BAY 61-3606 with paclitaxel or cisplatin this effect was sustained after 48 h (Supplementary Figure S4A).

Of note, after 24 h incubation with BAY 61-3606, paclitaxel or the combination temozolomide-BAY 61-3606 increased SYK protein levels could be observed (Figure 7A). This effect was not sustained after 48 h (Supplementary Figure S4A). However, after 48 h a clear reduction in SYK protein levels could be detected in cells treated with a combination of BAY 61-3606 and chemotherapeutic drugs compared to treatment with drugs alone (Supplementary Figure S4A).

After 48 and 72 h incubation, a significant decrease in cell viability was evident for all drugs in combination with BAY 61-3606 in SH-SY5Y cells as compared to the chemotherapeutic drugs alone (Table 2).

In SK-N-BE(2) cells the apparent increase in cleaved PARP after combined treatment with BAY 61-3606 and paclitaxel was accompanied by a decrease in cell viability after 48 h and 72 h (Table 2). Comparing the combinations to treatment with BAY 61-3606 alone, a significant difference was observed for paclitaxel and cisplatin but not doxorubicin and temozolomide after 48 h and 72 h in SH-SY5Y cells, indicating that monotherapy with 0.4 µM BAY 61-3606 is comparable to a combination of temozolomide or doxorubicin and BAY 61-3606.

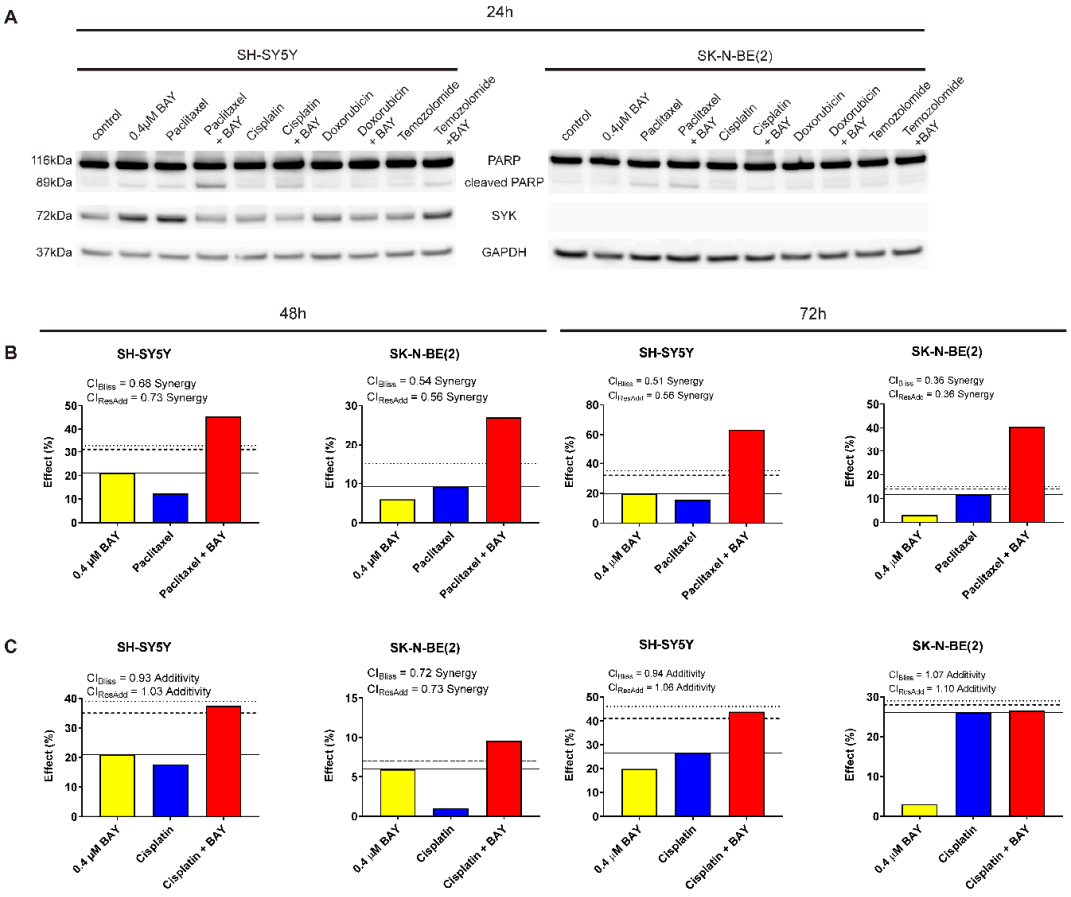

Figure 7. The selective SYK inhibitor BAY 61-3606 enhances the effect of chemotherapeutic drugs in neuroblastoma cells. (**A**) PARP cleavage and SYK expression were determined by western blot after 24 h monotherapy or combinations of 0.4 µM BAY 61-3606, 20 nM paclitaxel, 5 nM doxorubicin, 100 µM temozolomide and cisplatin (1 µM or 3 µM for SH-SY5Y and SK-N-BE(2), respectively). Illustration of drug combination effects for 0.4 µM BAY 61-3606 and paclitaxel (**B**) as well as 0.4 µM BAY 61-3606 and cisplatin (**C**) in SH-SY5Y and SK-N-BE(2) cells after 48 h and 72 h treatment. The continuous horizontal line indicates the effect of the highest single agent, the dashed line denotes expected additive effect calculated by the Bliss independence model, and the dotted line shows expected additive effect calculated by response additivity. Combination index (CI), given from the Bliss independence model and the response additivity, and effect are specified for each combination.

Table 2. Cell viability of SH-SY5Y and SK-N-BE(2) after treatment with 0.4 μM BAY 61-3606, chemotherapeutic drugs or combinations of both.

		SH-SY5Y			SK-N-BE(2)		
	Treatment	**Cell viability (%) Mean ± SD**	***p* value Drug vs. combination**	***p* value BAY vs. combination**	**Cell viability (%) Mean ± SD**	***p* value Drug vs. combination**	***p* value BAY vs. combination**
48 h	0.4 μM BAY	79.01 ± 6.26			94.04 ± 7.72		
	Paclitaxel	87.71 ± 7.83			90.89 ± 7.86		
	Paclitaxel + BAY	54.65 ± 3.26	**<0.001**	**<0.001**	72.98 ± 9.33	**<0.001**	**<0.001**
	Cisplatin	82.33 ± 9.01			98.94 ± 6.48		
	Cisplatin + BAY	62.47 ± 5.82	**<0.001**	**<0.001**	90.49 ± 7.46	0.052	>0.999
	Doxorubicin	100.5 ± 9.59			102 ± 9.68		
	Doxorubicin + BAY	77.97 ± 8.01	**<0.001**	>0.999	93.69 ± 8.78	0.121	>0.999
	Temozolomide	107 ± 11.17			107.7 ± 3.65		
	Temozolomide + BAY	76.81 ± 4.82	**<0.001**	>0.999	100 ± 4.36	0.132	0.181
72 h	0.4 μM BAY	80.20 ± 7.62			96.97 ± 6.89		
	Paclitaxel	84.53 ± 4.60			88.29 ± 5.19		
	Paclitaxel + BAY	36.79 ± 3.14	**<0.001**	**<0.001**	59.48 ± 8.81	**<0.001**	**<0.001**
	Cisplatin	73.38 ± 5.89			73.99 ± 2.95		
	Cisplatin + BAY	56.25 ± 5.72	**<0.001**	**<0.001**	73.53 ± 5.94	>0.999	**<0.001**
	Doxorubicin	102.2 ± 8.37			101.3 ± 7.56		
	Doxorubicin + BAY	78.57 ± 7.16	**<0.001**	>0.999	93.99 ± 9.68	0.053	>0.999
	Temozolomide	107.7 ± 6.13			102.7 ± 4.28		
	Temozolomide + BAY	74.21 ± 5.99	**<0.001**	0.217	99.74 ± 6.68	>0.999	>0.999

Cell viability was measured by MTT assay after 48 and 72 h. The control was set as 100% viable cells. Data are presented as mean ± SD from at least three independent experiments. Using two-way ANOVA, a significant effect was observed for both treatment and between cell lines $p < 0.001$; Bonferroni's multiple comparison test was used to evaluate differences between treatments, and p values < 0.05 were considered as statistically significant.

Using Bliss independence and response additivity calculations, we determined whether the chemotherapeutic drug-BAY 61-3606 combination was synergistic, additive or antagonistic in regard to cell viability. The combinations of BAY 61-3606 and doxorubicin or temozolomide could not be analyzed with these methods due to the limited effects of these drugs as single agents at concentrations used in this study. A synergistic effect was determined for paclitaxel in combination with BAY 61-3606 in both SH-SY5Y and SK-N-BE(2) cells after 48 and 72 h (Figure 7B). Additionally, cisplatin in combination with BAY 61-3606 displayed a mainly additive effect in SH-SY5Y and SK-N-BE(2) cells after 48 and 72 h (Figure 7C).

A 24 h treatment with a higher BAY 61-3606 concentration (0.8 μM) in combination with any of the drugs resulted in a more pronounced increase in cleaved PARP in SH-SY5Y cells but not in the SYK-negative SK-N-BE(2) cells (Supplementary Figure S5A) after 24 h. However, after 48 h higher levels of PARP were observed in the combinations compared to treatment with chemotherapeutic drugs alone for the majority of drugs in SH-SY5Y and to a lesser extent in SK-N-BE(2) cells (Supplementary Figure S4B). Furthermore, a significant decrease in cell viability was observed for both cell lines comparing chemotherapeutic drug vs. combination with BAY 61-3606 after 48 and 72 h (Supplementary Table S2). However, when comparing the combinations to treatment with BAY 61-3606 alone, a significant difference in cell viability occurred for combinations of BAY 61-3606 with paclitaxel, cisplatin and temozolomide in SH-SY5Y cells after 48 h, and paclitaxel as well as cisplatin after 72 h. In SYK-negative SK-N-BE(2) cells combination of paclitaxel, cisplatin or doxorubicin and BAY 61-3606 after 72 h and paclitaxel as well as cisplatin after 48 h demonstrated a significant difference compared to monotherapy with BAY 61-3606.

A synergistic effect was determined for paclitaxel in combination with 0.8 μM BAY 61-3606 in both SH-SY5Y and SK-N-BE(2) cells after 48 and 72 h (Supplementary Figure S5B). Additionally, cisplatin in combination with 0.8 μM BAY 61-3606 displayed a less consistent effect, the combinational effects were mainly additive in SH-SY5Y and SK-N-BE(2) cells after 48 and 72 h (Supplementary Figure S5C) but some of the combinations were classified as synergistic or antagonistic using Bliss independence and response additivity calculations.

2.8. Transfection with an Active SYK Variant Increases the Cell Viability of Neuroblastoma Cells Independent of Endogenous SYK Levels

To further explore the effect of SYK on neuroblastoma cell viability, we transfected SH-SY5Y, SK-N-BE(2), and SK-N-AS cells with expression vectors encoding different FLAG-tagged SYK variants (SYK wt = SYK wild type, SYK B = short SYK splice variant B, SYK Y130E = constitutive active SYK, SYK K402R = kinase dead SYK, SYK RR42/195KK = SYK with inactive SH2 domains). After 48 h, we measured the cell viability and confirmed transfection efficiency by evaluating exogenous SYK expression levels using western blot (Figure 8). SYK overexpression that exceeded the endogenous SYK levels was evident. Constitutive active SYK Y130E increased cell viability of all three neuroblastoma cell lines in comparison to transfection with the empty vector independent of the presence/absence of endogenous SYK (Figure 8A). Transfection with SYK wt significantly increased the cell viability of SK-N-AS cells and SYK RR42/195KK increased the cell viability of SH-SY5Y cells. A minor, reproducible reduction in cell viability after transfection with the kinase dead SYK mutant was observed in SH-SY5Y and SK-N-BE(2) cells, which was however not statistically significant.

Following transfection, all SYK variants were detected in the three cell lines by western blot although SYK RR42/195K was expressed at somewhat lower levels (Figure 8B).

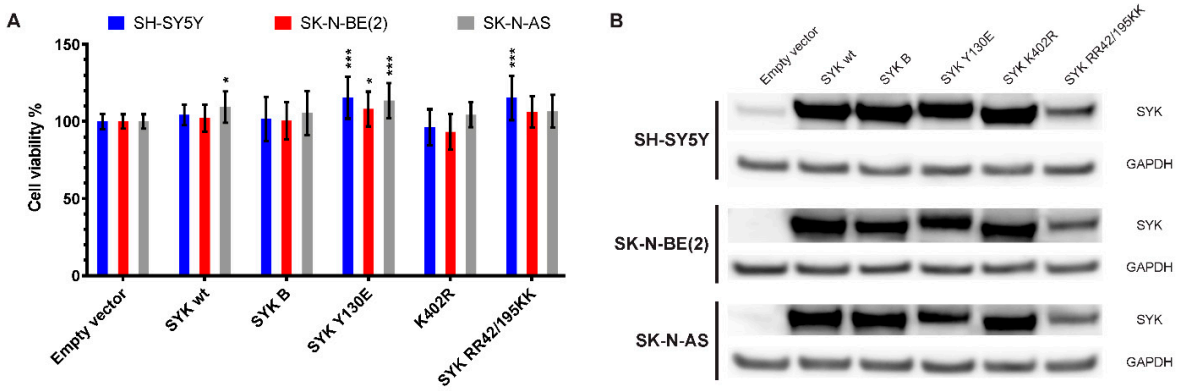

Figure 8. Transfection with an active SYK variant increases the cell viability of neuroblastoma cells independent of endogenous SYK levels. Cells were transfected with expression plasmids encoding different SYK variants and the cell viability was measured after 48 h by MTT assay (**A**). The empty vector control was set as 100% viable cells. Data are presented as mean ± SD from six independent experiments. Statistical comparisons were made using two-way ANOVA and a difference was observed between the SYK variants and between cell lines $p < 0.001$. The Dunnett's multiple comparison test was used to evaluate the difference between empty vector and different SYK variants: * $p < 0.05$, *** $p < 0.001$. Western blot analysis was used to evaluate the presence of SYK following transfection, ensuring sufficient transfection efficiency (**B**). SYK wt = SYK wild type, SYK B = short SYK splice variant B, SYK Y130E = constitutive active SYK, SYK K402R = kinase dead SYK, SYK RR42/195KK = SYK with inactive SH2 domains.

3. Discussion

There is a need for further advancements in the treatment of neuroblastoma to improve the survival of high-risk patients and reduce acute and long-term toxic effects in neuroblastoma survivors. Targeted therapies exhibit great potential used either alone or more particularly in combination with conventional drugs [41,44].

In two other pediatric cancers, retinoblastoma and Ewing sarcoma, SYK promotes tumor cell survival and SYK inhibition, using small molecule inhibitors, was identified as a promising treatment option for these diseases [35,36].

In the present study, we observed that *SYK* expression was higher in four different neuroblastoma cohorts compared to neural crest cells and benign neurofibroma. Moreover, we demonstrate that SYK is present in neuroblastoma tissues and to a lesser extent in neuroblastoma cell lines. Inhibition of SYK using small molecule inhibitors alone or in combination with chemotherapeutic drugs as well as knockdown of SYK by siRNA impaired the cell viability of SYK expressing neuroblastoma cells. Additionally, SYK inhibition decreased phosphorylation of Akt and ERK1/2 indicating Akt and MAPK signaling as potential downstream targets of SYK in neuroblastoma. Furthermore, constitutive active SYK increased neuroblastoma cell viability independent of endogenous SYK expression. Taken together, our findings indicate a tumorigenic involvement of SYK in neuroblastoma.

We observed the presence of SYK protein in the majority of neuroblastoma tissues analyzed in this study. A positive staining of SYK and p-SYK was observed in both the cytoplasm and the nucleus with a more pronounced nuclear staining for p-SYK. The presence of SYK in different cellular compartments (cytoplasm, nucleus, membrane) has previously been described [37,45,46].

Furthermore, we compared the presence of SYK protein in *MYCN*-amplified and non-*MYCN*-amplified tumor tissue and did not observe differences between the two groups. Of note, by examining publicly available gene expression datasets, we detected a negative correlation between *MYCN* and *SYK* in neuroblastoma. In contrast, a positive correlation between *SYK* and *MYC* was discerned. *MYCN*-amplification occurs in about 20% of neuroblastomas and is associated with aggressive tumors and poor survival [47–49]. Furthermore, *MYC* has also been identified as an independent prognostic marker for poor survival in neuroblastoma [50] and is predominantly

expressed by non-*MYCN*-amplified tumors [51]. A link between SYK and MYC has been previously demonstrated in Ewing sarcoma and hematopoietic cells [36,52]. Therefore, a potential connection between SYK and MYC in neuroblastoma is highly interesting and warrants further investigation.

In contrast to neuroblastoma tumor tissue, SYK protein was only detected in two out of ten neuroblastoma cell lines by western blot. This is in accordance with previous findings by Alaminos et al. reporting more frequent methylation of the *SYK* promoter in neuroblastoma cell lines (60%) compared to tumor tissue (11%) [53]. In subsequent work by Margetts et al. and Grau et al. no aberrant hypermethylation of the *SYK* promoter was observed in tumor tissue or highly infiltrated bone marrow [54–56]. Yu et al. recently demonstrated that EGF stimulates SYK-mediated migration and invasion in ovarian cancer cells. The authors suggested that SYK function might be regulated by environmental stimuli [11]. Therefore, one could speculate that the absence of a specific stimulus, which is present in the tumor microenvironment, could lead to the downregulation of *SYK* expression in neuroblastoma cells lines. However, additional studies are necessary to determine if known factors, such as specific cytokines and chemokines, present in the neuroblastoma tumor microenvironment may affect SYK expression and function.

Complex phosphorylation events on tyrosine residues are required for the regulation of SYK functions by mediating conformational changes and creating docking stations for other proteins [8,57,58]. Phosphorylation of Tyr352 and/or Tyr348 (Tyr346 and Tyr342 in mouse SYK) provides binding sites for various proteins such as phospholipase Cγ, Vav-1 and 2 as well as Akt, and ERK, linking SYK to different signaling pathways and cellular functions [8,59–62]. Furthermore, Tyr352 has been linked to constitutive SYK activation [63]. The Tyr525/526 residues are located in the SYK activation loop. These phosphorylation sites likely provide important docking sites for other proteins thereby mediating intracellular signaling. However, mutations in these sites affect the in vitro catalytic activity only marginally [8,64,65]. Phosphorylation of Tyr323 in SYK promotes binding of Cbl protein family members causing ubiquitination and possibly degradation of SYK. However, Tyr323 is also an important binding site for PI3K indicating multiple functions of this phosphorylation site (reviewed in [8]).

We determined the status of these three well-established SYK phosphorylation sites (Tyr352, Tyr525/526, and Tyr323) and found that all were phosphorylated under normal growth conditions in the SYK expressing SH-SY5Y neuroblastoma cells, suggesting the presence of catalytically active SYK.

We observed a weaker nuclear staining of both total SYK and p-SYK in neuroblastoma cell lines as compared to neuroblastoma tissue. It has previously been demonstrated that SYK splice variants display differences in cellular localization and function [37,66,67] and that EGF can modulate SYK splicing pattern [66]. These findings indicate that the cellular localization of SYK may be affected by environmental stimuli and changes in splicing pattern. Therefore, the presence of specific stimuli in the neuroblastoma tumor microenvironment as well potential differences/changes in SYK splicing pattern compared to neuroblastoma cell lines may contribute to the observed differences in staining pattern. In our study, we observed that siRNA-mediated SYK downregulation reduced neuroblastoma cell growth. However, we did not achieve a complete SYK knockdown. Since SYK is a protein kinase, residual SYK protein could provide an explanation for the significant, but modest effect on the cell viability.

Therefore, we investigated the effects of commercially available SYK inhibitors BAY 61-3606 [68], R406 [69], PRT062607 (P505-15) [70] and GS-9973 [71] on neuroblastoma survival. Using increasing inhibitor concentrations, we compared the effect on cell viability in neuroblastoma cells with and without detectable SYK protein levels (SH-SY5Y and SK-N-BE(2), respectively). We determined at least one concentration for each inhibitor at which a significant reduction in cell viability was observed in SH-SY5Y but not SK-N-BE(2) cells, indicating an effect on cell viability that can likely be attributed to specific SYK inhibition.

PRT062607 and GS-9973 significantly reduced the viability of SH-SY5Y but not SK-N-BE(2) cells at a concentration of 1 μM. This is in line with recent work by Sun et al. where 1 μM PRT062607 and GS-9973 significantly impaired clonogenicity and cell viability of Ewing sarcoma

cell lines [36]. A dose-dependent impairment of cell viability as well as increased caspase-3 activity has been previously reported in retinoblastoma cells after treatment with BAY 61-3606 and R406 [35]. We observed that these inhibitors significantly decreased SH-SY5Y cell viability as compared to SK-N-BE(2) cells at concentrations of 0.1–0.6 μM and 0.8–1 μM, respectively.

Of note, inhibitor concentrations >1 μM also significantly reduced the cell viability of SK-N-BE(2) cells that exhibit no apparent SYK expression suggesting off-target effects for all four inhibitors when used at higher concentrations. Kinase inhibitors commonly display off-target effects that can be beneficial but need to be carefully evaluated at the mechanistic level. For example, the SYK inhibitor BAY 61-3606 has been reported to inhibit JNK [72]. JNK inhibition has previously been demonstrated to reduce the apoptotic effect of chemotherapeutic drugs such as doxorubicin in SH-SY5Y cells [73]. Therefore, off-target effects of BAY 61-3606 on JNK could potentially impair doxorubicin function and not display a potentiating effect as seen in our studies. Furthermore, work by Colado et al. demonstrated that GS-9973 and R406 can impair T-cell function via off-target effects on the SYK homolog ZAP-70 [74]. We screened the neuroblastoma cell lines used in this study for ZAP-70 presence and found it expressed at protein level only in SK-N-DZ cells (Supplementary Figure S6). Since this cell line was not used in the inhibitor studies, potential off-target effects on ZAP-70 can be excluded. However, these are just two of many potential proteins that may be the target of non-selective inhibition.

Various downstream targets for SYK have been described in health and disease [4,8]. ERK- and Akt-mediated signaling is known to be affected by SYK inhibition in CLL and Ewing sarcoma [20,36]. We observed that Akt and ERK1/2 phosphorylation was decreased by the SYK inhibitors BAY 61-3606, R406 and PRT062607, but not GS-9973. A possible explanation could be differences in the kinetics of GS-9973 mediated SYK inhibition. Since we only examined two time points, (4 h and 24 h) rapid and transient effects might not have been detected. PI3K/Akt- and MAPK-mediated signaling was previously shown to promote neuroblastoma tumorigenesis [75–79]. Therefore, a decrease in Akt and ERK1/2 phosphorylation and activity could contribute to the impaired cell viability.

Yu et al. demonstrated an increased expression of SYK in paclitaxel-resistant ovarian cancer cells and that paclitaxel in combination with the SYK inhibitor R406 increased apoptosis in vitro and impaired tumor growth in vivo [33]. Paclitaxel is a chemotherapeutic drug that is rarely used for the treatment of neuroblastoma. It was, however, included in this study to determine if the additive effect seen in ovarian cancer cells [33] could also be observed in neuroblastoma cell lines. We furthermore analyzed the effect of three drugs used in first-line treatment and/or refractory and relapsed neuroblastoma: cisplatin, doxorubicin, and temozolomide.

We compared the cell viability of neuroblastoma cells treated with cytostatic drugs alone or in combination with the pharmacological SYK inhibitor BAY 61-3606. Synergetic and additive effects were observed in SYK expressing SH-SY5Y cells for paclitaxel- BAY 61-3606 and cisplatin-BAY 61-3606 combination, respectively. Furthermore, 0.4 μM BAY 61-3606 potentiated the effects of doxorubicin and temozolomide in SH-SY5Y cells. Interestingly, a synergetic effect of BAY 61-3606 in combination with paclitaxel was also observed in SK-N-BE(2), a cell line without significant expression of SYK protein. Although BAY 61-3606 concentrations applied in this study are rather low, off-target effects are likely the cause for the observed effect.

Furthermore, we observed increased amounts of cleaved PARP in the SYK-positive SH-SY5Y cells after treatment with BAY 61-3606 (0.4 and 0.8 μM) in combination with the tested drugs after 24 h, particularly when 0.8 μM BAY 61-3606 was used. We propose that the decrease in cell viability in SH-SY5Y cells may be attributed to an increase in apoptosis, whereas the decrease in cell viability in SYK-negative SK-N-BE(2) cells might rather be due to reduced proliferation than increased apoptosis. However, further experiments are required to determine the detailed mechanisms.

In addition, we also demonstrate that transient transfection with a constitutively active SYK variant increased the cell viability of neuroblastoma cell lines independent of endogenous SYK expression. This suggests that SYK has tumor-promoting functions in neuroblastoma. Previous work reported a tumor-suppressing role for SYK in breast cancer, among others. Transfection of breast cancer

cells with a wild-type SYK encoding vector suppressed invasive outgrowth in Matrigel and impaired tumor growth and metastasis in mice [26]. We did, however, not observe any inhibitory effect on the cell viability of transfected neuroblastoma cell lines expressing exogenous SYK. Taken together, this suggests that SYK functions as a tumor-promoting molecule in neuroblastoma rather than having a tumor-suppressing effect.

To further evaluate the potential therapeutic use of SYK inhibitors in neuroblastoma both as a single agent and in combination with existing chemotherapeutic drugs, in vivo studies are necessary. Since SYK is widely expressed by hematopoietic cells, potential negative effects on the immune cells of the tumor microenvironment have to be carefully evaluated using immunocompetent neuroblastoma animal models. Recent work in glioma demonstrated that SYK inhibition impaired the mobility and infiltration of B cells and CD11b+ leukocytes in addition to reducing proliferation and migration of tumor cells [34].

4. Materials and Methods

4.1. Microarray Gene Expression

Gene expression analysis was performed using the MegaSampler feature of the publicly available R2: Genomics Analysis and Visualization Platform (http://r2.amc.nl).

4.2. Reagents and Antibodies

The selective SYK inhibitors GS-9973 (Entospletinib) and R406 were purchased from Selleck Chemicals Europe (Munich, Germany). BAY 61-3606 and PRT062607 were obtained from Calbiochem/Merck (Merck Life Science AS, Oslo, Norway) and ApexBio (Houston, TX, USA), respectively. Paclitaxel, cisplatin, doxorubicin, and temozolomide were bought from Sigma-Aldrich Norway AS (Oslo, Norway). The antibodies used in this study are listed in Table 3.

Table 3. Antibodies.

Antibody	Application	Source
Anti-SYK	WB, IP	#1240, Santa Cruz Biotechnology
Anti-SYK	WB	#13198, Cell Signaling Technology
Anti-SYK	ICC/IHC	#HPA001384, Sigma
Anti-Phospho-ZAP-70 (Tyr319)/SYK (Tyr352)	WB	#2701, Cell Signaling Technology
Anti-Phospho-SYK (Tyr323)	WB	#2715, Cell Signaling Technology
Anti-Phospho-SYK (Tyr525/526)	ICC	#2710, Cell Signaling Technology
Anti-Phospho-SYK (pTyr525)	IHC	#SAB4503839, Sigma
Anti-PARP	WB	#9542, Cell Signaling Technology
Anti-Phospho-p44/42 MAPK (Erk1/2) (Thr202/Tyr204)	WB	#4370, Cell Signaling Technology
Anti-p44/42 MAPK (Erk1/2)	WB	#4695, Cell Signaling Technology
Anti-Phospho-Akt (Ser473) (D9E)	WB	#4060, Cell Signaling Technology
Anti-Akt	WB	#9272, Cell Signaling Technology
Anti-GAPDH	WB	#47724, Santa Cruz Biotechnology
Goat Anti-Rabbit IgG H&L (HRP)	WB	#6721, Abcam
Rabbit Anti-Mouse IgG H&L (HRP)	WB	#97046, Abcam
Goat anti-Rabbit IgG (H+L), Alexa Fluor 488	ICC	# A-11008, Thermo Fisher Scientific

4.3. Human Tissue Samples and Cell Lines

Human tissue samples were obtained, with informed consent (written or verbal) provided by the parents or guardians for the use of tumor samples in research, in accordance with the ethical approval from the Stockholm Regional Ethical Review Board and the Karolinska University Hospital Research Ethics Committee (approval ID 2009/1369-31/1 and 03-736). Neuroblastoma tumor tissue was collected at the Karolinska University Hospital, snap-frozen in liquid nitrogen and stored at −80 °C until further use.

The human cell lines SK-N-AS, SK-N-SH, SK-N-DZ, SK-N-FI, SH-EP1, Kelly, SH-SY5Y, and IMR-32 as well as THP-1, Jurkat E6.1, and U937 cells were obtained from the ATCC (American Type Culture Collection, LGC Standards GmbH, Wesel, Germany). SK-N-BE(2) cells were purchased from DSMZ (Deutsche Sammlung von Mikroorganismen und Zellkulturen, Braunschweig, Germany). The cell lines were cultivated in RPMI-1640 medium containing L-glutamine and sodium bicarbonate (Sigma-Aldrich Norway AS, Oslo, Norway) supplemented with 10% heat-inactivated fetal bovine serum (FBS; Thermo Fisher Scientific Inc., Waltham, MA, USA). LAN-6 cells were a kind gift from Deborah Tweddle, Newcastle University and were grown in Iscove's Modified Dulbecco's Medium (Sigma-Aldrich Norway AS, Oslo, Norway) supplemented with GlutaMAX™ and 10% heat-inactivated FBS. All cell lines were cultivated at 37 °C in humidified air with 5% CO_2 and mycoplasma tests were performed regularly using the MycoAlert™ PLUS Mycoplasma Detection Kit (Lonza, Basel, Switzerland). The identity of the human neuroblastoma cell lines was confirmed by STR-profiling performed at the Centre of Forensic Genetics, University of Tromsø, Norway.

4.4. Immunohistochemistry (IHC)

Formalin-fixed, paraffin-embedded tissue sections were deparaffinized using xylene (VWR International, Oslo, Norway) and a series of graded alcohols (Sigma-Aldrich Norway AS, Oslo, Norway) followed by rehydration and washing in phosphate buffered saline (PBS, Biochrom GmbH, Berlin, Germany). Antigen retrieval was performed in sodium citrate buffer (pH 6) in a microwave oven. After blocking of endogenous peroxidase with 0.3% H_2O_2 for 15 min, unspecific antibody binding sites were blocked with 5% BSA in PBS (AppliChem, Darmstadt, Germany) for 45 min. The sections were incubated with the primary antibody overnight at 4 °C. The following day sections were thoroughly washed in PBS and incubated with SignalStain®Boost IHC Detection Reagent, HRP, Rabbit (Cell Signaling Technology, Leiden, Netherlands) and kept for 1 h at room temperature. Following washes in PBS, the sections were incubated with Liquid DAB+ Substrate solution (Dako, Agilent Technologies, Inc., Santa Clara, CA, USA). A matched isotype control was used as a control for nonspecific staining. The sections were examined with a BX43 microscope (Olympus, Tokyo, Japan) and images were acquired with an Olympus DP26 camera.

4.5. RNA Isolation and RT-PCR

Total RNA was isolated using the NucleoSpin®TriPrep Kit (MACHEREY-NAGEL GmbH & Co. KG, Düren, Germany) and RNA quantity and quality was determined with a NanoDrop™ 2000 spectrometer (Thermo Fisher Scientific Inc.). One µg RNA was used as input for cDNA synthesis with the iScript™ cDNA Synthesis Kit (Bio-Rad Laboratories AB, Oslo, Norway).

PCR was set up as a 25 µl reaction mix containing 2 µL cDNA, 12.5 µL AccuStart™ II GelTrack PCR SuperMix (Quanta Biosciences, Gaithersburg, MD, USA), 400 nM of each primer (Sigma-Aldrich Norway AS, Oslo, Norway) and 10.1 µL of ultra-pure H_2O (Biochrom GmbH, Berlin, Germany). The PCR run was performed in a T100™ Thermal Cycler (Bio-Rad Laboratories AB) as follows: 2 min at 94 °C and 35 cycles of 94 °C for 20 s, 61 °C for 30 s and 72 °C for 90 s. The following intron spanning primer sets were used: APRT (housekeeping) 5′ CCCGAGGCTTCCTCTTTGGC 3′ (sense) and 5′ CTCCCTGCCCTTAAGCGAGG-3′ (antisense) [80], SYK 5′ CATGTCAAGGATAAGAACATCAT AGA 3′ (sense) and 5′ AGTTCACCACGTCATAGTAGTAATT 3′ (antisense) [26], SYK L/S 5′ TTTTGGAGGCCGTCCACAAC '3 (sense) and 5′ ATGGGTAGGGCTTCTCTCTG 3′ (antisense) [37].

All primer sets used in this study were intron-spanning to avoid false positive signals caused by amplification of residual traces of genomic DNA. PCR products were analyzed by gel electrophoresis. The 2% SeaKem®LE Agarose gel (Lonza) was stained with GelRed™ (Biotium, Inc., Hayward, CA, USA) and visualized under UV light in the BioDoc-It™ Imaging System (UVP, LLC, Upland, CA, USA).

4.6. Immunocytochemistry (ICC) and Western Blot

Cells were grown in 8-well µ-Slide dishes (iBidi GmbH, Munich, Germany) until they reached approximately 70% confluence. Following a brief rinse with PBS the cells were fixed with 4% formaldehyde (Alfa Aesar, VWR International, Oslo, Norway) for 20 min. After three washes with PBS, unspecific binding sites were blocked with 5% goat serum (Sigma-Aldrich Norway AS) in PBS containing 0.3% Triton-X-100 (Sigma-Aldrich Norway AS) for 1 h. The cells were incubated with primary antibodies diluted in 1% bovine serum albumin (BSA; AppliChem, Darmstadt, Germany) in PBS containing 0.3% Triton-X-100 overnight at 4 °C. After three washes with PBS, the cells were incubated with the secondary antibodies diluted in 1% bovine serum albumin in PBS containing 0.3% Triton-X-100 for 1 h at room temperature, protected from light. Following three washes with PBS, the nuclei were stained with Hoechst 33342 (ImmunoChemistry Technologies, LLC, Bloomington, IN, USA) for 10 min. The cells were washed 3x with PBS and covered with Mounting Medium for fluorescence microscopy (iBidi GmbH). Subsequently, the cells were examined using a Zeiss LSM780 confocal microscope (Carl Zeiss AG, Oberkochen, Germany). Images were taken with the same microscope settings (laser intensity, gain etc.) and identical image processing parameters were applied to allow comparison between the cell lines. Western blots were performed as previously described [81].

4.7. Immunoprecipitation (IP)

Cells were washed twice with cold PBS and lysed by addition of lysis buffer containing 50 mM Tris-HCl (pH 8.0), 150 mM NaCl, 0.1% Triton X-100, 1 mM DTT and 1 mM EDTA (Sigma-Aldrich Norway AS, Oslo, Norway) as well Halt™ Protease and Phosphatase Inhibitor Cocktail (Thermo Fisher Scientific Inc.). Following sonication and centrifugation, the protein concentration was determined using a Protein Quantification Assay (MACHEREY-NAGEL GmbH & Co. KG). A sample of the supernatant was taken as "input control", supplemented with NuPAGE®LDS Sample Buffer (4X) (Thermo Fisher Scientific Inc.) as well as 100 mM DTT (AppliChem, Darmstadt, Germany) and incubated for 10 min at 70 °C. Cell lysate containing approximately 800 µg protein was pre-cleared with an irrelevant IgG2a antibody (same class as the SYK antibody used for IP) to reduce unspecific binding. Afterwards, the samples were incubated with the anti-SYK antibody (1 µg) rotating at 4 °C overnight followed by incubation with 80 µl of a 50% Sepharose G beads/lysis buffer solution (GE Healthcare, Oslo, Norway) for 1 h rotating at 4 °C. The beads were washed three times with lysis buffer and two times with 50 mM Tris-HCl, pH 8.0. Afterwards, the beads were incubated in sample buffer containing NuPAGE®LDS Sample Buffer (4×), ultrapure H_2O as well as 100 mM DTT for 10 min at 70 °C. The samples were subsequently used for western blot analysis.

4.8. siRNA-Mediated SYK Silencing

Two pre-designed SYK siRNAs were used in this study: ID-s13679 (siRNA 1) and ID-s13681 (siRNA 2) as well as a scramble control #1 siRNA (cat# 4392420 and 4390843, Ambion, Thermo Fisher Scientific Inc.). Cells were seeded into 24- and 6-well plates for cell viability assay and western blot analysis, respectively. After 24 h, the cells were transfected with the different siRNAs using Lipofectamine RNAiMAX reagent (Thermo Fisher Scientific Inc.) according to the manufacturer's specifications. Briefly, cells were incubated with 5 pmol (24-well plate) or 30 pmol siRNA (6-well plate) per well in Opti-MEM (Thermo Fisher Scientific Inc.) for 4 h followed by the removal of the transfection mix and addition of fresh Opti-MEM. After 72 h the cell viability was assessed and cells were harvested for western blot analysis. Densitometry was performed using Fiji software [82].

4.9. Cell Viability Assay

To assess the effect of the commercially available SYK inhibitors BAY 61-3606, R406, GS-9973 (Entospletinib) and PRT062607 alone as well as BAY61-3606 in combination with paclitaxel, cisplatin,

doxorubicin and temozolomide on the cell viability of SH-SY5Y and SK-N-BE(2) neuroblastoma cells the colorimetric MTT (3-(4,5-dimethylthiazol-2-yl)-2,5-diphenyltetrazodium bromide)-assay was used [83]. The cells were seeded in 96-well plates in full growth media. As an exception, cells treated with GS-9973 and PRT062607 were seeded in Opti-MEM to reduce cell viability variations attributed to residual serum. After 24 h, the cells were washed once with Opti-MEM before incubation with SYK inhibitors alone for 24 and 48 h or a combination of chemotherapeutic drugs with BAY61-3606 for 48 and 72 h. Control cells received the corresponding drug vehicle at the highest concentration present in the drug-treated cells. BAY 61-3606 and doxorubicin were dissolved in water, R406, GS-9973, PRT062607, and temozolomide in DMSO, paclitaxel in ethanol, and cisplatin in 0.9% saline. After 24, 48 or 72 h the MTT solution (10 µL of 5 mg MTT, Sigma-Aldrich Norway AS, per ml phosphate buffered saline) was added to each well and incubated for additional 3 h. To facilitate formazan crystal solubilizing, 70 µL of the solution were carefully removed from each well, 100 µL isopropanol containing 0.04 M HCl were added and mixed thoroughly. In addition, the plates were placed on an orbital shaker for 1 h at room temperature. The absorbance was measured with a CLARIOstar plate reader (BMG LABTECH, Ortenberg, Germany) at 590 nm. The experiment was performed at least three times with at least three parallels per treatment. The cell viability was calculated as the ratio of the mean OD of treated cells over vehicle treated control cells (100% living cells). The cell viability assay for the siRNA and SYK plasmid studies were performed in 24-well plates. The amounts of MTT solution and acidic isopropanol were adjusted correspondingly.

4.10. Cell Signaling Study

To investigate the effect of commercially available SYK inhibitors on MAPK- and Akt- mediated signaling SH-SY5Y cells were seeded in 6-well plates in full growth medium. The next day, the cells were washed in Opti-MEM and treated with BAY 61-3606, R406, GS-9973 (entospletinib), PRT062607 or corresponding vehicle controls (water for BAY 61-3606 and DMSO for R406, GS-9973, and PRT062607) for 4 or 24 h. Following incubation, the cells were washed with PBS and harvested in RIPA Lysis and Extraction Buffer containing Halt™ Protease and Phosphatase Inhibitor Cocktail (Thermo Fisher Scientific Inc.) and analyzed by western blot. Densitometry was performed using Fiji software. Phosphorylated and total protein were normalized to their respective GAPDH loading control (pERK/GAPDH, ERK/GAPDH, pAkt/GAPDH, Akt/GAPDH). Ratios of pERK/ERK and pAkt/Akt were calculated using the normalized values. The respective vehicle control was set as 1 and the ratios were calculated.

4.11. Transfection with SYK Plasmids

The following, previously described FLAG-tagged plasmids were used in this study: pCAF1 empty expression vector, SYK wt = SYK wild type, SYK B = short SYK splice variant B, SYK Y130E = constitutive active SYK, SYK K402R = kinase dead SYK, SYK RR42/195KK = SYK with inactive SH2 domains [26,46]. Cells were seeded in 24- (cell viability assay) or 6-well plates (western blot) in full growth media. The following day the cells were transfected using jetPRIME®transfection reagent (Polyplus-transfection®, Illkirch, France) according to the provided manual (1 µg DNA per well in a 6-well plate and 0.25 µg DNA per well in a 24-well plate). After 5 h, the media containing the transfection mix was removed and fresh media was added. After 48 h, cell viability was determined and cells were harvested for western blot.

4.12. Drug Combination Analysis

To determine whether the chemotherapeutic drug-SYK inhibitor combinations displayed a synergistic or additive effect, highest single agent, response additivity and Bliss independence calculations were performed on the cell viability data as described in [84]. Highest single agent method proves the superiority of the drug combination compared to its single agents and was assessed with statistical testing (two-way ANOVA). Response additivity and the Bliss Independence model

both compares the observed drug combination effect to the expected additive effect and thereby calculates a combination index. For Response additivity the expected additive effect is calculated as following: E(A) + E(B) and for the Bliss Independence: E(A) + E(B) − E(A)*E(B) where E is the effect produced by drug A and B. A combination index <0.9 was defined as synergistic, 0.9–1.1 as additive and >1.1 as antagonistic.

4.13. Statistical Analysis

GraphPad Prism software (versions 7 and 8, GraphPad Inc., San Diego, CA, USA) was used for statistical analysis and graph design. Fisher's exact test was used to test the statistical significance of the association between two categories. Two-way ANOVAs and Dunnett or Bonferroni post-tests were applied to assess two independent variables (differences between cell lines and the effect of treatment). Two-tailed one sample t-tests were used for the statistical analysis of the cell signaling studies.

5. Conclusions

Our findings demonstrate the presence of functional SYK in neuroblastoma tissue as well as certain neuroblastoma cell lines and indicate that pharmacological SYK inhibition may be a potential therapeutic approach that can be used to support conventional chemotherapy in SYK-expressing neuroblastomas.

Supplementary Materials: The following are available online at http://www.mdpi.com/2072-6694/11/2/202/s1, Table S1: Clinical features of neuroblastoma tumors, Table S2: Cell viability of SH-SY5Y and SK-N-BE(2) after treatment with 0.8 μM BAY 61-3606, chemotherapeutic drugs or combinations of both, Figure S1: The expression of *SYK* is negatively correlated to *MYCN* but positively to *MYC* in neuroblastoma tissue, Figure S2: IHC of neuroblastoma tumors negative for SYK and p-SYK, Figure S3: Inhibition of SYK decreases the cell viability of neuroblastoma cells, Figure S4: Combination of chemotherapeutic drugs and the selective SYK inhibitor BAY 61-3606 promotes PARP cleavage in neuroblastoma cells, Figure S5: The selective SYK inhibitor BAY 61-3606 enhances the effect of chemotherapeutic drugs in neuroblastoma cells, Figure S6: ZAP70 is expressed in at least one neuroblastoma cell line.

Author Contributions: Conceptualization: B.S., C.T., U.M.; data curation: C.T., G.D., M.W., A.V., U.M.; formal analysis: C.T., G.D., M.W., A.V., B.S., P.K.; funding acquisition: B.S., U.M., P.K., J.I.J.; investigation: C.T., G.D., B.S., U.M., A.V., M.W.; methodology C.T., B.S., U.M., G.D., M.W., P.C., A.V., J.I.J., P.K.; project administration: B.S., U.M., C.T; resources: B.S., U.M., P.C., P.K., J.I.J., A.V.; software: M.W., C.T.; supervision: B.S., U.M.; validation: C.T., G.D., M.W., P.C., A.V., U.M., B.S., J.I.J., P.K.; visualization: C.T., G.D., M.W., P.C., A.V., U.M., B.S.; writing – original draft: C.T., B.S., U.M., G.D., M.W., P.C., J.I.J.; writing – review & editing: C.T., B.S., U.M., G.D., M.W., P.C., J.I.J., A.V., P.K.

Funding: This study was funded with grants from the University of Tromsø, The Norwegian Childhood Cancer Society, Erna and Olav Aakre Foundation for Cancer Research (A20310), Tromsø, Norway, the Swedish Childhood Cancer Foundation, the Swedish Cancer Foundation, the Swedish Research Council, the Swedish Foundation for Strategic Research (www.nnbcr.se) and the Cancer Research Foundations of Radiumhemmet. PC is a staff scientist at the Centre National de la Recherche Scientifique and supported by the Institut National du Cancer and Plan Cancer (ASC14021FSA).

Acknowledgments: We thank Julia Cserna and Marianne Marken for their help with the SYK inhibitor pilot studies, Lotta Elfman for her assistance with the neuroblastoma tissues, and Joe Hurley for proofreading.

Conflicts of Interest: The authors declare no conflict of interest.

References

1. Hunter, T. Tyrosine phosphorylation: thirty years and counting. *Curr. Opin. Cell Biol.* **2009**, *21*, 140–146. [CrossRef] [PubMed]
2. Teruko, T.; Alexandra, K. Tyrosine Kinases as Targets for Anti-Inflammatory Therapy. *Antiinflam. AntiAllergy Agents Med. Chem.* **2007**, *6*, 47–60. [CrossRef]
3. Krause, D.S.; Van Etten, R.A. Tyrosine kinases as targets for cancer therapy. *N. Engl. J. Med.* **2005**, *353*, 172–187. [CrossRef] [PubMed]
4. Mocsai, A.; Ruland, J.; Tybulewicz, V.L. The SYK tyrosine kinase: a crucial player in diverse biological functions. *Nat. Rev. Immunol.* **2010**, *10*, 387–402. [CrossRef] [PubMed]

5. Yagi, S.; Suzuki, K.; Hasegawa, A.; Okumura, K.; Ra, C. Cloning of the cDNA for the deleted syk kinase homologous to ZAP-70 from human basophilic leukemia cell line (KU812). *Biochem. Biophys. Res. Commun.* **1994**, *200*, 28–34. [CrossRef] [PubMed]
6. Rowley, R.B.; Bolen, J.B.; Fargnoli, J. Molecular cloning of rodent p72Syk. Evidence of alternative mRNA splicing. *J. Biol. Chem.* **1995**, *270*, 12659–12664. [CrossRef] [PubMed]
7. Latour, S.; Chow, L.M.; Veillette, A. Differential intrinsic enzymatic activity of Syk and Zap-70 protein-tyrosine kinases. *J. Biol. Chem.* **1996**, *271*, 22782–22790. [CrossRef] [PubMed]
8. Geahlen, R.L. Syk and pTyr'd: Signaling through the B cell antigen receptor. *Biochim. Biophys. Acta* **2009**, *1793*, 1115–1127. [CrossRef] [PubMed]
9. Turner, M.; Mee, P.J.; Costello, P.S.; Williams, O.; Price, A.A.; Duddy, L.P.; Furlong, M.T.; Geahlen, R.L.; Tybulewicz, V.L. Perinatal lethality and blocked B-cell development in mice lacking the tyrosine kinase Syk. *Nature* **1995**, *378*, 298–302. [CrossRef] [PubMed]
10. Baudot, A.D.; Jeandel, P.Y.; Mouska, X.; Maurer, U.; Tartare-Deckert, S.; Raynaud, S.D.; Cassuto, J.P.; Ticchioni, M.; Deckert, M. The tyrosine kinase Syk regulates the survival of chronic lymphocytic leukemia B cells through PKCdelta and proteasome-dependent regulation of Mcl-1 expression. *Oncogene* **2009**, *28*, 3261–3273. [CrossRef] [PubMed]
11. Yu, Y.; Suryo Rahmanto, Y.; Lee, M.H.; Wu, P.H.; Phillip, J.M.; Huang, C.H.; Vitolo, M.I.; Gaillard, S.; Martin, S.S.; Wirtz, D.; et al. Inhibition of ovarian tumor cell invasiveness by targeting SYK in the tyrosine kinase signaling pathway. *Oncogene* **2018**. [CrossRef]
12. Angibaud, J.; Louveau, A.; Baudouin, S.J.; Nerriere-Daguin, V.; Evain, S.; Bonnamain, V.; Hulin, P.; Csaba, Z.; Dournaud, P.; Thinard, R.; et al. The immune molecule CD3zeta and its downstream effectors ZAP-70/Syk mediate ephrin signaling in neurons to regulate early neuritogenesis. *J. Neurochem.* **2011**, *119*, 708–722. [CrossRef]
13. Hatterer, E.; Benon, A.; Chounlamountri, N.; Watrin, C.; Angibaud, J.; Jouanneau, E.; Boudin, H.; Honnorat, J.; Pellier-Monnin, V.; Noraz, N. Syk kinase is phosphorylated in specific areas of the developing nervous system. *Neurosci. Res.* **2011**, *70*, 172–182. [CrossRef] [PubMed]
14. Noraz, N.; Jaaoini, I.; Charoy, C.; Watrin, C.; Chounlamountri, N.; Benon, A.; Malleval, C.; Boudin, H.; Honnorat, J.; Castellani, V.; et al. Syk kinases are required for spinal commissural axon repulsion at the midline via the ephrin/Eph pathway. *Development* **2016**, *143*, 2183–2193. [CrossRef]
15. Wu, C.; Orozco, C.; Boyer, J.; Leglise, M.; Goodale, J.; Batalov, S.; Hodge, C.L.; Haase, J.; Janes, J.; Huss, J.W., 3rd; et al. BioGPS: an extensible and customizable portal for querying and organizing gene annotation resources. *Genome Biol.* **2009**, *10*, R130. [CrossRef] [PubMed]
16. Uhlen, M.; Fagerberg, L.; Hallstrom, B.M.; Lindskog, C.; Oksvold, P.; Mardinoglu, A.; Sivertsson, A.; Kampf, C.; Sjostedt, E.; Asplund, A.; et al. Proteomics. Tissue-based map of the human proteome. *Science* **2015**, *347*, 1260419. [CrossRef] [PubMed]
17. Geahlen, R.L. Getting Syk: spleen tyrosine kinase as a therapeutic target. *Trends Pharmacol. Sci.* **2014**, *35*, 414–422. [CrossRef]
18. D'Aura Swanson, C.; Paniagua, R.T.; Lindstrom, T.M.; Robinson, W.H. Tyrosine kinases as targets for the treatment of rheumatoid arthritis. *Nat. Rev. Rheumatol.* **2009**, *5*, 317–324. [CrossRef]
19. Markham, A. Fostamatinib: First Global Approval. *Drugs* **2018**, *78*, 959–963. [CrossRef]
20. Buchner, M.; Fuchs, S.; Prinz, G.; Pfeifer, D.; Bartholome, K.; Burger, M.; Chevalier, N.; Vallat, L.; Timmer, J.; Gribben, J.G.; et al. Spleen tyrosine kinase is overexpressed and represents a potential therapeutic target in chronic lymphocytic leukemia. *Cancer Res.* **2009**, *69*, 5424–5432. [CrossRef]
21. Feng, G.; Wang, X. Role of spleen tyrosine kinase in the pathogenesis of chronic lymphocytic leukemia. *Leuk. Lymphoma* **2014**, *55*, 2699–2705. [CrossRef] [PubMed]
22. Young, R.M.; Hardy, I.R.; Clarke, R.L.; Lundy, N.; Pine, P.; Turner, B.C.; Potter, T.A.; Refaeli, Y. Mouse models of non-Hodgkin lymphoma reveal Syk as an important therapeutic target. *Blood* **2009**, *113*, 2508–2516. [CrossRef]
23. Boros, K.; Puissant, A.; Back, M.; Alexe, G.; Bassil, C.F.; Sinha, P.; Tholouli, E.; Stegmaier, K.; Byers, R.J.; Rodig, S.J. Increased SYK activity is associated with unfavorable outcome among patients with acute myeloid leukemia. *Oncotarget* **2015**, *6*, 25575–25587. [CrossRef] [PubMed]
24. Yanagi, S.; Inatome, R.; Takano, T.; Yamamura, H. Syk expression and novel function in a wide variety of tissues. *Biochem. Biophys. Res. Commun.* **2001**, *288*, 495–498. [CrossRef] [PubMed]

25. Krisenko, M.O.; Geahlen, R.L. Calling in SYK: SYK's dual role as a tumor promoter and tumor suppressor in cancer. *Biochim. Biophys. Acta* **2015**, *1853*, 254–263. [CrossRef] [PubMed]
26. Coopman, P.J.; Do, M.T.; Barth, M.; Bowden, E.T.; Hayes, A.J.; Basyuk, E.; Blancato, J.K.; Vezza, P.R.; McLeskey, S.W.; Mangeat, P.H.; et al. The Syk tyrosine kinase suppresses malignant growth of human breast cancer cells. *Nature* **2000**, *406*, 742–747. [CrossRef] [PubMed]
27. Layton, T.; Stalens, C.; Gunderson, F.; Goodison, S.; Silletti, S. Syk tyrosine kinase acts as a pancreatic adenocarcinoma tumor suppressor by regulating cellular growth and invasion. *Am. J. Pathol.* **2009**, *175*, 2625–2636. [CrossRef] [PubMed]
28. Hoeller, C.; Thallinger, C.; Pratscher, B.; Bister, M.D.; Schicher, N.; Loewe, R.; Heere-Ress, E.; Roka, F.; Sexl, V.; Pehamberger, H. The non-receptor-associated tyrosine kinase Syk is a regulator of metastatic behavior in human melanoma cells. *J. Invest. Dermatol.* **2005**, *124*, 1293–1299. [CrossRef] [PubMed]
29. Yuan, Y.; Wang, J.; Li, J.; Wang, L.; Li, M.; Yang, Z.; Zhang, C.; Dai, J.L. Frequent epigenetic inactivation of spleen tyrosine kinase gene in human hepatocellular carcinoma. *Clin. Cancer Res.* **2006**, *12*, 6687–6695. [CrossRef] [PubMed]
30. Goodman, P.A.; Wood, C.M.; Vassilev, A.; Mao, C.; Uckun, F.M. Spleen tyrosine kinase (Syk) deficiency in childhood pro-B cell acute lymphoblastic leukemia. *Oncogene* **2001**, *20*, 3969–3978. [CrossRef]
31. Ghotra, V.P.; He, S.; van der Horst, G.; Nijhoff, S.; de Bont, H.; Lekkerkerker, A.; Janssen, R.; Jenster, G.; van Leenders, G.J.; Hoogland, A.M.; et al. SYK is a candidate kinase target for the treatment of advanced prostate cancer. *Cancer Res.* **2015**, *75*, 230–240. [CrossRef] [PubMed]
32. Udyavar, A.R.; Hoeksema, M.D.; Clark, J.E.; Zou, Y.; Tang, Z.; Li, Z.; Li, M.; Chen, H.; Statnikov, A.; Shyr, Y.; et al. Co-expression network analysis identifies Spleen Tyrosine Kinase (SYK) as a candidate oncogenic driver in a subset of small-cell lung cancer. *BMC Syst. Biol.* **2013**, *7*, S1. [CrossRef] [PubMed]
33. Yu, Y.; Gaillard, S.; Phillip, J.M.; Huang, T.C.; Pinto, S.M.; Tessarollo, N.G.; Zhang, Z.; Pandey, A.; Wirtz, D.; Ayhan, A.; et al. Inhibition of Spleen Tyrosine Kinase Potentiates Paclitaxel-Induced Cytotoxicity in Ovarian Cancer Cells by Stabilizing Microtubules. *Cancer Cell* **2015**, *28*, 82–96. [CrossRef] [PubMed]
34. Moncayo, G.; Grzmil, M.; Smirnova, T.; Zmarz, P.; Huber, R.M.; Hynx, D.; Kohler, H.; Wang, Y.; Hotz, H.R.; Hynes, N.E.; et al. SYK Inhibition Blocks Proliferation and Migration of Glioma Cells, and Modifies the Tumor Microenvironment. *Neuro Oncol.* **2018**. [CrossRef] [PubMed]
35. Zhang, J.; Benavente, C.A.; McEvoy, J.; Flores-Otero, J.; Ding, L.; Chen, X.; Ulyanov, A.; Wu, G.; Wilson, M.; Wang, J.; et al. A novel retinoblastoma therapy from genomic and epigenetic analyses. *Nature* **2012**, *481*, 329–334. [CrossRef] [PubMed]
36. Sun, H.; Lin, D.C.; Cao, Q.; Pang, B.; Gae, D.D.; Lee, V.K.M.; Lim, H.J.; Doan, N.; Said, J.W.; Gery, S.; et al. Identification of a Novel SYK/c-MYC/MALAT1 Signaling Pathway and Its Potential Therapeutic Value in Ewing Sarcoma. *Clin. Cancer Res.* **2017**, *23*, 4376–4387. [CrossRef] [PubMed]
37. Wang, L.; Duke, L.; Zhang, P.S.; Arlinghaus, R.B.; Symmans, W.F.; Sahin, A.; Mendez, R.; Dai, J.L. Alternative splicing disrupts a nuclear localization signal in spleen tyrosine kinase that is required for invasion suppression in breast cancer. *Cancer Res.* **2003**, *63*, 4724–4730. [PubMed]
38. Matthay, K.K.; Maris, J.M.; Schleiermacher, G.; Nakagawara, A.; Mackall, C.L.; Diller, L.; Weiss, W.A. Neuroblastoma. *Nat. Rev. Dis. Primers* **2016**, *2*, 16078. [CrossRef]
39. Steliarova-Foucher, E.; Colombet, M.; Ries, L.A.G.; Moreno, F.; Dolya, A.; Bray, F.; Hesseling, P.; Shin, H.Y.; Stiller, C.A.; Bouzbid, S.; et al. International incidence of childhood cancer, 2001-10: A population-based registry study. *Lancet Oncol.* **2017**, *18*, 719–731. [CrossRef]
40. Berlanga, P.; Canete, A.; Castel, V. Advances in emerging drugs for the treatment of neuroblastoma. *Expert. Opin. Emerg. Drugs* **2017**, *22*, 63–75. [CrossRef]
41. Johnsen, J.I.; Dyberg, C.; Fransson, S.; Wickstrom, M. Molecular mechanisms and therapeutic targets in neuroblastoma. *Pharmacol. Res.* **2018**, *131*, 164–176. [CrossRef] [PubMed]
42. Zhang, J.; Billingsley, M.L.; Kincaid, R.L.; Siraganian, R.P. Phosphorylation of Syk activation loop tyrosines is essential for Syk function. An in vivo study using a specific anti-Syk activation loop phosphotyrosine antibody. *J. Biol. Chem.* **2000**, *275*, 35442–35447. [CrossRef] [PubMed]
43. Taylor, N.; Jahn, T.; Smith, S.; Lamkin, T.; Uribe, L.; Liu, Y.; Durden, D.L.; Weinberg, K. Differential activation of the tyrosine kinases ZAP-70 and Syk after Fc gamma RI stimulation. *Blood* **1997**, *89*, 388–396. [PubMed]
44. Tolbert, V.P.; Matthay, K.K. Neuroblastoma: clinical and biological approach to risk stratification and treatment. *Cell Tissue Res.* **2018**, *372*, 195–209. [CrossRef] [PubMed]

45. Zhou, F.; Hu, J.; Ma, H.; Harrison, M.L.; Geahlen, R.L. Nucleocytoplasmic trafficking of the Syk protein tyrosine kinase. *Mol. Cell. Biol.* **2006**, *26*, 3478–3491. [CrossRef] [PubMed]
46. Zyss, D.; Montcourrier, P.; Vidal, B.; Anguille, C.; Merezegue, F.; Sahuquet, A.; Mangeat, P.H.; Coopman, P.J. The Syk tyrosine kinase localizes to the centrosomes and negatively affects mitotic progression. *Cancer Res.* **2005**, *65*, 10872–10880. [CrossRef] [PubMed]
47. Brodeur, G.M.; Seeger, R.C.; Schwab, M.; Varmus, H.E.; Bishop, J.M. Amplification of N-myc in untreated human neuroblastomas correlates with advanced disease stage. *Science* **1984**, *224*, 1121–1124. [CrossRef]
48. Seeger, R.C.; Brodeur, G.M.; Sather, H.; Dalton, A.; Siegel, S.E.; Wong, K.Y.; Hammond, D. Association of multiple copies of the N-myc oncogene with rapid progression of neuroblastomas. *N. Engl. J. Med.* **1985**, *313*, 1111–1116. [CrossRef]
49. Thompson, D.; Vo, K.T.; London, W.B.; Fischer, M.; Ambros, P.F.; Nakagawara, A.; Brodeur, G.M.; Matthay, K.K.; DuBois, S.G. Identification of patient subgroups with markedly disparate rates of MYCN amplification in neuroblastoma: A report from the International Neuroblastoma Risk Group project. *Cancer* **2016**, *122*, 935–945. [CrossRef]
50. Wang, L.L.; Teshiba, R.; Ikegaki, N.; Tang, X.X.; Naranjo, A.; London, W.B.; Hogarty, M.D.; Gastier-Foster, J.M.; Look, A.T.; Park, J.R.; et al. Augmented expression of MYC and/or MYCN protein defines highly aggressive MYC-driven neuroblastoma: a Children's Oncology Group study. *Br. J. Cancer* **2015**, *113*, 57–63. [CrossRef]
51. Breit, S.; Schwab, M. Suppression of MYC by high expression of NMYC in human neuroblastoma cells. *J. Neurosci. Res.* **1989**, *24*, 21–28. [CrossRef] [PubMed]
52. Minami, Y.; Nakagawa, Y.; Kawahara, A.; Miyazaki, T.; Sada, K.; Yamamura, H.; Taniguchi, T. Protein tyrosine kinase Syk is associated with and activated by the IL-2 receptor: Possible link with the c-myc induction pathway. *Immunity* **1995**, *2*, 89–100. [CrossRef]
53. Alaminos, M.; Davalos, V.; Cheung, N.K.; Gerald, W.L.; Esteller, M. Clustering of gene hypermethylation associated with clinical risk groups in neuroblastoma. *J. Nat. Cancer Inst.* **2004**, *96*, 1208–1219. [CrossRef] [PubMed]
54. Margetts, C.D.; Morris, M.; Astuti, D.; Gentle, D.C.; Cascon, A.; McRonald, F.E.; Catchpoole, D.; Robledo, M.; Neumann, H.P.; Latif, F.; et al. Evaluation of a functional epigenetic approach to identify promoter region methylation in phaeochromocytoma and neuroblastoma. *Endocr. Relat. Cancer* **2008**, *15*, 777–786. [CrossRef] [PubMed]
55. Grau, E.; Martinez, F.; Orellana, C.; Canete, A.; Yanez, Y.; Oltra, S.; Noguera, R.; Hernandez, M.; Bermudez, J.D.; Castel, V. Epigenetic alterations in disseminated neuroblastoma tumour cells: influence of TMS1 gene hypermethylation in relapse risk in NB patients. *J. Cancer Res. Clin. Oncol.* **2010**, *136*, 1415–1421. [CrossRef] [PubMed]
56. Grau, E.; Martinez, F.; Orellana, C.; Canete, A.; Yanez, Y.; Oltra, S.; Noguera, R.; Hernandez, M.; Bermudez, J.D.; Castel, V. Hypermethylation of apoptotic genes as independent prognostic factor in neuroblastoma disease. *Mol. Carcinog.* **2011**, *50*, 153–162. [CrossRef] [PubMed]
57. Cottat, M.; Yasukuni, R.; Homma, Y.; Lidgi-Guigui, N.; Varin-Blank, N.; Lamy de la Chapelle, M.; Le Roy, C. Phosphorylation impact on Spleen Tyrosine kinase conformation by Surface Enhanced Raman Spectroscopy. *Sci. Rep.* **2017**, *7*, 39766. [CrossRef]
58. Bohnenberger, H.; Oellerich, T.; Engelke, M.; Hsiao, H.-H.; Urlaub, H.; Wienands, J. Complex phosphorylation dynamics control the composition of the Syk interactome in B cells. *European J. Immunol.* **2011**, *41*, 1550–1562. [CrossRef]
59. Law, C.L.; Chandran, K.A.; Sidorenko, S.P.; Clark, E.A. Phospholipase C-gamma1 interacts with conserved phosphotyrosyl residues in the linker region of Syk and is a substrate for Syk. *Mol. Cell. Biol.* **1996**, *16*, 1305–1315. [CrossRef]
60. Deckert, M.; Tartare-Deckert, S.; Couture, C.; Mustelin, T.; Altman, A. Functional and physical interactions of Syk family kinases with the Vav proto-oncogene product. *Immunity* **1996**, *5*, 591–604. [CrossRef]
61. Groesch, T.D.; Zhou, F.; Mattila, S.; Geahlen, R.L.; Post, C.B. Structural basis for the requirement of two phosphotyrosine residues in signaling mediated by Syk tyrosine kinase. *J. Mol. Biol.* **2006**, *356*, 1222–1236. [CrossRef] [PubMed]
62. Simon, M.; Vanes, L.; Geahlen, R.L.; Tybulewicz, V.L. Distinct roles for the linker region tyrosines of Syk in FcepsilonRI signaling in primary mast cells. *J. Biol. Chem.* **2005**, *280*, 4510–4517. [CrossRef] [PubMed]

63. Carsetti, L.; Laurenti, L.; Gobessi, S.; Longo, P.G.; Leone, G.; Efremov, D.G. Phosphorylation of the activation loop tyrosines is required for sustained Syk signaling and growth factor-independent B-cell proliferation. *Cell. Signal.* **2009**, *21*, 1187–1194. [CrossRef] [PubMed]
64. Zhang, J.; Kimura, T.; Siraganian, R.P. Mutations in the activation loop tyrosines of protein tyrosine kinase Syk abrogate intracellular signaling but not kinase activity. *J. Immunol.* **1998**, *161*, 4366–4374. [PubMed]
65. Papp, E.; Tse, J.K.; Ho, H.; Wang, S.; Shaw, D.; Lee, S.; Barnett, J.; Swinney, D.C.; Bradshaw, J.M. Steady state kinetics of spleen tyrosine kinase investigated by a real time fluorescence assay. *Biochemistry* **2007**, *46*, 15103–15114. [CrossRef]
66. Prinos, P.; Garneau, D.; Lucier, J.F.; Gendron, D.; Couture, S.; Boivin, M.; Brosseau, J.P.; Lapointe, E.; Thibault, P.; Durand, M.; et al. Alternative splicing of SYK regulates mitosis and cell survival. *Nat. Struct. Mol. Biol* **2011**, *18*, 673–679. [CrossRef]
67. Hong, J.; Yuan, Y.; Wang, J.; Liao, Y.; Zou, R.; Zhu, C.; Li, B.; Liang, Y.; Huang, P.; Wang, Z.; et al. Expression of variant isoforms of the tyrosine kinase SYK determines the prognosis of hepatocellular carcinoma. *Cancer Res.* **2014**, *74*, 1845–1856. [CrossRef]
68. Yamamoto, N.; Takeshita, K.; Shichijo, M.; Kokubo, T.; Sato, M.; Nakashima, K.; Ishimori, M.; Nagai, H.; Li, Y.F.; Yura, T.; et al. The orally available spleen tyrosine kinase inhibitor 2-[7-(3,4-dimethoxyphenyl)-imidazo [1,2-c]pyrimidin-5-ylamino]nicotinamide dihydrochloride (BAY 61-3606) blocks antigen-induced airway inflammation in rodents. *J. Pharmacol. Exp. Ther.* **2003**, *306*, 1174–1181. [CrossRef]
69. Braselmann, S.; Taylor, V.; Zhao, H.; Wang, S.; Sylvain, C.; Baluom, M.; Qu, K.; Herlaar, E.; Lau, A.; Young, C.; et al. R406, an orally available spleen tyrosine kinase inhibitor blocks fc receptor signaling and reduces immune complex-mediated inflammation. *J. Pharmacol. Exp. Ther.* **2006**, *319*, 998–1008. [CrossRef]
70. Coffey, G.; DeGuzman, F.; Inagaki, M.; Pak, Y.; Delaney, S.M.; Ives, D.; Betz, A.; Jia, Z.J.; Pandey, A.; Baker, D.; et al. Specific inhibition of spleen tyrosine kinase suppresses leukocyte immune function and inflammation in animal models of rheumatoid arthritis. *J. Pharmacol. Exp. Ther.* **2012**, *340*, 350–359. [CrossRef]
71. Currie, K.S.; Kropf, J.E.; Lee, T.; Blomgren, P.; Xu, J.; Zhao, Z.; Gallion, S.; Whitney, J.A.; Maclin, D.; Lansdon, E.B.; et al. Discovery of GS-9973, a selective and orally efficacious inhibitor of spleen tyrosine kinase. *J. Med. Chem.* **2014**, *57*, 3856–3873. [CrossRef]
72. Lin, Y.C.; Huang, D.Y.; Chu, C.L.; Lin, W.W. Anti-inflammatory actions of Syk inhibitors in macrophages involve non-specific inhibition of toll-like receptors-mediated JNK signaling pathway. *Mol. Immunol.* **2010**, *47*, 1569–1578. [CrossRef] [PubMed]
73. Fey, D.; Halasz, M.; Dreidax, D.; Kennedy, S.P.; Hastings, J.F.; Rauch, N.; Munoz, A.G.; Pilkington, R.; Fischer, M.; Westermann, F.; et al. Signaling pathway models as biomarkers: Patient-specific simulations of JNK activity predict the survival of neuroblastoma patients. *Sci. Signal.* **2015**, *8*, ra130. [CrossRef] [PubMed]
74. Colado, A.; Almejún, M.B.; Podaza, E.; Risnik, D.; Stanganelli, C.; Elías, E.E.; Dos Santos, P.; Slavutsky, I.; Fernández Grecco, H.; Cabrejo, M.; et al. The kinase inhibitors R406 and GS-9973 impair T cell functions and macrophage-mediated anti-tumor activity of rituximab in chronic lymphocytic leukemia patients. *Cancer Immunol. Immunother.* **2016**, *66*, 461–473. [CrossRef] [PubMed]
75. Singh, A.; Ruan, Y.; Tippett, T.; Narendran, A. Targeted inhibition of MEK1 by cobimetinib leads to differentiation and apoptosis in neuroblastoma cells. *J. Exp. Clin. Cancer Res.* **2015**, *34*, 104. [CrossRef] [PubMed]
76. Vieira, G.C.; Chockalingam, S.; Melegh, Z.; Greenhough, A.; Malik, S.; Szemes, M.; Park, J.H.; Kaidi, A.; Zhou, L.; Catchpoole, D.; et al. LGR5 regulates pro-survival MEK/ERK and proliferative Wnt/beta-catenin signalling in neuroblastoma. *Oncotarget* **2015**, *6*, 40053–40067. [CrossRef] [PubMed]
77. Johnsen, J.I.; Segerstrom, L.; Orrego, A.; Elfman, L.; Henriksson, M.; Kagedal, B.; Eksborg, S.; Sveinbjornsson, B.; Kogner, P. Inhibitors of mammalian target of rapamycin downregulate MYCN protein expression and inhibit neuroblastoma growth in vitro and in vivo. *Oncogene* **2008**, *27*, 2910–2922. [CrossRef]
78. King, D.; Yeomanson, D.; Bryant, H.E. PI3King the lock: targeting the PI3K/Akt/mTOR pathway as a novel therapeutic strategy in neuroblastoma. *J. Pediatr. Hematol. Oncol.* **2015**, *37*, 245–251. [CrossRef]
79. Segerstrom, L.; Baryawno, N.; Sveinbjornsson, B.; Wickstrom, M.; Elfman, L.; Kogner, P.; Johnsen, J.I. Effects of small molecule inhibitors of PI3K/Akt/mTOR signaling on neuroblastoma growth in vitro and in vivo. *Int. J. Cancer* **2011**, *129*, 2958–2965. [CrossRef]

80. Figenschau, Y.; Knutsen, G.; Shahazeydi, S.; Johansen, O.; Sveinbjornsson, B. Human articular chondrocytes express functional leptin receptors. *Biochem. Biophys. Res. Commun.* **2001**, *287*, 190–197. [CrossRef]
81. Tümmler, C.; Snapkov, I.; Wickstrom, M.; Moens, U.; Ljungblad, L.; Maria Elfman, L.H.; Winberg, J.O.; Kogner, P.; Johnsen, J.I.; Sveinbjornsson, B. Inhibition of chemerin/CMKLR1 axis in neuroblastoma cells reduces clonogenicity and cell viability in vitro and impairs tumor growth in vivo. *Oncotarget* **2017**, *8*, 95135–95151. [CrossRef] [PubMed]
82. Schindelin, J.; Arganda-Carreras, I.; Frise, E.; Kaynig, V.; Longair, M.; Pietzsch, T.; Preibisch, S.; Rueden, C.; Saalfeld, S.; Schmid, B.; et al. Fiji: an open-source platform for biological-image analysis. *Nat. Methods* **2012**, *9*, 676–682. [CrossRef] [PubMed]
83. Mosmann, T. Rapid colorimetric assay for cellular growth and survival: application to proliferation and cytotoxicity assays. *J. Immunol. Methods* **1983**, *65*, 55–63. [CrossRef]
84. Foucquier, J.; Guedj, M. Analysis of drug combinations: current methodological landscape. *Pharmacol. Res. Perspect.* **2015**, *3*, e00149. [CrossRef] [PubMed]

Supplementary Material

SYK Inhibition Potentiates the Effect of Chemotherapeutic Drugs on Neuroblastoma Cells *In Vitro*

Conny Tümmler, Gianina Dumitriu, Malin Wickström, Peter Coopman, Andrey Valkov, Per Kogner, John Inge Johnsen, Ugo Moens and Baldur Sveinbjörnsson

Table S1. Clinical features of neuroblastoma tumors.

	Number (%)
Age	
<18 month	22 (52%)
>18 month	20 (48%)
Gender	
Female	22 (52%)
Male	20 (48%)
INSS Stage	
1	10 (24%)
2	9 (21%)
3	11 (26%)
4	10 (24%)
4s	2 (5%)
MYCN amplification	10 (24%)
1p deletion	9 (21%)
11q deletion	3 (7%)
17q gain	7 (17%)
Treated tissue	13 (31%)
Untreated tissue	26 (62%)
Information not available	3 (7%)

Table 2. Cell viability of SH-SY5Y and SK-N-BE(2) after treatment with 0.8 μM BAY 61-3606, chemotherapeutic drugs or combinations of both.

		SH-SY5Y			SK-N-BE(2)		
	Treatment	Cell viability (%) Mean ± SD	P value Drug vs. combination	P value BAY vs. combination	Cell viability (%) Mean ± SD	P value Drug vs. combination	P value BAY vs. combination
48 h	0.8μM BAY	51.26 ± 7.83			82.4 ± 8.79		
	Paclitaxel	87.71 ± 7.83			90.89 ± 7.86		
	Paclitaxel + BAY	31.63 ± 2.23	**<0.001**	**<0.001**	54.61 ± 4.12	**<0.001**	**<0.001**
	Cisplatin	82.33 ± 9.01			98.94 ± 6.48		
	Cisplatin + BAY	42.53 ± 2.96	**<0.001**	**0.001**	73.21 ± 5.16	**<0.001**	**<0.001**
	Doxorubicin	100.5 ± 9.59			102 ± 9.68		
	Doxorubicin + BAY	49.15 ± 6.39	**<0.001**	>0.999	76.06 ± 8.81	**<0.001**	0.167
	Temozolomide	107 ± 11.17			107.7 ± 3.65		
	Temozolomide + BAY	44.56 ± 3.83	**<0.001**	**0.018**	76.81 ± 3.85	**<0.001**	0.304
72 h	0.8μM BAY	45.38 ±7.87			82 ± 9.05		
	Paclitaxel	84.53 ± 4.6			88.29 ± 5.19		
	Paclitaxel + BAY	21.79 ± 1.28	**<0.001**	**<0.001**	38.07 ± 4.55	**<0.001**	**<0.001**
	Cisplatin	73.38 ± 5.89			73.99 ± 2.95		
	Cisplatin + BAY	36.68 ± 4.99	**<0.001**	**<0.001**	61.53 ± 4.99	**<0.001**	**<0.001**
	Doxorubicin	102.2 ± 8.37			101.3 ± 7.56		
	Doxorubicin + BAY	47.36 ± 6.6	**<0.001**	>0.999	75.18 ± 8.05	**<0.001**	**0.008**
	Temozolomide	107.7 ± 6.13			102.7 ± 4.28		
	Temozolomide + BAY	40.55 ± 2.79	**<0.001**	0.997	80.87 ± 6.6	**<0.001**	>0.999

Cell viability was measured by MTT assay after 48 and 72 h. The control was set as 100% viable cells. Data are presented as mean ± SD from at least three independent experiments. Using two-way ANOVA, a significant effect was observed for both treatment and between cell lines $p < 0.001$; Bonferroni's multiple comparison test was used to evaluate differences between treatments and p values < 0.05 were considered as statistically significant.

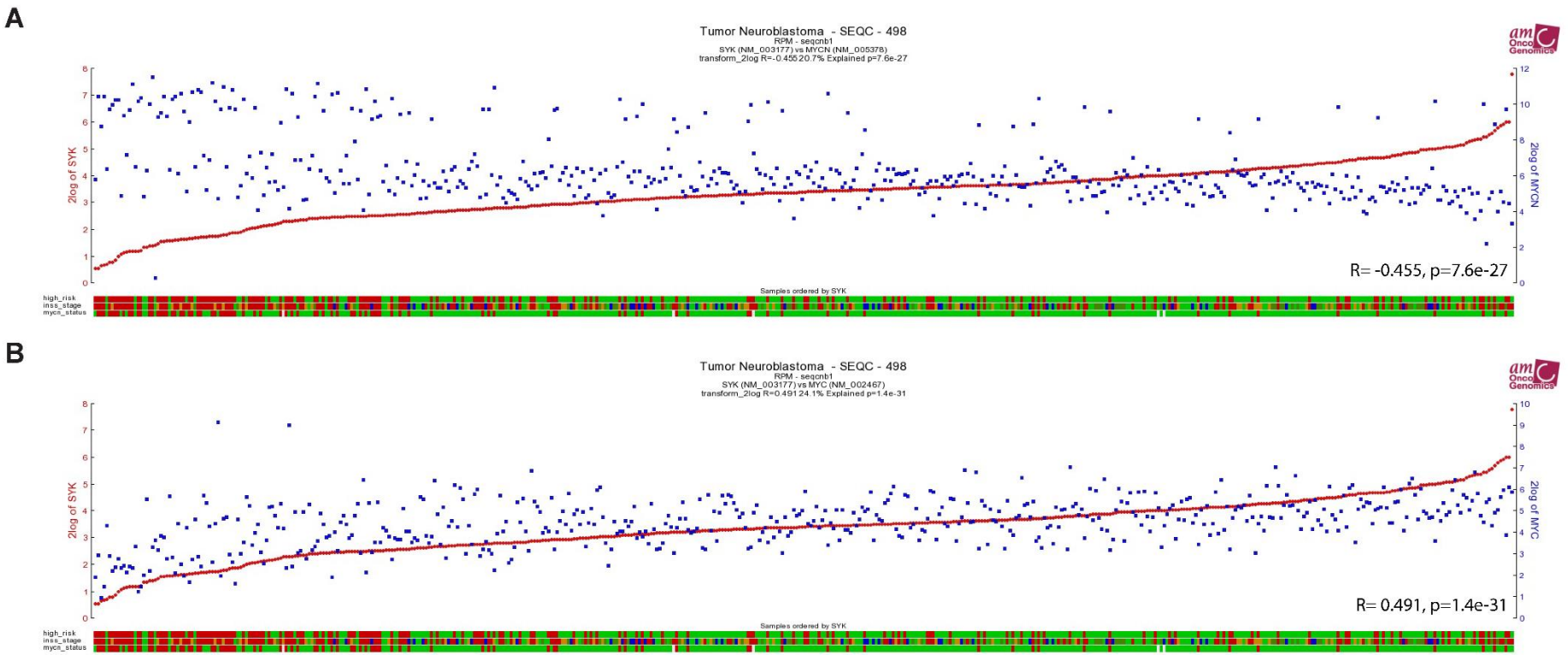

Figure S1. The expression of *SYK* is negatively correlated to *MYCN* but positively to *MYC* in neuroblastoma tissue. Gene expression data were analyzed using the R2 database http://r2.amc.nl. (**A**) Correlation of *SYK* and *MYCN* expression in neuroblastoma tissue using the SEQC dataset (n = 498). (**B**) Correlation of *SYK* and *MYC* expression in neuroblastoma tissue using the SEQC dataset (n = 498).

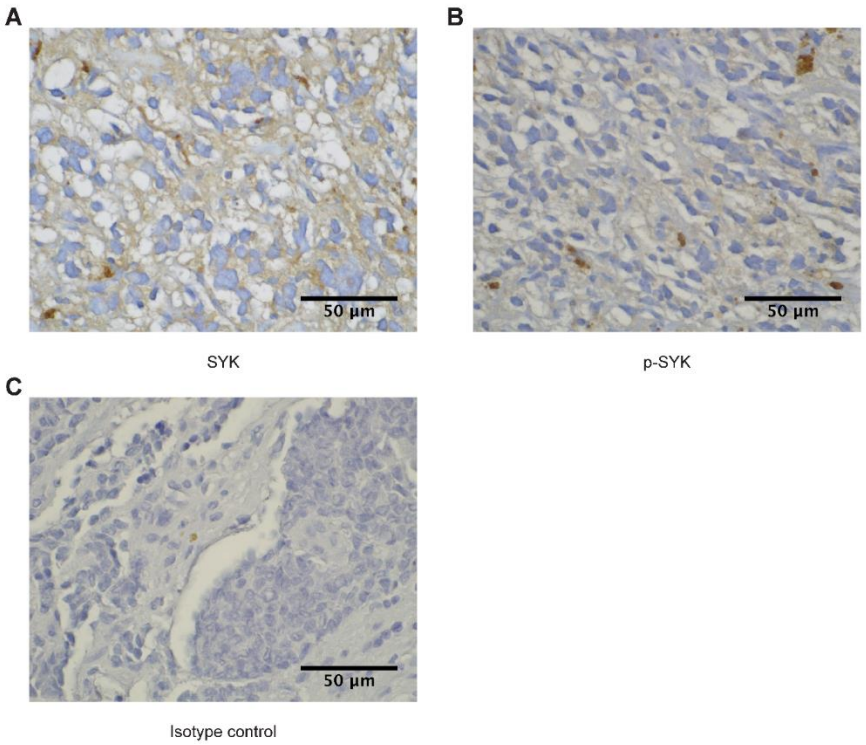

Figure S2. IHC of neuroblastoma tumors negative for SYK and p-SYK. Representative images of immunoperoxidase labeled tumor sections negative for SYK (**A**) and p-SYK (**B**). (**C**) Isotype control, where the primary antibody was replaced with the appropriate rabbit isotype antibody. Images were captured at a magnification of 900×.

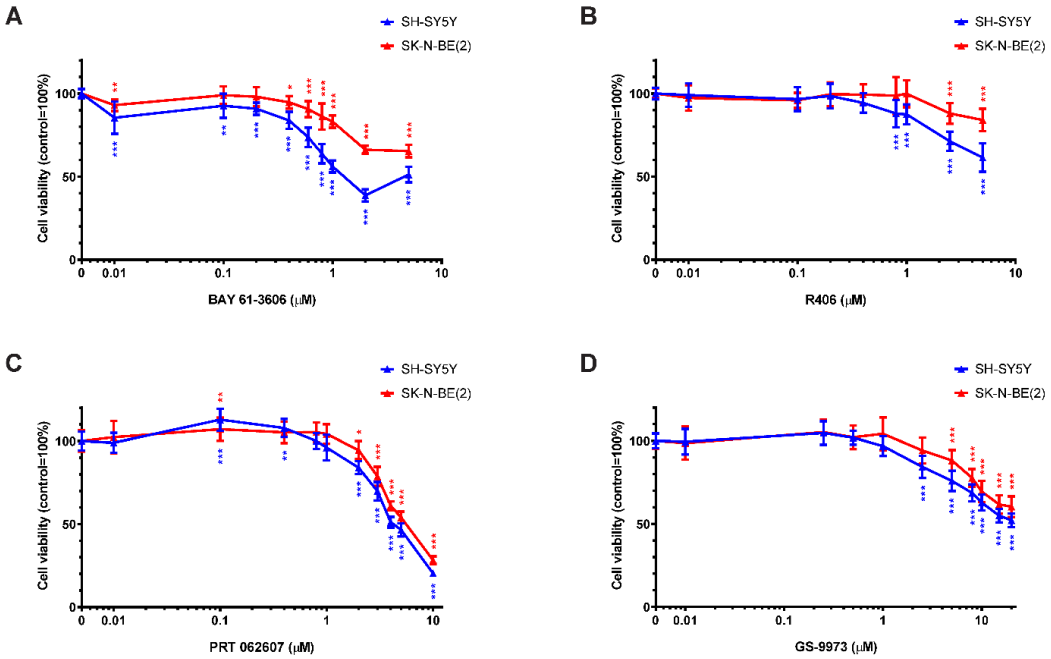

Figure S3. Inhibition of SYK decreases the cell viability of neuroblastoma cells. Cell viability was measured in SH-SY5Y and SK-N-BE(2) cells by MTT assay after 24 h incubation with increasing concentrations of the SYK inhibitors BAY 61-3606 (**A**) R406 (**B**) PRT 062607 (**C**) GS-9973 (**D**). The control was set as 100% viable cells. Data are presented as mean ± SD from three independent experiments. Using two-way ANOVA, a significant difference between cell lines and significant effect of the inhibitor $p < 0.001$ was seen. Dunnett's multiple comparison test was used to evaluate the difference between vehicle treated control cells and the various inhibitor concentrations* $p < 0.05$ ** $p < 0.01$ *** $p < 0.001$.

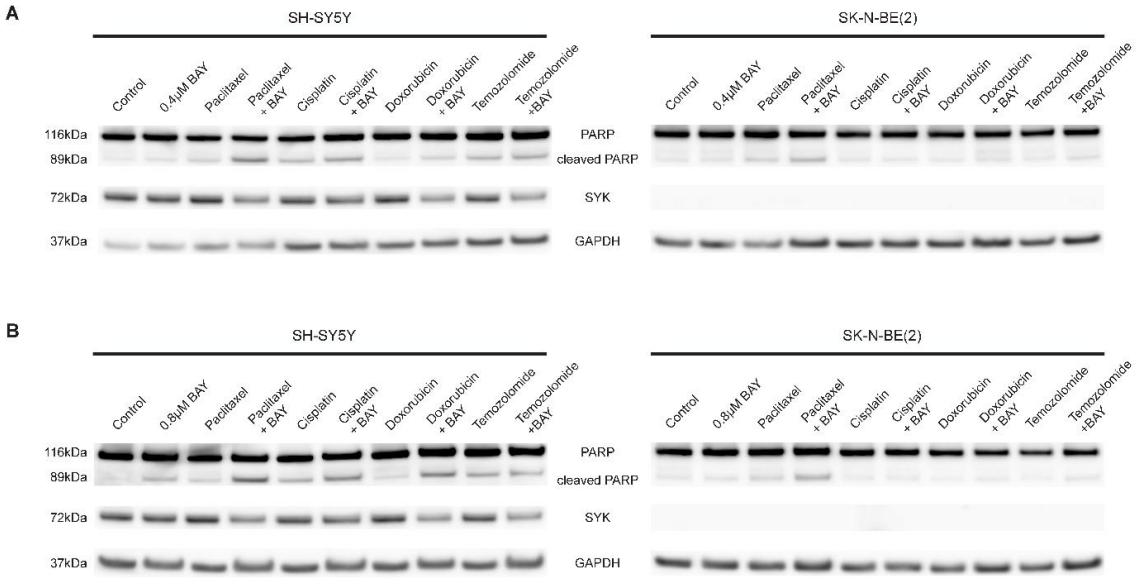

Figure S4. Combination of chemotherapeutic drugs and the selective SYK inhibitor BAY 61-3606 promotes PARP cleavage in neuroblastoma cells. PARP cleavage and SYK expression were determined by western blot after 48 h monotherapy or combinations of 0.4 µM (**A**) or 0.8 µM (**B**) BAY 61-3606, 20 nM paclitaxel, 5 nM doxorubicin, 100 µM temozolomide and cisplatin (1 µM or 3 µM for SH-SY5Y and SK-N BE(2), respectively).

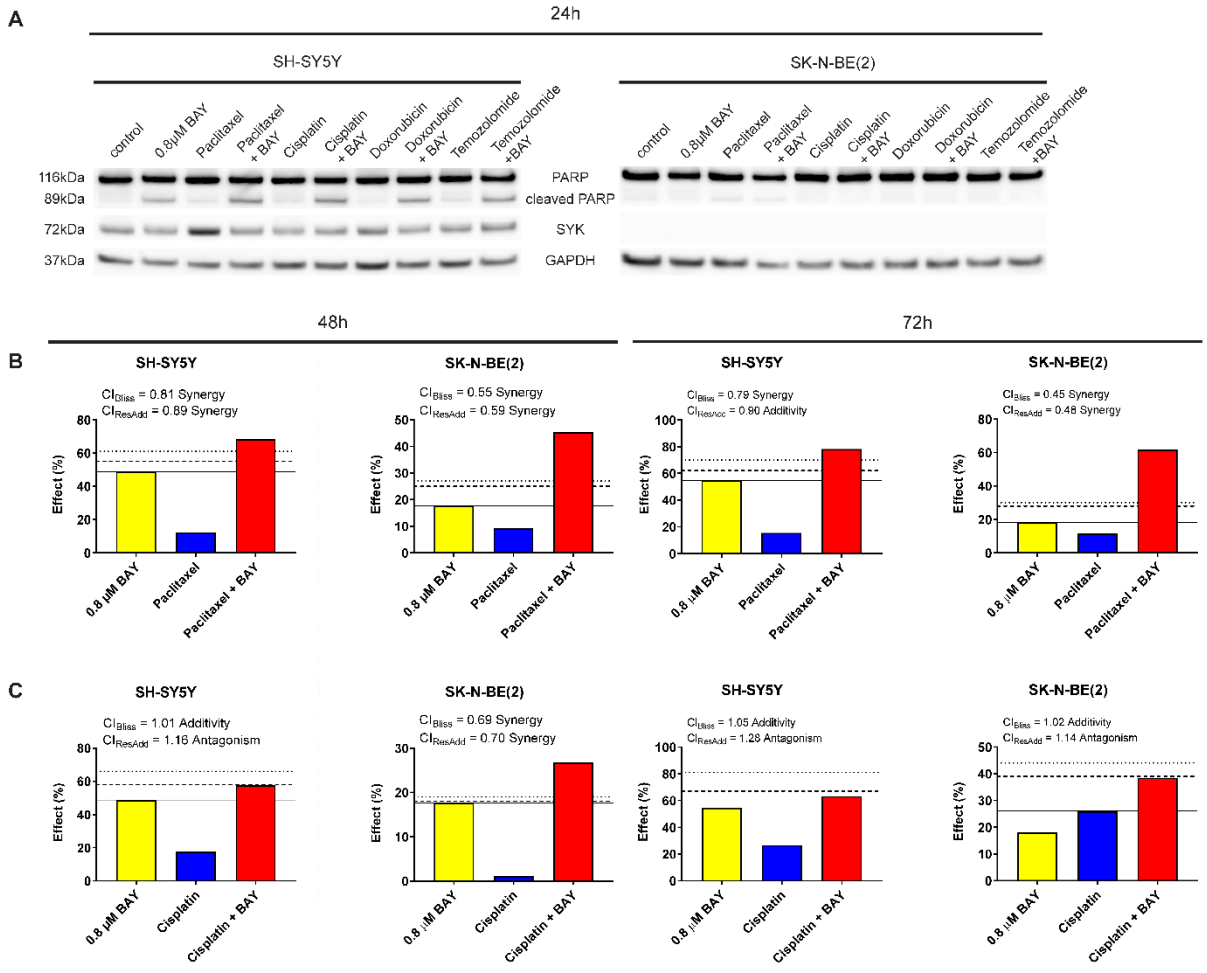

Figure 5. The selective SYK inhibitor BAY 61-3606 enhances the effect of chemotherapeutic drugs in neuroblastoma cells. (**A**) PARP cleavage and SYK expression were determined by western blot after 24 h monotherapy or combinations of 0.8 µM BAY 61-3606, 20 nM paclitaxel, 5 nM doxorubicin,

100 μM temozolomide and cisplatin (1 μM or 3 μM for SH-SY5Y and SK-N-BE(2), respectively). Illustration of drug combination effects for 0.8 μM BAY 61-3606 and paclitaxel (**B**) as well as 0.8 μM BAY 61-3606 and cisplatin (**C**) in SH-SY5Y and SK-N-BE(2) cells after 48 h and 72 h treatment. The continuous horizontal line indicates the effect of the highest single agent, the dashed line denotes expected additive effect calculated by the Bliss independence model, and the dotted line shows expected additive effect calculated by response additivity. Combination index (CI), given from the Bliss independence model and the response additivity, and effect are specified for each combination.

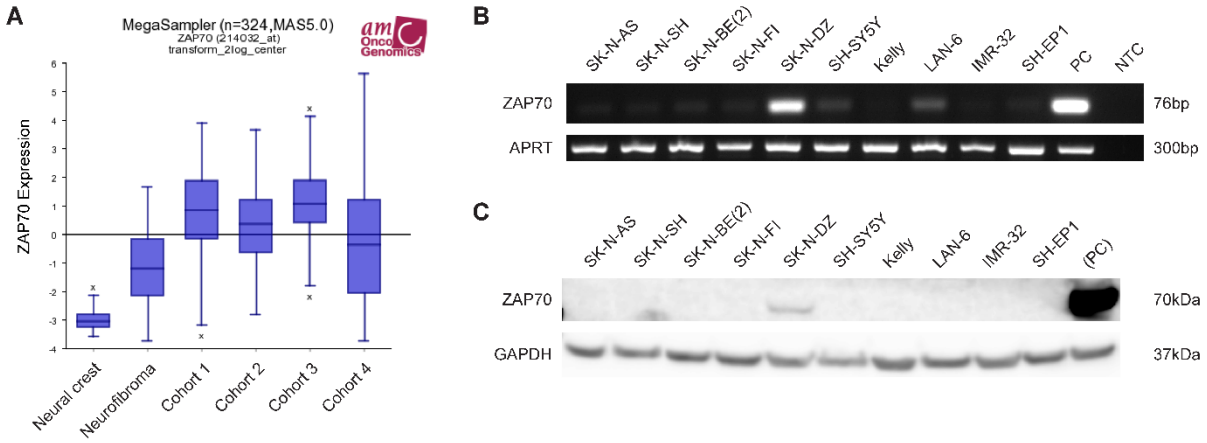

Figure S6. ZAP70 is expressed in at least one neuroblastoma cell line**.** Expression data were analyzed using the R2 database http://r2.amc.nl. (**A**) The expression of *ZAP70* was compared between neural crest (Etchevers n = 5), benign neurofibroma (Miller n = 86) and 4 neuroblastoma cohorts (cohort 1: Versteeg n = 88, cohort 2: Delattre n = 4, cohort 3: Hiyama n = 51, cohort 4: Lastowska n = 30). (**B**) RT-PCR analysis demonstrating the expression *ZAP70* mRNA in some of the examined neuroblastoma cell lines. Jurkat cells were used as a positive control (PC). NTC, no template control. (**C**) western blot of ZAP70 with Jurkat cells as a positive control.

PAPER III

The Interleukin 17 Family and Interleukin 23 in the Neuroblastoma Microenvironment

Conny Tümmler[1], Marianne Marken[1], Andrey Valkov[2], Nina Eissler[3], Per Kogner[3], John Inge Johnsen[3], Ugo Moens[1] and Baldur Sveinbjörnsson[1,3]

[1] Molecular Inflammation Research Group, Department of Medical Biology, Faculty of Health Sciences, University of Tromsø; Hansine Hansens veg 18; 9019 Tromsø; Norway;
[2] Department of Clinical Pathology, University Hospital of Northern Norway; Sykehusveien 38; 9019 Tromsø; Norway;
[3] Childhood Cancer Research Unit, Department of Women's and Children's Health, Karolinska Institutet; Tomtebodav 18A; 17177 Stockholm; Sweden;

Abstract:

Neuroblastoma is a pediatric cancer arising from neural crest cells in the developing sympathetic nervous system. It is the most common extra-cranial solid tumor in children and the most deadly cancer of infancy. Increasing knowledge of the neuroblastoma microenvironment has led to promising new therapeutic approaches. Inflammatory mediators are important contributors to the tumor microenvironment and several of these have been linked to pro-tumorigenic functions in neuroblastoma. In this work, we examined the expression and prognostic value of the interleukin 17 family members, their receptors, and the associated interleukin 23, a heterodimer consisting of the IL-23p19 and IL-12p40 subunit. We observed increased expression of *IL17A*, *IL17C*, *IL17F*, *IL17RA*, *IL17RB*, and *IL17RD* in neuroblastoma compared to neural crest cells and benign neurofibroma. Furthermore, we found that high expression of *IL17RA*, *IL17RB*, *IL17RD*, *IL17A*, *IL17B, IL17C*, *IL25* (also knowns as IL-17E), and *IL17F* correlated with a reduced overall survival probability. In addition, IL-17RA, IL-17RB, and IL-17RC protein was present in neuroblastoma cell lines and tumor tissue. Moreover, we detected IL-23p19 protein in neuroblastoma cell lines and neuroblastoma tissue. While stimulation with recombinant IL-17 proteins only affected the cell viability of neuroblastoma cell lines modestly, we observed that stimulation with IL-17A and IL-17B modulated *in vitro* migration of neuroblastoma cells. Furthermore, IL-17A, IL-17B, and IL-25 affected hepatocyte growth factor levels in SK-N-AS cell supernatants and an effect of IL-25 on Dickkopf-related protein 1 secretion was seen in SK-N-BE(2) and SK-N-AS cells.

This study demonstrates the presence of functional IL-17 receptors in neuroblastoma and the potential of selected IL-17 family members as prognostic factors.

Keywords: Pediatric cancer, Inflammation, Cytokines, Tumor microenvironment

1. Introduction

Cancer-related inflammation is a well-recognized enabling factor of tumorigenesis, as persistent inflammatory processes can contribute to every stage of cancer development [1, 2]. Cytokines and chemokines are important mediators of inflammation and several of them have been identified as promising drug targets for cancer therapy [3, 4].

The IL-17 family is comprised of six interleukins (IL-17A-F) with important functions in inflammation and host defense against pathogens [5]. IL-17A, the first discovered family member, and IL-17F are signature cytokines of Th17 helper cells and bind as IL-17A homodimers or IL-17A/F heterodimers to IL-17RA/RC [6-9]. Complex roles for IL-17A and IL-17F have been described in different autoimmune diseases and cancers [10, 11]. Pro-tumorigenic functions have been demonstrated in, for example colorectal cancer [12, 13], breast cancer [14-18], pancreatic cancer [19, 20], and glioma [21, 22]. Tumor-promoting functions of IL-17A have been linked to promoting proliferation, migration, angiogenesis, and metastasis, and to immune cell modulation, for example recruitment and activation of MDSCs and regulatory T cells [11]. Tumor-suppressing functions of IL-17A and IL-17-producing cells have been indicated in, among other, sarcoma and colorectal cancer models [23] and gastric cancer [24], and are often connected to the recruitment and activation of tumor-suppressing immune cells, such as NK cells and T cells.

The functions of the remaining IL-17 family members in carcinogenesis are less extensively studied. IL-17B and its receptor IL-17RB have been implicated in the tumorigenesis of breast cancer [25, 26] and gastric cancer [27, 28]. IL-25 (also known as IL-17E) signals through a heterodimer of IL17RA/RB [29, 30] and anti-tumorigenic effects have been demonstrated in breast cancer [31-33] and colon cancer [31, 34]. While tumor-promoting functions have been observed for IL-17C, whose receptor is an IL-17RA/RE heterodimer, in colorectal cancer and lung cancer [35, 36], IL-17D delayed growth of transplanted melanoma tumor cells *in vivo* [37]. Furthermore, *IL17D* expression was decreased in advanced glioma and metastatic prostate cancer [37]. The receptor for IL-17D remains to date unknown.

IL-17A/F expression and secretion occurs often in response to IL-23 in the major IL-17A/F producing cells (Th17, γδ T cells, ILC3, and NKT cells), linking IL-17A/F functions to IL-23 [38, 39]. However, IL-23-independent IL-17A production has also been observed [40-42]. IL-23, a member of the IL-12 family, is a pro-inflammatory cytokine consisting of the IL-23p19 and the IL-12p40 subunit [43]. Expressed by, among others, dendritic cells and macrophages, IL-23 has been implicated in host defense but also the pathogenesis of different inflammatory diseases, such as psoriasis and Crohn's disease [44-47]. Furthermore, IL-23 can promote tumor growth and metastasis in different cancers [48].

Neuroblastoma is the most frequently diagnosed childhood cancer in the first year of life and accounts for 6-10% of pediatric cancers worldwide [49, 50]. As a malignancy of the sympathetic nervous system, the majority of neuroblastomas arise in the adrenal medulla as well as paraspinal sympathetic ganglia [50, 51]. The clinical presentation of neuroblastomas is highly heterogenic, ranging from spontaneously regressing tumors that require minimal treatment or observation only to highly aggressive metastatic tumors requiring intensive multimodal therapy [52]. Despite advances in diagnosis and treatment, 12-15% of cancer-related deaths in children are accounted for by neuroblastomas, indicating the need for a deeper understanding of neuroblastoma biology and novel therapeutic approaches [53]. An increasing understanding of the complex neuroblastoma microenvironment has led to the identification of potential new therapeutic targets including various inflammatory mediators and pathways [54], such as the COX/mPGES/ PGE_2 pathway [55-60] and the IL-6/IL-6R axis [61, 62].

The aim of this study was to investigate the presence and function of the IL-17 family and IL-23 in the neuroblastoma microenvironment.

2. Material and Methods

2.1. Gene expression analysis

The publically available R2: Genomics Analysis and Visualization Platform (http://r2.amc.nl) was used to perform gene expression analyses. The MegaSampler feature was employed to compare gene expression between neural crest, benign neurofibroma and different neuroblastoma cohorts. Furthermore, RNA sequencing data from the SEQC-498-RPM dataset were examined to determine correlations between high and low gene expression and overall survival probability.

2.2. Cell lines and human tissue samples

The human neuroblastoma cell lines SK-N-AS, SK-N-SH, SK-N-DZ, SK-N-FI, SH-EP1, Kelly, SH-SY5Y, and IMR-32 were obtained from the ATCC (American Type Culture Collection, LGC Standards GmbH, Wesel, Germany) and SK-N-BE(2) cells were purchased from DSMZ (Deutsche Sammlung von Mikroorganismen und Zellkulturen, Braunschweig, Germany). LAN-6 cells were a kind gift from Deborah Tweddle, Newcastle University. The identity of the cell lines was confirmed by STR profiling performed at the Centre of Forensic Genetics, University of Tromsø, Norway. Additionally, THP-1, A431, HepG2, and Jurkat E6.1, serving as control cell lines, were obtained from the ATCC. All cell lines were cultivated at 37 °C in humidified air with 5% CO_2 in RPMI-1640 medium containing L-glutamine and sodium bicarbonate (Sigma-Aldrich Norway AS, Oslo, Norway) supplemented with 10% heat-inactivated fetal bovine serum (FBS; Thermo Fisher Scientific Inc., Waltham, MA, USA). Mycoplasma tests were regularly performed using the MycoAlert™ PLUS Mycoplasma Detection Kit (Lonza, Basel, Switzerland).

Human neuroblastoma tissue samples were collected at the Karolinska University Hospital with written or verbal informed consent for the use of tumor samples in research provided by the parents or guardians. Sample collection and subsequent use was in accordance with the ethical approval from the Stockholm Regional Ethical Review Board and the Karolinska University Hospital Research Ethics Committee (approval ID 2009/1369-31/1 and 03-736). Following resection, the tissue samples were snap-frozen in liquid nitrogen and stored at -80 °C until further use.

2.3. Reagents and antibodies

Recombinant human IL-17A, IL-17B, IL-25, and IL-17A/F were purchased from R&D Systems, Inc. (Minneapolis, MN, USA). Antibodies used in this study are listed in Table 1.

Table 1: Antibodies (*WB=western blot; IHC=immunohistochemistry; ICC=immunocytochemistry)

Antibody	Application*	Source
Anti-IL-17RA	WB	#sc-376374, Santa Cruz
Anti-IL-17RA	IHC	#MAB1771, R&D Systems
Anti-IL-17RB	WB, IHC	#AF1207, R&D Systems
Anti-IL-17RC	WB, IHC	#bs-2607R, Bioss Antibodies
Anti-IL-23	ICC, IHC	#HPA001554, Sigma
Anti-GAPDH	WB	#47724, Santa Cruz
Goat Anti-Rabbit IgG H&L (HRP)	WB	#6721, abcam
Rabbit Anti-Mouse IgG H&L (HRP)	WB	#97046, abcam
Goat anti-Rabbit IgG (H+L), Alexa Fluor 488	ICC	# A-11008, Thermo Fisher Scientific

2.4. Immunohistochemistry (IHC)

IHC was performed as described in [63] with the following modifications. With respect to the primary antibody source, the SignalStain® Boost IHC Detection Reagent, HRP for rabbit or mouse was used (Cell Signaling Technology, Leiden, Netherlands). As substrate served the SignalStain® DAB Substrate Kit (Cell Signaling Technology).

2.5. RNA isolation, cDNA synthesis, and RT-PCR

Total RNA was isolated with the NucleoSpin® TriPrep Kit (MACHEREY-NAGEL GmbH & Co. KG, Düren, Germany) according to the user manual. RNA quantity and quality was determined using a NanoDrop™ 2000 spectrometer (Thermo Fisher Scientific Inc.) followed by cDNA synthesis with the iScript™ cDNA Synthesis Kit (Bio-Rad Laboratories AB, Oslo, Norway). The PCR reaction was performed in a 25 µl mix containing 12.5 µl AccuStart™ II GelTrackPCR SuperMix (Quanta Biosciences, Gaithersburg, MD, USA), 400 nM of each primer (Sigma-Aldrich Norway AS, Oslo, Norway), 2 µl cDNA and 10.1 µl of ultra-pure H_2O (Biochrom GmbH, Berlin, Germany). Primer sequences were retrieved from the Primer Bank http://pga.mgh.harvard.edu/primerbank/index.html, the qPrimerDepot [64], scientific literature or designed using Primer-BLAST https://www.ncbi.nlm.nih.gov/tools/primer-blast/. A complete overview of primer sequences and sources is displayed in Table 2. Of note, all primer sets were intron spanning to avoid false positive signals caused be amplification of residual genomic DNA. PCR runs (2 min at 94 °C and 35 cycles of 94 °C for 20 s, 60 °C for 30 s and 72 °C for 90 s) were performed in a T100™ Thermal Cycler (Bio-Rad Laboratories AB). PCR products were analyzed by gel electrophoresis on a 2% SeaKem® LE Agarose gel (Lonza) stained with GelRed™ (Biotium, Inc., Hayward, CA, USA) and visualized in the BioDoc-It® 220 Imaging System (UVP, LLC, Upland, CA, USA).

140 **Table 2: Primer sets**

Target		Sequence	Source
APRT	Fw	CCCGAGGCTTCCTCTTTGGC	**[65]**
	Rv	CTCCCTGCCCTTAAGCGAGG	
IL-17RA	Fw	AGTTCCACCAGCGATCCAAC	Primer Bank 313151200c2
	Rv	GTCTGAGGCAGTCATTGAGGC	
IL-17RB	Fw	TACCCCGAGAGCCGACCGTT	**[26]**
	Rv	GGCATCTGCCCGGAGTACCCA	
IL-17RC	Fw	TCGTCCTAACGGAGTCAGGT	qPrimerDepot
	Rv	TACTGGAATCAGGTCCAGGG	
IL-17RD	Fw	CTCCGTCTTCTTTACGGTCAAC	Primer Bank 166063982c1
	Rv	TCCCCACTGGATTCAAGTAGG	
IL-17RE	Fw	TCCCACACGGATGACAGTTTC	Primer Bank ID 24430203c1
	Rv	GAAGAGGCCCCGTTGAAGAC	
IL-17A	Fw	ATGTGGTAGTCCACGTTCCC	qPrimerDepot
	Rv	TCCACCTCACCTTGGAATCT	
IL-17B	Fw	GCCACTGGACCTGGTGTCACG	**[26]**
	Rv	CTGGGGTCGTGGTTGATGCTGT	
IL-17C	Fw	CCCTGGAGATACCGTGTGGA	Primer Bank ID 27477078c2
	Rv	GGGACGTGGATGAACTCGG	
IL-17D	Fw	GCCCTGGGCCTACAGAATC	Primer Bank ID 19923715a1
	Rv	CGCCCTGTTTGTCGATGCT	
IL-25 (IL-17E)	Fw	CAGGTGGTTGCATTCTTGGC	Primer Bank ID 291045205c1
	Rv	GAGCCGGTTCAAGTCTCTGT	
IL-17F	Fw	CCTACTTTGGGGATTTTCCG	qPrimerDepot
	Rv	CTGCACAAAGTAAGCCACCA	
IL-23 (1)	Fw	CTCAGGGACAACAGTCAGTTC	Primer Bank ID 28144902c1
	Rv	ACAGGGCTATCAGGGAGCA	
IL-23 (2)	Fw	ACTCAGTGCCAGCAGCTTTC	qPrimerDepot
	Rv	CCACACTGGATATGGGGAAC	
IL-23 (3) (sequencing)	Fw	CAGGCTCAAAGCAAGTGGAAGTGGGC	Primer-BLAST
	Rv	GAGATCTGAGTGCCATCCTTGAGCTG	
IL-12B	Fw	CAGGTCACTATTCAATGGGATGC	Primer Bank ID 24430211c1
	Rv	GCAGTTCTTAATTGCTGCTTGG	
IL-23R	Fw	ATTGGACTCTCCGTCCTGC	qPrimerDepot
	Rv	TCCGGATACCAATCCAATTC	

141

2.6. Western blot

Western blots were performed as previously described in [66].

2.7. Cell Viability assay

Colorimetric MTT (3-(4,5-dimethylthiazol-2-yl)-2,5-diphenyltetrazodium bromide)-assays [67] were performed to assay the effect of recombinant human IL-17A, IL-17B, IL-25, or IL-17A/F on the cell viability of neuroblastoma cell lines. Briefly, cells were seeded in 96-well plates in RPMI containing 10% FBS. The following day cells were washed and serum-starved for 24 h by incubation in Opti-MEM (Thermo Fisher Scientific Inc.). Afterwards, the cells were stimulated with recombinant IL-17 proteins for 48 h or 72 h. The recombinant proteins were reconstituted in the vehicle recommended by the supplier; IL-17A and IL-17B in PBS (phosphate buffered saline) containing 0.2% human serum albumin (Octapharma, Manchester, UK), IL-25 in 4mM HCl containing 0.2% human serum albumin, and IL-17A/F in 4mM HCl. Control cells were incubated with amounts of vehicle corresponding to the highest concentration of vehicle present in the treated cells. The MTT stock solution was prepared as 5 mg MTT (Sigma-Aldrich Norway, AS) per 1 ml PBS and 10 µl MTT stock were added to each well after 48 h or 72 h. After additional 3-4 h incubation, 70 µl solution were carefully removed and 100 µl isopropanol containing 0.04 M HCl were added. Formazan solubilization was achieved through vigorous mixing and additional incubation on an orbital shaker for 1 h. Absorbance at 590 nm was measured using a CLARIOstar plate reader (BMG LABTECH, Ortenberg, Germany). Cell viability was calculated as the ratio of stimulated cells over vehicle control cells (100% living cells). The experiment was performed at least three times with a minimum of four parallels per stimulation.

2.8. HGF and Dkk-1 ELISA

Human hepatocyte growth factor (HGF) and Dickkopf-related protein 1 (Dkk-1) DuoSet ELISAs (R&D Systems, Inc.) were used to measure the concentration of HGF and Dkk-1 in cell supernatants according to the user manual. The cells were seeded in 24-well plates in full growth medium. The following day the cells were washed briefly with PBS and serum-starved in Opti-MEM for 24h. Stimulation with recombinant human IL-17A, IL-17B, IL-25 or IL-17A/F was performed in triplicates for 1 h or 24h. Appropriate amounts of vehicle, corresponding to the highest amount used in the treated cells, were added to the control cells. Following stimulation, supernatants from the same treatment were pooled and centrifuged at 4 °C for 5 min at 1500rpm to remove cells and cell debris. The supernatants were stored at -80 °C until use. *In vitro migration (scratch) assay*

SK-N-BE(2) cells were seeded in 6-well plates and cultured in RPMI-1640 containing 10 % FBS. The following day, the cells were serum-starved in Opti-MEM for 24 h. Thereafter, the cells were scratched

using a 1000 µL tip and stimulated with 25 ng/ml IL-17A or IL-17B in Opti-MEM for 48 h. Cell migration was monitored using the Celldiscoverer 7 microscope (Carl Zeiss AG, Oberkochen, Germany) for live cell imaging with pictures being taken every two hours.

2.10. Immunocytochemistry (ICC)

Cells were grown in full growth media in 8-well µ-Slides (iBidi GmbH) over night. The cells were washed briefly with PBS and fixed for 20 min with 4% formaldehyde (Alfa Aesar, VWR International, Oslo, Norway). After 3 x 5 min washes with PBS the cells were incubated for 1 h in PBS containing 0.03% Triton™ X-100 (Sigma-Aldrich Norway AS) for membrane permeabilization and 5% goat serum (Sigma-Aldrich Norway AS) to block unspecific binding sites. Incubation with the primary antibody in PBS containing 0.3% Triton™ X-100 and 1% bovine serum albumin or a corresponding isotype control (Thermo Fisher Scientific Inc.) took place at 4 °C over night. Following 3 x 5 min washes in PBS the cells were incubated with the secondary antibody diluted in PBS containing 0.3% Triton™ X-100 and 1% BSA (BSA; AppliChem, Darmstadt, Germany) for 1 h at room temperature. Afterwards, the cells were washed 3 x 5 min washes in PBS and incubated for 10 min with Hoechst 33342 (ImmunoChemistry Technologies, LLC, Bloomington, IN, USA) diluted in PBS for nuclear staining. After 3 x 5 min washes in PBS the cells were covered with Mounting Medium for fluorescence microscopy (iBidi GmbH) and examined using a Zeiss LSM780 confocal microscope (Carl Zeiss AG).

2.11. IL-23 cloning and sequencing

RNA from neuroblastoma cells was isolated using the Nucleospin® TriPrep Kit (Macherey-Nagel) according to the manufacturer's instructions. The RNA concentration was determined with a NanoDrop™ ND2000 (Thermo Fisher Scientific Inc.). cDNA was synthesized with the iScript Select cDNA Synthesis Kit (Bio-Rad Laboratories) according to the manufacturer's instructions using Oligo dT primers to ensure reverse transcription of mRNA.

For PCR amplification, the MyFi DNA polymerase (Bioline, Alexandria, New South Wales, Australia) was used in the following setup: 8 µL of cDNA, 2 µL MyFi DNA polymerase, 10 µL MyFi Reaction Buffer, 20 ng of each primer (Table 2), dH_2O to 50 µL. Amplification was carried out in the T100™ Thermal Cycler (Bio-Rad Laboratories) under the following PCR conditions: 1 min denaturation at 95 °C; 35 cycles of 15 s denaturation at 95 °C, 15 s annealing at 60 °C, 15 s elongation at 72 °C and a final extension for 10 min at 72 °C.

PCR products were analyzed by gel electrophoresis on a 2% SeaKem® LE Agarose gel (Lonza) stained with GelRed™ (Biotium Inc.) at 115 V and visualized under UV light in the BioDoc-It® 220 Imaging System (UVP, LLC). DNA fragment sizes were estimated by comparison to a low-molecular-weight marker (1 Kb Plus DNA Ladder; Thermo Fisher Scientific Inc.). Bands of interest were excised

from the gel and the DNA was extracted using the Wizard® SV Gel and PCR Clean-Up System (Promega Biotech AB, Nacka, Sweden). A re-amplification of the DNA was performed in a 25 µL PCR followed by gel electrophoresis and gel extraction as described above. PCR products were cloned into a TOPO vector using the TOPO 2.1 TA Cloning® Kit (Thermo Fisher Scientific Inc.) according to the manufacturer's instructions with the modification of using 9 µL purified PCR product per 1 µL vector. The plasmids were transformed into competent *E. coli* DH5α cells, which were cultured in SOC medium and plated on LA plates containing 100 mg/ml ampicillin. Colonies containing the IL-23 insert were identified by PCR and cultured in LB broth with 100 mg/ml ampicillin. Plasmids were purified using the NucleoSpin® Plasmid Miniprep Kit (Macherey-Nagel) according to the manufacturer's instructions. The sequencing reactions were performed using M13 forward and reverse primers and the BigDye™ Terminator v3.1 Cycle Sequencing Kit (Thermo Fisher Scientific Inc.) and products were analyzed on the Applied Biosystems™ 3130xl DNA Analyzer (Thermo Fisher Scientific Inc.).

2.12. Graph design and statistical analysis

GraphPad Prism software (versions 8, GraphPad Inc., San Diego, CA, USA) was used for Graph design and statistical analysis. One-way ANOVAs and Dunnett's post-test were applied to assess effects of recombinant IL-17 proteins on cell viability and HGF and Dkk-1 secretion.

3. Results

3.1. *Expression of several IL-17 family members is increased in neuroblastoma and predicts poor overall survival probability*

The publically available R2: Genomics Analysis and Visualization Platform (http://r2.amc.nl) was used to investigate IL-17 family gene expression in neuroblastoma. We observed increased expression of *IL17RA* (Figure 1A), *IL17RB* (Figure 1B), *IL17A* (Figure 1D) and to a lesser extend *IL17F* (Figure 1G) in four neuroblastoma cohorts compared to neural crest cells and benign neurofibroma. While a higher expression of *IL17RC*, *IL17B*, and *IL25* was apparent in the neuroblastoma cohorts in comparison to neurofibroma, the same trend was not discernable in comparison to neural crest cells (Figure 1C, 1E, and 1F). In addition, we found an increase of *IL17C* in the neuroblastoma cohorts (supplementary Figure 1D) compared to neural crest cells and neurofibroma, and for *IL17RD* and *IL17D* (supplementary Figure 1A and 1D) a difference between the neuroblastoma cohorts and neurofibroma was seen. In contrast, higher expression of *IL17RE* was observed in the neuroblastoma cohorts in comparison to the neural crest but not neurofibroma (supplementary Figure 1B).

Furthermore, we examined the SEQC-RPM-seqcnb1 RNA sequencing dataset with data from 498 patients and observed that high expression of *IL17RA* (Figure 1A), *IL17RB* (Figure 1B), *IL17A* (Figure 1D), *IL17B* (Figure 1E), *IL25* (Figure 1F), *IL17F* (Figure 1G), and *IL17RD* and *IL17C* (supplementary Figure 1A and D) correlated to a reduced overall survival probability. In contrast, high expression of *IL17RC* (Figure 1C), *IL17RE* (supplementary Figure 1B), and *IL17D* (supplementary Figure 1E) correlated to an increased survival probability.

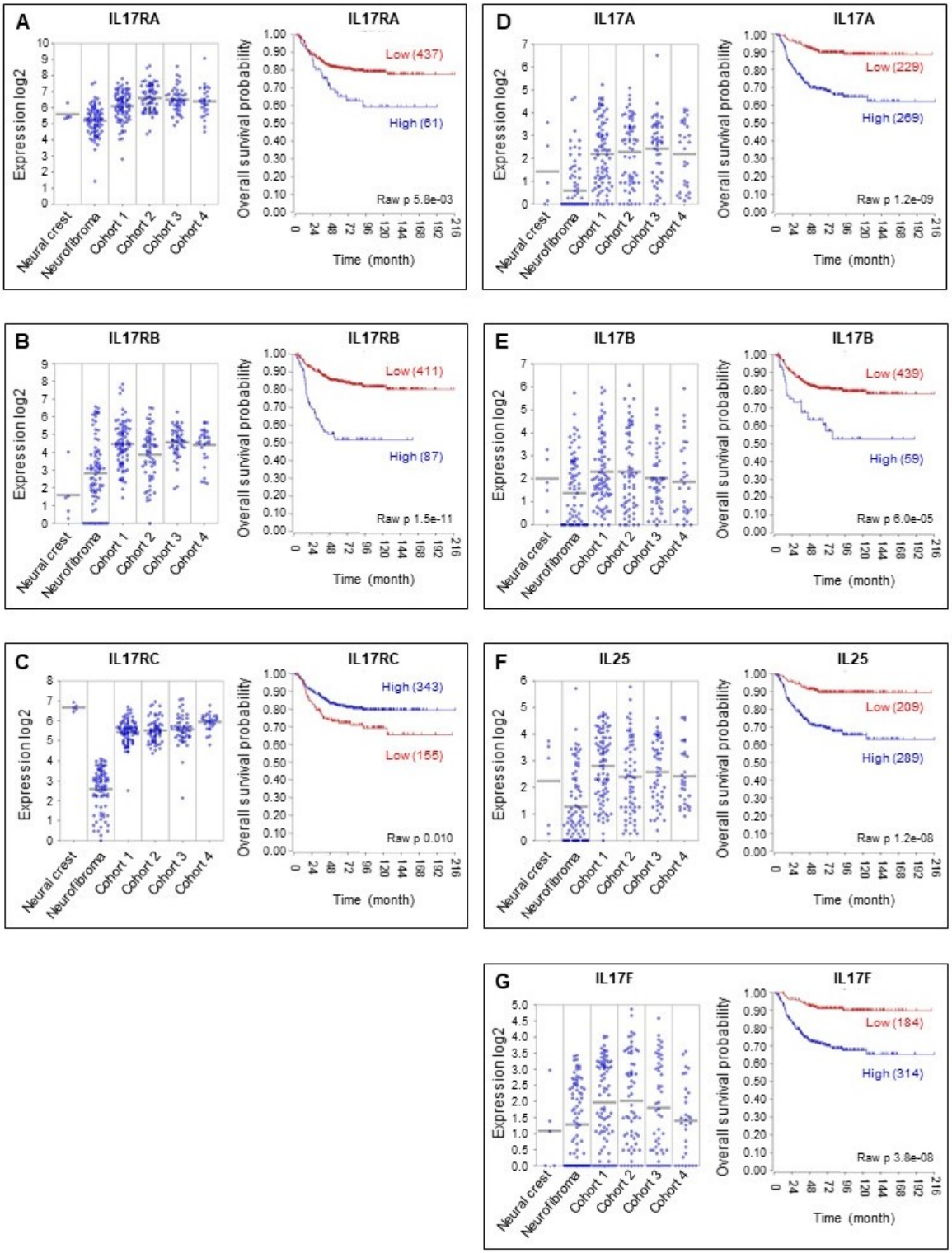

Figure 1: Expression of several IL-17 family members is increased in neuroblastoma and predicts poor overall survival probability.

Gene expression data were analyzed using the R2 database http://r2.amc.nl. The expression of *IL17RA* **(A)**, *IL17RB* **(B)**, *IL17RC* **(C)**, *IL-17A* **(D)**, *IL17B* **(E)**, *IL25* **(F)**, and *IL17F* **(G)** was compared between neural crest cells (Etchevers n=5), benign neurofibroma (Miller n=86) and 4 neuroblastoma cohorts (cohort 1: Versteeg, n=88, cohort 2: Delattre, n=64, cohort 3: Hiyama, n=51, cohort 4: Lastowska, n=30) using the MegaSampler feature. In addition, the prognostic value of IL-17 family members was evaluated in the SEQC-RPM-seqcnb1 dataset (n=498) using Kaplan-Meier survival estimates. The Kaplan-Meier scanning tool determines the most optimal cutoff between high and low gene expression and the lowest p-value (log-rank test) to evaluate significant differences between tumors with high or low expression of the respective gene.

3.2. *The receptors IL-17RA, IL-17RB, and IL-17RC are present in neuroblastoma tissue*

To evaluate the presence of IL-17RA, IL-17RB, and IL-17RC protein in neuroblastoma, we performed IHC on a panel of neuroblastoma tumors from different clinical stages and biological subsets. Figure 2 displays a representative staining from a neuroblastoma comprised of areas with poor differentiation and little Schwannian stroma and areas with a greater proportion of Schwannian stroma and differentiating cells (Figure 2E).

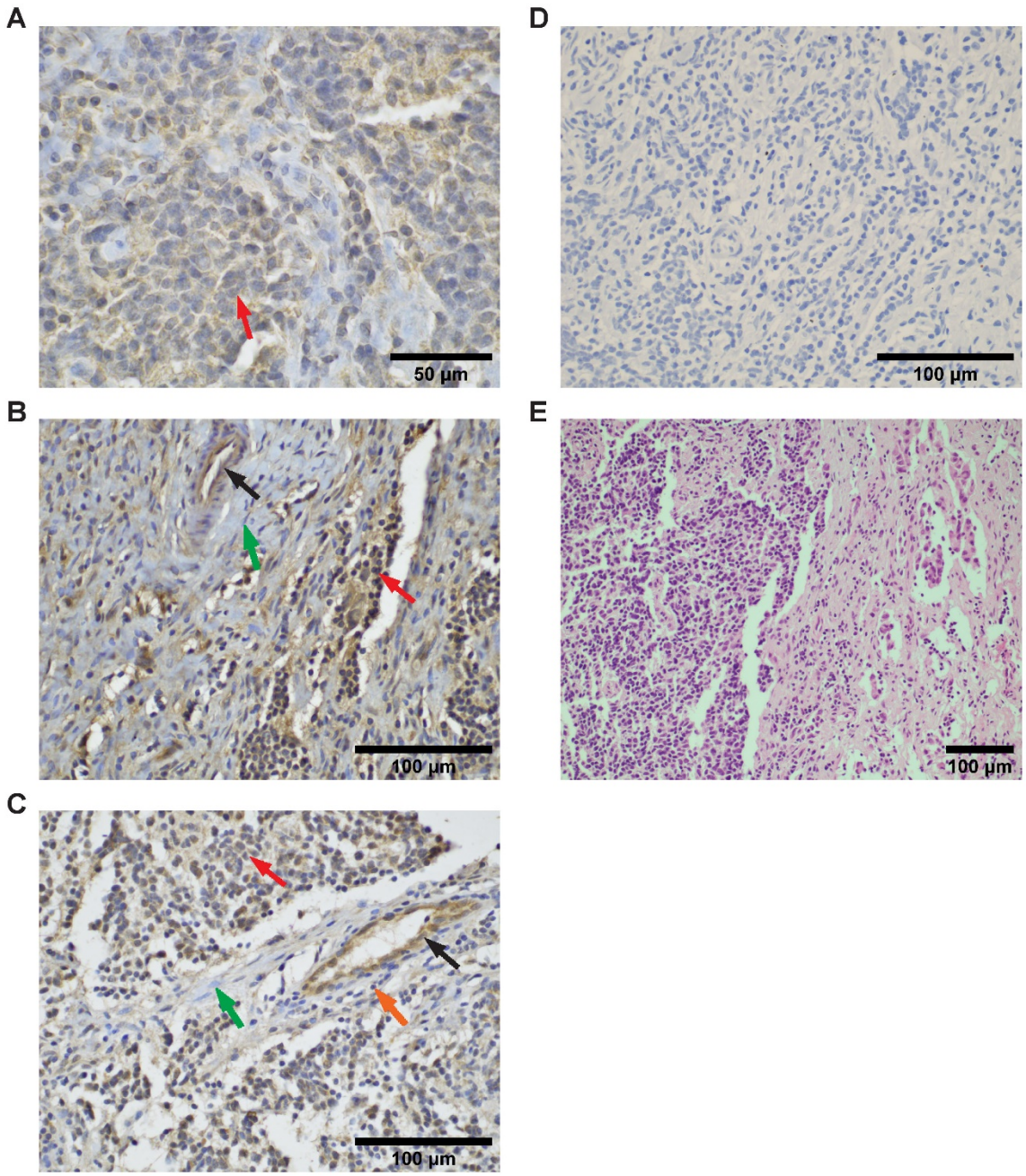

Figure 2: IL-17RA, IL-17RB, and IL-17RC protein are present in neuroblastoma tissue.
The presence of IL-17RA **(A)**, IL-17RB **(B)**, and IL-17RC **(C)** was determined using immunoperoxidase staining. Red arrows indicate neuroblasts, black arrows endothelial cells, green arrows fibroblasts, and orange arrows lymphocytes. Panel **D** and **E** displays isotype control staining and H&E staining respectively. The displayed images are representative stainings from a panel of neuroblastomas.

Neuroblasts displaying membranous positivity for IL-17RA were observed throughout the tissue section at varying degrees of staining intensity (Figure 2A, red arrow). IL-17RB positivity was observed in neuroblasts (Figure 2B red arrow) and endothelial cells (black arrow), while stromal cells were weakly positive or negative for IL-17RB (green arrow). A positive staining for IL-17RC was apparent in neuroblasts (Figure 2C, red arrow) and endothelial cells (black arrow) while stromal cells (green arrow) and lymphocytes (orange arrow) displayed no staining. Isotype control labeling (Figure 2D) was performed to ensure the absence of unspecific secondary antibody binding.

Among our panel of tissues, we noticed an intermixed ganglioneuroblastoma (supplementary Figure 2A) displaying pronounced lymphocyte infiltration. A big proportion of the infiltrate was identified as T cells by positive CD3 labeling (supplementary Figure 2B). Furthermore, a weak positive staining for IL-17A was observed among those T cells (supplementary Figure 2C).

3.3. *Several IL-17 receptor family members are expressed in neuroblastoma cell lines*

Using RT-PCR, we determined mRNA expression of the IL-17 family in neuroblastoma cell lines (Figure 3 and supplementary Figure 3). *IL17RC* mRNA was present at comparable levels in all neuroblastoma cell lines, whereas *IL17RA* and *IL17RB* were expressed at varying levels among the neuroblastoma cell lines (Figure 3A). In addition, we observed *IL17RD* expression in the majority and IL17RE expression in all neuroblastoma cell lines (supplementary Figure 3). Furthermore, we detected *IL17B* (Figure 3B) and *IL17D* (supplementary Figure 3) mRNA in the majority of neuroblastoma cells. Relatively low levels of *IL17F* were observed in some neuroblastoma cell lines, while *IL17A* and *IL25* expression was essentially absent (Figure 3B). Of note, in some neuroblastoma cell lines *IL17C* transcripts were detected (supplementary Figure 3).

As a prerequisite for functional studies, we determined the presence of IL-17RA, IL-17RB, and IL17RC protein in neuroblastoma cell lines using western blots (Figure 3C). IL-17RA was detected in SK-N-AS, SK-N-BE(2), SK-N-DZ, SK-N-FI, IMR-32, and SH-EP1 cells. Furthermore, a very faint band was observed for SK-N-SH cells. Moreover, IL-17RB and IL-17RC protein was present in all neuroblastoma cell lines. Of note, THP-1, A431, HepG2, and Jurkat cells served as controls in the expression studies based on the gene expression levels of IL-17 family members described for those cells in the human protein atlas www.proteinatlas.org and expression atlas https://www.ebi.ac.uk/gxa/home databases [68, 69].

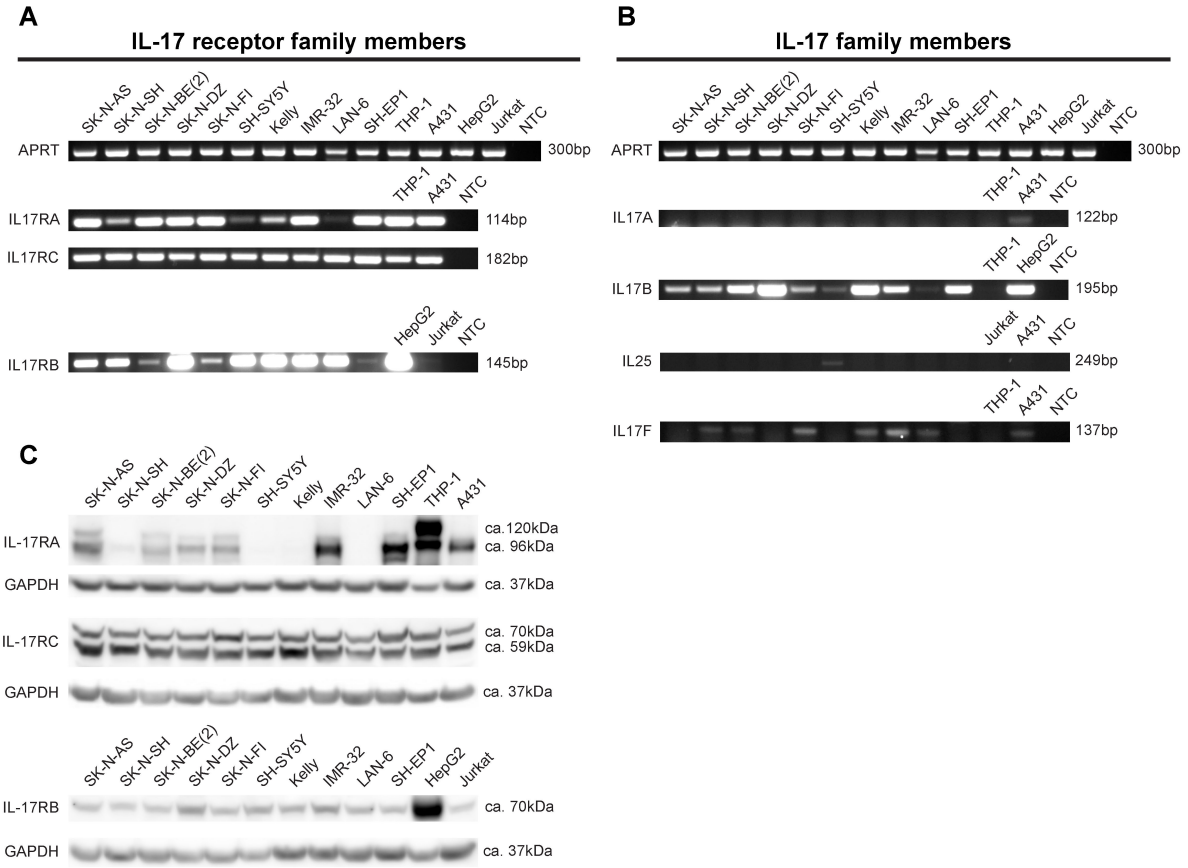

Figure 3: Several IL-17 receptor family members are expressed in neuroblastoma cell lines
RT-PCR analysis demonstrating mRNA expression of *IL17RA*, *IL17RB*, *IL17RC* **(A)** and *IL17B* **(B)** in different neuroblastoma cell lines. Low or no expression of *IL17A*, *IL25*, and *IL17F* among the examined cell lines **(B)**. Expression of the APRT housekeeping gene was examined to ensure equal RNA input. NTC, no template control. IL-17RA protein was detected by western blot in the majority of neuroblastoma cell lines and IL-17RB and IL-17RC protein were present in all examined neuroblastoma cell lines **(C)**. GAPDH was used as a loading control. THP-1, A431, HepG2, and Jurkat cells served as control cell lines for RT-PCR and western blot.

3.4. *Recombinant IL-17 proteins affect the cell viability of neuroblastoma cell lines only marginally*

To investigate the effect of IL-17 proteins on the cell viability of neuroblastoma cell lines, we stimulated SK-N-AS, SK-N-BE(2), SK-N-DZ, and SH-SY5Y cells with different concentrations of IL-17A homodimer, IL-17A/F heterodimer, IL-17B, and IL-25 for 48 h or 72 h and determined the cell viability by MTT assay. Table 3 and supplementary Table 1 display the cell viabilities after 48 h and 72 h, respectively. While IL-17A did not display a significant effect, IL-17A/F, IL-17B, and IL-25 modestly increased the cell viability of SK-N-AS cells after 48 h. The effect was sustained for IL-17A/F and to a lesser extend IL-17B after 72 h. Moreover, a significant decrease in cell viability was apparent following stimulation with high concentrations of IL-17A and IL-25 after 72 h. In contrast, IL-17A increased the cell viability of SK-N-BE(2) after 48 h and to a lesser extend 72 h. In addition, an increase in cell viability was seen in response to IL-17B after 48 h. Although a marginal increase in cell viability of SK-N-DZ cells

was observed after stimulation with IL-17A, IL-17B, and IL-17A/F after 48 h, the effect was not statistically significant. However, a significant decrease in cell viability occurred following stimulation with high levels of IL-25 after 48. In SH-SY5Y cells, a modest increase in cell viability was observed in response to IL-17A/F, IL-17B, and IL-25 whereas after 72 h a marginal decrease in cell viability was noticed following stimulation with high concentrations of IL-17A/F and IL-25.

Table 3: Cell viability of SK-N-AS, SK-N-BE(2), SK-N-DZ, and SH-SY5Y after stimulation with IL 17A, IL 17A/F, IL 17B or IL-25 for 48h

Treatment		SK-N-AS		SK-N-BE(2)		SK-N-DZ		SH-SY5Y	
		Cell viability (%) Mean ± SD	P value ctr. vs. treat.	Cell viability (%) Mean ± SD	P value ctr. vs. treat.	Cell viability (%) Mean ± SD	P value ctr. vs. treat.	Cell viability (%) Mean ± SD	P value ctr. vs. treat.
IL-17A	Control	100 ± 10.4		100 ± 12.4		100 ± 22.2		100 ± 16	
	0.01 ng/ml	101.4 ± 9.7	0.971	109.2 ± 11.9	0.004	97.7 ± 23.4	0.997	107.7 ± 15	0.086
	0.1 ng/ml	100.8 ± 9.3	0.997	109.8 ± 14	0.002	98.6 ± 29.6	>0.999	102.4 ± 15	0.944
	1 ng/ml	102.0 ± 11.7	0.883	107 ± 13.2	0.049	91.1 ± 23.3	0.559	106.1 ± 13.3	0.252
	10 ng/ml	100.1 ± 13.3	>0.999	104.9 ± 12.5	0.276	111.4 ± 28.2	0.314	107.8 ± 14.3	0.081
	100 ng/ml	96.4 ± 9.3	0.427	102.6 ± 13	0.848	102.5 ± 28.3	0.996	108.3 ± 16.6	0.055
IL-17A/F	Control	100 ± 8.7		100 ± 11.2		100 ±16.2		100 ± 12.8	
	0.01 ng/ml	108.6 ± 13.3	0.014	104.2 ± 11.2	0.514	104.7 ± 22.9	0.952	104.5 ± 15	0.721
	0.1 ng/ml	112.3 ± 12.8	<0.001	104.7 ± 10.2	0.393	116.5 ± 28.8	0.083	113.6 ± 15.3	0.004
	1 ng/ml	113.8 ± 8.7	<0.001	105.4 ± 12.9	0.264	111.4 ± 25.3	0.366	110.4 ± 12.2	0.041
	10 ng/ml	108.4 ± 13.7	0.017	101.7 ± 11.9	0.975	111.3 ± 31.5	0.374	110.8 ± 18.3	0.031
	100 ng/ml	108.3 ± 12.2	0.019	97.6 ± 10.9	0.935	112 ± 33.	0.488	112.1 ± 13.1	0.022
IL-17B	Control	100 ± 10.8		100 ± 11.9		100 ± 17.8		100 ± 12.1	
	0.01 ng/ml	107.3 ± 10.5	0.318	106.2 ± 15.7	0.319	111.4 ± 32.5	0.111	105.9 ± 14.3	0.367
	0.1 ng/ml	110.8 ± 14	0.048	111.7 ± 11.7	0.006	110.1 ± 21.7	0.195	108.7 ± 19.8	0.080
	1 ng/ml	112.9 ± 18.2	0.013	107.3 ± 10.5	0.175	111.8 ± 28	0.094	110.8 ± 17.3	0.015
	10 ng/ml	109.3 ± 16.6	0.127	107.3 ± 12.5	0.177	100.9 ± 18.0	>0.999	105.2 ± 13.5	0.509
	100 ng/ml	106.1 ± 21.9	0.493	107.4 ± 15.6	0.161	101.0 ± 26.1	>0.999	99.3 ± 12	>0.999
IL-25	Control	100 ± 7.9		100 ± 6		100 ± 11.9		100 ± 6.7	
	0.01 ng/ml	103.5 ± 13.1	0.681	100.5 ± 7.9	0.999	103.6 ± 16.6	0.806	105.6 ± 12.8	0.206
	0.1 ng/ml	109.2 ± 15.1	0.009	98.9 ± 9.1	0.960	100.2 ± 13.1	>0.999	108.8 ± 15.6	0.011
	1 ng/ml	104.9 ± 17.3	0.355	100.7 ± 9.7	0.994	103.5 ± 17.5	0.820	102.1 ± 16.2	0.935
	10 ng/ml	103.2 ± 15.5	0.762	96.8 ± 8.2	0.239	94.3 ± 16.7	0.384	107.3 ± 15.6	0.047
	100 ng/ml	97.4 ± 12.7	0.872	95 ± 9.7	0.023	84.7 ± 18.9	<0.001	100 ± 14	>0.999

Cell viability was measured by MTT assay after 48 h. The control was set as 100% viable cells. Data are presented as mean ± SD from at least three independent experiments. Dunnett's multiple comparison test was used to evaluate differences between control cells and the different concentrations of recombinant IL-17 proteins. P values of <0.05 were considered as statistically significant.

3.5. *IL-17 family members modulate the secretion of HGF and DKK-1 in neuroblastoma cells*

In order to investigate the effect of recombinant IL-17 proteins on cytokine secretion from neuroblastoma cell lines, we performed a pilot study using a cytokine profiler assay. Hepatocyte growth factor (HGF) and Dickkopf-related protein 1 (Dkk-1) were among the candidates whose secretion appeared to be modulated by IL-17 proteins (data not shown). Consequently, the effect of IL-17A, IL-17A/F, IL-17B and IL-25 was examined using ELISA kits to measure HGF and Dkk-1 in neuroblastoma cell supernatants. We observed that low concentrations of IL-17A (Figure 4A), IL-17B (Figure 4B), and IL-25 (Figure 4C) resulted in lower HGF amounts in SK-N-AS cell supernatants already after 1h incubation indicating a rapid response. Furthermore, while high amounts (50 ng/ml) of IL-17B and IL-25 did not affect the secretion of HGF, high amounts of IL-17A (25 or 50 ng/ml) stimulated the secretion of HGF. Of note, no clear effect on HGF secretion was seen following stimulation with IL-17A/F (data not shown).

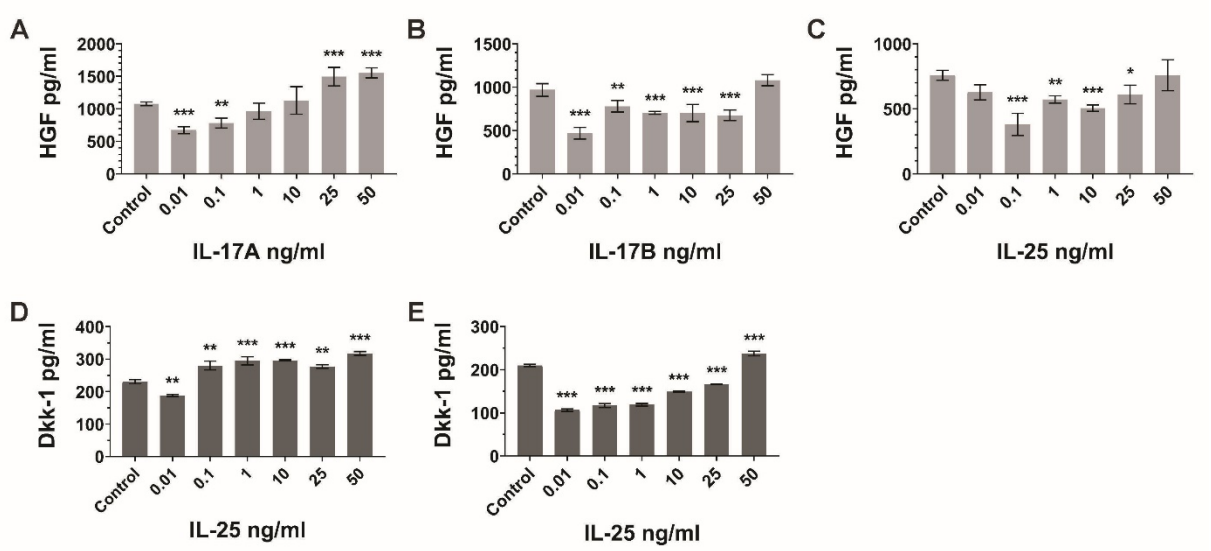

Figure 4: IL 17 family members modulate the secretion of HGF and DKK 1 in neuroblastoma cells.
Secreted HGF **(A-C)** and Dkk-1 **(D and E)** levels were determined by ELISA following stimulation with increasing concentrations of recombinant IL-17 proteins. Data are presented as mean ± SD. HGF levels in SK-N-AS cell supernatants after 1 h incubation with IL-17A **(A)**, IL-17B **(B)**, and IL-25 **(C)**. Dkk-1 level in cell supernatants of SK-N-AS **(D)** and SK-N-BE(2) **(E)** cells after IL-25 stimulation for 1h or 24h, respectively. Statistical analysis was performed using one-way ANOVAs and a significant effect of the stimulation $p<0.001$ was seen for all experiments. Dunnett's multiple comparison test was used to evaluate the difference between vehicle control and the different concentrations of IL-17A, IL-17B, and IL-25: * $p<0.05$; ** $p<0.01$; *** $p<0.001$.

Furthermore, we measured Dkk-1 in cell supernatants of SK-N-AS cells after 1 h and SK-N-BE(2) cells after 24 h of incubation with recombinant IL-25 (Figure 4D and 4E). While Dkk-1 is secreted rapidly from SK-N-AS cells, the secretion from SK-N-BE(2) cells occurs slower, therefore two different time points were chosen. While IL-25 stimulation resulted in increased Dkk-1 levels in SK-N-AS cell

supernatants at a range of 0.1-50 ng/ml, a decrease in Dkk-1 was observed in SK-N-BE(2) cell supernatants following stimulation with 0.01-25 ng/ml IL-25.

3.6. *IL-17A and IL-17B modulate in vitro migration of neuroblastoma cells*

Using an *in vitro* migration assay (scratch assay), we observed that IL-17A and IL-17B promoted the migration of SK-N-BE(2) cells as a more pronounced gap closure was observed after stimulation with 25 ng/ml recombinant protein (Figure 5).

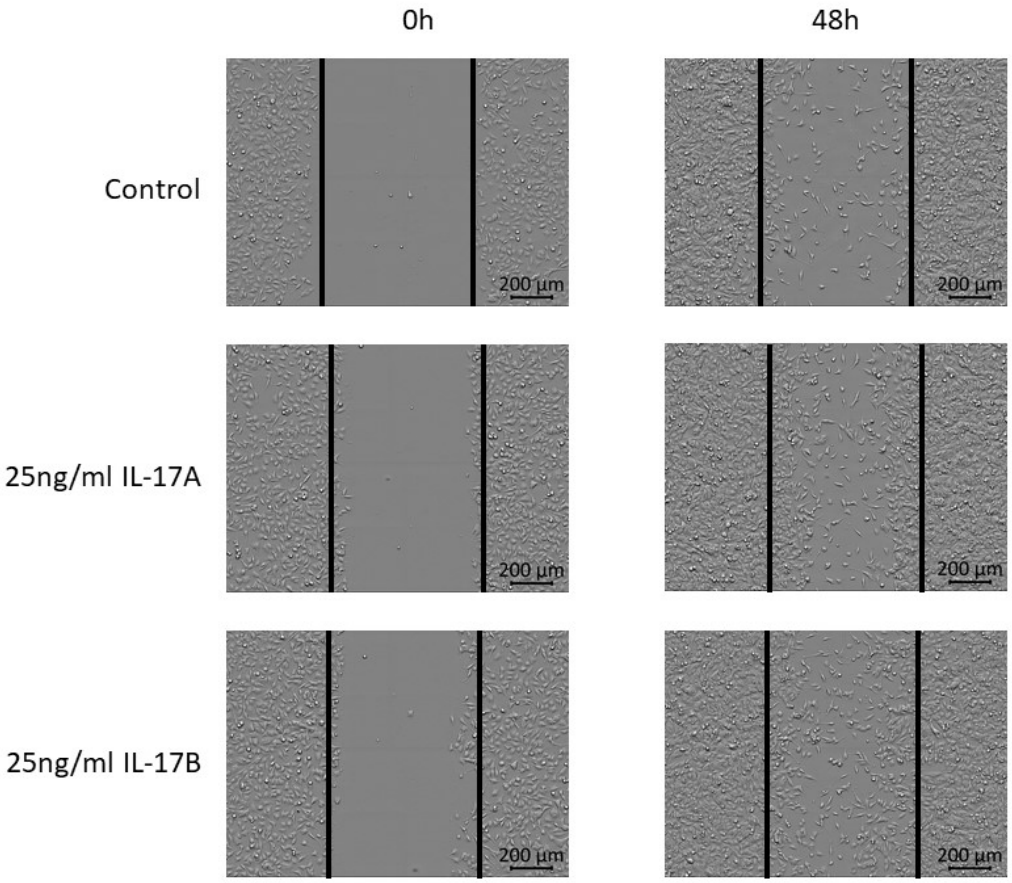

Figure 5: IL-17A and IL-17B promote *in vitro* migration of SK-N-BE(2) cells
In vitro migration of SK-N-BE(2) cells was determined by scratch assay. The figure displays representative images from three independent runs.

3.7. *IL-23p19 is expressed in neuroblastoma cell lines and tumor tissue*

Interleukin 23 is a heterodimeric interleukin consisting of the IL-12p40 and IL-23p19 subunit whose function is linked to IL-17A and IL-17F [39, 43]. Using RT-PCR, we determined the expression of *IL23A* (encoding the IL-23p19 subunit), *IL12B* (encoding the IL-12p40 subunit), and *IL23R* (Figure 6A). We detected *IL23A* transcripts in all of the examined neuroblastoma cell lines and the positive control cell lines THP-1 and A431. However, essentially no expression of *IL12B*, except for a faint band in LAN-6 cells, was observed in the neuroblastoma cell lines. Moreover, only a faint band could be seen in THP-1

and A431 cells serving as controls. With the exception of SK-N-AS cells, no or low expression of *IL23R* was detected.

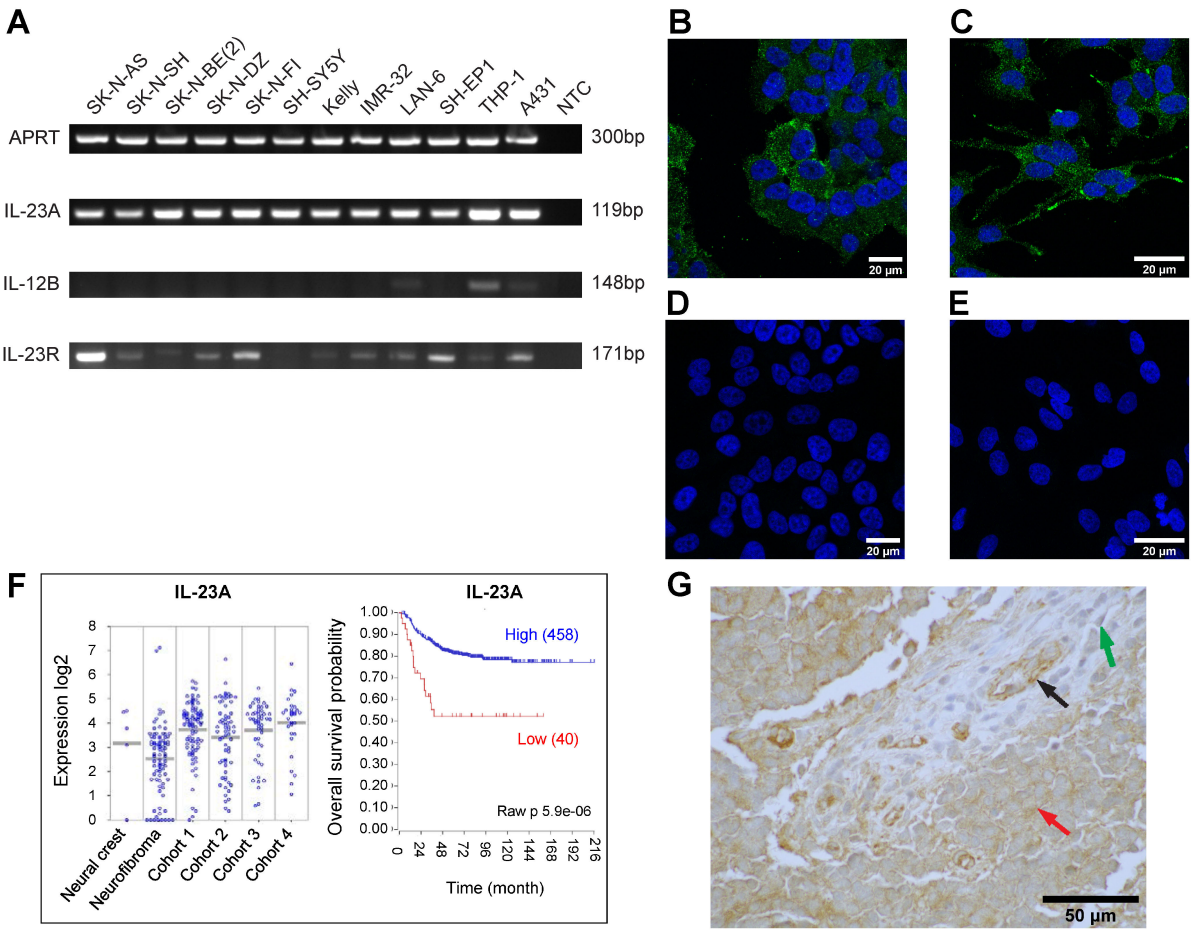

Figure 6: IL-23p19 is present in neuroblastoma cell lines and tumor tissue.
RT-PCR was used to examine the presence of *IL23A*, *IL12B*, and *IL23R* in neuroblastoma cell lines **(A)** with THP-1 and A431 cells serving as positive controls. NTC, no template control. Immunofluorescence labeling demonstrates the presence of IL-23p19 (green) in SK-N-AS **(B)** and SK-N-BE(2) **(C)** cells. The nuclei (blue) were stained with Hoechst 33342. Panel **(D)** and **(E)** display isotype control stainings for SK-N-AS and SK-N-BE(2), respectively. Gene expression data were analyzed using the R2 database http://r2.amc.nl. The expression of *IL23A* **(F)** was compared between neural crest cells (Etchevers n=5), benign neurofibroma (Miller n=86) and 4 neuroblastoma cohorts (cohort 1: Versteeg, n=88, cohort 2: Delattre, n=64, cohort 3: Hiyama, n=51, cohort 4: Lastowska, n=30). In addition, the prognostic value of *IL23A* was evaluated in the SEQC-RPM-seqcnb1 dataset (n=498) using Kaplan-Meier survival estimates. **(G)** Immunoperoxidase staining was used to evaluate the presence of IL-23p19 in neuroblastoma tissue. The red arrow indicates neuroblasts, black arrow endothelial cells, and green arrow fibroblasts. The image was captured at 900x and is a representative staining from a panel of neuroblastomas.

The presence of IL-23p19 protein was investigated using ICC. Both SK-N-AS and SK-N-BE(2) cells displayed a positive labeling for IL-23p19 in the cytoplasm (Figure 6B and 6C). While some cells demonstrated a strong staining in patch-like structures, other cells were less intensely stained. No staining was observed in cells incubated with an isotype control antibody instead of an IL-23p19-specifc antibody (Figure 6D and 6E).

In addition, we compared the expression of IL23A in four neuroblastoma cohorts to neural crest cells and benign neurofibroma using the publically available R2: Genomics Analysis and Visualization Platform (http://r2.amc.nl). While the expression of IL-23A is to some extend higher in the neuroblastoma cohorts compared to neurofibroma, no difference to the neural crest cells was apparent (Figure 6F). Furthermore, we observed that low IL23A expression correlated to decreased overall survival probability (Figure 6F).

Moreover, we examined the expression of IL-23p19 in a panel of neuroblastomas. Figure 6G displays a representative staining with positive cytoplasmic and membranous labeling in neuroblasts (red arrow) and endothelial cells (black arrow), whereas stromal cells showed a weak positive-negative staining (green arrow).

In a pilot study, we investigated the presence of IL-23p19 positive cells in the TH-MYCN neuroblastoma mouse model. Using flow cytometry, we observed the presence of IL-23p19 in $CD11b^{+}$ myeloid cells and tumor or tumor-stroma cells ($CD45^{-}$) in tumor-bearing mice (supplementary Figure 4A). Intracellular staining of splenocytes (supplementary Figure 4A) and cytokine analysis in sera (supplementary Figure 4C) from tumor-bearing mice did not indicate increased IL23 expression compared to wild-type animals, however, cytokine analysis of dissociated organs or tumor material confirmed an increased expression of IL-23p19 in spleens and tumors from tumor-bearing TH-MCYN mice (supplementary Figure 4B). Of note, we also observed elevated levels of IL-1β and IL-10 in the tumor and spleen (supplementary Figure 4D and 4E) and increased IL-1β in the sera (supplementary Figure 4C) from tumor-bearing mice. Furthermore, no changes in IL-17A and IL-17F were apparent (supplementary Figure 4C).

3.8. *Neuroblastoma cell lines contain different splice variants of IL23A*

Using RT-PCR and different *IL23A*-specifc primer combinations, we obtained distinct PCR-product pattern for each primer set in both neuroblastoma and control cell lines (Figure 7A). Consequently, we designed primers spanning the entire *IL23A* gene to amplify whole *IL23A* transcript variants. The resulting PCR products were separated by gel electrophoresis and the highlighted bands were sequenced (Figure 7B). The obtained sequences (supplementary material) demonstrated the presence of *IL23A* transcripts at different stages of splicing with three, two or one intron remaining (Figure 7C). Of note, the sequencing results indicated that the introns of the *IL23A* transcript are spliced out in a specific order with intron 3 being removed first followed by intron 2 and lastly intron 1. Furthermore, we observed a short transcript containing part of exon 1 and exon 4 (blue and green segment in variant 5) (Figure 7C) that were spliced together in frame.

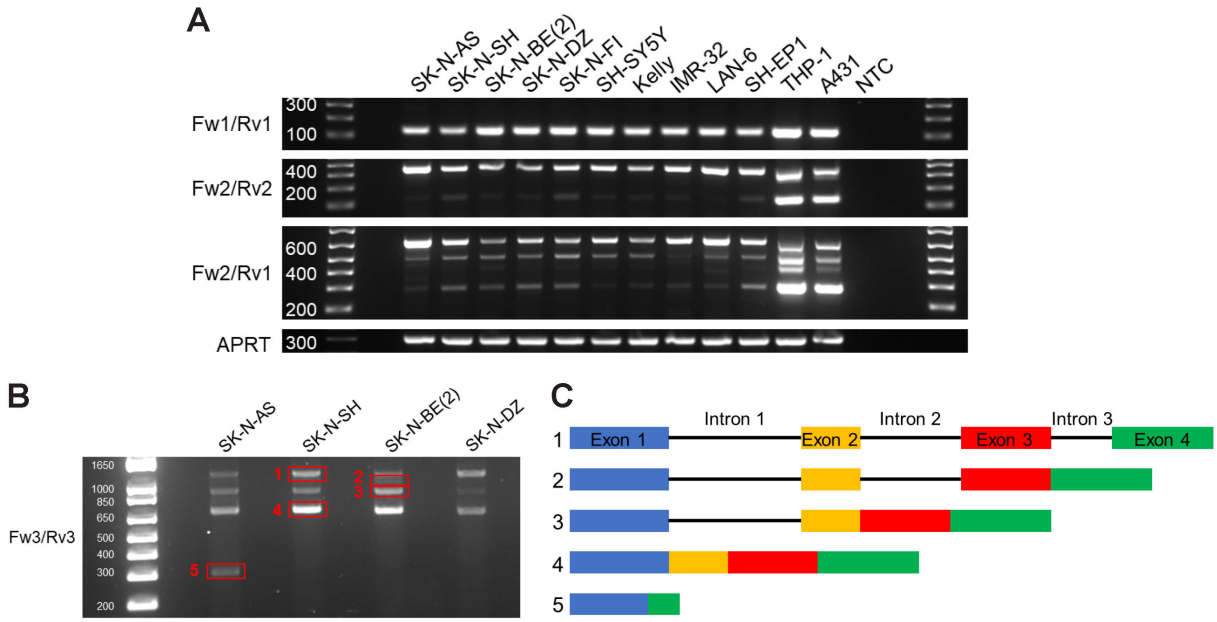

Figure 7: Neuroblastoma cell lines contain different splice variants of IL23A.
(A) IL23A transcripts were analyzed by RT-PCR using two different primer sets (Fw1/Rv1 and Fw2/Rv2) or a combination of both (Fw2/Rv1). APRT served as a housekeeping gene ensuring equal RNA input for all cell lines. **(B)** Full-length IL23A transcripts were amplified and DNA from the highlighted bands was extracted and sequenced. **(C)** Schematic drawing of the obtained sequences with numbers corresponding to the specific bands in panel **(B)**.

4. Discussion

Neuroblastomas are a clinically and biologically heterogenic group of cancers occurring in early childhood with a median age of 18 month at diagnosis [52]. In recent years, the complex interactions within the neuroblastoma microenvironment have gained increased attention and have led to promising novel therapeutic approaches [52, 54]. The IL-17 family is a group of inflammatory cytokines and their receptors with important functions in host defense and autoimmunity [5]. In particular, the IL-23/IL-17A axis has been implicated in autoimmune diseases, such as psoriasis, and different cancers, where both tumor-promoting and tumor-suppressing effects have been observed [11, 39].

In the present study, we investigated the expression of the IL-17 family and their potential prognostic implication in neuroblastoma. We observed that high expression of the receptors *IL17RA*, *IL17RB*, *IL17RD* and the interleukins *IL17A*, *IL17B*, *IL17C*, *IL25*, and *IL17F* correlated with a reduced overall survival probability in a large (n=498) neuroblastoma dataset. Furthermore, we noticed a positive correlation between *IL17RB* as well as *IL17RD* and the *MYCN* oncogene (supplementary Figure 5A); while a negative correlation was observed between *IL17RA* and *MYCN* using the same dataset. This observation was confirmed using an additional dataset (supplementary Figure 5B). *MYCN*-amplification is an important marker for highly aggressive tumors and poor survival [70, 71] and a potential link between *MYCN* and *IL17RB* as well as *IL17RD* should be investigated further.

In addition, we examined the expression of the IL-17 family members in neuroblastoma cell lines and observed mRNA for IL17RA-RE, IL17B, and IL17D in the majority of examined neuroblastoma cell lines. Although the expression of *IL17RE* and *IL17RD* in neuroblastoma is very interesting and should be investigated further, we focused in this study on the, to date, best understood IL-17 receptors, IL-17RA, IL-17RB, and IL-17RC whose protein we detected both in neuroblastoma cell lines and tissues. While IL-17RA is ubiquitously expressed in different cell types with higher levels in hematopoietic tissues, higher IL-17RC expression has been observed in non-immune cells [72]. Interestingly, despite lower expression of IL-17RA in fibroblasts, epithelial and endothelial cells compared to immune cells they are particularly responsive to IL-17A [72]. Of note, preliminary results indicate that IL-17B protein is present in neuroblastoma cell lines. However, further studies are necessary to confirm the data.

Furthermore, we evaluated the effect of IL-17A and IL-17A/F (ligands for IL-17RA/RC), IL-17B (ligand for IL-17RB), and IL-25 (ligand for IL-17RA/RB) on cell viability, *in vitro* migration, and the release of HGF and Dkk-1. We observed only marginal effects of IL-17 proteins on the cell viability of neuroblastoma cell lines *in vitro.* Similar observations have previously been made in cervical cancer cells and non-small cell lung cancer in which stimulation or transfection with IL-17A did not affect *in vitro* cell growth [73, 74]. However, overexpression of IL-17A promoted tumor growth *in vivo* [73, 74]. Modest *in vitro* effects but potent *in vivo* functions of IL-17s have been previously described in

immunity and inflammation and can to some extend be explained by the ability of IL-17 to work potently in concert with other cytokines and inflammatory mediators, such as TNFα and IL-1β [75]. In the context of cancer biology, IL-17A can contribute to the tumor microenvironment by stimulating the release of pro-angiogenic factors, for example VEGF [76] and cytokines and chemokines, such as IL-6 [73, 77], CXCL1, CXCL5, CXCL6, and CXCL8 [74]. Furthermore, IL-17 can contribute to the recruitment of tumor-supporting cells, such as suppressive myeloid cells [78, 79]. IL-17A is a multifunctional cytokine and can therefore also display potent anti-tumor functions, for example through the recruitment of NK cells and indirect activation of T cells [24, 80].

Of note, we observed a marginal effect of IL-17A/F and IL-25 on the cell viability of SH-SY5Y although those cells did not express detectable levels of IL-17RA protein (determined by western blot). However, recently a functional IL-17F/IL-17RC axis has been observed and IL-17RD was described as an alternative receptor for IL-17A [81, 82]. The continuous emergence of novel IL-17 ligand/receptor combinations may indicate that additional, to date unknown, combinations exist that might explain the effects we observed in the SH-SY5Y cell line.

In this study, IL-17A, IL-17B, and IL-25 affected HGF secretion in SK-N-AS cells. While low concentrations of IL-17A, IL-17B, and IL-25 reduced HGF levels in SK-N-AS supernatants, high concentrations had no effect or in the case of IL-17A increased HGF secretion. HGF signals through c-MET and is known to promote proliferation, migration, angiogenesis, metastasis, and drug resistance in cancer [83, 84]. In neuroblastoma, elevated HGF is a marker of poor prognosis and promotes neuroblastoma progression [85, 86]. Furthermore, c-MET inhibition reduces neuroblastoma proliferation and migration [87].

In addition, IL-25 modulated the secretion of Dkk-1 in SK-N-AS and SK-N-BE(2) cells. While IL-25 increased the levels of Dkk-1 in the supernatant of SK-N-AS cells it was decreased in SK-N-BE(2) cells following IL-25 stimulation, indicating cell-type specific effects of IL-25. Dkk-1 is an antagonist of canonical Wnt signaling [88]. In neuroblastoma, MYCN downregulates Dkk-1 and upregulation of Dkk-1 reduces the proliferation of a *MYCN*-amplified cell line indicating anti-tumorigenic functions [89]. Interestingly, Dkk-1 also displays immunomodulatory functions. Dkk-1 neutralization in mice injected with Lewis lung carcinoma cells reduced MDSC numbers, increased the presence of CD4+ and CD8+ T cells, and impaired tumor growth [90]. Concentration-dependent and cell type-specific effects of IL-17A, IL-17B, and IL-25 on HGF and Dkk-1 secretion by neuroblastoma cells indicate a fine tuned cellular responses to IL-17 family members. Further studies are required to investigate responses to IL-17s more detailed and in the context of the tumor microenvironment.

In this study, we observed that stimulation with IL-17A and IL-17B promoted the *in vitro* migration of SK-N-BE(2). A stimulatory effect of IL-17A on cell migration has previously been described in, among

others, glioma [22] and gastric cancer [91]. Moreover, IL-17B has been demonstrated to promote proliferation and migration of gastric cancer cells [27].

Considering the multifunctional role of Interleukin 17 family members in immunity, inflammatory diseases, and cancer, *in vivo* studies are necessary to determine the effects of IL-17s on the different components of the neuroblastoma microenvironment.

IL-17A and IL-17F functions are closely connected to IL-23 since IL-17A/F secretion from the major IL-17A/F producing cells (Th17, γδ T cells, ILC3, and NKT cells) occurs in response to IL-23 [38, 39]. However, IL-23 independent IL-17A/F expression has also been described in NKT and γδ T cells [40-42]. The IL-23/IL-17 axis has been linked to different autoimmune diseases, such as psoriasis and Crohn's disease [10]. However, there is increasing evidence that cellular sources of IL-17A and the microenvironmental context must be taken into account when targeting the IL-23/IL-17 axis. While in psoriasis neutralization of IL-23, IL-17A, and IL-17RA has been demonstrated as a promising therapeutic approach, IL-23 blockade but not IL-17A blockade protected against inflammatory gut diseases in a preclinical model [10]. A thorough understanding of both IL-23 and IL-17 function is, therefore, necessary to evaluate their role in any context. Consequently, we investigated the presence of IL-23 in neuroblastoma and observed IL-23p19 presence in both neuroblastoma cell lines and tumor tissue. However, we did not detect any significant expression of *IL12B* mRNA in neuroblastoma cell lines. *IL12B* encodes the IL-12p40 subunit that forms functional IL-23 together with the IL-23p19 subunit [43]. While IL-23 is mainly expressed by dendritic cell and macrophages, other sources, such as mouse intestinal epithelial cells, have also been described [92]. Moreover, expression of IL-23p19 but not IL-12p40 has been observed in different cells, for example, gastric and intestinal epithelial cells and keratinocytes [92]. Espígol-Frigolé et al. demonstrated that endothelial cells express IL-23p19, but not IL-12p40, and that IL-23p19 associates with gp130 promoting STAT3 (signal transducer and activator of transcription 3) activation [93]. Further studies are therefore necessary to determine whether IL-23p19 has IL-12p40-independent functions in neuroblastoma or if specific stimuli are required to induce *IL12B* expression.

Using the publically available R2 database http://r2.amc.nl, we observed that low IL-23 expression correlated to a poor overall survival probability. Cytokine expression is known to be very dynamic and post-transcriptional regulation is frequently observed. Several mechanisms have also been described that regulate IL23A RNA stability and decay [92]. Therefore, presence of transcripts does not necessarily correlate to protein presence and cytokine function. In this study, we observed that *IL23A* transcripts are present at different splice stages in neuroblastoma cells. Specific stimuli might promote or inhibit splicing of *IL23A* transcripts to enable a rapid increase or decrease in IL-23p19 protein. Additional studies are required to determine whether specific stimuli known to regulate *IL23A* expression in other cell types, such as TNFα, IL-10, PGE_2, affect *IL23A* expression in neuroblastoma

cells. Furthermore, we detected a short IL-23A splice variant where the beginning of exon 1 is spliced, in frame, to the end of exon 4. Whether this variant is translated into a peptide chain and has biological activity remains to be examined.

In a pilot study, we observed the presence of IL-23p19 positive myeloid cells and tumor or stroma cells in the transgenic TH-MYCN mouse model, indicating that this model is suitable to investigate the role of IL-23 in neuroblastoma tumorigenesis *in vivo*. However, we did not observe any difference in IL-17A and IL-17F serum levels between tumor-bearing and wildtype mice. Of note, we also observed increased levels of IL-1β in serum, spleens, and tumors of tumor-bearing mice in comparison to wildtype mice. IL-1β is a master regulator of inflammation with diverse pro-tumorigenic functions [94].

5. Conclusion

Our findings demonstrate the presence and prognostic value of different IL-17 family members in neuroblastoma. Furthermore, recombinant IL-17 proteins modulate cell migration and Dkk-1 and HGF levels *in vitro*. In addition, IL-23p19 is present in neuroblastoma cell lines and tumor tissue. However, the specific functions of the IL-17 family and IL-23 in the neuroblastoma tumor microenvironment and their potential as therapeutic targets remains to be investigated.

Abbreviations

IL- Interleukin, HGF- Hepatocyte growth factor, Dkk-1- Dickkopf-related protein 1, MDSC- Myeloid-derived suppressor cell, NK cells- Natural killer cells, Th cells- Helper T cells, ILC- Innate lymphoid cell, NKT cell- Natural killer T cell, COX- Cyclooxygenase, PGE_2- Prostaglandin E2, mPGES- Microsomal prostaglandin E synthase-1

Funding

This study was funded with grants from the University of Tromsø, The Norwegian Childhood Cancer Society, The Norwegian Childhood Cancer Society Region Troms and Finnmark, Erna and Olav Aakre Foundation for Cancer Research (A20310), Tromsø, Norway, the Swedish Childhood Cancer Foundation, the Swedish Cancer Foundation, and the Swedish Foundation for Strategic Research (www.nnbcr.se).

Acknowledgements

We thank Maria Ludvigsen for her assistance with the RT-PCRs and *in vitro* migration assays, Dr. Tweddle for the kind gift of LAN-6 cells, and the Centre of Forensic Genetics, University of Tromsø for STR profiling.

Conflict of interest

The authors declare no conflict of interest.

Supplementary Material

Supplementary Figure 1: Expression of *IL17RD* and *IL17C* is increased in neuroblastoma and predicts poor overall survival probability

Supplementary Figure 2: IL-17A is present in a intermixed ganglioneuroblastoma with high T cell infiltration

Supplementary Figure 3: Expression of IL17RD, IL17RE, IL17C, and IL17D in neuroblastoma cell lines

Supplementary Figure 4: IL 23p19 is increased in myeloid cells and tumor and/or stroma cells of tumor-bearing TH-MYCN mice

Supplementary Figure 5: Correlation between IL17RB, IL17RD, IL17RA and MYCN expression

Supplementary Table 1: Cell viability of SK-N-AS, SK-N-BE(2), SK-N-DZ, and SH-SY5Y after stimulation with IL 17A, IL 17A/F, IL 17B or IL-25 for 72h

Supplementary Material and Methods

Appendix: Sequences of *IL23A* splice variants

References

1. Colotta F, Allavena P, Sica A, Garlanda C, Mantovani A. Cancer-related inflammation, the seventh hallmark of cancer: links to genetic instability. Carcinogenesis. 2009;30(7):1073-81.

2. Hanahan D, Weinberg RA. Hallmarks of cancer: the next generation. Cell. 2011;144(5):646-74.

3. Crusz SM, Balkwill FR. Inflammation and cancer: advances and new agents. Nature Reviews Clinical Oncology. 2015;12(10):584-96.

4. Coussens LM, Zitvogel L, Palucka AK. Neutralizing tumor-promoting chronic inflammation: a magic bullet? Science. 2013;339(6117):286-91.

5. Monin L, Gaffen SL. Interleukin 17 Family Cytokines: Signaling Mechanisms, Biological Activities, and Therapeutic Implications. Cold Spring Harb Perspect Biol. 2018;10(4).

6. Wright JF, Bennett F, Li B, Brooks J, Luxenberg DP, Whitters MJ, et al. The human IL-17F/IL-17A heterodimeric cytokine signals through the IL-17RA/IL-17RC receptor complex. Journal of immunology. 2008;181(4):2799-805.

7. Wright JF, Guo Y, Quazi A, Luxenberg DP, Bennett F, Ross JF, et al. Identification of an interleukin 17F/17A heterodimer in activated human CD4+ T cells. J Biol Chem. 2007;282(18):13447-55.

8. Yao Z, Spriggs MK, Derry JM, Strockbine L, Park LS, VandenBos T, et al. Molecular characterization of the human interleukin (IL)-17 receptor. Cytokine. 1997;9(11):794-800.

9. Rouvier E, Luciani MF, Mattei MG, Denizot F, Golstein P. CTLA-8, cloned from an activated T cell, bearing AU-rich messenger RNA instability sequences, and homologous to a herpesvirus saimiri gene. Journal of immunology. 1993;150(12):5445-56.

10. Bianchi E, Rogge L. The IL-23/IL-17 pathway in human chronic inflammatory diseases-new insight from genetics and targeted therapies. Genes Immun. 2019.

11. Yuzhalin AE, Kutikhin AG. Interleukin-17 Superfamily and Cancer. Interleukins in Cancer Biology2015. p. 261-89.

12. Wang K, Kim MK, Di Caro G, Wong J, Shalapour S, Wan J, et al. Interleukin-17 receptor a signaling in transformed enterocytes promotes early colorectal tumorigenesis. Immunity. 2014;41(6):1052-63.

13. Housseau F, Wu S, Wick EC, Fan H, Wu X, Llosa NJ, et al. Redundant Innate and Adaptive Sources of IL17 Production Drive Colon Tumorigenesis. Cancer research. 2016;76(8):2115-24.

14. Benevides L, da Fonseca DM, Donate PB, Tiezzi DG, De Carvalho DD, de Andrade JM, et al. IL17 Promotes Mammary Tumor Progression by Changing the Behavior of Tumor Cells and Eliciting Tumorigenic Neutrophils Recruitment. Cancer research. 2015;75(18):3788-99.

15. Cochaud S, Giustiniani J, Thomas C, Laprevotte E, Garbar C, Savoye AM, et al. IL-17A is produced by breast cancer TILs and promotes chemoresistance and proliferation through ERK1/2. Sci Rep. 2013;3:3456.

16. Coffelt SB, Kersten K, Doornebal CW, Weiden J, Vrijland K, Hau CS, et al. IL-17-producing gammadelta T cells and neutrophils conspire to promote breast cancer metastasis. Nature. 2015;522(7556):345-8.

17. Nam JS, Terabe M, Kang MJ, Chae H, Voong N, Yang YA, et al. Transforming growth factor beta subverts the immune system into directly promoting tumor growth through interleukin-17. Cancer research. 2008;68(10):3915-23.

18. Zhu X, Mulcahy LA, Mohammed RA, Lee AH, Franks HA, Kilpatrick L, et al. IL-17 expression by breast-cancer-associated macrophages: IL-17 promotes invasiveness of breast cancer cell lines. Breast Cancer Res. 2008;10(6):R95.

19. Zhang Y, Zoltan M, Riquelme E, Xu H, Sahin I, Castro-Pando S, et al. Immune Cell Production of Interleukin 17 Induces Stem Cell Features of Pancreatic Intraepithelial Neoplasia Cells. Gastroenterology. 2018;155(1):210-23 e3.

20. McAllister F, Bailey JM, Alsina J, Nirschl CJ, Sharma R, Fan H, et al. Oncogenic Kras activates a hematopoietic-to-epithelial IL-17 signaling axis in preinvasive pancreatic neoplasia. Cancer cell. 2014;25(5):621-37.

21. Parajuli P, Anand R, Mandalaparty C, Suryadevara R, Sriranga PU, Michelhaugh SK, et al. Preferential expression of functional IL-17R in glioma stem cells: potential role in self-renewal. Oncotarget. 2016;7(5):6121-35.

22. Wang B, Zhao CH, Sun G, Zhang ZW, Qian BM, Zhu YF, et al. IL-17 induces the proliferation and migration of glioma cells through the activation of PI3K/Akt1/NF-kappaB-p65. Cancer letters. 2019;447:93-104.

23. Ma Y, Aymeric L, Locher C, Mattarollo SR, Delahaye NF, Pereira P, et al. Contribution of IL-17-producing gamma delta T cells to the efficacy of anticancer chemotherapy. The Journal of experimental medicine. 2011;208(3):491-503.

24. Wang JT, Li H, Zhang H, Chen YF, Cao YF, Li RC, et al. Intratumoral IL17-producing cells infiltration correlate with antitumor immune contexture and improved response to adjuvant chemotherapy in gastric cancer. Ann Oncol. 2019;30(2):266-73.

25. Huang CK, Yang CY, Jeng YM, Chen CL, Wu HH, Chang YC, et al. Autocrine/paracrine mechanism of interleukin-17B receptor promotes breast tumorigenesis through NF-kappaB-mediated antiapoptotic pathway. Oncogene. 2014;33(23):2968-77.

26. Laprevotte E, Cochaud S, du Manoir S, Lapierre M, Dejou C, Philippe M, et al. The IL-17B-IL-17 receptor B pathway promotes resistance to paclitaxel in breast tumors through activation of the ERK1/2 pathway. Oncotarget. 2017;8(69):113360-72.

27. Bie Q, Sun C, Gong A, Li C, Su Z, Zheng D, et al. Non-tumor tissue derived interleukin-17B activates IL-17RB/AKT/beta-catenin pathway to enhance the stemness of gastric cancer. Sci Rep. 2016;6:25447.

28. Bie Q, Zhang B, Sun C, Ji X, Barnie PA, Qi C, et al. IL-17B activated mesenchymal stem cells enhance proliferation and migration of gastric cancer cells. Oncotarget. 2017;8(12):18914-23.

29. Rickel EA, Siegel LA, Yoon BR, Rottman JB, Kugler DG, Swart DA, et al. Identification of functional roles for both IL-17RB and IL-17RA in mediating IL-25-induced activities. Journal of immunology. 2008;181(6):4299-310.

30. Lee J, Ho WH, Maruoka M, Corpuz RT, Baldwin DT, Foster JS, et al. IL-17E, a novel proinflammatory ligand for the IL-17 receptor homolog IL-17Rh1. J Biol Chem. 2001;276(2):1660-4.

31. Benatar T, Cao MY, Lee Y, Lightfoot J, Feng N, Gu X, et al. IL-17E, a proinflammatory cytokine, has antitumor efficacy against several tumor types in vivo. Cancer Immunol Immunother. 2010;59(6):805-17.

32. Furuta S, Jeng YM, Zhou L, Huang L, Kuhn I, Bissell MJ, et al. IL-25 causes apoptosis of IL-25R-expressing breast cancer cells without toxicity to nonmalignant cells. Sci Transl Med. 2011;3(78):78ra31.

33. Yin SY, Jian FY, Chen YH, Chien SC, Hsieh MC, Hsiao PW, et al. Induction of IL-25 secretion from tumour-associated fibroblasts suppresses mammary tumour metastasis. Nat Commun. 2016;7:11311.

34. Thelen TD, Green RM, Ziegler SF. Acute blockade of IL-25 in a colitis associated colon cancer model leads to increased tumor burden. Sci Rep. 2016;6:25643.

35. Song X, Gao H, Lin Y, Yao Y, Zhu S, Wang J, et al. Alterations in the microbiota drive interleukin-17C production from intestinal epithelial cells to promote tumorigenesis. Immunity. 2014;40(1):140-52.

36. Jungnickel C, Schmidt LH, Bittigkoffer L, Wolf L, Wolf A, Ritzmann F, et al. IL-17C mediates the recruitment of tumor-associated neutrophils and lung tumor growth. Oncogene. 2017;36(29):4182-90.

37. O'Sullivan T, Saddawi-Konefka R, Gross E, Tran M, Mayfield SP, Ikeda H, et al. Interleukin-17D mediates tumor rejection through recruitment of natural killer cells. Cell Rep. 2014;7(4):989-98.

38. Gaffen SL, Jain R, Garg AV, Cua DJ. The IL-23-IL-17 immune axis: from mechanisms to therapeutic testing. Nature reviews Immunology. 2014;14(9):585-600.

39. Veldhoen M. Interleukin 17 is a chief orchestrator of immunity. Nature immunology. 2017;18(6):612-21.

40. Lee JS, Tato CM, Joyce-Shaikh B, Gulen MF, Cayatte C, Chen Y, et al. Interleukin-23-Independent IL-17 Production Regulates Intestinal Epithelial Permeability. Immunity. 2015;43(4):727-38.

41. Yoshiga Y, Goto D, Segawa S, Ohnishi Y, Matsumoto I, Ito S, et al. Invariant NKT cells produce IL-17 through IL-23-dependent and -independent pathways with potential modulation of Th17 response in collagen-induced arthritis. Int J Mol Med. 2008;22(3):369-74.

42. Hasegawa E, Sonoda KH, Shichita T, Morita R, Sekiya T, Kimura A, et al. IL-23-independent induction of IL-17 from gammadeltaT cells and innate lymphoid cells promotes experimental intraocular neovascularization. Journal of immunology. 2013;190(4):1778-87.

43. Oppmann B, Lesley R, Blom B, Timans JC, Xu Y, Hunte B, et al. Novel p19 protein engages IL-12p40 to form a cytokine, IL-23, with biological activities similar as well as distinct from IL-12. Immunity. 2000;13(5):715-25.

44. Teng MW, Bowman EP, McElwee JJ, Smyth MJ, Casanova JL, Cooper AM, et al. IL-12 and IL-23 cytokines: from discovery to targeted therapies for immune-mediated inflammatory diseases. Nature medicine. 2015;21(7):719-29.

45. Happel KI, Zheng M, Young E, Quinton LJ, Lockhart E, Ramsay AJ, et al. Cutting edge: roles of Toll-like receptor 4 and IL-23 in IL-17 expression in response to Klebsiella pneumoniae infection. Journal of immunology. 2003;170(9):4432-6.

46. Lyakh L, Trinchieri G, Provezza L, Carra G, Gerosa F. Regulation of interleukin-12/interleukin-23 production and the T-helper 17 response in humans. Immunological reviews. 2008;226:112-31.

47. Sheibanie AF, Tadmori I, Jing H, Vassiliou E, Ganea D. Prostaglandin E2 induces IL-23 production in bone marrow-derived dendritic cells. FASEB journal : official publication of the Federation of American Societies for Experimental Biology. 2004;18(11):1318-20.

48. Yan J, Smyth MJ, Teng MWL. Interleukin (IL)-12 and IL-23 and Their Conflicting Roles in Cancer. Cold Spring Harb Perspect Biol. 2018;10(7).

49. Stiller CA, Parkin DM. International variations in the incidence of neuroblastoma. International journal of cancer Journal international du cancer. 1992;52(4):538-43.

50. Matthay KK, Maris JM, Schleiermacher G, Nakagawara A, Mackall CL, Diller L, et al. Neuroblastoma. Nat Rev Dis Primers. 2016;2:16078.

699 51. Vo KT, Matthay KK, Neuhaus J, London WB, Hero B, Ambros PF, et al. Clinical, biologic, and prognostic
700 differences on the basis of primary tumor site in neuroblastoma: a report from the international
701 neuroblastoma risk group project. Journal of clinical oncology : official journal of the American Society of
702 Clinical Oncology. 2014;32(28):3169-76.

703 52. Tolbert VP, Matthay KK. Neuroblastoma: clinical and biological approach to risk stratification and
704 treatment. Cell Tissue Res. 2018;372(2):195-209.

705 53. Irwin MS, Park JR. Neuroblastoma: paradigm for precision medicine. Pediatr Clin North Am.
706 2015;62(1):225-56.

707 54. Borriello L, Seeger RC, Asgharzadeh S, DeClerck YA. More than the genes, the tumor microenvironment in
708 neuroblastoma. Cancer letters. 2015.

709 55. Carlson LM, Rasmuson A, Idborg H, Segerstrom L, Jakobsson PJ, Sveinbjornsson B, et al. Low-dose aspirin
710 delays an inflammatory tumor progression in vivo in a transgenic mouse model of neuroblastoma.
711 Carcinogenesis. 2013;34(5):1081-8.

712 56. Johnsen JI, Lindskog M, Ponthan F, Pettersen I, Elfman L, Orrego A, et al. Cyclooxygenase-2 is expressed
713 in neuroblastoma, and nonsteroidal anti-inflammatory drugs induce apoptosis and inhibit tumor growth
714 in vivo. Cancer research. 2004;64(20):7210-5.

715 57. Johnsen JI, Lindskog M, Ponthan F, Pettersen I, Elfman L, Orrego A, et al. NSAIDs in neuroblastoma therapy.
716 Cancer letters. 2005;228(1-2):195-201.

717 58. Kock A, Larsson K, Bergqvist F, Eissler N, Elfman LHM, Raouf J, et al. Inhibition of Microsomal Prostaglandin
718 E Synthase-1 in Cancer-Associated Fibroblasts Suppresses Neuroblastoma Tumor Growth. EBioMedicine.
719 2018;32:84-92.

720 59. Larsson K, Kock A, Idborg H, Arsenian Henriksson M, Martinsson T, Johnsen JI, et al. COX/mPGES-1/PGE2
721 pathway depicts an inflammatory-dependent high-risk neuroblastoma subset. Proc Natl Acad Sci U S A.
722 2015;112(26):8070-5.

723 60. Rasmuson A, Kock A, Fuskevag OM, Kruspig B, Simon-Santamaria J, Gogvadze V, et al. Autocrine
724 prostaglandin E2 signaling promotes tumor cell survival and proliferation in childhood neuroblastoma.
725 PLoS One. 2012;7(1):e29331.

726 61. Ara T, Nakata R, Sheard MA, Shimada H, Buettner R, Groshen SG, et al. Critical role of STAT3 in IL-6-
727 mediated drug resistance in human neuroblastoma. Cancer research. 2013;73(13):3852-64.

728 62. Ara T, Song L, Shimada H, Keshelava N, Russell HV, Metelitsa LS, et al. Interleukin-6 in the bone marrow
729 microenvironment promotes the growth and survival of neuroblastoma cells. Cancer research.
730 2009;69(1):329-37.

731 63. Tümmler C, Dumitriu G, Wickström M, Coopman P, Valkov A, Kogner P, et al. SYK Inhibition Potentiates
732 the Effect of Chemotherapeutic Drugs on Neuroblastoma Cells in Vitro. Cancers (Basel). 2019;11(2):202.

733 64. Cui W, Taub DD, Gardner K. qPrimerDepot: a primer database for quantitative real time PCR. Nucleic Acids
734 Res. 2007;35(Database issue):D805-9.

735 65. Figenschau Y, Knutsen G, Shahazeydi S, Johansen O, Sveinbjornsson B. Human articular chondrocytes
736 express functional leptin receptors. Biochem Biophys Res Commun. 2001;287(1):190-7.

737 66. Tümmler C, Snapkov I, Wickstrom M, Moens U, Ljungblad L, Maria Elfman LH, et al. Inhibition of
738 chemerin/CMKLR1 axis in neuroblastoma cells reduces clonogenicity and cell viability in vitro and impairs
739 tumor growth in vivo. Oncotarget. 2017;8(56):95135-51.

67. Mosmann T. Rapid colorimetric assay for cellular growth and survival: application to proliferation and cytotoxicity assays. J Immunol Methods. 1983;65(1-2):55-63.

68. Petryszak R, Keays M, Tang YA, Fonseca NA, Barrera E, Burdett T, et al. Expression Atlas update--an integrated database of gene and protein expression in humans, animals and plants. Nucleic Acids Res. 2016;44(D1):D746-52.

69. Uhlen M, Fagerberg L, Hallstrom BM, Lindskog C, Oksvold P, Mardinoglu A, et al. Proteomics. Tissue-based map of the human proteome. Science. 2015;347(6220):1260419.

70. Brodeur GM, Seeger RC, Schwab M, Varmus HE, Bishop JM. Amplification of N-myc in untreated human neuroblastomas correlates with advanced disease stage. Science. 1984;224(4653):1121-4.

71. Seeger RC, Brodeur GM, Sather H, Dalton A, Siegel SE, Wong KY, et al. Association of multiple copies of the N-myc oncogene with rapid progression of neuroblastomas. The New England journal of medicine. 1985;313(18):1111-6.

72. Gaffen SL. Structure and signalling in the IL-17 receptor family. Nature reviews Immunology. 2009;9(8):556-67.

73. Tartour E, Fossiez F, Joyeux I, Galinha A, Gey A, Claret E, et al. Interleukin 17, a T-cell-derived cytokine, promotes tumorigenicity of human cervical tumors in nude mice. Cancer research. 1999;59(15):3698-704.

74. Numasaki M, Watanabe M, Suzuki T, Takahashi H, Nakamura A, McAllister F, et al. IL-17 enhances the net angiogenic activity and in vivo growth of human non-small cell lung cancer in SCID mice through promoting CXCR-2-dependent angiogenesis. Journal of immunology. 2005;175(9):6177-89.

75. McGeachy MJ, Cua DJ, Gaffen SL. The IL-17 Family of Cytokines in Health and Disease. Immunity. 2019;50(4):892-906.

76. Pan B, Shen J, Cao J, Zhou Y, Shang L, Jin S, et al. Interleukin-17 promotes angiogenesis by stimulating VEGF production of cancer cells via the STAT3/GIV signaling pathway in non-small-cell lung cancer. Sci Rep. 2015;5:16053.

77. Wang L, Yi T, Kortylewski M, Pardoll DM, Zeng D, Yu H. IL-17 can promote tumor growth through an IL-6-Stat3 signaling pathway. The Journal of experimental medicine. 2009;206(7):1457-64.

78. Chung AS, Wu X, Zhuang G, Ngu H, Kasman I, Zhang J, et al. An interleukin-17-mediated paracrine network promotes tumor resistance to anti-angiogenic therapy. Nature medicine. 2013;19(9):1114-23.

79. He D, Li H, Yusuf N, Elmets CA, Li J, Mountz JD, et al. IL-17 promotes tumor development through the induction of tumor promoting microenvironments at tumor sites and myeloid-derived suppressor cells. Journal of immunology. 2010;184(5):2281-8.

80. Martin-Orozco N, Muranski P, Chung Y, Yang XO, Yamazaki T, Lu S, et al. T helper 17 cells promote cytotoxic T cell activation in tumor immunity. Immunity. 2009;31(5):787-98.

81. Su Y, Huang J, Zhao X, Lu H, Wang W, Yang XO, et al. Interleukin-17 receptor D constitutes an alternative receptor for interleukin-17A important in psoriasis-like skin inflammation. Sci Immunol. 2019;4(36).

82. De Luca A, Pariano M, Cellini B, Costantini C, Villella VR, Jose SS, et al. The IL-17F/IL-17RC Axis Promotes Respiratory Allergy in the Proximal Airways. Cell Rep. 2017;20(7):1667-80.

83. Xiang C, Chen J, Fu P. HGF/Met Signaling in Cancer Invasion: The Impact on Cytoskeleton Remodeling. Cancers (Basel). 2017;9(5).

84. Owusu BY, Galemmo R, Janetka J, Klampfer L. Hepatocyte Growth Factor, a Key Tumor-Promoting Factor in the Tumor Microenvironment. Cancers (Basel). 2017;9(4).

85. Skoldenberg EG, Larsson A, Jakobson A, Hedborg F, Kogner P, Christofferson RH, et al. The angiogenic growth factors HGF and VEGF in serum and plasma from neuroblastoma patients. Anticancer Res. 2009;29(8):3311-9.

86. Hecht M, Papoutsi M, Tran HD, Wilting J, Schweigerer L. Hepatocyte growth factor/c-Met signaling promotes the progression of experimental human neuroblastomas. Cancer research. 2004;64(17):6109-18.

87. Crosswell HE, Dasgupta A, Alvarado CS, Watt T, Christensen JG, De P, et al. PHA665752, a small-molecule inhibitor of c-Met, inhibits hepatocyte growth factor-stimulated migration and proliferation of c-Met-positive neuroblastoma cells. BMC Cancer. 2009;9:411.

88. Huang Y, Liu L, Liu A. Dickkopf-1: Current knowledge and related diseases. Life sciences. 2018;209:249-54.

89. Koppen A, Ait-Aissa R, Hopman S, Koster J, Haneveld F, Versteeg R, et al. Dickkopf-1 is down-regulated by MYCN and inhibits neuroblastoma cell proliferation. Cancer letters. 2007;256(2):218-28.

90. D'Amico L, Mahajan S, Capietto AH, Yang Z, Zamani A, Ricci B, et al. Dickkopf-related protein 1 (Dkk1) regulates the accumulation and function of myeloid derived suppressor cells in cancer. The Journal of experimental medicine. 2016;213(5):827-40.

91. Jiang YX, Yang SW, Li PA, Luo X, Li ZY, Hao YX, et al. The promotion of the transformation of quiescent gastric cancer stem cells by IL-17 and the underlying mechanisms. Oncogene. 2017;36(9):1256-64.

92. Welsby I, Goriely S. Regulation of Interleukin-23 Expression in Health and Disease. Advances in experimental medicine and biology. 2016;941:167-89.

93. Espigol-Frigole G, Planas-Rigol E, Ohnuki H, Salvucci O, Kwak H, Ravichandran S, et al. Identification of IL-23p19 as an endothelial proinflammatory peptide that promotes gp130-STAT3 signaling. Sci Signal. 2016;9(419):ra28.

94. Voronov E, Dotan S, Krelin Y, Song X, Elkabets M, Carmi Y, et al. Unique Versus Redundant Functions of IL-1alpha and IL-1beta in the Tumor Microenvironment. Front Immunol. 2013;4:177.

Supplementary Material

Supplementary Figure 1

Expression of IL17RD and IL17C is increased in neuroblastoma and predicts poor overall survival probability

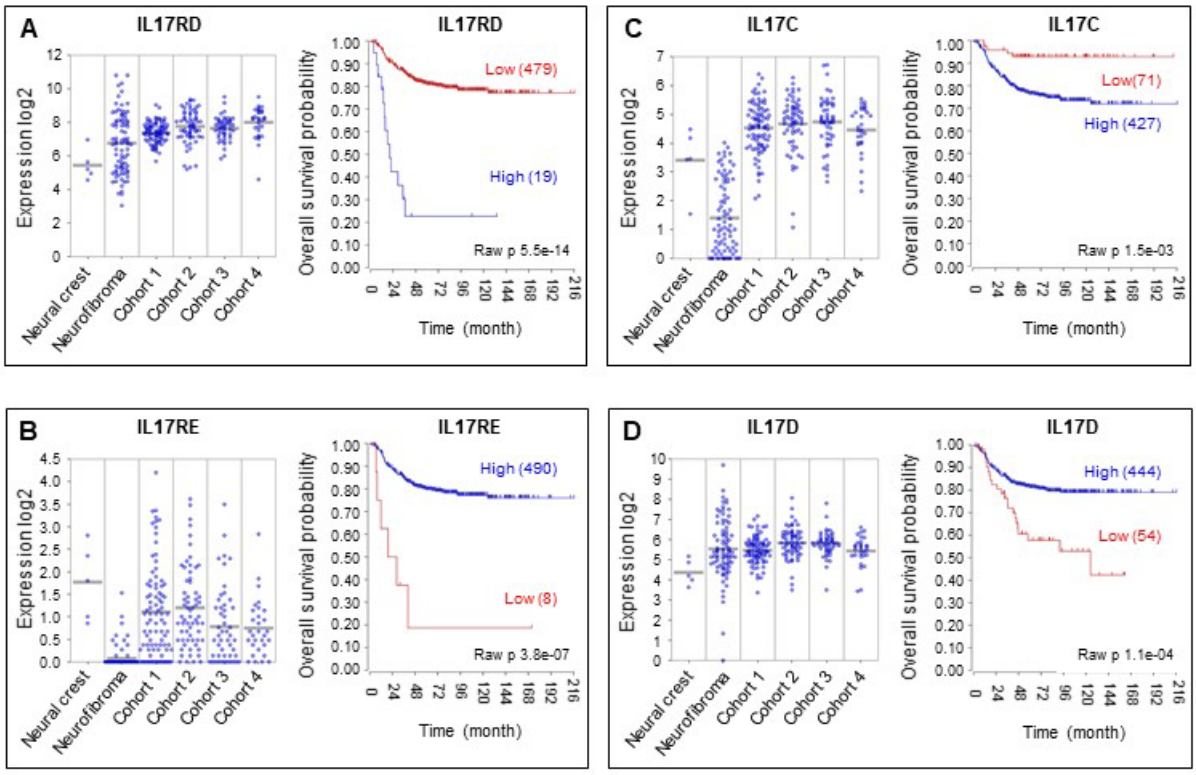

Supplementary Figure 1:
Gene expression data was analyzed using the R2 database http://r2.amc.nl. The expression of *IL17RD* **(A)**, *IL17RE* **(B)**, *IL17C* **(C)** and, *IL-17D* **(D)** was compared between neural crest cells (Etchevers n=5), benign neurofibroma (Miller n=86) and 4 neuroblastoma cohorts (cohort 1: Versteeg, n=88, cohort 2: Delattre, n=64, cohort 3: Hiyama, n=51, cohort 4: Lastowska, n=30) using the MegaSampler feature. In addition, the prognostic value of IL-17 family members was evaluated in the SEQC-RPM-seqcnb1 data set (n=498) using Kaplan-Meier survival estimates. The Kaplan-Meier scanning tool determines the most optimal cutoff between high and low gene expression and the lowest p-value (log-rank test) to evaluate significant differences between tumors with high or low expression of the respective gene.

Supplementary Figure 2

IL-17A is present in a intermixed ganglioneuroblastoma with high T cell infiltration

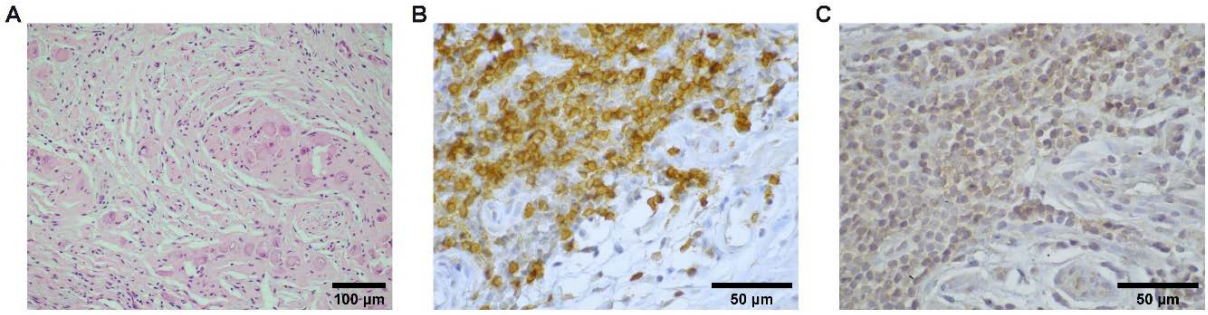

Supplementary Figure 2: IL-17A is present in an intermixed ganglioneuroblastoma.
The presence of CD3 (B) and IL-17A(C) was determined by immunoperoxidase staining. Panel A displays an H&E staining of the tissue. Images were captured at 300x (A) and 900x (B and C).

Supplementary Figure 3

Expression of IL17RD, IL17RE, IL17C, and IL17D in neuroblastoma cell lines

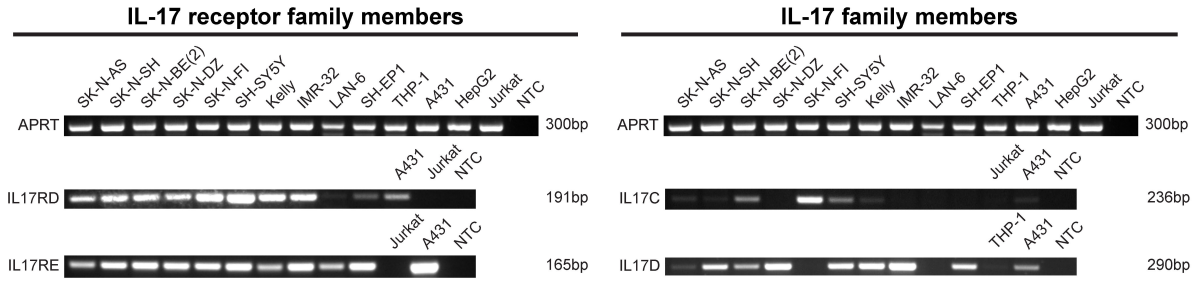

Supplementary Figure 3: Expression of IL17RD, IL17RE, IL17C, and IL17D in neuroblastoma cell lines
RT-PCR analysis demonstrating mRNA expression of *IL17RD*, *IL17RE*, *IL17C* and *IL17D* in different neuroblastoma cell lines. Expression of the APRT housekeeping gene was examined to ensure equal RNA input. THP-1, A431, and Jurkat cells served as control cell lines. NTC, no template control

Supplementary Figure 4

IL-23p19 is increased in myeloid cells and tumor and/or stroma cells of tumor-bearing TH-MYCN mice

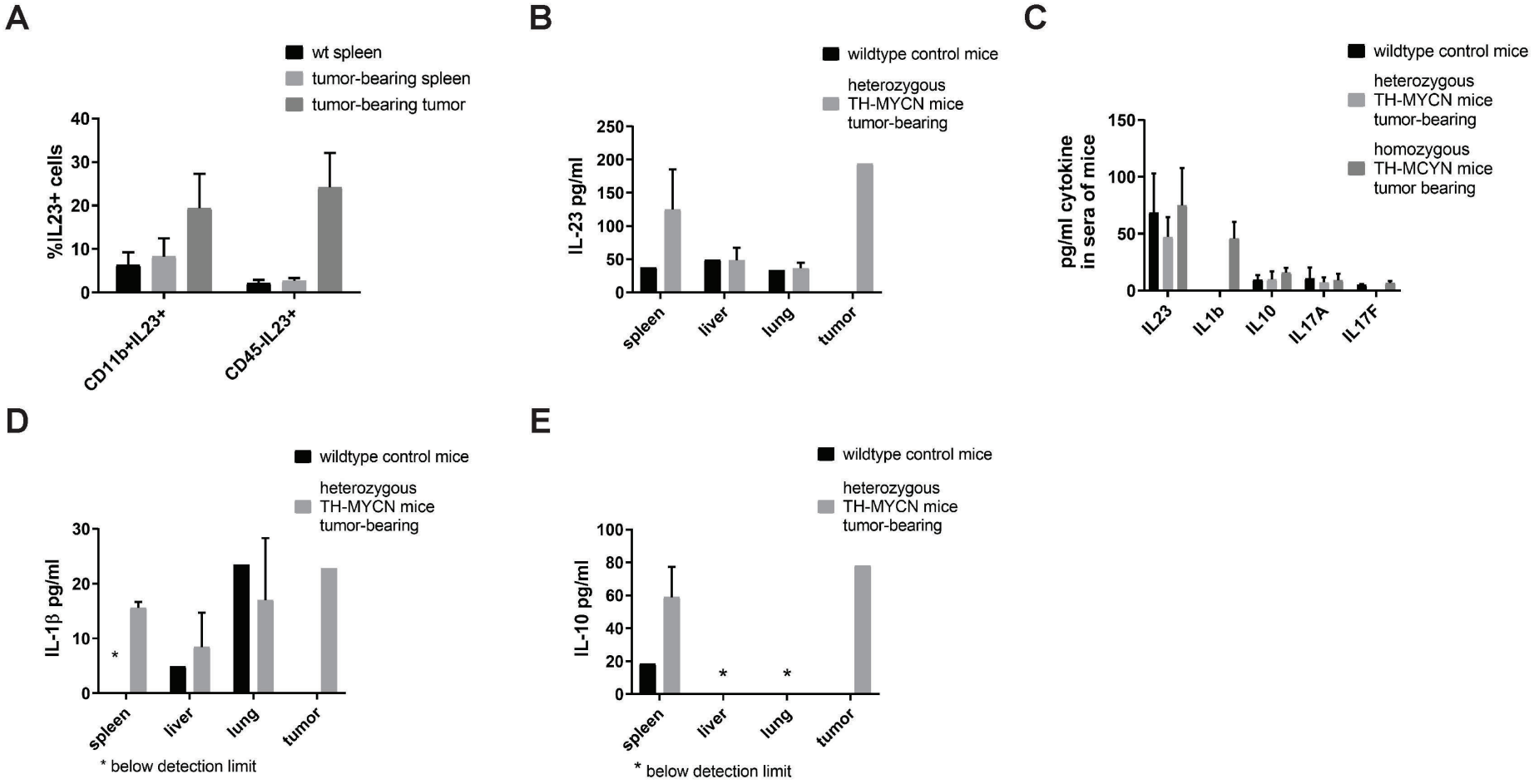

Supplementary Figure 4: IL-23p19 is increased in myeloid cells and tumor and/or stroma cells of tumor-bearing TH-MYCN mice.
(A) Intracellular staining of IL-23p19 in $CD11b^+$ cells isolated from spleen and tumor of tumor-bearing or wildtype mice as well as $CD45^-$ cells from tumors. **(B-E)** Cytokine analysis of IL-23p19 **(B)**, IL-1β **(D)**, and IL-10 **(E)** in organs or sera **(C)** of tumor-bearing or wildtype mice (n=2 for wt mice, n=3 for tumor-bearing mice).

Supplementary Figure 5

Correlation between IL17RB, IL17RD, IL17RA and MYCN expression

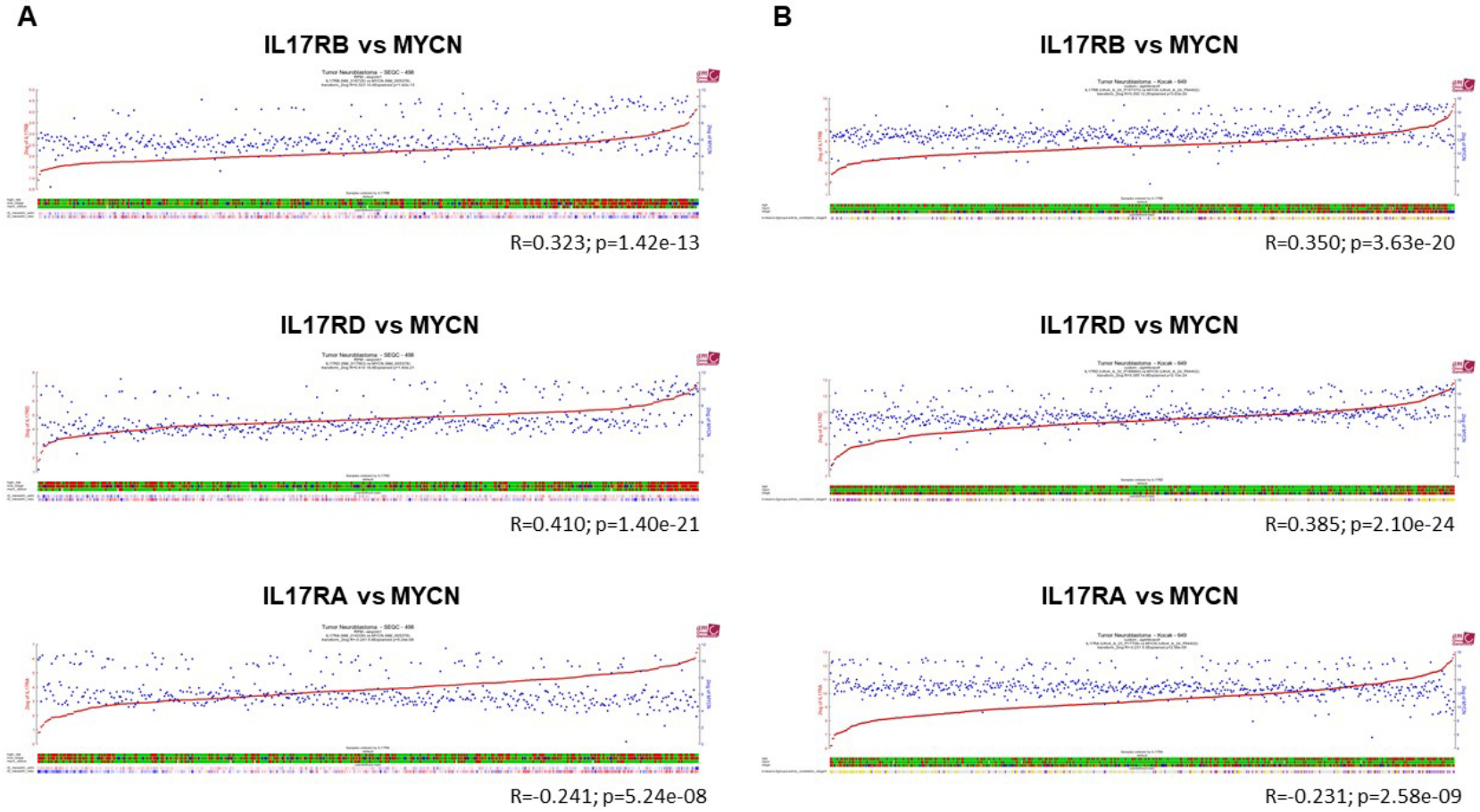

Supplementary Figure 5: Correlation between IL17RB, IL17RD, IL17RA and MYCN expression
Expression data was analyzed using the R2 database http://r2.amc.nl. The SEQC-RPM-seqcnb1 data set (n=498) **(A)** and the Kocak data set (n=649) **(B)** were used to correlate *IL17RB*, *IL17RD* and *IL17RA* expression to MYCN expression.

Supplementary Table 1: Cell viability of SK-N-AS, SK-N-BE(2), SK-N-DZ, and SH-SY5Y after stimulation with IL-17A, IL-17A/F, IL-17B or IL-25 for 72h

Treatment		SK-N-AS		SK-N-BE(2)		SK-N-DZ		SH-SY5Y	
		Cell viability (%) Mean ± SD	P value ctr. vs. treat.	Cell viability (%) Mean ± SD	P value ctr. vs. treat.	Cell viability (%) Mean ± SD	P value ctr. vs. treat.	Cell viability (%) Mean ± SD	P value ctr. vs. treat.
IL-17A	Control	100 ± 12.2		100 ± 12.6		100 ± 23.7		100 ± 18.9	
	0.01 ng/ml	105 ± 12.9	0.187	108.3 ± 12.4	0.018	95.6 ± 30.3	0.971	104 ± 19.6	0.784
	0.1 ng/ml	106 ± 9.6	0.072	105.5 ± 12.7	0.204	89.8 ± 32.1	0.509	102.7 ± 25.3	0.957
	1 ng/ml	102.3 ± 10.4	0.849	105.6 ± 14.4	0.196	105.9 ± 40	0.905	106.3 ± 15.04	0.446
	10 ng/ml	98.1 ± 13.4	0.925	104 ± 14.5	0.517	105.3 ± 37	0.936	106.2 ± 15.8	0.449
	100 ng/ml	92.8 ± 10.5	0.019	95.4 ± 14.4	0.365	100.1 ± 31.1	>0.999	98.7 ± 17.4	0.998
IL-17A/F	Control	100 ± 7.6		100 ± 8.2		100 ± 16.3		100 ± 8.4	
	0.01 ng/ml	106.5 ± 9.9	0.006	105 ± 13.9	0.707	108.3 ± 20.6	0.189	102.1 ± 9.9	0.824
	0.1 ng/ml	108.2 ± 9.3	<0.001	104.7 ± 19.1	0.755	107.0 ± 22.8	0.335	100.3 ± 9.5	>0.999
	1 ng/ml	109.6 ± 9.7	<0.001	103.1 ± 17.5	0.938	109.9 ± 20.7	0.076	102.3 ± 11.6	0.763
	10 ng/ml	106.6 ± 7.3	0.005	97.9 ± 17.4	0.989	107.7 ± 23.53	0.253	100.6 ± 8.2	0.999
	100 ng/ml	98.3 ± 6.7	0.943	97.04 ± 19.7	0.981	104.1 ± 17.7	0.904	94.2 ± 10.2	0.028
IL-17B	Control	100 ± 6.8		100 ± 8.4		100 ± 16.8		100 ± 18.22	
	0.01 ng/ml	102.7 ± 7.1	0.525	100.9 ± 12.4	0.998	108.8 ± 17.4	0.222	104.5 ± 19.2	0.854
	0.1 ng/ml	104.7 ± 8.1	0.076	101 ± 11.4	0.997	118.2 ± 19.6	<0.001	106.5 ± 15.04	0.572
	1 ng/ml	106 ± 7.6	0.01	101.9 ± 10.9	0.962	108.5 ± 20.7	0.256	102.7 ± 19.8	0.980
	10 ng/ml	101.4 ± 5.3	0.952	101.3 ± 9.9	0.992	111.4 ± 23.4	0.067	107.8 ± 18.56	0.386
	100 ng/ml	103.7 ± 6.2	0.221	101.3 ± 14.7	0.993	103.2 ± 20	0.946	95.7 ± 11.5	0.873
IL-25	Control	100 ± 8.3		100 ± 7.7		100 ± 9.9		100 ± 6.2	
	0.01 ng/ml	103.0 ± 11.8	0.543	105.1 ± 11.9	0.146	97.8 ± 9.5	0.953	100.1 ± 9.3	>0.999
	0.1 ng/ml	105.0 ± 11.2	0.103	102.1 ± 13.3	0.890	93.2 ± 10.5	0.138	100.3 ± 9.1	>0.999
	1 ng/ml	100.6 ± 11.9	>0.999	102.5 ± 10.8	0.794	91.5 ± 14.7	0.034	101.2 ± 7.6	0.936
	10 ng/ml	94.9 ± 10.2	0.084	105.2 ± 11.8	0.128	87.7 ± 12.2	<0.001	98.0 ± 8.4	0.627
	100 ng/ml	93.2 ± 7.6	0.009	98.5 ± 12.7	0.971	75.2 ± 12.7	<0.001	92.0 ± 8.1	<0.001

Cell viability was measured by MTT assay after 72 h. The control was set as 100% viable cells. Data are presented as mean ± SD from at least three independent experiments. Dunnett's multiple comparison test was used to evaluate differences between control cells and stimulation with different concentrations of recombinant IL-17 proteins. P values <0.05 were considered as statistically significant.

Supplementary Material and Methods

IHC

The following antibodies were used for CD3 and IL-17A immunoperoxidase staining: IL-117A: #sc-374218, Santa Cruz Biotechnology, CD3: #A0452, Agilent Technologies, Dako

TH-MYCN murine neuroblastoma model

TH-MYCN mice (Weiss et al. EMBO J 1997) were kept as continuous inbreeding at the animal facilities of the Karolinska Institutet in Stockholm under the ethical permit number N42/12. Abdomens of mice were palpated every second day to monitor tumor growth and sacrificed for further analysis once substantial tumors had developed, as described in [1, 2].

Flow cytometry

Single cell suspensions of spleens or tumors were obtained by passing organs through cell strainers, and erythrocytes were lysed using 1x Erylysis buffer (Sigma). Up to 1×10^6 cells were placed in FACS tubes, washed with PBS, and stained for 20 min at room temperature with pre-mixed surface marker antibodies and life dead markers (Invitrogen) in 20–50 µL PBS. Cells were washed in PBS, resuspended in FACS buffer (PBS+10% heat-inactivated FCS) and stored at 4°C before measurements. For intracellular staining of IL23 cells were fixed in BD Cytofix/Cytoperm buffer (BD Bioscience) for 30 min at room temperature and washed with 1× BD PermWash (BD Bioscience) buffer. Cells were incubated with intracellular antibodies (anti-IL23 or isotype control) in 1× BD PermWash buffer for 45 min at room temperature. After a final wash, cells were acquired at the NovoCyte Flow Cytometer (ACEA Biosciences) and analysed by NovoExpress software (ACEA).

The following Flow antibodies were used: CD11b (clone M1/70, Biolegend), CD45 (30-F11, Biolegend), IL23p19 clone 320244, Novus Biologicals) and corresponding isotype control IgG2ak.

Cytokine analysis in mouse organs and sera

Blood samples were taken from euthanized mice by cardiac puncture. Following blood clotting (30min) the samples were centrifuged for 10min at 1000xg. Serum was transferred into new tubes an stored at -80˚C until further use. Organs were homogenized in T-PER tissue extraction buffer containing protease and phosphatase inhibitors (Thermo Fisher Scientific Inc.). Following sonication samples were centrifuged for 5min at 10000xg to remove tissue debris. Cytokine content of sera and tissue lysates was determined using a LEGENDplex™ kit (BioLegend, San Diego, CA, USA) according to the supplied manual.

1. Eissler N, Mao Y, Brodin D, Reutersward P, Andersson Svahn H, Johnsen JI, et al. Regulation of myeloid cells by activated T cells determines the efficacy of PD-1 blockade. Oncoimmunology. 2016;5(12):e1232222.
2. Mao Y, Eissler N, Blanc KL, Johnsen JI, Kogner P, Kiessling R. Targeting Suppressive Myeloid Cells Potentiates Checkpoint Inhibitors to Control Spontaneous Neuroblastoma. Clin Cancer Res. 2016;22(15):3849-59.

Appendix

Sequence 1

Forward:

CTAGAATTAGGGCGATTGGGCCCTCTAGATGCATGCTCGAGCGGCCGCCAGTGTGATGGA
TATCTGCAGAATTCGCCCTTCAGGCTCAAAGCAAGTGGAAGTGGGCAGAGATTCCACCAG
GACTGGTGCAAGGCGCAGAGCCAGCCAGATTTGAGAAGAAGGCAAAAAGATGCTGGGGAG
CAGAGCTGTAATGCTGCTGTTGCTGCTGCCCTGGACAGCTCAGGGCAGAGCTGTGCCTGG
GGGCAGCAGCCCTGCCTGGACTCAGTGCCAGCAGCTTTCACAGAAGCTCTGCACACTGGC
CTGGAGTGCACATCCACTAGTGGGACACATGGTGAGTGGCAGCCCCTGGAGCCTAACAGG
AGTCCAGGCTCTCCAAGGCTGTGGCAGAAGACCGTGACCTTGAGTGGAAGCTGGAGGGTT
GAAGACCATTAGGGAGTAAGAGAGGACAAGAGAGTAGGGTTCCTGGGAGAGTCATGGGCC
TGAGGGTCCAGGTTGGCTTCAGAAGTACTATCTTACTTCTTCATTCTTTCCACCTCTTCC
TTCATTCCAGGATCTAAGAGAAGAGGGAGATGAAGAGACTACAAATGATGTTCCCCATAT
CCAGTGTGGAGATGGCTGTGACCCCCAAGGACTCAGGGACAACAGTCAGGTACCACTGGG
ATGTGGCTGGGCAATGAAGGAGAGGGGACTGAGAACATGGCTGGGTACCATGGTAAACCA
GAAGTTGTGTCTGAAAATAGTAAGAAACTGGGTGAGTCTTCAGTGAATGGAGTAGGAAGA
GGGTGTCCTCTTTCATTGCTTTCTTTTCTCCCTAGTTCTGCTTGCAAAGGATCCACCAGG
GTCTGATTTTTTTATGAGAAGCTGCTAGGATCGGATATTTTCACAGGGGAGCCTTCTCTG
CTCCCTGATAGCCCTGTGGACCAGCTTCATGCCTCCCTACTGGGCCTCAGCCAACTCCTG
CAGTACGAAGTAAGGGGCGTGGAGGATGGGGGCTTGCAGTGTCAGAGACAGAGGTTGGGG
AGTTTAAAGGTTTAAGAGTCTTCTCTGGACTGTGTCCTATGTTCCCTATCCAGCTGAGGG
TCAACCAACTGGGGAGACTTCAGCAGATTTCAGGCCCTTCAGTTCCCAGACAGCCCATTG
GCAGCGTTACTCTCGCTTCAAAATTACGT

Reverse:

ACATGGTCGAGCTCGGATCCACTAGTAACGGCCGCCAGTGTGCTGGAATTCGCCCTTGAG
ATCTGAGTGCCATCCTTGAGCTGCTGCCTTTAGGGACTCAGGGTTGCTGCTCCATGGGCA
AAGACCCGGGCGGCTACAGCCACAAAGGCCTGGAGGCTGCGAAGGATTTTGAAGCGGAGA
AGGAGACGCTGCCATGGCTGGCTGGGACTGAGGCTTGGAATCTGCTGAGTCTCCCAGTGG
TGACCCTCAGGCTGAAAGGACATAGGACACAGTCAGAGAAGACTCTAAACCCTTAACCCC
CAACCCTCTGTCTCTGACACCTGCAAGCCCCCATCCTCCACGCCCCTACTTCGTACCTGC
AGGAGTTGGCTGAGGCCCAGTAGGGAGGCATGAAGCTGGTCCACAGGGCTATCAGGGAGC
AGAGAAGGCTCCCCTGTGAAAATATCCGATCCTAGCAGCTTCTCATAAAAAATCAGACCC
TGGTGGATCCTTTGCAAGCAGAACTAGGGAGAAAAGAAAGCAATGAAAGAGGACACCCTC
TTCCTACTCCATTCACTGAAGACTCACCCAGTTTCTTACTATTTTCAGACACAACTTCTG
GTTTACCATGGTACCCAGCCATGTTCTCAGTCCCCTCTCCTTCATTGCCCAGCCACATCC
CAGTGGTACCTGACTGTTGTCCCTGAGTCCTTGGGGGTCACAGCCATCTCCACACTGGAT
ATGGGGAACATCATTTGTAGTCTCTTCATCTCCCTCTTCTCTTAGATCCTGGAATGAAGG
AAGAGGTGGAAAGAATGAAGAAGTAAGATAGTACTTCTGAAGCCAACCTGGACCCTCACG
CCCATGACTCTCCCAGGAACCCTACTCTCTTGTCCTCTCTTACTCCCTAATGGTCTTCAA
CCCTCCAGCTTCCACTCAAAGGTCACGGTCTTCTGCCACAGCCCTTGGAGAGCCTGGACT
CCTGTTTAGGCTCCAGGGGCTGCCCACTCACCATGTGTCCCACTAGTGGGATGTGCACTC
CAGGCCCAGTGTGCAGAGCTTTCTGTGAAAGCCTGCCTGGGCAACTGAGTCAAGTCAGAC
TGCTGCTCCAGGCACAGCCTCTGCCCCTGGAAGCC

Sequence 2

Forward:

CAAAACGGCGATTGGGCCCTCTAGATGCATGCTCGAGCGGCCGCCAGTGTGATGGATATC
TGCAGAATTCGCCCTTGAGATCTGAGTGCCATCCTTGAGCTGCTGCCTTTAGGGACTCAG
GGTTGCTGCTCCATGGGCAAAGACCCGGGCGGCTACAGCCACAAAGGCCTGGAGGCTGCG
AAGGATTTTGAAGCGGAGAAGGAGACGCTGCCATGGCTGGCTGGGACTGAGGCTTGGAAT
CTGCTGAGTCTCCCAGTGGTGACCCTCAGGCTGCAGGAGTTGGCTGAGGCCCAGTAGGGA
GGCATGAAGCTGGCCCACAGGGCTATCAGGGAGCAGAGAAGGCTCCCCTGTGAAAATATC

CGATCCTAGCAGCTTCTCATAAAAAATCAGACCCTGGTGGATCCTTTGCAAGCAGAACTA
GGGAGAAAAGAAAGCAATGAAAGAGGACACCCTCTTCCTACTCCATTCACTGAAGACTCA
CCCAGTTTCTTACTATTTTCAGACACAACTTCTGGTTTACCATGGTACCCAGCCATGTTC
TCAGTCCCCTCTCCTTCATTGCCCAGCCACATCCCAGTGGTACCTGACTGTTGTCCCTGA
GTCCTTGGGGGTCACAGCCATCTCCACACTGGATATGGGGAACATCATTTGTAGTCTCTT
CATCTCCCTCTTCTCTTAGATCCTGGAATGAAGGAAGAGGTGGAAAGAATGAAGAAGTAA
GATAGTACTTCTGAAGCCAACCTGGACCCTCAGGCCCATGACTCTCCCAGGAACCCTACT
CTCTTGTCCTCTCTTACTCCCTAATGGCCTTCAACCCTCCAGCTTCCACTCAAGGTCACG
GTCTTCTGCCACAGCCTTGGAGAGCCTGGACTCCTGTTAGGCTCCAGGGGCTGCCACTCA
CCATGTGTCCCACTAGTGGATGTGCACTCCAGGCCAGTGTGCAGAGCTTCTGTGAAAGCT
GCTGGCACTGAGTCCAGGCACGGCTGCTGCCCCCCAGGCACAGCTCTGCCCTGAGCTGTC
CAGGGCAGCAGCACAGCAGCATTACAGCTCTGCTCCCCAGCATCTTTTTTGCCGTTCTTC
TCAAGTCTGCCTGCTCTGCGCCTTTGCACCAAGTTCCTGGGTGGAATTCCTTCCTGTGC

Reverse:

GCTTTCGAGCTCGGATCCACTAGTAACGGCCGCCAGTGTGCTGGAATTCGCCCTTCAGGC
TCAAAGCAAGTGGAAGTGGGCAGAGATTCCACCAGGACTGGTGCAAGGCGCAGAGCCAGC
CAGATTTGAGAAGAAGGCAAAAAGATGCTGGGGAGCAGAGCTGTAATGCTGCTGTTGCTG
CTGCCCTGGACAGCTCAGGGCAGAGCTGTGCCTGGGGGCAGCAGCCCTGCCTGGACTCAG
TGCCAGCAGCTTTCACAGAAGCTCTGCACACTGGCCTGGAGTGCACATCCACTAGTGGGA
CACATGGTGAGTGGCAGCCCCTGGAGCCTAACAGGAGTCCAGGCTCTCCAAGGCTGTGGC
AGAAGACCGTGACCTTGAGTGGAAGCTGGAGGGTTGAAGGCCATTAGGGAGTAAGAGAGG
ACAAGAGAGTAGGGTTCCTGGGAGAGTCATGGGCCTGAGGGTCCAGGTTGGCTTCAGAAG
TACTATCTTACTTCTTCATTCTTTCCACCTCTTCCTTCATTCCAGGATCTAAGAGAAGAG
GGAGATGAAGAGACTACAAATGATGTTCCCCATATCCAGTGTGGAGATGGCTGTGACCCC
CAAGGACTCAGGGACAACAGTCAGGTACCACTGGGATGTGGCTGGGCAATGAAGGAGAGG
GGACTGAGAACATGGCTGGGTACCATGGTAAACCAGAAGTTGTGTCTGAAAATAGTAAGA
AACTGGGTGAGTCTTCAGTGAATGGAGTAGGAAGAGGGTGTCCTCTTTCATTGCTTTCTT
TTCTCCCTAGTTCTGCTTGCAAAGGATCCACCAGGGTCTGATTTTTTATGAGAAGCTGCT
AGGATCGGATATTTTCACAGGGGAGCCTTCTCTGCTCCCTGATAGCCCTGTGGGCCAGCT
TCATGCCTCCCTACTGGGCCTCAGCCAACTCCTGCAGCCTGAGGGTCACCACTGGGGAGA
CTCAGCAGATTCCAAAGCCTCAGTCCCAGCCAGCCATGGCAGCGTCTCCCTTCTCCGCTT
CAAAATCCCTTCGCAGCCCTCCCAGGCCCTTTGTGGGCTGTAGCCCGCCCCGGATCTTTG
GCTCATGGAGCCAGTACCCCGTGCAGTCCCCTTAAAAGGCAAGCAAGCCTCCAAA

Sequence 3

Forward:

AACAATACGGCGATTGGGCCCTCTAGATGCATGCTCGAGCGGCCGCCAGTGTGATGGATA
TCTGCAGAATTCGCCCTTCAGGCTCAAAGCAAGTGGAAGTGGGCAGAGATTCCACCAGGA
CTGGTGCAAGGCGCAGAGCCAGCCAGATTTGAGAAGAAGGCAAAAAGATGCTGGGGAGCA
GAGCTGTAATGCTGCTGTTGCTGCTGCCCTGGACAGCTCAGGGCAGAGCTGTGCCTGGGG
GCAGCAGCCCTGCCTGGACTCAGTGCCAGCAGCTTTCACAGAAGCTCTGCACACTGGCCT
GGAGTGCACATCCACTAGTGGGACACATGGTGAGTGGCAGCCCCTGGAGCCTAACAGGAG
TCCAGGCTCTCCAAGGCTGTGGCAGAAGACCGTGACCTTGAGTGGAAGCTGGAGGGTTGA
AGGCCATTAGGGAGTAAGAGAGGACAAGAGAGTAGGGTTCCTGGGAGAGTCATGGGCCTG
AGGGTCCAGGTTGGCTTCAGAAGTACTATCTTACTTCTTCATTCTTTCCACCTCTTCCTT
CATTCCAGGATCTAAGAGAAGAGGGAGATGAAGAGACTACAAATGATGTTCCCCATATCC
AGTGTGGAGATGGCTGTGACCCCCAAGGACTCAGGGACAACAGTCAGTTCTGCTTGCAAA
GGATCCACCAGGGTCTGATTTTTTATGAGAAGCTGCTAGGATCGGATATTTTCACAGGGG
AGCCTTCTCTGCTCCCTGATAGCCCTGTGGGCCAGCTTCATGCCTCCCTACTGGGCCTCA
GCCAACTCCTGCAGCCTGAGGGTCACCACTGGGAGACTCAGCAGATTCCAAGCCTCAGTC
CCAGCCAGCCATGGCAGCGTCTCCTTCTCCGCTTCAAAATCCTTCGCAGCCTCCAGGCCT
TTGTGGCTGTAGCCGCCCGGGTCTTTGCCCATGGAGCAGCAACCCTGAGTCCCTAAAGGC
AGCAGCTCAAGGATGGCACTCAGATCTCAAGGGCGAATTCCAGCACACTGGGCGGCCCGT
ACTAGTGGGATCCGAGCTCGGTACAAGCTTGGCGTAATCATGGTCATAGCTGTTTCCTGT
GTGAATTGTTATCGCTCACAATCCACAACAACTACGAGTCGAAGGCCATAATGTTAAGTC

TTGGATGACCTGTAAAT

Reverse:

GACTGTCGAGCTCGGATCCACTAGTAACGGCCGCCAGTGTGCTGGAATTCGCCCTTGAGA
TCTGAGTGCCATCCTTGAGCTGCTGCCTTTAGGGACTCAGGGTTGCTGCTCCATGGGCAA
AGACCCGGGCGGCTACAGCCACAAAGGCCTGGAGGCTGCGAAGGATTTTGAAGCGGAGAA
GGAGACGCTGCCATGGCTGGCTGGGACTGAGGCTTGGAATCTGCTGAGTCTCCCAGTGGT
GACCCTCAGGCTGCAGGAGTTGGCTGAGGCCCAGTAGGGAGGCATGAAGCTGGCCCACAG
GGCTATCAGGGAGCAGAGAAGGCTCCCCTGTGAAAATATCCGATCCTAGCAGCTTCTCAT
AAAAAATCAGACCCTGGTGGATCCTTTGCAAGCAGAACTGACTGTTGTCCCTGAGTCCTT
GGGGGTCACAGCCATCTCCACACTGGATATGGGGAACATCATTTGTAGTCTCTTCATCTC
CCTCTTCTCTTAGATCCTGGAATGAAGGAAGAGGTGGAAAGAATGAAGAAGTAAGATAGT
ACTTCTGAAGCCAACCTGGACCCTCAGGCCCATGACTCTCCCAGGAACCCTACTCTCTTG
TCCTCTCTTACTCCCTAATGGCCTTCAACCCTCCAGCTTCCACTCAAGGTCACGGTCTTC
TGCCACAGCCTTGGAGAGCCTGGACTCCTGTTAGGCTCCAGGGGCTGCCACTCACCATGT
GTCCCACTAGTGGATGTGCACTCCAGGCCAGTGTGCAGAGCTTCTGTGAAAGCTGCTGGC
ACTGAGTCCAGGCAGGGCTGCTGCCCCCAGGCACAGCTCTGCCCTGAGCTGTCCAGGGCA
GCAGCAACAGCAGCATTACAGCTCTGCTCCCCAGCATCTTTTTTGCCTTCTTCTCAAATC
TGGCTGGCTCTGCGCCTTGCACCAGTCCTGGTGGAATCTCTGCCCACTTCCACTTGCTTT
GAGCCTGAAAGGGCGAATTCTGCAGATATCCATCACACTGGCGGCCGCTCGAGCATGCAT
CTAGAGGGCCCAATTTCGCCCTATAGTGAGTCGTATTTACAATTCACTGGGTCGTTCGAT
TTTACCAACCGGTCGGTGGACTGGGAAAAAACCCCCTTGGGGGCCGGATTTTAAAC

Sequence 4

Forward:

ATGCAAATAGGGCGATTGGGCCTCTAGATGCATGCTCGAGCGGCCGCCAGTGTGATGGAT
ATCTGCAGAATTCGCCCTTGAGATCTGAGTGCCATCCTTGAGCTGCTGCCTTTAGGGACT
CAGGGTTGCTGCTCCATGGGCAAAGACCCGGGCGGCTACAGCCACAAAGGCCTGGAGGCT
GCGAAGGATTTTGAAGCGGAGAAGGAGACGCTGCCATGGCTGGCTGGGACTGAGGCTTGG
AATCTGCTGAGTCTCCCAGTGGTGACCCTCAGGCTGCAGGAGTTGGCTGAGGCCCAGTAG
GGAGGCATGAAGCTGGCCCACAGGGCTATCAGGGAGCAGAGAAGGCTCCCCTGTGAAAAT
ATCCGATCCTAGCAGCTTCTCATAAAAAATCAGACCCTGGTGGATCCTTTGCAAGCAGAA
CTGACTGTTGTCCCTGAGTCCTTGGGGGTCACAGCCACCTCCACACTGGATATGGGGAAC
ATCATTTGTAGTCTCCTCATCTTCCCCTTCTCTTAGATCCATGTGTCCCACTAGTGGATG
TGCACTCCAGGCCAGTGTGCAGAGCTTCTGTGAAAGCTGCTGGCACTGAGTCCAGGCGGG
GCTGCTGCCCCCAGGCACAGCTCTGCCCTGAGCTGTCCAGGGCAGCAGCAACAGCAGCAT
TACAGCTCTGCTCCCCAGCATCTTTTTGCCTTCTTCTCAAATCTGGCTGGCTCTGCGCCT
TGCACCAGTCCTGGTGGAATCTCTGCCCACTTCCACTTGCTTTGAGCCTGAAGGGCGAAT
TCCAGCACACTGGCGGCCGTTACTAGTGGATCCGAGCTCGGTACCAAGCTTGGCGTAATC
ATGGTCATAGCTGTTTCCTGTGTGAAATTGTTATCCGCTCACAATTCCACACAACATACG
AAGCCGGGAAGCATAAAGTGTAAAGCCTGGGGTGCCTAAATGAGTGAGCTAACTCACATT
AAATTGCGTTGCGCTCACTGCCCGCTTTTCCAGTTCGGGAAAACCTGGTCCGTGCCAGCT
GCAATAAATTGAAATCGGGCCCAAACGCCGGCGGGGGAAGAAGGCCGGGTTTGCCGTTAT
TTGGGGCGGCTCTTTCGGCATTCCTTCGGCTCAACTTGAACATCGGCTTACGGCCATCGA
GATCAGATTACGGCTTGGCGGCACAGACCGTATACCAGCTTCACTCCAAGGTGCCGTATT
ACCGCAGAATATCATTAC

Reverse:

GCTTTCGAGCTCGGATCCACTAGTAACGGCCGCCAGTGTGCTGGAATTCGCCCTTCAGGC
TCAAAGCAAGTGGAAGTGGGCAGAGATTCCACCAGGACTGGTGCAAGGCGCAGAGCCAGC
CAGATTTGAGAAGAAGGCAAAAAGATGCTGGGGAGCAGAGCTGTAATGCTGCTGTTGCTG
CTGCCCTGGACAGCTCAGGGCAGAGCTGTGCCTGGGGGCAGCAGCCCCGCCTGGACTCAG
TGCCAGCAGCTTTCACAGAAGCTCTGCACACTGGCCTGGAGTGCACATCCACTAGTGGGA
CACATGGATCTAAGAGAAGGGGAAGATGAGGAGACTACAAATGATGTTCCCCATATCCAG
TGTGGAGGTGGCTGTGACCCCCAAGGACTCAGGGACAACAGTCAGTTCTGCTTGCAAAGG

ATCCACCAGGGTCTGATTTTTTATGAGAAGCTGCTAGGATCGGATATTTTCACAGGGGAG
CCTTCTCTGCTCCCTGATAGCCCTGTGGGCCAGCTTCATGCCTCCCTACTGGGCCTCAGC
CAACTCCTGCAGCCTGAGGGTCACCACTGGGAGACTCAGCAGATTCCAAGCCTCAGTCCC
AGCCAGCCATGGCAGCGTCTCCTTCTCCGCTTCAAAATCCTTCGCAGCCTCCAGGCCTTT
GTGGCTGTAGCCGCCCGGGTCTTTGCCCATGGAGCAGCAACCCTGAGTCCCTAAAGGCAG
CAGCTCAAGGATGGCACTCAGATCTCAAGGGCGAATTCTGCAGATATCCATCACACTGGC
GGCCGCTCGAGCATGCATCTAGAGGGCCCAATTCGCCCTATAGTGAGTCGTATTACAATT
CACTGGCCGTCGTTTTACAACGTCGTGACTGGGAAAACCCTGGCGTTACCCAACTTAATC
GCCTTGCAGCACATCCCCCCTTTCGCCAGCTGGCGTAATAGCGAAGAGGCCCGCACCGAT
CGCCCTTCCCAACAGTTTGCGCAGCCTGAATGGCGAATGGACGCGCCCTGTAGCGGGCGC
ATTAAGCGCGGGCGGGTGTGGGTGGGTTTACGCGCAGGCGTGACCGCTACACTTTGCCCA
GCGTCCTAGCGCCGCTCCGTTTCGCTTTTCTTCCCTTTCCATTTTTCTTTCGATCCA

Sequence 5

Forward:

GTCTGTCGAGCTCGGATCCACTAGTAACGGCCGCCAGTGTGCTGGAATTCGCCCTTCAGG
CTCAAAGCAAGTGGAAGTGGGCAGAGATTCCACCAGGACTGGTGCAAGGCGCAGAGCCAG
CCAGATTTGAGAAGAAGGCAAAAAGATGCTGGGGAGCAGAGCTGTAATGCTGCTGTTGCT
GCTGCCCTGGACAGCTCAGGGCAGAGCTGTGCCTGGGGGCAGCAGCCCTGCCTGGACTCA
GTGCCAGCAGCTTTCACAGAAGCTCTGCACACTGGCTGTAGCCGCCCGGGTCTTTGCCCA
TGGAGCAGCAACCCTGAGTCCCTAAAGGCAGCAGCTCAAGGATGGCACTCAGATCTCAAG
GGCGAATTCTGCAGATATCCATCACACTGGCGGCCGCTCGAGCATGCATCTAGAGGGCCC
AATTCGCCCTATAGTGAGTCGTATTACAATTCACTGGCCGTCGTTTTACAACGTCGTGAC
TGGGAAAACCCTGGCGTTACCCAACTTAATCGCCTTGCAGCACATCCCCCTTTCGCCAGC
TGGCGTAATAGCGAAGAGGCCCGCACCGATCGCCCTTCCCAACAGTTGCGCAGCCTGAAT
GGCGAATGGACGCGCCCTGTAGCGGCGCATTAAGCGCGGCGGGTGTGGTGGTTACGCGCA
GCGTGACCGCTACACTTGCCAGCGCCCTAGCGCCCGCTCCTTTCGCTTTCTTCCCTTCCT
TTCTCGCCACGTTCGCCGGCTTTCCCCGTCAAGCTCTAAATCGGGGGCTCCCTTTAGGGT
TCCGATTTAGTGCTTTACGGCACCTCGACCCCAAAAAACTTGATTAGGGTGATGGTTCAC
GTAGTGGGCCATCGCCCCTGATAGACGGTTTTTCGCCCTTTGACGTTGGAGTCCACGTTT
CTTTAATAGTGGACTCTTGTTCCAAACTGGAAACAACACTCAACCCTATCTCGGGTCTAT
TCTTTTGATTTATAAGGATTTTGCCGATTTCGGCCTATTGGTTAAAAAAATGAGCTGATT
AACAAAAATTTAACGCGAAATTTTAACAAAATTTCAAGTGCAGGACTTGCCTTAAGAAGC
CGGACACGTAGAAGTCAAGTTCCGCCAGAAACCGTGCCTGGACCCCCGGGA

Reverse:

ATGCAATACGGCGATTGGGCCCTCTAGATGCATGCTCGAGCGGCCGCCAGTGTGATGGAT
ATCTGCAGAATTCGCCCTTGAGATCTGAGTGCCATCCTTGAGCTGCTGCCTTTAGGGACT
CAGGGTTGCTGCTCCATGGGCAAAGACCCGGGCGGCTACAGCCAGTGTGCAGAGCTTCTG
TGAAAGCTGCTGGCACTGAGTCCAGGCAGGGCTGCTGCCCCCAGGCACAGCTCTGCCCTG
AGCTGTCCAGGGCAGCAGCAACAGCAGCATTACAGCTCTGCTCCCCAGCATCTTTTTGCC
TTCTTCTCAAATCTGGCTGGCTCTGCGCCTTGCACCAGTCCTGGTGGAATCTCTGCCCAC
TTCCACTTGCTTTGAGCCTGAAGGGCGAATTCCAGCACACTGGCGGCCGTTACTAGTGGA
TCCGAGCTCGGTACCAAGCTTGGCGTAATCATGGTCATAGCTGTTTCCTGTGTGAAATTG
TTATCCGCTCACAATTCCACACAACATACGAGCCGGAAGCATAAAGTGTAAAGCCTGGGG
TGCCTAATGAGTGAGCTAACTCACATTAATTGCGTTGCGCTCACTGCCCGCTTTCCAGTC
GGGAAACCTGTCGTGCCAGCTGCATTAATGAATCGGCCAACGCGCGGGGAGAGGCGGTTT
GCGTATTGGGCGCTCTTCCGCTTCCTCGCTCACTGACTCGCTGCGCTCGGTCGTTCGGCT
GCGGCGAGCGGTATCAGCTCACTCAAAGGCGGTAATACGGTTATCCACAGAATCAGGGGA
TAACGCAGGAAAGAACATGTGAGCAAAAGGCCAGCAAAAGGCCAGGAACCGTAAAAAGGC
CGCGTTGCTGGCGTTTTTCCATAGGCTCCGCCCCCCTGACGAGCATCACAAAATCGACGC
TCAAGTCAGAGGTGGCGAAACCCGACAGGACTATAAAGATACCAGGCGTTTCCCCCTGGG
AAGCTCCCTCGTGCGCTCTCTGTTCCGACCCTGCCGCTTACCCGGATACCTGTCGCCTTC
TCCCTTTCGGGAAGCGTGGCGCTTTTCTCATAGCTCACGCTGTAAGGTATCTCAGTTTCG
ATGTAAGTCGTCGCTTCAGCTTGGGCTGTGATGCACGAACTCCCCCGGTTCCAGGCCGGA
CCGGCCTGTGGGCT